

The respiratory chain in *Neisseria* species

Xi Li

PhD

University of York
Department of Biology
April 2013

Abstract:

This work presents the organization of respiratory chain in *Neisseria* species. The localization of redox proteins was determined. Lipid-modified azurin (Laz) and nitrite reductase (AniA) are mainly associated with outer membrane. All c-type cytochrome proteins are mainly associated with inner membrane.

Cytochrome c_5 is the major electron donor to AniA. Reduced form cytochrome c_5 is able to donate electrons to AniA at a physiologically relevant rate. In addition, the second haem domain of cytochrome c_5 is the direct donor to AniA. It presents a potential problem for inter-electron transfer between c_5 and AniA, which are associated with inner and outer membrane respectively. Trihaem CcoP is the alternative electron donor to AniA in *N. gonorrhoeae*. The 3rd haem domain of *N. gonorrhoeae* CcoP is able to donate electrons to AniA at a physiologically relevant rate, suggesting there is alternative route for nitrite reduction in *N. gonorrhoeae*. *N. elongata* cytochrome is an electron donor to AniA. *N. elongata* cytochrome which has high degree of similarity with c_5 , is confirmed to donate electrons to AniA at a physiologically relevant rate, suggesting *N. elongata* has one other route for nitrite reduction.

Laz is not involved in nitrite reduction. Laz is able to receive electrons from cytochrome c_5 at physiological relevant rate, but cannot donate electrons to AniA. Based on laz mutagenesis study, laz mutant strain has limited affect on growth and nitrite usage compared to the wild type strain.

Cytochrome c_x is not involved in oxygen reduction. Cytochrome c_x has presumably been found to be involved in oxygen reduction in *N. meningitidis*, but not in *N. gonorrhoeae*. *N. meningitidis* carrying an *N. gonorrhoeae ccoP* gene has a similar growth rate as the growth rate of the wild type strain and also c_x mutant strains.

Table of Content:

Chapter 1 General introduction	1
1.1 Biology and genetics of <i>N. meningitidis</i>	1
1.2 Pathogenesis of <i>N. meningitidis</i>	2
1.3 Respiration in <i>N. meningitidis</i>	5
1.4 Denitrification during oxygen limiting respiration in <i>Neisseria</i> species	6
1.5 Electron transport chain in <i>Neisseria</i> species	7
1.6 Terminal redox reductases	10
1.6.1 Nitrite reductase AniA.....	10
1.6.2 Cytochrome <i>cbb</i> ₃ oxidase	15
1.6.3 Nitric oxide reductase NorB	21
1.7 Regulation of nitrite reduction in <i>Neisseria</i> species.....	22
1.8 Major electron carriers	24
1.8.1 Cytochrome <i>c</i> ₅	26
1.8.2 Cytochrome <i>c</i> ₄	28
1.8.3 Cytochrome <i>c</i> _x	29
1.8.4 Lipid-modified azurin (Laz)	30
1.9 Potential electron carriers in other <i>Neisseria</i> species?	33
1.10 Inter-protein electron transfer for nitrite reduction in denitrification in <i>Neisseria</i>	

species.....	34
1.11 Aims and objectives of this work:	36
Chapter 2 Method and Material	37
2.1 Bacterial strains and plasmids used in this work	37
2.1.1 Bacterial strains used in this work	37
2.1.2 Bacterial plasmid used in this work.....	40
2.2 Growth of cells.....	42
2.2.1 Growth of <i>Neisseria meningitidis</i> and <i>Neisseria lactamica</i>	42
2.2.2 Growth of <i>Escherichia coli</i>	42
2.2.3 Preparation of bacterial frozen stocks.....	43
2.2.4 Preparation of antibiotic selective media	43
2.2.5 Bacterial Growth assay	43
2.3 Fractionation of cells.....	44
2.3.1 Preparation of <i>N. meningitidis</i> whole cell extract.....	44
2.3.2 Preparation of <i>N. lactamica</i> periplasm, cytoplasm and inner and outer membranes	44
2.3.3 Extraction of chromosomal DNA.....	46
2.3.4 Transformation of <i>N. meningitidis</i> strains by TSB method	47
2.4 Genetic techniques	48
2.4.1 The polymerase chain reaction:.....	48

2.4.1.1	Generation of c_5 , c_x constructs:	48
2.4.1.2	Generation of the first haem and the second haem domain of c_5 , laz , <i>N. elongata</i> cytochrome and the 3 rd haem domain of <i>N. gonorrhoeae ccoP</i> constructs....	49
2.4.2	Restriction digestion of PCR product and pET22b+ vector.....	51
2.4.3	Ligation of inserts into pET 22b(+) plasmid.....	51
2.4.4	Transformation of DH5 α and BL21 (λ)DE3 <i>E. coli</i> cells:	52
2.4.5	Colony PCR	52
2.4.6	Preparation of <i>E. coli</i> plasmid DNA.....	52
2.4.7	Preparation of <i>E. coli</i> competent cells	53
2.5	Protein purification	53
2.5.1	Preparing <i>E. coli</i> cell crude extract:.....	53
2.5.2	Extraction of periplasmic proteins from <i>E. coli</i> BL21 (λ)DE3.	54
2.5.3	Nickel Affinity Chromatography.....	54
2.5.4	Ion exchange chromatography	54
2.5.5	Protein concentration determination.....	55
2.5.6	Desalting and buffer-exchanging of protein samples	55
2.6	Analytical techniques	56
2.6.1	SDS-PAGE.....	56
2.6.2	Coomassie stain.....	58
2.6.3	Western blot	58
2.6.4	Haem stain (Chemiluminescent method)	59

2.6.5 Spectra of protein samples	60
2.6.6 Pyridine haemochrome	60
2.7 Stopped-flow kinetics experiment	60
2.8 <i>In vivo</i> <i>N. meningitidis</i> nitrite usage assay:	61
Chapter 3 Localization of redox proteins in <i>Neisseria</i> species.....	62
3.1 Introduction	62
3.2 Commensal <i>Neisseria lactamica</i> is closely related to <i>Neisseria meningitidis</i>:	66
3.3 Subcellular localization of c-type cytochrome proteins:	69
3.4 Membrane localization of redox proteins:	71
3.5 Discussion:	73
Chapter 4 Biochemical basis of inter-protein electron transfer for nitrite	
reduction in denitrification in <i>N. meningitidis</i>	78
4.1 Introduction	78
4.2 Purification and characterization of cytochrome <i>c</i>₅	80
4.2.1 Construction and purification of cytochrome <i>c</i> ₅	80
4.2.2. Characterization of cytochrome <i>c</i> ₅	84
4.2.2.1 Spectra properties of reduced and oxidized cytochrome <i>c</i> ₅	84
4.2.2.2 Pyridine heamochrome to measure the concentration of cytochrome <i>c</i>	
.....	84

4.3 Purification and characterization of nitrite reductase AniA	86
4.4 Steady state cytochrome c_5 nitrite reductase AniA interaction	89
4.5 Stopped flow kinetics of cytochrome c_5 and nitrite reductase AniA interaction.....	91
4.5.1 The second order electron transfer rate constant between cytochrome c_5 and nitrite reductase AniA	91
4.5.2 Salt dependence of cytochrome c_5 and AniA interaction:	93
4.5.3 pH dependence of cytochrome c_5 and AniA interaction:	95
4.6 Over-expression of monohaem domains of cytochrome c_5	97
4.7 Stopped-flow kinetics of inter-protein electron transfer reaction from reduced first haem domain and second haem domain of cytochrome c_5 to nitrite reductase AniA..	103
4.7.1: Stopped-flow kinetics of first haem domain of cytochrome c_5 and AniA interaction.....	103
4.7.2 Stopped flow kinetics of second haem domain of cytochrome c_5 with AniA:	105
4.8: Over-expression of cytochrome c_x and c_4:	108
4.9: Stopped-flow kinetics of inter-protein electron transfer reaction from reduced cytochrome c_x to nitrite reductase AniA.	113
4.10: Intra-protein electron transfer between two haem containing domains of c_5 during nitrite reduction:	118
4.11: Salt and pH dependence of intra-protein electron between two haem containing domains of c_5:	121

4.12: Discussion	126
-------------------------------	------------

Chapter 5 : Inter-protein electron transfer for nitrite reduction in

denitrification in other <i>Neisseria</i> species:	135
---	------------

5.1 Introduction	135
-------------------------------	------------

5.2 Over-expression and characterization of the third haem domain of CcoP of cytochrome <i>cbb₃</i> complex from <i>N. gonorrhoeae</i>.	140
---	------------

5.3 Stopped-flow kinetics of inter-protein electron transfer reaction from reduced third haem domain of CcoP of <i>cbb₃</i> to nitrite reductase AniA.	143
--	------------

5.3.1 The second order electron transfer rate constant between 3 rd haem domain of <i>N. gonorrhoeae</i> CcoP and nitrite reductase AniA.....	143
--	-----

5.3.2 Salt dependence of the 3 rd haem domain of <i>N. gonorrhoeae</i> CcoP and nitrite reductase AniA interaction	145
---	-----

5.3.3 pH dependence of 3 rd haem domain of <i>N. gonorrhoeae</i> CcoP nitrite reductase AniA interaction.	147
---	-----

5.4 Over-expression and characterization of cytochrome c family protein from <i>N. elongata</i>	149
--	------------

5.5 Steady state <i>N. elongata</i> cytochrome and nitrite reductase AniA interaction	153
--	------------

5.6 Stopped-flow kinetics of inter-protein electron transfer reaction from reduced <i>N. elongata</i> cytochrome c to nitrite reductase AniA	155
---	------------

5.7: Discussion	159
------------------------------	------------

Chapter 6 Characterization of lipid-modified Azurin (Laz)	165
6.1 Introduction	165
6.2 Over-expression and characterization of Laz	169
6.3 Steady state kinetics of inter-protein electron transfer reaction from Laz to nitrite reductase AniA and cytochrome c_5 to Laz	173
6.4 Stopped flow kinetics of inter-protein electron transfer reaction from cytochrome c_5 to Laz, and from Laz to AniA	176
6.5 Growth of laz mutant strain under microaerobic conditions.	179
6.6 Discussion.	182
Chapter 7 : Are cytochrome c_x and c_4 still electron donors to cbb_3 oxidase, when <i>N. meningitidis</i> is carrying an ectopic copy of <i>N. gonorrhoeae ccoP</i>?	186
7.1 Introduction	186
7.2 Visualization of cytochrome profiles in <i>N. meningitidis</i> MC58 and MF64 by haem staining	190
7.3 Growth properties of cytochrome deficient mutants of <i>N. meningitidis</i> MC58 and MF64	194
7.4 Comparing <i>N. meningitidis</i> c_x mutants in published construct and new construct	197
7.5 Discussion	200

Chapter 8 : General discussion and conclusion: 205

Reference..... 212

Tables and Illustrations

Chapter 1 General introduction:

- Figure 1.1 Proposed complete denitrification pathway in bacteria
- Figure 1.2 Proposed electron transport chains in *N. meningitidis*.
- Figure 1.3 Proposed structure of soluble AniA
- Figure 1.4 Amino acid alignment of AniA and other copper containing nitrite reductase.
- Figure 1.5 Proposed organization of fixNOQP operon in *N. meningitidis*.
- Figure 1.6 Primary structure of cytochrome *c*₅.
- Figure 1.7 Predicted function of Laz in *Neisseria* respiratory metabolism.
- Figure 1.8 Predicted nitrite reduction network in *Neisseria* species

Chapter 2 Method and Material:

- Table 2.1: Bacterial strains used in this work
- Table 2.2: Bacterial plasmid used in this work.
- Table 2.3: Antibiotic concentration used in this work.
- Figure 2.1: Preparation of ultracentrifuge tube for *N. lactamica* inner membrane and outer membrane separation:

Table 2.4: Oligonucleotides primers used in amplifying cytochrome c_5 and c_x in this work.

Table 2.5: Oligonucleotides primers used in amplifying the first haem and the second haem domain of c_5 , laz , *N. elongata* cytochrome and the 3rd haem domain of *N. gonorrhoeae ccoP*.

Table 2.6 Protocol for preparation of SDS-PAGE.

Chapter 3: Localization of redox proteins in *Neisseria* species

Figure 3.1 Electron flow between membranes in *N. meningitidis*.

Table 3.1 Results of NCBI Blast searches: *N. meningitidis* MC58 redox genes were searched against *N. lactamica* ST640 to find homologous sequences and identities.

Figure 3.2 Primary structure comparison of AniA in *N. meningitidis* MC58(N. men) and *N. lactamica* ST640(N. lac).

Figure 3.3 Primary structure comparison of Laz of *N. meningitidis* MC58(N. men) and *N. lactamica* ST640(N. lac).

Figure 3.4 *N. lactamica* cells were fractionated into periplasm, cytoplasm and membrane.

Figure 3.5 *N. lactamica* cells were fractionated into periplasm, cytoplasm and membrane using lysozyme treatment and osmotic shock.

Figure 3.6 Predicted model of electron flow between membranes in *N. meningitidis*.

Chapter 4: Biochemical basis of inter-protein electron transfer for nitrite reduction in denitrification in *N. meningitidis*:

Figure 4.1 SDS-PAGE analysis of cytochrome c_5 from each step of purification process.

Figure 4.2 Molecular mass of soluble c_5 detected by electrospray mass spectrometry.

Figure 4.3 Absorption spectra of purified cytochrome c_5 :

Figure 4.4 SDS-PAGE analysis of Anion exchange chromatography fractions of crude periplasmic extract and purified AniA

Figure 4.5 Spectral features of reduced and oxidized AniA by UV-VIS spectroscopy.

Figure 4.6 Spectral analysis of reduced c_5 and oxidized AniA interaction is measured between 350nm-650nm.

Figure 4.7 The electron-transfer between AniA and cytochrome c_5 was performed in 50mM Tris(pH 7.5).

Figure 4.8 The salt dependence of cytochrome c_5 and AniA interaction was performed in 50mM Tris(pH 7.5)with salt present(0mM-500mM) :

- Figure 4.9 pH-dependence of AniA and cytochrome *c*₅ interaction was performed in 50 mM Tris with vary pH conditions (5.5-8.5)
- Table 4.1 Primary sequences of first haem domain and second haem domain of cytochrome *c*₅ from *N. meningitidis* MC58.
- Figure 4.10 PCR product of first haem domain of cytochrome *c*₅ with flanking regions.
- Figure 4.11 Colony PCR screens of *E. coli* DH5 α transformants for pET22b+ plasmid with insertion of first haem domain of cytochrome *c*₅ gene.
- Figure 4.12 PCR product of the second haem domain of cytochrome *c*₅ with flanking regions.
- Figure 4.13 Colony PCR screen of *E. coli* DH5 α transformants for pET22b⁺ plasmid with insertion of second haem domain of cytochrome *c*₅ gene.
- Figure 4.14 Expression of the 1st haem domain and the 2nd haem domain of cytochrome *c*₅ protein in *E. coli*.
- Figure 4.15 Molecular mass of the first haem domain of cytochrome *c*₅ detected by electrospray mass spectroscopy.
- Figure 4.16 The salt dependence of first haem domain of cytochrome *c*₅ and AniA interaction was performed in 50mM Tris (pH 7.5) with salt present (0mM-500mM).
- Figure 4.17 The electron-transfer between AniA and second haem domain of cytochrome *c*₅ was performed in 50mM Tris(PH7.5)

- Figure 4.18 The salt dependence of the second haem domain of cytochrome c_5 and AniA interaction was performed in 50mM Tris(pH 7.5) with salt present (0mM-500mM)
- Figure 4.19 PCR product of plasmid c_x -pETYSBL3C.
- Figure 4.20 Purified c_x from nickel affinity chromatography.
- Figure 4.21 Purification of cytochrome c_4 protein in from ion exchange chromatography analyzed by SDS-PAGE.
- Figure 4.22 Salt dependence of cytochrome c_x and AniA interaction by stopped-flow kinetics.
- Figure 4.23 The electron-transfer between AniA and cytochrome c_4 . Stopped-flow kinetics of inter-protein electron-transfer reaction from reduced cytochrome c_4 to AniA.
- Figure 4.24 The salt dependence of cytochrome c_4 and AniA interaction by stopped flow kinetics.
- Figure 4.25 The electron-transfer between AniA and cytochrome c_5 analyzed by 5-parameter double exponential equation.
- Figure 4.26 Salt dependence of intra-protein electron transfer between two haem containing of domains of cytochrome c_5 was performed in 50mM Tris(pH7.5) with salt present(0mM-500mM).
- Figure 4.27 pH dependence of intra-protein electron transfer between two haem containing domains of cytochrome c_5 was performed in 50 mM Tris

with vary pH (5.5-8.5).

Figure 4.28 Proposed model of soluble *c*₅ and AniA interaction *in vitro*.

Figure 4.29 pH dependence of intra-protein electron transfer between two monohaem domains of cytochrome *c*₅.

Chapter 5: Inter-protein electron transfer for nitrite reduction in denitrification in other *Neisseria* species:

Figure 5.1 Domain architectures of neisserial CcoP subunit of *cbb*₃ oxidase.

Figure 5.2 Primary protein sequence comparison of *N. gonorrhoeae* CcoP(NGO 1371) and *N. meningitidis* *c*₅ (NMB 1677).

Figure 5.3 Primary protein sequence comparison of *N. elongata* cytochrome *c* (NEIELOOT_00905) and cytochrome *c*₅ (NMB 1677).

Figure 5.4 PCR product of 3rd haem domain of *ccoP*.

Figure 5.5 Colony PCR screen of 3rd haem domain of *ccoP* of *N. gonorrhoeae*.

Figure 5.6 SDS-PAGE analysis of Ni affinity chromatography fractions of crude periplasmic extract and purified 3rd haem domain of *N. gonorrhoeae* CcoP.

Figure 5.7 Absorption spectra of purified cytochrome CcoP.

Figure 5.8 Stopped-flow kinetics of inter-protein electron-transfer reaction from

- reduced cytochrome CcoP to AniA was performed in 50mM Tris (pH7.5).
- Figure 5.9 The salt dependence of reduced 3rd haem domain cytochrome CcoP and AniA was performed in 50 mM Tris(pH7.5 with salt present (0-500mM).
- Figure 5.10 pH-dependence of AniA and reduced cytochrome CcoP interaction was performed in 50mM Tris with vary pH conditions(5.5-8.5)
- Figure 5.11 PCR product of cytochrome c family protein from *N. elongata*
- Figure 5.12 Colony PCR screen of cytochrome c family protein from *N. elongata* gene ligated into pET22b+ vector inserted in *E. coli* DH5 α transformants.
- Figure 5.13 SDS-PAGE analysis of Ni affinity chromatography fractions of crude periplasmic extract and purified cytochrome c family protein from *N. elongata*.
- Figure 5.14 Absorbance spectra of purified *N. elongata* cytochrome c: Spectra were recorded at room temperature in 50mM Tris buffer (pH7.5).
- Figure 5.15 Spectral analysis of *N. elongata* cytochrome and oxidized AniA interaction is measured between 350nm to 700nm.
- Figure 5.16 The electron transfer between AniA and *N. elongata* cytochrome c was performed in 50mM Tris (pH7.5)
- Figure 5.17 Proposed pathways for electron transfer from NADH

dehydrogenase(H) to terminal reductase (*cbb₃*, AniA and NorB) in *N. meningitidis* and *N. gonorrhoeae*.

Chapter 6: Characterization of lipid-modified Azurin (Laz)

- Figure 6.1 Predicted *Neisseria* Laz structure: a. Predicted *Neisseria* Laz domain structure.
- Figure 6.2 PCR product of *laz* gene with EcoRI and NcoI restriction digested sites exhibit a size of 516bp.
- Figure 6.3 Colony PCR screen for *laz* inserted in pET 22b(+) plasmid
- Figure 6.4 Expression of meningococcal sLaz protein from *E. coli*.
- Figure 6.5 UV-visible spectrum of reduced and oxidized soluble Laz buffered in 50mM Tris (pH7.5).
- Figure 6.6 Spectral analysis of reduced *c₅* and oxidized Laz interaction is measured between 400nm-700nm.
- Figure 6.7 Spectral analysis of reduced Laz and oxidized AniA interaction is measured between 400nm-800nm.
- Figure 6.8 The 2nd order rate constant for cytochrome *c₅* and Laz interaction
- Figure 6.9 Stopped-flow kinetics of inter-protein electron-transfer reaction from reduced Laz to oxidized AniA was performed at wavelength (455nm,

600nm, 626nm)

Figure 6.10 Colony PCR screen of *laz* with disrupted gene in *N. meningitidis* MC58.

Figure 6.11 Growth of *N. meningitidis* under oxygen limited conditions.

Figure 6.12 The predicted function of Laz in *N. meningitidis*.

Chapter 7: Are cytochrome c_x and c_4 still electron donors to cbb_3 oxidase, when *N. meningitidis* is carrying an ectopic copy of *N. gonorrhoeae ccoP*?

Figure 7.1 Comparison of cytochrome c_x difference in *N. meningitidis* (NMB0717) and *N. gonorrhoeae* (NGO0292).

Figure 7.2 Cytochrome profiles of *N. meningitidis* MC58 and MF64.

Figure 7.3 Colony PCR Colony PCR screen for c_x gene with erythromycin resistance gene cassette (ery^r) and c_4 gene with spectinomycin resistance gene cassette (spc^r) insert in *N. meningitidis* MF64 transformants.

Figure 7.4 Cytochrome profiles of respiratory cytochrome c_x , c_4 mutant extracts show altered expression of cytochrome in *N. meningitidis* MC58 and MF64.

Figure 7.5 Growth of *N. meningitidis* cytochrome c_x mutants under aerobic conditions.

Figure 7.6 Growth of *N. meningitidis* cytochrome c_4 mutants under aerobic conditions.

Figure 7.7 Cytochrome profiles of c_x mutant and wild type strains under the same growth conditions.

Figure 7.8 Proposed electron transport chains in *N. meningitidis* MC58.

Chapter 8: General discussion and conclusion:

Table 8.1 Summary of the rate constants for potential electron donors and AniA interaction in this work.

Figure 8.1 Proposed electron transport chains from NADH to nitric oxide, oxygen and nitrite in *N. meningitidis*, *N. gonorrhoeae* and *N. elongata*.

Figure 8.2 The predicted model of electron transfer between c_5 and AniA in *Neisseria* species.

Abbreviations

ABS	Absorbance
APS	Ammonium persulphate
AniA	Aerobically inducible protein A from <i>Neisseria</i> sp.
AI	Auto-induction medium
BHI	Brain Heart infusion
BSA	Bovine serum albumin
CSF	Cerebrospinal fluid
CBA/HBA	Columbia-blood Aga
CTAB	Cetyltrimethylammonium bromide
Cyc.	C-type cytochrome
DDM	n-Dodecyl β -D-maltoside
DMSO	Dimethyl sulfoxide
DUS	DNA uptake signal sequence
EDTA	Ethylenediaminetetraacetic acid
FNR	Fumarate nitrate reduction regulator
HCO	Haem-copper oxidases
IPTG	Isopropyl β -D-1-thiogalactopyranoside
LB	Lysogeny broth
LCR	Low complexity region

MHB	Mueller-Hinton broth
NDH	NADH dehydrogenase
OD	Optical density
PBS	Phosphate buffer saline
PEG	Polyethylene glycol
Rpm	Revolutions per minute
Redox	Reduction-oxidation
SDS	Sodium Dodecyl Sulfate
SDS PAGE	Sodium dodecyl sulphate polyacrylamide gel electrophoresis
SNP	Single-nucleotide polymorphism
TBE	Tris-borate-EDTA buffer
TSB	Transforming Storage Buffer
UV	Ultraviolet

Acknowledgements:

It has been a wonderful time for me working in the Moir lab for four years. I would like to thank to my supervisor Dr. James Moir for all his support and guidance throughout my project. He has been a fabulous source of inspiration and support for these years. I have learned many things and gained valuable experiences.

I would also like to thanks to all members of Moir's lab. Dr. James Edwards was always there with technical and theoretical advice. Many thanks to Marie Chiara Catenazzi, Andrew Schofield and Rachel Yale for the helping, sharing. Thanks to Dr. Andrew Leech for all the help and advice on stopped-flow work. Many thanks to Dr. J.M. Koomey for the gift of the *N. elongata* subsp. *Glycolytica* ATCC 29315. Thanks to Dr. Neil Bruce and Dr. Christoph Baumann for monitoring my progress on my teaching committee.

Most thanks go to my father Hongwei Li and my mother Yongqin Sun for your unconditional love, and for believing in me and supporting me. And also thanks to my husband Lichao Wang for the believing in every way for every decision and making my PhD life happy and memorable.

Author's Declaration:

I declare that all of the work present in this thesis is my own, original work unless explicitly stated in the text.

Xi Li, May 2013

Chapter 1

General introduction:

1.1 Biology and genetics of *N. meningitidis* :

The human restricted pathogen *Neisseria meningitidis* is a Gram negative, non-spore forming, capsulated, and non-motile β -proteobacteria (a class that includes *Bordetella*, *Burkholderia*, *Kingella*, and *Methylobacter*) in the family *Neisseriaceae*. The majority of organisms in this family are part of the normal flora of mammals and non-pathogenic, including *N. lactamica*, *N. elongata*, *N. sicca*, *N. subflava*, and *N. mucosa*. There are two species of genus *Neisseria* that can cause human disease: *N. meningitidis* and *N. gonorrhoeae*. *N. meningitidis* shares more than 95% sequence similarity with non-capsular, sexually-transmitted human pathogen *N. gonorrhoeae* (Kawai et al. 2006). Both pathogens are obligate human parasites. The natural habitat of *N. meningitidis* (also called meningococcus), is only in the human nasopharynx and oropharynx. It is the most common cause of bacterial meningitis, the causative agent of meningococcal septicaemia, and is the most common infectious infant and child disease in developed countries (Hart and Thomson 2006).

Strains within this species are classified by chemical composition and immunological characteristics of polysaccharide capsule encoded by pathogenicity island in the genome. Out of the 13 serogroups identified, five major serogroups (A, B, C, Y, and W135) of *N. meningitidis* as determined by capsular polysaccharide typing) are responsible for meningococcal disease (Gotschlich et al. 1969). Strains of serogroup B

and C cause the majority of infection in Europe and the United States. Strains of serogroup A are more prevalent in sub-Saharan Africa. *N. meningitidis* serogroup A (Z2491), serogroup B (MC58) and serogroup C (FAM18) complete genome sequences have been published. Genetic analysis shows that serogroup B (MC58) has only 10% difference in genome form to that of serogroup A, which might leads to different spreading patterns through human population (Tetelin et al. 2000).

There are three major islands for horizontal DNA transfer, involving genes encoding proteins involved in bacterial pathogenicity and capsulation and also encoding toxic and immunogenic proteins (Tetelin et al. 2000). *N. meningitidis* contains more genes undergo phase variation an adaptation to the changing environment of the host and facilitate invasion, even including overcoming of the immune response) than other pathogens studies to date, a mechanism that control gene expression and also enable the bacteria to survival of humoral immune surveillance (Tetelin et al. 2000).

1.2 Pathogenesis of *N. meningitidis*:

There are 11 *Neisseria* species that colonize humans, including two pathogenic species, *N. meningitidis* and *N. gonorrhoeae*. *N. meningitidis* is an opportunistic human pathogen, which colonizes as part of the normal flora of the nasopharynx of about 5 - 10% of the human population. Human nasopharyngeal mucosa is the only natural reservoir of *N. meningitidis*. These carriers do not exhibit clinical symptoms, which may be due to the successful competition for resources between all resident commensal organisms. This competition is important for limiting the growth of

pathogenic strains. Secretory IgA in the respiratory tract has an important role in inhibiting the pathogenic bacteria, but the occasional invasion of *N. meningitidis* is also able to lead to the life threatening disease and results in mortality in 20-50% of patients presenting severe disease. *N. meningitidis* enters the bloodstream, crosses the blood brain barrier and meninges leading to meningitis and septicaemia. Treatment involves the high dose of antibiotic therapy which is successful in the early stages of infection, however, approximately 10 - 15% treated patients will die (Fraser et al. 2006).

Meningococcal disease continues to have a major public health impact worldwide. Community- acquired meningitis occurs among small children and young adults with close and prolonged contact is required for transmission. The highest risk group in children is between the ages of 6 months and 6 years. The incidence of the disease drops with the increasing age due to the development of acquired immunity in nasopharyngeal mucosa (Frasch et al. 2001).

Generally, meningococcal infectious disease is rare and also needs to fulfill four conditions, including (1) Host needs to have contact with a virulent strain. (2) Colonization by the certain strain. (3) Penetration of the bacteria through the mucosa surface of the host. (4) Survival and outgrowth of the bacteria in the bloodstream (van Deuren et al. 2000). Infection caused by *N. meningitidis* is responsible for morbidity and mortality worldwide, which can occasionally manifest itself by crossing the blood-brain barrier to inflame the membrane called meninges surrounding the brain or as bacterial septicaemia and systemic shock.

Cell adhesion of *N. meningitidis* is crucial for colonization of nasopharyngeal mucosal surfaces. In addition, biofilm formation of human pathogen *N. meningitidis* is likely important in meningococcal colonization. It was reported that about 30% of carriage isolates and 12.5% of invasive-disease isolates formed biofilms and lack a capsule (Yi et al. 2004). The genes for capsule biosynthesis are down regulated upon contact with the host epithelial and facilitate meningococcal adherence (Yi et al. 2004). Type IV Pili are major adhesions that contribute to attachment to mucosa surfaces of the host cells (van Deuren et al. 2000). The other virulence determinants of *N. meningitidis* are contributed by outer membrane proteins and opacity proteins (Opa and Opc) (van Deuren et al. 2000).

The use of polysaccharide vaccine for control of serogroup C and A disease in young children has been established (Morleya and Pollardb 2001). The protein-polysaccharide conjugate vaccine against serogroup A and C (followed by Y and W135) has a dramatic effect on the epidemiology of disease and was introduced in 2000 (Morleya and Pollardb 2001). However, a safe, immunogenic and effective vaccine against serogroup B meningococcus is lacking in the market. There is a need to understand the basic physiology of these medically and economically important pathogens as a basis for identifying novel targets for therapy and improving the diagnosis.

1.3 Respiration in *N. meningitidis*:

When an external electron acceptor is presented, respiration is a catabolic pathway through which organic compounds can be oxidized to carbon dioxide via the TCA cycle. During aerobic respiration, oxygen is utilized as an electron acceptor. However, in the absence of oxygen, other inorganic or organic compounds can be used by bacteria as alternative terminal electron acceptors, including nitrate, nitrite, sulphur, sulphate, carbonate, ferric ion, fumarate ion and trimethylamine N-oxide.

Oxygen respiration in *Neisseria* species relies on the sole terminal oxygen reductase (cytochrome *cbb₃* oxidase), which is essential for viability in *Neisseria* species. Cytochrome *cbb₃* oxidase in other species of bacteria is typically associated with microaerobic conditions and has a high oxygen affinity (Pitcher and Watmough 2004), which could be a potential target for development of therapies. Under oxygen limiting conditions, *N. meningitidis* can use nitrogen compounds as electron acceptors to support growth and expressed nitrite and nitric reductase enabling *Neisseria* to catalyze a truncated denitrification pathway (Rock et al. 2005; Anjum et al. 2002).

Electrons flow to oxygen is able to generate more protons translocation along electron transport chain, which produces more ATP, than that of flow to nitrite. In electrochemically aspect, the positive redox potential of oxygen reduction O_2/H_2O (+820 mV) is higher than that of nitrite reduction NO_2^-/NO (+348 mV). So in *Neisseria* species, oxygen is more favorable source of terminal electron acceptor than nitrite.

1.4 Denitrification during oxygen limiting respiration in *Neisseria* species:

Denitrification is one type of respiration, which uses nitrogen species as the terminal electron acceptors, as an alternative to oxygen. The reduction of nitrate to nitrogen is the complete process of the denitrification pathway. Normally, the denitrification pathway is only activated under oxygen limiting conditions (oxygen is the preferred electron acceptor), and is inhibited when denitrifying bacteria are cultured in aerobic conditions. The denitrification process is the process of reduction of nitrate to dinitrogen gas, and involves four distinct enzymes, including nitrate reductase, nitrite reductase, nitric oxide reductase, and nitrous oxide reductase (Figure 1.1).

On occasions, aerobic denitrification is found in *Thiospharea pantorropa* and *Alcaligenes faecalis* (Bell et al. 1990; Van Niel et al. 1992). *Paracoccus* species is a good model for study complete denitrification in bacteria (Bell et al. 1990). However, some other bacteria can only perform some of the steps of denitrification.

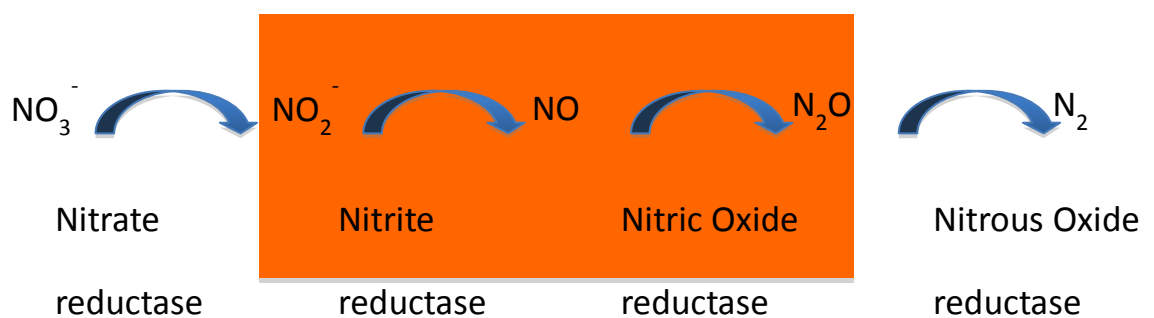


Figure 1.1: Proposed complete denitrification pathway in bacteria. Orange squared pathway is partial denitrification in *Neisseria* species.

Under oxygen limiting conditions, *N. meningitidis* catalyzes a truncated denitrification and use nitrite and nitric oxide as electron acceptor, which they use to supplement growth (Rock et al. 2005). This is highlighted in the orange square (Figure 1.1). The denitrification system is present also as a detoxification system for protecting bacteria from nitrosative stress *via* inducible nitric oxide synthase from the host cells. The activation of detoxification of NO has also been shown to enhance the survival of *N. meningitidis* in human macrophages and in nasopharyngeal mucosa (Stevanin et al. 2005).

1.5 Electron transport chain in *Neisseria* species:

Like typical Gram negative bacteria, *Neisseria* species possess an envelope consisting of two lipid bilayers. It is found that redox cofactor containing respiratory proteins embedded in the inner membrane and periplasm function as electron carriers or redox enzymes. One unusual aspect of the arrangement in *N. meningitidis* is that some of the existing redox active proteins (AniA, Laz, cytochrome c peroxidase (CCP)) were predicted to be tethered to the outer membrane.

There are three different respiratory substrates in the *Neisseria* species, including nitrite, nitric oxide, and oxygen. In *N. meningitidis*, most of the electrons transfer is towards to oxygen under aerobic conditions. Cytochrome *cbb₃* oxidase (the only oxygen terminal reductase in the *Neisseria* species) is the favored terminal reductase. However, nitrite and nitric oxide are favored electron terminal acceptors under microaerobic conditions. This process consists of reduction of nitrite to nitric oxide via nitrite reductase AniA and reduction of nitric oxide to nitrous oxide via nitric oxide reductase NorB (Anjum et al, 2002).

The major electron source is from cytoplasm, including succinate, pyruvate, malate,

NADH, and lactate. Reduction of ubiquinone by each of these substrates is done by its specific catalytic enzymes in the cytoplasmic membrane. Ubiquinone (Q) is the sole quinone in *N. meningitidis*, as *N. meningitidis* genome lacks a mannaquinone synthetic pathway. Q is reduced by inner membrane component NADH dehydrogenase (NADH DH). Ubiquinol is then oxidized by cytochrome *bc₁* complex in the ubiquinol pool, and can be oxidized directly by NorB. Based on genetic analysis and a cytochrome *bc₁* complex specific inhibitor study, NorB receives electrons directly from quinol directly, but not via c-type cytochrome or lipid modified azurin (Laz) (Deeudom et al. 2006).

There are three predicted electron carrying low spin cytochromes (*c_x*, *c₄* and *c₅*) and a lipid modified azurin (Laz) in *Neisseria* which might function as electron carriers between *bc₁* cytochrome and terminal reductase, including nitrite reductase AniA, and *cbb₃* oxidase. Based on previous published data, the involvement of the Laz protein in *Neisseria* respiratory metabolism is still not clear. Cytochrome *bc₁* complex specific inhibitor (myxothiazol) study has shown the electron flow to nitrite reductase AniA, and oxygen reductase *cbb₃*, but not NO reductase NorB, via *bc₁* complex (Deeudom et al. 2006). Cytochrome *c_x* and *c₄* mutagenesis study showed mutants in *c_x*, *c₄*, and *c_x* & *c₄* have a decreased capacity to reduce oxygen under aerobic conditions (Deeudom et al. 2008). It also indicates there may be alternative routes for oxygen reduction in *N. meningitidis*. In addition, cytochrome *c₅* mutagenesis study showed mutants in *c₅* failed to reduce nitrite under the denitrifying conditions. It suggests that cytochrome *c₅* provides the sole electron transferring pathway to nitrite reductase AniA in *N. meningitidis*. It is possible that these electron donors have an overlapping function and even the same function under different external conditions in *N. meningitidis*

(Figure 1.2).

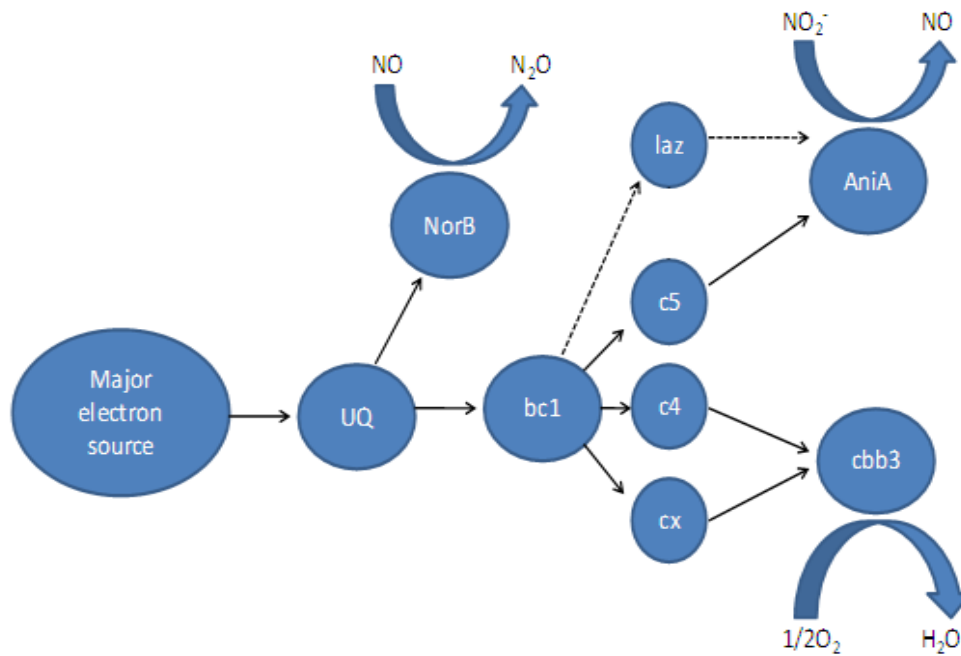


Figure 1.2: Proposed electron transport chains in *N. meningitidis*. The dotted line represents the predicted involvement of Laz in electron pathways (Deeudom et al. 2006 & 2008).

1.6 Terminal redox reductases:

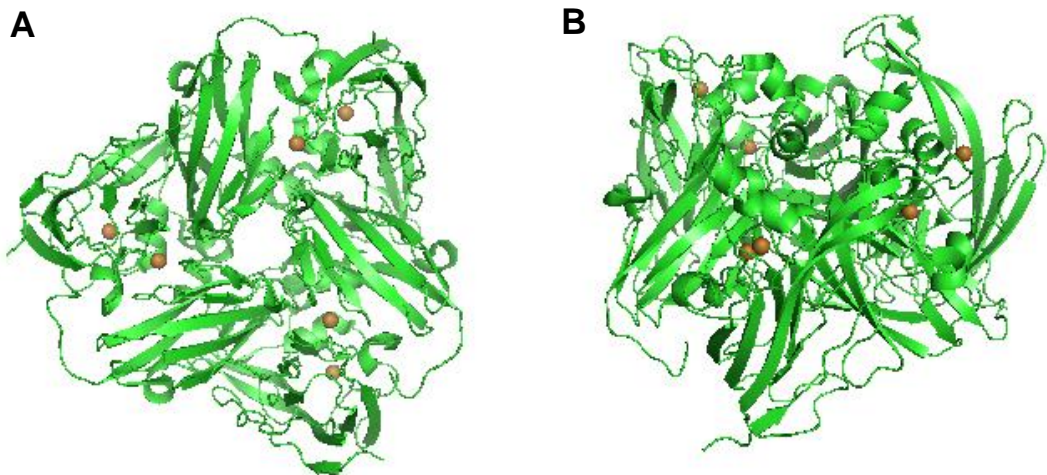
1.6.1 Nitrite reductase AniA

Neisseria species can denitrify nitrite dependent on aniA (anaerobically induced protein A) expression (originally named Pan1). AniA is encoded by NMB1623, which is the only gene predicted to encode a nitrite reductase in *N. meningitidis*. The published molecular structure of AniA indicates that it is a trimer composed of three identical monomers (Boulanger and Murphy, 2002). Each monomer of AniA consists of one atom of type I copper and one atom of type II copper, and that the ligands to the type I and type II copper atoms are the same as those of NirK from other bacteria (Figure 1.3). AniA is predicted to be tethered to the outer membrane with a linker region at the N-terminus, which is unique from other NirKs (Figure 1.4). Type I copper ligands are associated with His 143, His 94, Cys135, and Met 148 (Figure 1.3). The type I copper site of AniA gives the protein a distinctive blue color and shows the visible characteristic spectrum peaks at 458nm and 585nm (Boulanger and Murphy, 2002). Type II copper ligands are associated with His99, His134, His289, and a water molecule (Figure 1.3). The globular domain of the copper type I site of AniA is predicted to be able to accept electrons from either soluble small c-type cytochromes or cupredoxin Laz and transfer electrons to the type II copper (catalytic center for nitrite reduction), which is located in a deeper groove of the enzyme. Type II copper is finally reduced. Then an electron is passed to nitrite leading to reduction of nitrite to nitric oxide, according to the following equation, $\text{NO}_2^- + 2\text{H}^+ + \text{e}^- \rightarrow \text{NO} +$

H₂O (Kukimoto et al, 1994) .

The localization of AniA was firstly described as an outer membrane associated protein in *N. gonorrhoeae* based on selective solubilization of the cytoplasmic membrane using detergent dodecyl sarcosinate (Clark 1987). AniA was also predicted as an outer membrane associated protein in other *Neisseria* species including *N. meningitidis* and other commensal *Neisseria* species, based on the same differential detergent solubilization (Hoehn and Clark 1990). As the location of AniA was only determined biochemically by using differential detergent solubilization method, the investigation of localization of AniA in *Neisseria* species by isolating intact membranes and separating inner membrane and outer membrane protein could be addressed in our research.

Nitrite reductase AniA catalyzes the reduction of nitrite oxide to nitric oxide in *Neisseria meningitidis*, and has an important role in microaerobic respiration and growth under the denitrifying conditions.



C

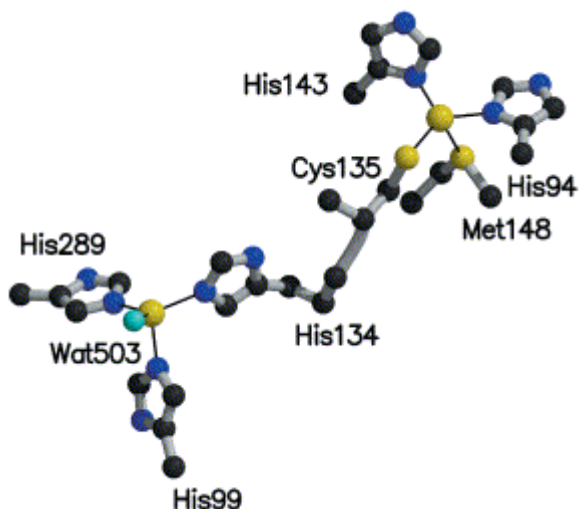


Figure 1.3: Proposed structure of soluble AniA: A&B. One trimer of AniA with each monomer containing two copper ions. A. Top view of AniA; B. Side view of AniA. C. Type I and Type II copper sites located in one AniA monomer. The copper binding sites are shown in balls and sticks showing the covalent linkage. Copper I ligands are two histidines (His143, His94), one cysteine (Cys135) and one methionine (Met 148). Copper II ligands are three histidines (His99, His134, His289) and one water molecule (blue ball). Nitrite binds to Copper II by replacing the water molecule (Based on Manu Deedom's PhD thesis and Boulanger and Murphy, 2002)

Figure 1.4: Amino acid alignment of AniA and other copper containing nitrite reductase. Sequence codes as follow: AxNIR, *Achromobacter xylosoxidans* (NZ_GL982453.1); RsNIR, *Rhodobacter sphaeroides* (AAB05767.1) HmNIR, *Haloarcula marismortui* (CAB93142.1); AniA: *Neisseria meningitidis* MC58 (NC_003112.2). Type I and Type II copper atoms ligands are highlighted in green and pink color, respectively. The yellow highlighted is predicted putative flexible linker regions/LCR of AniA. The regions shown begin after the predicted type II signal peptidase cleavage sites (LAAC, red in color), and leaves cysteine residue at the N-terminus, and end at the beginning of predicted globular domain of AniA in *N. meningitidis*. Amino acids alanine(A), glutamate (E), proline (P), serine (S) and theronine(T) are in bold and are predicted to be involved in forming the linker region.

1.6.2 Cytochrome *cbb*₃ oxidase

*cbb*₃ belongs to the haem-copper oxidase (HCO) superfamily and is well described in proteobacteria (Pitcher and Watmough 2004). Cytochrome *cbb*₃ type oxidase has a K_M for dioxygen of 7nM, significantly higher affinity than other members of HCO superfamily (K_M of cytochrome *bo*₃ is 0.15 - 0.35 μ M; K_M of mitochondrial cytochrome *aa*₃ is 0.1-1 μ M) (Pitcher and Watmough 2004).

Cytochrome *cbb*₃ oxidase catalyzes the reduction of dioxygen to water and translocates protons across the cytoplasmic membrane to periplasm, and terminates the oxygen electron transport chain. It has similar function as mitochondria cytochrome c oxidase. *cbb*₃ oxidase contains c-type cytochrome domain in place of Cu_A domain of other HCOs. *cbb*₃ oxidase utilized soluble c-type cytochromes as electron donors, but not quinol. It catalyzes the following reaction: $\text{Cyc.}_{\text{Red}} + 1/2 \text{O}_2 + 2\text{H}^+ \rightarrow \text{Cyc.}_{\text{ox}} + \text{H}_2\text{O}$. There are four subunits that assemble *cbb*₃ oxidase in *P. stutzeri* (well established in literatures), as *ccoNOQP*. CcoN is a dihaem b-type cytochrome, containing two b-type hemes (*b*₃ and *b*) and one copper ion (Cu_B). CcoO is the mono haem c-type cytochrome. The redox center of *cbb*₃ is located at CcoO subunit that accepting electrons from c-type cytochromes. CcoO subunit transfers electrons to catalytic center CcoN. CcoN has high reduction potential among subunits in *cbb*₃ oxidase (Midpoint redox potential CcoN>CcoO=CcoP) (Pitcher and Watmough 2004). CcoO and CcoP have similar reduction potential. CcoN and CcoO are necessary for assembly of the multimeric oxidase and independently of CcoP

subunit involvement (Zufferey et al. 1996). CcoQ is the small membrane bound protein. It isn't essential for complex formation (Zufferey et al. 1996) and absent from *P. stutzeri* *cbb₃* oxidase. The function of CcoP subunit in *cbb₃* oxidase is not fully understood. It contained redox activity, might provide an alternative electron pathway to the core enzyme. However, as CcoO-CcoN subcomplex is catalytically active in oxygen reduction in *B. japonicum* and *P. denitrificans*, it indicates CcoP is not essential for *cbb₃* oxidase catalytic activity (Zufferey et al. 1996).

Cytochrome *cbb₃* oxidase is the only respiratory oxidase in the *Neisseria* species. *N. meningitidis* cytochrome *cbb₃* oxidase subunits are encoded by four genes of the operon *fixNOQP*. NMB1725, NMB1724, and NMB1723 are predicted to encode gene *fixN*, *fixO*, and *fixP*, respectively.

FixQ does not have a locus number yet, but appears to be present downstream of *fixO* (Figure 1.5). In *Neisseria*, cytochrome *cbb₃* oxidase appears to get electrons from c-type cytochromes rather than quinol. The organization of operon and proposed structural complex is shown in Figure 1.5. *cbb₃* oxidase consists the core enzyme CcoN and two c-type cytochrome containing subunits CcoO and CcoP. CcoQ does not have a redox cofactor. CcoO and CcoP in *N. meningitidis* are monohaem and dihaem proteins. Comparative analysis of the subunits of *cbb₃* oxidase of *N. meningitidis* with *N. gonorrhoeae* reveals unexpected differences. The dihaem CcoP is present in more than 50 *N. meningitidis* strains, in contrast, trihaem version CcoP is present in more than 50 sequences from other *Neisseria* species. The loss of the extra haem domain might reveal a species level adaption (Aspholm 2010).

BLAST searches have shown that the second haem domain of cytochrome *c₅* (predicted electron donor to AniA) shares more than 74% with the third haem domain of subunit III *CcoP* of the cytochrome *cbb₃* oxidase of *N. gonorrhoeae* (Deeudom et al., 2008). A single nucleotide polymorphism results in *CcoP* truncation acts as a species adaptation of *N. meningitidis*.

It was also shown that introducing *c₅* insertion mutation into *N. meningitidis* MC58 strain carrying alleles encoding *N. gonorrhoeae* trihaem *CcoP* is still capable of reducing nitrite under the denitrifying conditions and showing remarkable similar growth rate to the wildtype strain (Aspholm 2010). The trihaem *ccoP* allele was epistatic to *c₅* suggesting that trihaem *CcoP* and *c₅* are overlapping functionally in supporting AniA-dependent nitrite reduction in *N. gonorrhoeae* (Aspholm 2010).

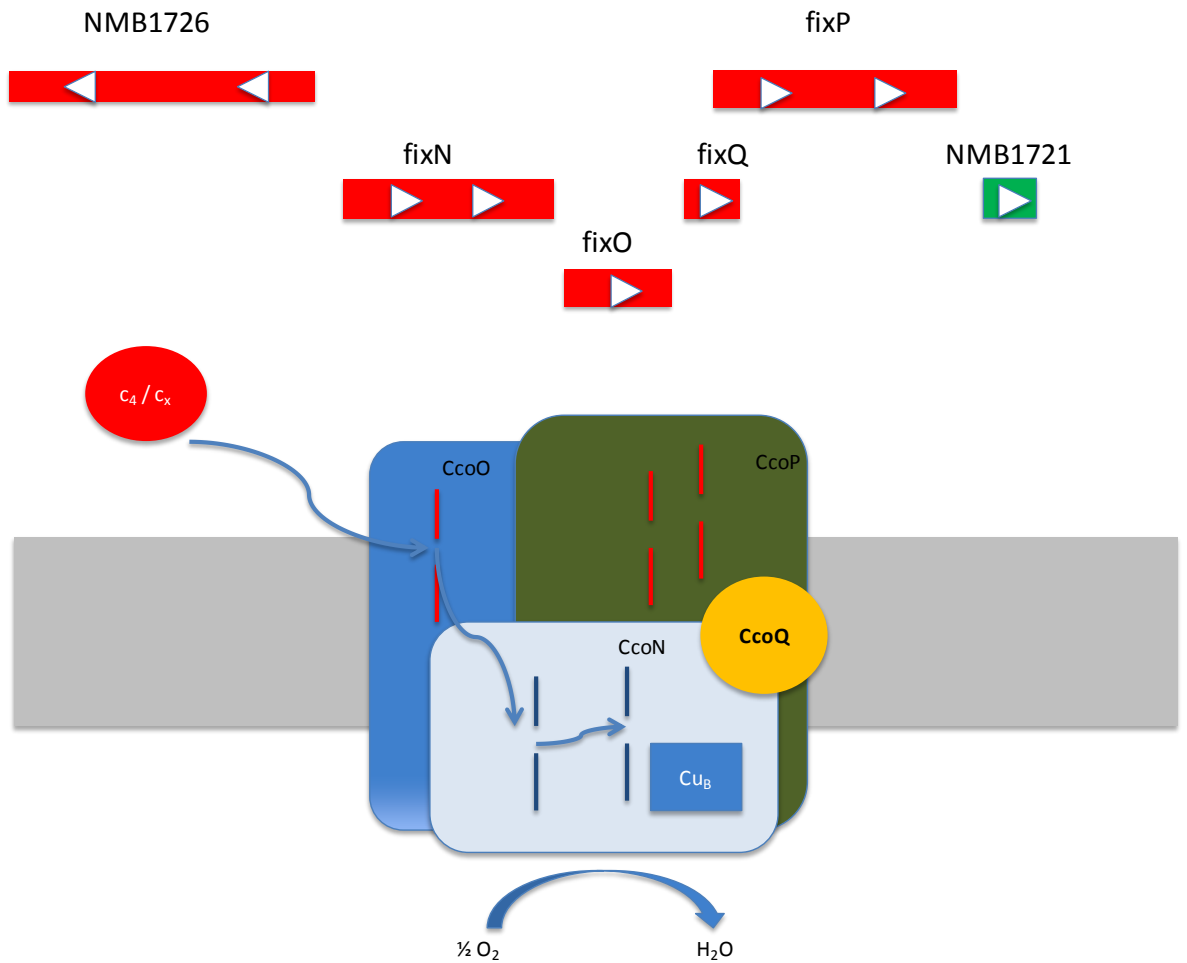
The extension of *CcoP* might also transfer electrons across the periplasm from the cytochrome *bc₁* complex in the cytoplasmic membrane to AniA in the outer membrane (Hopper 2009). In the trihaem *CcoP*, there is an AlaSerPro-rich low complexity region (LCR) that separates the second and third haem domains and also includes the O-linked glycan occupancy sites. Cytochrome *c₅* also possesses an AlaSerPro-rich LCR that also contained O-linked glycan attachments sites between the two haem domains. Like the active trimer form of AniA is predicted to tether to outer membrane by three distinct linker regions, cytochrome *cbb₃* oxidase is predicted to be integrated into the inner membrane in order to fulfill the role in proton pumping for ATP

synthesis (Aspholm 2010). Encompassing both the AlaSerPro-rich LCR and the haem containing domains of *c₅* and trihaem CcoP might be important for functioning to bridge a potential periplasmic gap for inter-protein electron transfer in nitrite reduction in the *Neisseria* species.

If tri-haem CcoP is able to donate electrons to AniA directly in *N. gonorrhoeae*, it will broaden our knowledge that a terminal oxidase acts as an electron carrier to a different terminal reductase. The extra haem c containing domains are quite common on oxidases. In the extremely thermophilic bacterium *Thermus thermophilus*, cytochrome *caa₃* variant of *aa₃* has been thought to allow the oxidase to interact with *bc₁* complex directly (Janzon et al. 2007).

The high affinity to oxygen of cytochrome *cbb₃* oxidase might suggest that the *Neisseria* species have an adaptation to live in oxygen limiting conditions in the human host and also has a important role in successful colonization of the nasopharynx and oropharynx.

A.



B.

ttgcgtaaagtaggtactccttacagtgatgaggaaattgcgaaagcacctgaggctttgg
 caaacaatccgagctggatgctgtagtcgcctatctgcaaggattgggtctggctttga

aaaacgtaaggtaacatc**atggatattaacggatttcgtgctctcttcacggtatggatc**
 M D I N G I R A L F T V W I

ttatctgtttcctggttggactctatatcgtcttcaacaggcgaataagaaaaactac
 F I C F L L V L Y I V F N R R N K K N Y

gataatgccgcaaacagcatttttgatgaaaaccaagatgcgcaagataagaaaagcgaa
 D N A A N S I F D E N Q D A Q D K K S E

aaccgttaatattgtgataacggagcaaaacaatgaacacaacatcccaatttaccagta
 N R -

atctctggaatatatatattgcagttattgtcttactgagctttatcgctttggcttggc
 tgctgctgtctcaaatggtgtcaaacgtccgaagaaggcggaagaagtacaaactacgg
 gtcatgagtgggacggcatt

Figure 1.5: Proposed organization of *fixNOQP* operon in *N. meningitidis*. A. The *fixNOQP* operon of *N. meningitidis* encodes the four structural proteins that comprise the cytochrome *cbb*₃ oxidase complex. CcoO and CcoN subunits are the core enzyme of *cbb*₃ oxidase. The redox centre CcoO is predicted to receive electrons from c-type cytochromes (*c*_x or *c*₄) and transfer to catalytic centre CcoN. The function of *N. meningitidis* of CcoP is still unclear. Copper ion (Cu_B) and haem b are blue in color. Haem c is red in color. B. *ccoQ* gene does not have a locus number yet, but appears to be present downstream of *ccoO* gene. It is a small membrane bound protein of 56 amino acids.

1.6.3 Nitric oxide reductase NorB:

Nitric oxide reductase (NOR) is an integral membrane protein that catalyzes the reduction of nitric oxide (NO) to nitrous oxide (N₂O), according to the following equation:



NOR is often involved in denitrification pathways of microorganisms. There are three types of NOR identified, including cNOR (cytochrome *bc*₁ complex that receive electrons from c-type cytochromes or azurin), qNOR (cytochrome b type complex lacking cytochrome c component that receive electrons from quinol), and qCu_ANOR (qNOR containing a CuA at electron entry site). *Meningococcus* NorB is predicted to be encoded by NMB 1622, a b-type cytochrome of the qNOR type. It is highly conserved with gonococcal NorB.

As NorB is qNOR type nitric oxide reductase, the enzyme is expected to accept electrons from quinol pool directly. NorB appears to have multiple transmembrane domains indicating that it is integral to the cytoplasmic membrane. Based on genetic analysis and cytochrome *bc*₁ complex specific inhibitor study (myxothiazol), NorB appears to receive electrons from quinol directly but not via cytochrome downstream of the *bc*₁ complex (Deeudom et al. 2006). NorB is found to be required for denitrifying growth. It was found *N. meningitidis* norB mutant strain is unable to grow in the presence of nitrite under microaerobic conditions. NorB has been shown to protect *N. meningitidis* against exogenous added NO and NO-related compounds

(Anjum et al. 2002).

1.7 Regulation of nitrite reduction in *Neisseria* species.

Denitrification in *N. meningitidis* is involved with anaerobic respiration, an organism which utilizes three respiratory substrates including oxygen, nitrite and nitric oxide. The regulation of gene expression to respond to environmental changes during aerobic and anaerobic transition is important for the *Neisseria* species to maintain bacterial growth. Multiple sensors and regulators act simultaneously to support the growth and keep the toxic intermediates under acceptable level, and to sense the concentration of each respiratory substrate in the environment.

In *N. meningitidis*, *ainA* gene is tightly regulated by four regulators, including FNR(fumarate and nitrite reductase), NarP, FUR(ferric uptake regulator), and NsrR. Both of *aniA* and *norB* gene promoters exist in the same region, as they are divergently transcribed. The expression of *aniA* gene is induced by FNR, and also requires the binding of FNR to its promoter (Fnr boxes are upstream of *aniA* and *norB* promoter region) in *N. meningitidis* (Rock et al. 2005). Under denitrifying conditions, FUR is also required for induction of *aniA* promoter (Edwards et al. 2012). FUR/NarP bind independently to adjacent sites on the *aniA* promoter (Edwards et al. 2012). In addition, the activation via FUR/NarP is dependent on the topological arrangement relative to the RNA polymerase binding site (Edwards et al. 2012). FUR and NarP are not the repressor of NsrR, as FUR and NarP are required for *aniA* expression in *nsrR*-deficient *N. meningitidis* under denitrifying conditions.

Species-specific SNP (between *N. meningitidis* and *N. gonorrhoeae*) in *aniA* promoter region are predicted to be important for altered regulator binding to DNA and also promoter activation by activator NarP and FNR. *N. gonorrhoeae* *aniA* promoter binds to NarP tighter than does the equivalent region in *N. meningitidis* (Edwards et al. 2012). However, *N. gonorrhoeae* *aniA* promoter binds to FNR more weakly than does the equivalent region in *N. meningitidis* (Edwards et al. 2012). Variations in *aniA* promoter regions in two pathogenic species *N. meningitidis* and *N. gonorrhoeae* appear to have been selected to benefit these two *Neisseria* species to tune differently their responses to environmental changes during aerobic and anaerobic transition (Edwards et al. 2012).

1.8 Major electron carriers:

In *N. meningitidis*, cytochrome *bc₁* complex is predicted to be oxidized by c-type cytochromes or azurin in periplasm. The function of soluble c-type cytochromes is usually to receive electrons from the quinone-cytochrome b system and transfer them to the terminal reductase, including cytochrome oxidase and nitrite reductase. They act as electron carriers that carry electrons towards terminal reductase in proteobacteria in the periplasm. These soluble c-type cytochromes are often involved in aerobic respiration and nitrite reduction. They act as electron mediators transferring electrons from cytochrome *bc₁* complex to terminal reductase. It is similar to the way that cytochrome c donates electrons from *bc₁* complex to cytochrome c oxidase in mitochondria. In *Paracoccus denitrificans*, cytochrome *c₅₅₀* is structurally similar to cytochrome *c₂* in photosynthetic bacteria, able to receive electrons from cytochrome *bc₁* complex and donate electrons to terminal reductase *aa₃* oxidase, *cbb₃* oxidase and also *cd₁* nitrite reductase (Pearson et al. 2003 and Otten et al, 2001). Membrane associated cytochrome *c₅₅₂* functions only in electron transfer from *bc₁* complex to terminal reductase *aa₃* oxidase (Pearson et al. 2003).

Haem c is covalently attached to the protein via thioether bridges between C2-C3 positions and involving sulfhydryl groups of cysteinyl residues in the protein. The conserved haem-binding site is C-XX-CH and histidine provides an axial ligand to the haem iron) (Jones and Poole 1985). Depending on the localization of haem group attached to the protein, c-type cytochromes can be classified into three groups: I.

single haem attached to the site close to the N-terminal of protein (cytochrome *c*, *c*₂, *c*₅₅₁, *c*₅₅₅, and *c*₄); II. haem attached to the site close to the C-terminal of the protein (cytochrome *c*') and III. Multi-haems associated in protein (*c*₃) (Jones and Poole 1985).

Depending on the redox potentials, two major c-type cytochromes identified in the respiratory chain of many species of bacteria. High redox potential cytochrome *c* receives electrons from specialized primary dehydrogenases or cytochrome *c* directly in Gram-negative methylotrophic, sulphur- ammonia oxidizing bacteria (Jones and Poole 1985). The other type of cytochrome *c* transfers electrons from quinone-cytochrome *b* systems to terminal reductase without involvement of a proton motive quinone cycle (Jones and Poole 1985).

Depending on haem-iron coordination which makes cytochrome different electron spin, cytochromes are classified into low spin haem and high spin haem. If hexacoordination with two axial iron ligands which are His-Fe-His or His-Fe-Met, this haem is usually low spin (Ambler 1991). High spin haems are typical pentacoordination with a His ligand and the other axial coordination site composed of being occupied by small molecules, e.g. O₂, NO (Ambler 1991).

There are three electron carrying low spin c-type cytochromes predicted to function as electron carriers electrons from cytochrome *bc*₁ complex to terminal reductase *cbb*₃ oxidase, and AniA in *N. meningitidis*.

Three predicted cytochromes *c*₃, *c*₄ and *c*₅ previously were identified as involved in the respiratory chains. It is possible that some of the cytochromes might have similar or

overlapping functions to the same terminal reductase. The differences in their biophysical or biochemical properties might provide bacterial advantages to function most effectively under different environmental conditions such as pH, ionic strength, and redox state.

1.8.1 Cytochrome c_5

NMB1677 is predicted to encode a membrane associated di-haem cytochrome with molecular mass of 30 kDa. Cytochrome c_5 is highly conserved among *Neisseria* species. The amino acid residues 1-12 of cytochrome c_5 are predicted to be exposed in the cytoplasm while the residues 13-32 are predicted to be localized in the cytoplasmic membrane. The two haem-containing soluble domains (residues 33-279) are predicted to be exposed in the periplasm (Figure 1.6).

```
MKQLRDNKAQGSALFTLVSGIVIVIAVLYFLIKLAGSGSFGDVDATEAATQTRIQ
PVGQLTMGDGIPVGERQGEQIFGKICIQCHAADSNVNPAPKLEHNGDWAPRIA
QGFDTLFQHALNGFNAMPAKGGAADLTDQELKRAITYMANKSGGSFPNPDEA
APADNAASGTASAPADSAAPAEAKAEDKGAAAPAVGVDGKKVFEATCQVCHG
GSIPGIPGIGKKDDWAPRIKKGKETHLKHLEGFNAMPAKGGNAGLSDDDEVKA
AVDYMANQSGAK
```

Figure 1.6: Primary structure of cytochrome c_5 . The Amino acid residues predicted to be exposed in cytoplasm were highlighted in green color. The amino acid residues predicted to be localized in cytoplasmic membrane were

highlighted in pink color. Two haem binding domains were highlighted in blue color.

Introduction of a *c₅* mutant into *N. meningitidis* MC58 leads to a clear defect in AniA-dependent nitrite reduction under microaerobic condition, and this growth defect is associated with an inability to reduce nitrite (Deeudom et al. 2008). It suggests *c₅* is crucial for reduction of nitrite to nitric oxide and also has a significant role in donating electrons to the sole nitrite reductase AniA in *N. meningitidis*. Cytochrome *c₅* is the sole electron mediator between cytochrome *bc₁* complex and AniA in *N. meningitidis*. *c₅* is predicted as inner membrane associated protein. However, AniA is predicted as outer membrane associated protein. It is interesting to understand the mechanism by which inner membrane *c₅* gets electrons access to outer membrane AniA across periplasm. The existence of this pathway suggests there is a novel mechanism for inter-membrane electron transfer in *Neisseria* species.

In *N. gonorrhoeae*, a *c₅* mutant strain increases sensitivity to growth inhibition and also reduces nitrite at approx. 65% of the rate of wild type strain (Aspholm 2010). It is clear that *c₅* is an important electron carrier in nitrite reduction in *N. gonorrhoeae*, but it is also suggested that there is an alternative electron donor to nitrite reductase in this closely related species. However, in *N. gonorrhoeae*, either cytochrome *c₄* or cytochrome *c₅* is also determined to be involved in oxygen reduction and is crucial for gonococcal survival (Li et al. 2010). There are two haem binding domains with cytochrome *c₅*, which might suggest that two mono-haem domains are involved in different functions in respiration. The function of cytochrome *c₅* involved in

denitrification in *Neisseria* species is highlighted in our study.

1.8.2 Cytochrome c_4

NMB1805 is predicted to encode for periplasmic dihaem cytochrome c_4 (similar to c_4 from *Pseudomonas stutzeri*) with a molecular mass of 21.5 kDa.

Cytochrome c_4 is determined to be an important electron donor to terminal cytochrome cbb_3 complex in *N. meningitidis* (Deeudom et al. 2008). In *Vibrro cholera*, the natural mobile electron donor c_4 is the sole electron carrier between cytochrome bc_1 complex and cbb_3 oxidase (Chang et al. 2010). Cytochrome c_4 is common in β - , and γ - proteobacteria and sporadically distributed within the α -proteobacterial clade and a few other bacterial phyla (Chang et al. 2010). In β - , and γ - proteobacteria including cbb_3 oxidase as the sole oxygen reductase in the respiratory chain (e.g. *N. meningitidis* and *P. stutzeri*), it is shown that there is a strong correlation between cytochrome c_4 and cytochrome cbb_3 type oxygen reductase in aerobic respiration (Chang et al. 2010). It suggests cytochrome c_4 is the natural electron donor to cbb_3 oxidase.

1.8.3 Cytochrome c_x

Cytochrome c_x homologs are functioning as electron carriers between bc_1 complex and cytochrome c oxidase in aerobic respiratory chain. In *Paracoccus denitrificans*, a membrane bounded c-type cytochrome c_{552} is determined to be the electron carrier between cytochrome bc_1 and cytochrome aa_3 oxidase in the respiratory chain and also becomes an integral part of $c_{552}:aa_3$ supercomplex (Lipowski et al. 2006; Reincke et al. 1999). NMB0717 is predicted to encode for periplasmic monohaem cytochrome c_x (or c_2) with a molecular mass of 12.5kDa in *N. meningitidis*. Cytochrome c_x is determined to be a significant electron donor to terminal cytochrome oxidase cbb_3 complex in *N. meningitidis* (Deeudom et al. 2008). *Gonococcus* cytochrome c_x is orthologous to cytochrome c_x in *N. meningitidis*. However, in *N. gonorrhoeae*, cytochrome c_x was determined to not be involved in oxygen reduction (Li et al. 2010). Neither of cytochrome c_4 and c_x are required for nitrite reduction in *N. meningitidis* (Deeudom et al. 2008).

1.8.4 Lipid-modified azurin (Laz)

Laz is predicted to be encoded by NMB1533 and has a globular azurin domain similar to azurin. It is a predicted membrane protein.

It is also found that pseudoazurin is an efficient electron donor, which can rapidly donate electrons to blue and green type copper type nitrite reductase under denitrifying conditions (Murphy et al. 2002). Pseudoazurin is confirmed to donate electrons to copper type nitrite reductase at a physiological relative rate constant in *Achromobacter cycloclastes*. In *Alcaligenes xylosoxidans*, pseudoazurin is identified as a high affinity electron donor to copper type nitrite reductase (Kataoka et al. 2004). In *Paracoccus denitrificans*, pseudoazurin and cytochrome *c₅₅₀* (analogous to cytochrome *c₂*) function as electron donors from membrane-bound cytochrome *bc₁* complex to periplasmic cytochrome *cd₁* nitrite reductase (Pearson et al. 2003). In the thermophilic green gliding photosynthetic bacterium *Cloroflexus auerantiacus* cytochrome *bc₁* complex is predicted to use a class of small protein auracyanin A (related to pseudoazurin) as an electron acceptor (Van Driessche et al. 1999). It is also known that pseudoazurin like protein (plastocyanin) is functioning as an electron carrier between cytochrome bf complex and photosystem I in *Cyanobacteria* and *Arabidopsis* (De la Cerda et al. 2002; Gupta et al. 2002).

However, instead of being an electron carrier between *bc₁* complex and terminal reductase in nitrite reduction, azurin is involved in responding to redox stress related to changes in growth conditions in *P. aeruginosa* (Vijgenboom et al, 1997).

Gene NMB 1533 is predicted to encode lipid modified azurin in *N. meningitidis*, a blue copper protein in the cupredoxin family. Laz was predicted to have three domains including the lipoprotein signal peptide, the flexible linker peptide, and the globular azurin domain. The N-terminal linker region (predicted to attach to outer membrane and allow the globular azurin to move in periplasm) contains AAEAP repeat and may form an unstructured elongated region that will allow the core domain to get electrons from cytochrome *bc₁* complex and transfer them to terminal reductase in *Neisseria* species (Figure 1.7).

It is likely that Laz is involved in the activity of terminal reductase *cbb₃* or AniA, as in the presence of meningococcal membrane extract; Laz can be oxidized by either oxygen or nitrite (Dr. Manu Deedom, PhD thesis, unpublished data). In addition, mutant strains deficient in Laz have a limited effect on nitrite reduction indicating that Laz is the less important electron carrier between cytochrome *bc₁* complex and AniA (Deedom, PhD thesis, unpublished data).

Although the function of Laz is still unknown, Laz was also predicted to function as an electron carriers or electron buffer between *c₅* and AniA to build a multi-branched respiratory chain, or function as an azurin like electron carrier between cytochrome *bc₁* complex and terminal reductase (Figure 1.7). Details of Laz function involving electron transport, respiration and growth, is going to be discussed in the results section.

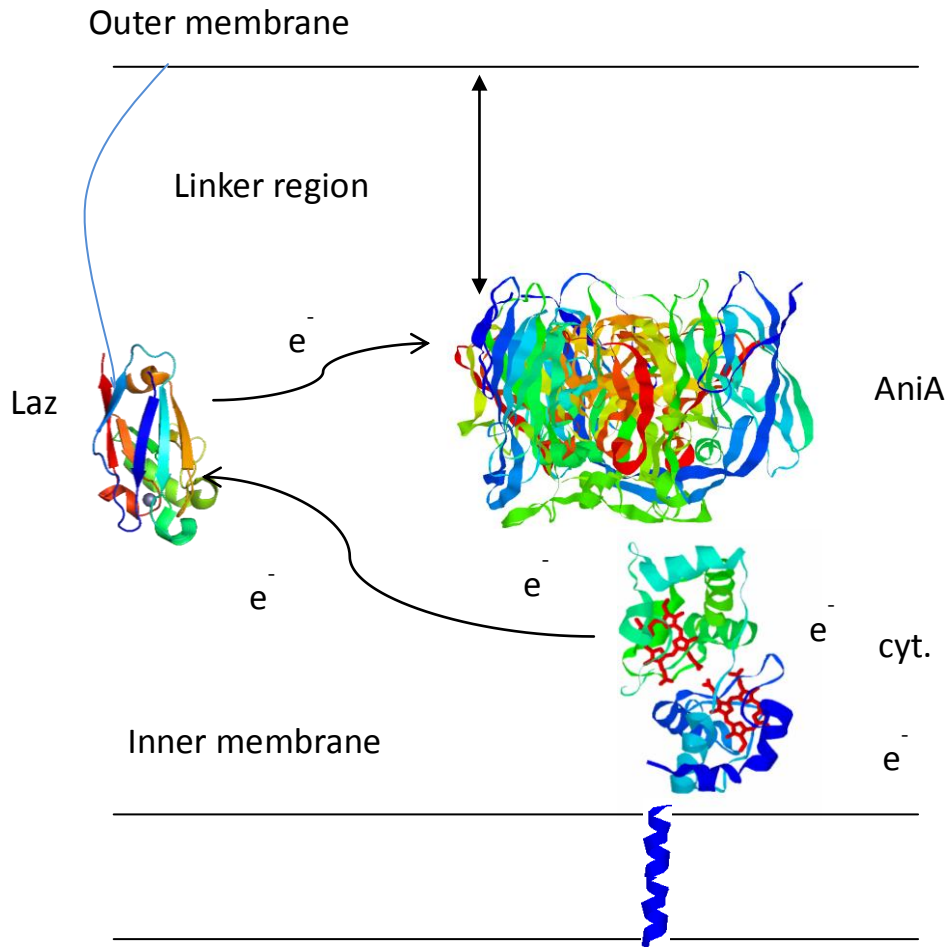


Figure 1.7: Predicted function of Laz in *Neisseria* respiratory metabolism. (I) Laz itself is able to donate electrons to AnIA directly. (II) Laz function as an electron buff is able to receive electrons from cytochrome c_5 and donate electrons to AnIA.

1.9 Potential electron carriers in other *Neisseria* species?

Are there any other potential electron carriers involved in respiration in *Neisseria* species? BLAST search shows a gene from *N. elongata* subsp. *glycolytica* ATCC 29315 has degree of similarity (more than 70%) with second haem domain of cytochrome *c*₅. This *N. elongata* cytochrome (NEIELOOT_00905) might be a potential electron carrier between *bc*₁ complex and AniA. If this prediction is true, *N. elongata* cytochrome is the natural electron carrier to AniA. If any c-type cytochrome shares a high degree of similarity with cytochrome *c*₅, it is possible to presume this cytochrome protein is functioning as an electron carrier in the respiratory chain. This extra electron transferring pathway to nitrite reductase AniA might benefit the *N. elongata* microaerobic growth under the denitrifying conditions and also pathogenesis of *N. elongata*. *N. elongata* was firstly described in 1970s and thought to be non-pathogenic. However, infective endocarditic and osteomyelitis caused by *N. elongata* is rare but important and often requires surgical intervention (Hsiao et al, 2008 and Haddow et al, 2003).

1.10 Inter-protein electron transfer for nitrite reduction in denitrification in *Neisseria* species

Under oxygen limited conditions, *aniA* gene is expressed and nitrite reduction proceeds. This nitrite reduction is performed by an efficient electron transfer reaction with a redox partner protein. However, the details of this mechanism during electron transfer are still unclear in *Neisseria* species. Redox partner proteins could be either c-type cytochrome or azurin, with copper containing nitrite reductase (CuNIR). In the case of *A. xylosoxidans* nitrite reduction, both azurin and *cyc* *c551* protein act as redox partners for nitrite reductase (A_xgNIR) *in vivo* (Nojiri et al. 2009 and Kataoka et al. 2004). It is possible that in *Neisseria* species there is more than one electron donor (including c-type cytochrome and azurin) donating electrons to the sole nitrite reductase AniA, to enable bacteria to survive in diverse conditions (Figure 1.8). There are three candidates predicted to be involved in nitrite reduction, including, cytochrome *c*₅, trihaem *N. gonorrhoeae* CcoP, and Laz.

Compared to oxygen respiration, nitrite reduction produces less biochemical energy. It is necessary to limit AniA activity under aerobic conditions for many reasons, including less production of ATP, production of NO inhibiting oxygen respiration, and the production of hydrogen peroxide causing oxidative damage. However, nitrite reduction is important for *N. meningitidis* to survive in the human host. Most of oxygen in the blood is bound to haemoglobin, only about 1.5% oxygen is freely dissolved in blood serum. As the low level of free dissolved oxygen in the blood, the survival of *N. meningitidis* in the blood is relied on anaerobic respiration (nitrite

reduction).

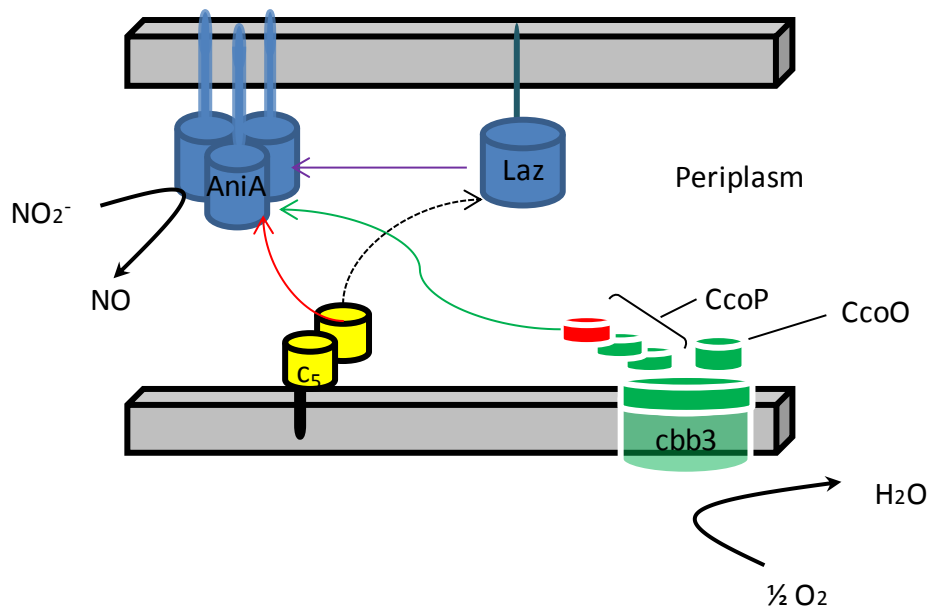


Figure 1.8: Predicted nitrite reduction network in *Neisseria* species: (I) Cytochrome c_5 donate electrons to nitrite reductase AnxA (Red line). (II) The 3rd haem domain of CcoP of *N. gonorrhoeae* cytochrome cbb_3 donates electrons to AnxA (Green line). (III) Laz donates electrons to AnxA (Purple line) or Laz receives electrons from cytochrome c_5 and then donate electrons to AnxA (Black dotted line).

1.11 Aims and objectives of this work:

The aims of this work are to determine the localization of redox proteins in *Neisseria* species. Ultimately, this work also aims to determine the nitrite reduction pathways in *Neisseria* species. The use of biochemistry and kinetics to study redox proteins involved in nitrite reduction and gain an insight of specificity of redox partners in the *Neisseria* species. One approach will involve heterologous expression of electron transferring redox proteins and identification of inter-protein electron transfer for nitrite reduction in denitrification by kinetics techniques in this project. In addition, another approach will involve the construction of bacterial strains defective in potential electron carrier proteins and characterization of mutants using various microbiological and biochemical techniques. This project will provide information about the organization of redox proteins in the *Neisseria* respiratory systems and also provide important information when considering the use of respiration as a potential target for developing novel anti-*Neisseria* therapies in the future.

Chapter 2

Method and Material

2.1 Bacterial strains and plasmids used in this work:

2.1.1 Bacterial strains used in this work :

Name	Description	Source
<i>Escherichia coli</i> DH5 α	General cloning strain carries F- ϕ 80dlacZ Δ M15 (lacZYA-argF) U169 <i>recA1 endA1 hsdR17</i> (r _k ⁻ , m _k ⁺) <i>phoA supE44 - thi-1 gyrA96 relA1</i>	Invitrogen
<i>Escherichia coli</i> BL21 (λ)DE3	Expression strain for cloning protein carries F ⁻ <i>ompT hsdS_B</i> (r _B ⁻ m _B ⁻) <i>gal dcm</i> (DE3)	Invitrogen
<i>N. meningitidis</i> MC58	Wild type	McGuinness <i>et al</i> , 1991
<i>N. meningitidis</i> MF64	<i>N. meningitidis</i> carrying an ectopic copy of <i>N. gonorrhoeae ccoP</i>	From Dr. J.M. Koomey
<i>N. lactamica</i> ST640	Wild type	(Bennett JS <i>et al</i> . 2010)
<i>N. elongata</i> subsp. <i>glycolytica</i> ATCC 29315	Wild type	From Dr. J.M. Koomey
<i>N. meningitidis</i> MC58 <i>c_x::spc^r</i>	Containing disrupted chromosomal copy of <i>c_x</i> gene	Deeudom <i>et al</i> . 2008
<i>N. meningitidis</i> MC58 <i>c₄::ery^r</i>	Containing disrupted chromosomal copy of <i>c₄</i> gene	Deeudom <i>et al</i> . 2008

<i>N. meningitidis</i> MF64 <i>c_x::spc^r</i>	Containing disrupted chromosomal copy of <i>c_x</i> gene in the wild type strain	In this work
<i>N. meningitidis</i> MF64 <i>c₄::ery^r</i>	Containing disrupted chromosomal copy of <i>c₄</i> gene in MF64 background	In this work
<i>N. meningitidis</i> MC58 <i>laZ::chl^r</i>	Containing disrupted chromosomal copy of <i>laZ</i> gene	Deeudom et al. 2008
<i>Escherichia coli</i> BL21 λDE3(pST2)- <i>c_x</i>	Containing plasmid borne copy of meningococcal <i>c_x</i> gene for expression of <i>c_x</i> protein with pST2 plasmid	In this work
<i>Escherichia coli</i> BL21 λDE3(pST2)- <i>c₅</i>	Containing plasmid borne copy of meningococcal <i>c₅</i> gene for expression of <i>c₅</i> protein with pST2 plasmid	In this work
<i>Escherichia coli</i> BL21 λDE3(pST2)- <i>c₄</i>	Containing plasmid borne copy of meningococcal <i>c₄</i> gene for expression of <i>c₄</i> protein with pST2 plasmid	In this work
<i>Escherichia coli</i> BL21 λDE3(pST2)- ccop	Containing plasmid borne copy of gonococcal 3 rd haem of <i>ccoP</i> gene for expression of 3 rd haem of CcoP protein with pST2 plasmid	In this work
<i>Escherichia coli</i> BL21 λDE3(pST2)- <i>N. elongata</i> cytochrome	Containing plasmid borne copy of <i>N. elongata</i> cytochrome gene for expression of <i>N. elongata</i> cytochrome protein with pST2 plasmid	In this work
<i>Escherichia coli</i> BL21 λDE3-Laz	Containing plasmid borne copy of meningococcal <i>laZ</i> gene for expression of Laz protein	In this work
<i>Escherichia coli</i> BL21 λDE3-AniA	Containing plasmid borne copy of meningococcal <i>aniA</i> gene for expression of AniA protein	From Dr. Melanie Thomson

<i>Escherichia coli</i> BL21 λ DE3(pST2)- 1H c_5	Containing plasmid borne copy of meningococcal 1 st haem domain of c_5 gene for expression of 1 st haem domain of c_5 protein with pST2 plasmid	In this work
<i>Escherichia coli</i> BL21 λ DE3(pST2)- 2H c_5	Containing plasmid borne copy of meningococcal 2 nd haem domain of c_5 for expression of 2 nd haem domain of c_5 protein with pST2 plasmid	In this work

Table 2.1: Bacterial strains used in this work.

2.1.2 Bacterial plasmid used in this work:

Name	Description	Source
pET22b ⁽⁺⁾	Cloning/Expression vector carries N-terminal <i>pelB</i> periplasmic leader sequence, and optional C-terminal HisTag sequence	Novegen
pST2	Plasmid containing chloramphenicol resistance gene cassette, derived from pACYC184 plasmid	Turner et al. 2005
pCR-Blunt II TOPO- <i>c_x</i> ::spec ^r	Containing a disrupted chromosomal copy of <i>c_x</i> gene by spectinomycin resistance gene cassette	Deeudom et al. 2008
pCR-Blunt II TOPO- <i>c₄</i> ::ery ^r	Containing a disrupted chromosomal copy of <i>c₄</i> gene by erythromycin resistance gene cassette	Deeudom et al. 2008
pCR-Blunt II TOPO- <i>laz</i> ::cam ^r	Containing a disrupted chromosomal copy of <i>laz</i> gene by chloramphenicol resistance gene cassette	Deeudom et al. 2008
pETYSBL3C- <i>c₅</i> C-terminal His tag	pETYSBL3C containing a copy of <i>c₅</i> gene (without the periplasm insertion) with C-terminal His tag for protein expression.	In this work
pETYSBL3C- <i>c₄</i>	pETYSBL3C containing a copy of <i>c₄</i> gene for protein expression.	In this work
pET22b(+)-1 st haem domain of <i>c₅</i>	pET22b ⁽⁺⁾ containing a copy of the 1 st haem domain of <i>c₅</i> gene for protein expression	In this work
pET22b(+)-2 nd haem domain of <i>c₅</i>	pET22b ⁽⁺⁾ containing a copy of the 2 nd haem domain of <i>c₅</i> gene for protein expression	In this work

3 rd haem <i>ccoP</i> - pET22b(+)	pET22b(+) containing a copy of 3 rd haem domain of <i>ccoP</i> of <i>N. gonorrhoeae cbb₃</i> oxidase gene for protein expression	In this work
NEIELOOT009 05-pET22b(+)	pET22b(+) containing a copy of <i>N. elongata</i> <i>NEIELOOT_00905</i> gene for protein expression	In this work
pET22b(+)- AniA	pET22b(+) containing a copy of <i>aniA</i> gene for protein expression	From Dr. Melanie Thomson
pET22b(+)-laz	pET22b(+) containing a copy of <i>laz</i> gene for protein expression	In this work

Table 2.2: Bacterial plasmid used in this work.

2.2 Growth of cells

2.2.1 Growth of *Neisseria meningitidis* and *Neisseria lactamica*:

All *Neisseria meningitidis* strains were grown in Columbia-blood Agar (CBA) or Muller-Hinton Broth (MHB) with 50mM NaHCO₃. *N. lactamica* ST640 strains were cultured in the same condition as *N. meningitidis*. Aerobic growth conditions were obtained in 5ml of MHB with 50mM NaHCO₃ in 50ml Falcon tube shaken at 200rpm, 37°C. Denitrification growth conditions was obtained in 20ml of MHB with 5mM sodium nitrite and 50mM NaHCO₃ in 30ml McCartney tube shaken at 90rpm, 37°C. For grown on CBA plates, the *Neisseria* plate cultures were incubated under 5% carbon dioxide, 37°C.

2.2.2 Growth of *Escherichia coli*:

E. coli strains were cultured aerobically in 5ml lysogeny Broth (LB , Tryptone 10g/L, Yeast extract 5g/L, NaCl 5g/L) in 50ml Falcon tube or on LB-agar plate (Tryptone 10g/L, Yeast extract 5g/L, NaCl 5g/L, agar 15g/L) at 37°C .

E. coli BL21 (λ)DE3 and BL21 (λ)DE3(pST2) expression strains were grown in Auto-induction(AI) medium at 30°C, continuously shaken at 200 rpm during growth. The composition of the AI growth medium was: Tryptone 10 g/L; Yeast extract 5g/L; glycerol 50 g/L; Glucose 5 g/L; lactose 20g/L; (NH₄)₂SO₄ 3.3g/L, KH₂PO₄ 16.3g/L. The medium was also supplemented with trace metals: MgSO₄ 1mM; FeCl₃, 50μM; CaCl₂, 20 μM; MnCl₂, 10 μM; ZnSO₄, 10 μM; CoCl₂, 2 μM; CuCl₂, 2 μM; NiCl₂, 2 μM; Na₂MoO₄, 2 μM; Na₂SeO₃, 2 μM; H₃BO₃, 2 μM.

2.2.3 Preparation of bacterial frozen stocks:

Bacterial strains were grown in liquid broth to the late log phase, which are ready for preparing the frozen stocks. 2-3ml of liquid culture was centrifuged at 6000 rpm for 1 minute. For all *E. coli* cell stocks, cell pellets were resuspended in 1ml of 50% LB broth and 50% glycerol. For all *Neisseria* cell stocks, cells pellets were resuspended in 1ml of 50% MHB and 50% glycerol. All bacterial stocks were stored at - 80°C.

2.2.4 Preparation of antibiotic selective media:

In order to prepare antibiotic selective media, antibiotic(s) was added to liquid media or molten agar. The final concentration of antibiotic(s) used for *E. coli* and *N. meningitidis* are shown below (Table 2.3) .

Antibiotic	<i>E. coli</i>	<i>N. meningitidis</i>
Ampicillin	80µg/ml	50 µg/ml
Kanamycin	50 µg/ml	50-80 µg/ml
Erythromycin	100 µg/ml	50 µg/ml
Chloramphenicol	50 µg/ml	2.5 µg/ml
Spectinomycin	100 µg/ml	50 µg/ml

Table 2.3 : Antibiotic concentration used in this work.

2.2.5 Bacterial Growth assay:

To ascertain the typical growth profiles of all *Neisseria* and *E. coli* strains in this project, growth assays were performed in aerobic and denitrifying conditions. All cultures were routinely set up in triplicates and optical density 600nm was monitored on an hourly base (in some cases 30 minutes) by removal 100 µl of the cell

suspension of each sample, which was measured using microcuvettes and an Eppendorf Biophotometer spectrophotometer (Eppendorf, Germany). It is possible to produce a curve of bacterial growth without compromising culture volume over 8-hour incubation. The mean average of the triplicates was used to produce growth curve. The standard deviation of mean was used as the error of the assay.

2.3 Fractionation of cells:

2.3.1 Preparation of *N. meningitidis* whole cell extract

N. meningitidis were grown on CBA with selective antibiotics overnight. A few colonies were collected and resuspended in 500 µl Bugbuster (Novagen) in a 1.5ml eppendorf tube, and incubated for 15 minutes at room temperature. Suspension was boiled at 90°C for 5 minutes and centrifuged for 5 minutes at 4000rpm. The supernatant contained *N. meningitidis* whole cell extract.

2.3.2 Preparation of *N. lactamica* periplasm, cytoplasm and inner and outer membrane:

Large broth *N. lactamica* cultures were grown in 500ml BHI with 50mM NaHCO₃ in a 2 L conical flask at 37°C. Cells were harvested by centrifugation at 5000 rpm for 20 minutes at 4°C after 5 hours incubation. Pellets were resuspended in 50ml buffer containing 500mM sucrose, 100mM Tris, 3mM EDTA (pH 8.0). After adding 1ml of 10 mg/ml lysozyme to the suspension, the mixture was incubated at 30°C for 30 minutes. Then it was centrifuged at 20 000rpm for 15 minutes at 4°C. The supernatant contained the periplasmic protein. Pellets were then resuspended in 100ml 10mM Tris buffer (pH 8.0). Adding 20 µl Dnase to the suspension, the

mixture was incubated for 30 minutes at 4 °C with slow stirring. After the incubation, it was centrifuged at 20 000rpm for 15 minutes at 4°C. The supernatant was the cytoplasmic protein. Pellet was resuspended in 25 ml buffer containing 10mM Tris (pH 8.0) with 1%(w/v) detergent n-Dodecyl β-D-maltoside (DDM). The mixture was incubated at 4°C for 30 minutes with slow stirring. After incubation, it was centrifuged at 6000g for 15 minutes at 4°C. The supernatant contained the solubilized membrane.

Sucrose density gradients were used to separate inner membrane and outer membranes. A step gradient was prepared in a 70ml ultracentrifuge tube consisting of 55%, 50%, 45%, 40%, 35%, and 30%(w/v) sucrose solutions (Turner et al. 2005). Each layer was loaded slowly before the next layer was added. The sucrose gradient was allowed to thaw slowly (Figure 2.1). The concentrated *N. lactamica* membrane prep (pellet following separation of membrane and cytoplasm) was mixed with the same volume of 50%(w/v) sucrose (reached the finally concentration of 25% sucrose) before loading on top of the sucrose gradients. Membranes were separated by ultracentrifugation for 12 hours at 38000 rpm, 4°C. After centrifugation, 1ml pipette was used to draw upper layer (containing inner membrane protein) and lower layer (containing outer membrane protein) samples slowly for further biochemical analysis.

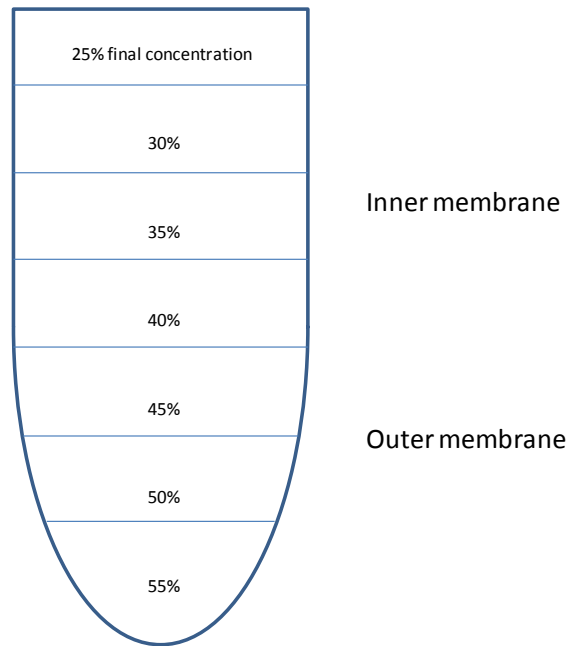


Figure 2.1: Preparation of ultracentrifuge tube for *N. lactamica* inner membrane and outer membrane separation: A sucrose gradient was used to separate inner membrane and outer membrane proteins. The concentrated *N. lactamica* sample was mixed with same volume 50% w/v sucrose, and reached the final concentration of 25% w/v sucrose.

2.3.3 Extraction of chromosomal DNA:

This method is based on the protocol used by Dr. Melanie Thomson. Chloroform: Isomylalcohol and cetyltrimethylammonium bromide (CTAB) were used to remove extract genomic material and remove carbohydrates. All solutions were prepared in DNase/RNase free water. The *Neisseria* strains of interested were cultured on CBA medium overnight. All colonies from the plate were collected and resuspended in 500 μ l Tris-EDTA (TE) buffer pH 8.0. The suspension was heated at 65 $^{\circ}$ C for 45 minutes before adding 1.25U RNase H (New England Biolabs, USA) and 100 μ l/ml lysozyme (the final concentration).The mixture was agitated gently and incubated at 37 $^{\circ}$ C overnight.

Following day, 30 μ l of 10% Sodium Dodecyl Sulfate (SDS) solution was added to mixture. The mixture was incubated for 1 hour at 37°C to lyse the cells completely. 80 μ l of 10% CTAB and 100 μ l of 5 M NaCl were added to the mixture before the incubation at 65°C for 10 minutes.

Then 800 μ l Chloroform: Isomyalcohol (24:1) solution was added to the mixture and tube was placed on a rotation-inverting shaker for 30 minutes at room temperature. The mixture was separated by centrifugation for 15 minutes at 6000 rpm. The clear upper supernatant containing genomic material was removed and placed in a clean tube. Then 800 μ l Chloroform: Isomyalcohol (24:1) solution was loaded on the top layer as before. And the mixture was centrifuged for 15 minutes at 6000 rpm. This process was repeated a further two times. After the third extraction, the upper supernatant was removed into a new centrifuge tube and then mixed with same volume of undiluted isopropanol. The genomic material was precipitated and pelleted in a tube and centrifuged for 20 minutes at maximum speed. Supernatant was removed and discarded. The pellet was resuspended in 300 μ l of 70% ethanol and centrifuged for 10 minutes at maximum speed. Ethanol was removed and pellets were dried overnight at 37°C. Next day, pellets were resuspended in 100 μ l water and the concentration was measured by Nanodrop (Thermo Scientific USA).

2.3.4 Transformation of *N. meningitidis* strains by TSB method (Bogdan et al, 2002):

N. meningitidis strains were cultured from frozen stocks on CBA plate overnight at 37°C. A few colonies were used to inoculate an aerobic growth culture of 5ml MHB with 50 mM NaHCO₃. The bacteria were cultured from OD₆₀₀ 0.05 to OD₆₀₀ 0.6 in about 2-3 hours. And 2-3ml of liquid culture was harvested and centrifuged for 5

minutes at 6000 rpm. The pellets were resuspended in 100 μ l Transforming Storage Buffer (TSB) which containing of MHB pH 6.5 with 10% PEG 4000, 10mM MgCl₂, 10 mM MgSO₄, 5% w/v DMSO, filter-sterilized. 10 μ l (200 ng/ μ l) of chromosomal DNA was added to the cells in TSB. And the other 10 μ l of water was added to the cells in TSB as control. These suspensions were incubated on ice for 50 minutes before adding 1ml pre-warmed MHB. The mixtures were cultured and shaken at 200 rpm for 1.5 hours, at 37°C. The cells were pelleted and resuspended in 50 μ l MHB. The suspension was spread on HBA containing the selective antibiotic and incubated at 37°C overnight. Resultant colonies were further verified by colony PCR.

2.4 Genetic techniques

2.4.1 The polymerase chain reaction:

2.4.1.1 Generation of c_5 , c_x constructs:

The cytochrome c_5 and c_x gene was originally cloned into the pETYSBLIC3C expression plasmid which contains a His tag at its N-terminus. It was found that the protein was soluble; however the protein appeared to lack an N-terminal His tag, presumably due to a cleavage of the mature protein. Another His tag was introduced to C-terminus of the cytochrome c_5 gene. A pair of complementary primers was designed according to a modified version of the quick change site-directed mutagenesis method (Table 2.4) (De la Cerda et al. 2002). The PCR was carried out following the standard protocol. The original c_x and c_5 cloned into pETYSBLIC3C with N-terminal His tag were used as the template DNA. Cytochrome c_5 and c_x PCR products were amplified by KOD enzyme (Roche, Germany), 100 pmol of each primer, 1mM MgCl₂, 5 μ l of dNTPs, 5 μ l of 10 \times buffer without MgCl₂, 0.5 μ l

template DNA (50 ng/μl) in 50 μl reaction mix with 1 cycle of initial denature at 94 °C for 2 minutes, 35 cycles of denature at 94 °C for 30 seconds, anneal at 55 °C for 30 seconds extension temperature at 72°C, for 1 minute, final extension at 72 °C for 3 minutes, and holding at 10 °C as long as necessary. The PCR reactions were digested with restriction enzyme Dpn I to digest the template DNA at 37 °C for 1 hour. The PCR product was purified by QIAquick PCR Purification Kit (QIAGEN, UK).

Name	Sequences	Description
c ₅ for	5'- ATCCGGTGCAAAATTCACCATCACCATCATCACTAATA ACGCGCCTTCTCCTCAC-3'	Forward primer to amplify cytochrome c ₅ with C-terminal His-tag
c ₅ reverse	5'- GTGGAATTTTGCACCGGATTTGGTTTGCCATATAGTCAACA GC-3'	Reverse primer to amplify cytochrome c ₅
c _x for	5'- CAAAAAGCAAAAAAACCCACCATCACCATCATCACTAAT AACGCGCCTTCTCCTCA-3'	Forward primer to amplify cytochrome c _x with C-terminal His-tag
c _x reverse	5'- GTGGTTTTTTTGCTTTTGCCTGTTTACGTCTTTTTCGG A-3'	Reverse primer to amplify cytochrome c _x

Table 2.4: Oligonucleotides primers used in amplifying cytochrome c₅ and c_x in this work. His tag was highlighted in green. Overlapping regions were highlighted in yellow.

2.4.1.2 Generation of the first haem and the second haem domain of c₅, laz, N. elongata cytochrome and the 3rd haem domain of N. gonorrhoeae ccoP constructs:

Primers of first and second haem domain of cytochrome c₅, third haem domain of ccoP and N. elongata cytochrome and laz are contained enzyme restriction sites to ensure the insertion into pET22b(+) vector. Boiled N. meningitis MC58 was used as template for all the genes derived from N. meningitidis. Boiled N. gonorrhoeae M6

was used as template for third haem domain of *ccoP* of *cbb₃* complex. *N. elongata* was kindly donated from Dr. Mike Koomey(University of Oslo).

The PCR was carried out following the standard protocol. PCR products were amplified by GoTaq® Green Master Mix (Promega, UK), 100 pmol of each primer, 0.5 µl template DNA (50 ng/µl) in 50 µl reaction mix with 1 cycle of initial denature at 94 for 5 minutes, 35 cycles of denature at 94 °C for 30 sec, anneal at 55 °C for 30 sec extension temperature at 72°C, for 1 minute, final extension at 72 °C for 3 minutes, and holding at 10 °C as long as necessary. The PCR product was purified by QIAquick PCR Purification Kit (QIAGEN, UK).

Name	Sequences	Description
1 st c ₅ For	5'-GCCAGCTGCGGGCAGCGGCTCGTTTCGGA-3'	Forward primer to amplify 1 st haem domain of cytochrome c ₅ with <u>PvuII</u>
1 st c ₅ Rev	5'-GCCTCGAGAGCGGCATTGTCGGCAGGCGCAG-3'	Reverse primer to amplify 1 st haem domain of cytochrome c ₅ with <u>XhoI</u>
2 nd c ₅ For	5'-GCCAGCTGCCCCTGCGGTTCGGCGTTG-3'	Forward primer to amplify 2 nd haem domain of cytochrome c ₅ with <u>PvuII</u>
2 nd c ₅ Rev	5'-GCCTCGAGGAATTTTGCACCGGATTGGTTTG-3'	Reverse primer to amplify 2 nd haem domain of cytochrome c ₅ with <u>XhoI</u>
ccoP For	5'-GCCAGCTGCCGCAAAGCGGATGGCAA-3'	Forward primer to amplify 3 rd haem domain of <i>ccoP</i> with <u>PvuII</u>
ccoP Rev	5'-GCCTCGAGGAACTTACCGCTGACTGGTTG-3'	Reverse primer to amplify 3 rd haem domain of <i>ccoP</i> with <u>XhoI</u>
NE For	5'-GCCAGCTGCTCCTGCTGCCAAAGTAG-3'	Forward primer to amplify <i>N. elongata</i> cytochrome with <u>PvuII</u>
NE Rev	5'-GCCTCGAGACCTTCGTTACCGCCTTTG-3'	Reverse primer to amplify <i>N. elongata</i> cytochrome with

		<u>XhoI</u>
Laz For	5' - <u>CCA TGG</u> CCT CTC AAG AAC CTG CCG CG- 3'	Forward primer to amplify <i>laz</i> with <u>NcoI</u>
Laz Rev	5' - <u>GAA TTC</u> CGG ATT AAT CGA CCA AAG TCA- 3'	Reverse primer to amplify <i>Laz</i> with <u>EcoRI</u>

Table 2.5: Oligonucleotides primers used in amplifying the first haem and the second haem domain of *c₅*, *laz*, *N. elongata* cytochrome and the 3rd haem domain of *N. gonorrhoeae ccoP*. Restriction enzymes cut sites were underlined.

2.4.2 Restriction digestion of PCR product and pET22b+vector:

Purified PCR products were digested with restriction enzymes to complement those in the MCS of the pET22b(+) vector. All the restriction digestions were done using protocols from the manufacture. All the restriction enzymes are from Promega and New England Biolabs.

2.4.3 Ligation of inserts into pET 22b(+) plasmid:

The ligation of digested DNA fragment with linearized plasmid was done using T4 DNA ligase (Promega UK) following the protocols from the manufacturer instructions.

2.4.4 Transformation of DH5 α and BL21 (λ)DE3 *E. coli* cells:

For each transformation, take 50 μ l competent cells and keep them in a sterile tube on ice. 2 μ l of ligated product was added to the competent cells and mixed well. And the mixture was maintained on ice for 5 minutes. The tube was placed in a water bath at 42 °C for 30 seconds, and then transferred the mixture to cool on ice for 3 minutes. Add 500 μ l LB medium, the mixture was mixed well and incubated at 37°C for 1 hour. All of the transformation was plated onto agar plates containing the appropriate antibiotic, incubated at 37°C over night.

2.4.5 Colony PCR

Colony PCR provides a quick method of determining which clones contain the desired insert. Select a few colonies from plate as template. PCR reaction was prepared the same as before, but replaced reverse primer with T7 reverse primer. PCR cycles are the same as before to check for the presence of the correctly sized insert.

2.4.6 Preparation of *E. coli* plasmid DNA

The frozen stock *E. coli* strain of interested was plated on LB agar plate with selective antibiotic and incubated at 37°C overnight. Following day, one colony was picked and grown in 5ml LB broth in 50ml falcon tube with selective antibiotics. Liquid culture was grown aerobically at 37 °C at 200 rpm overnight. Cells were harvested by centrifugation for 30-60 seconds at 4000 rpm. Plasmid DNA was extracted using QIAprep spin Miniprep Kit (QIAGEN, UK). Protocols were following the manufacturer's instructions. Plasmid DNA concentration was measured by Nanodrop (Thermo Scientific) and stored at -20°C.

2.4.7 Preparation of *E. coli* competent cells

Chemically competent cells of *E. coli* DH5 α , BL21 (λ)DE3, BL21 (λ)DE3(pST2) were used to all uptake plasmid containing cloned gene or mutant construct, or expression cloned gene of interest in this work. Competent cells were prepared by Hanahan method and stored at -80 °C (Hanahan 1983).

2.5 Protein purification

2.5.1 Preparing *E. coli* cell crude extract:

All the *E. coli* expression strains BL21 (λ)DE3(pST2) (pST2 is a plasmid containing the ccm genes from *E. coli* and conferring resistance to chloramphenicol) were cultured aerobically in AI medium supplemented with selective antibiotics (Turner et al. 2005). Co-expression of the ccm gene is necessary for assembly of c-type cytochrome in the *E. coli* periplasm under aerobic conditions. Broth cultures were grown overnight and harvested by centrifugation at 5000 rpm for 10 minutes at 4 °C. Pellets were resuspended in 50 mM Tris pH7.5 and sonicated for 2 minutes (10 seconds on/off time) at output level 4.0 using a Misonix 3000 sonicator (Qsonica, LLC USA). All soluble material containing cytochrome was centrifuged at 18,000 rpm for 40 minutes. Supernatant contained the cell crude extract and was filtered through a 0.45 μ m Millex® syringe filter (Merck Millipore, Germany) before applying to the column for further purification.

2.5.2 Extraction of periplasmic proteins from *E. coli* BL21 (λ)DE3.

The *E. coli* strain BL21 (λ)DE3 was used to express AniA and Laz. Cells were grown in 2×500 ml auto-induction media with 0.5 mM CuCl₂ containing 100 µg/ml ampicillin. Broth cultures were harvested by centrifugation at 4000 rpm for 15 minutes at 4 °C after 8 hours incubation time. Pellets were resuspended in 50 ml buffer containing 500 mM sucrose, 100 mM Tris, 3 mM EDTA (pH 8). After adding 1 ml of 20 mg/ml Hen Egg Lysozyme solution to the suspension, the mixture was incubated at 30 °C for 1 hour and then centrifuged at 6000 rpm for 15 minutes at 4 °C. The periplasmic protein was contained in the supernatant.

2.5.3 Nickel Affinity Chromatography

His tagged recombinant proteins were purified by pre-packed HisTrap™ Hp column (GE Healthcare, UK). HisTrap HP column was operated with a syringe and equilibrated with 5 column volumes of 40 mM imidazole 50 mM Tris (pH 7.5) washing buffer first. The crude extract was applied to the column, and washed with 5 column volumes of 40 mM imidazole 50 mM Tris (pH 7.5). His tagged recombinant proteins were bound to the Ni sepharose resin. And bound proteins were eluted with 5 column volumes of 500 mM imidazole 50 mM Tris (pH 7.5) buffer by a step gradient.

2.5.4 Ion exchange chromatography:

If the estimated isoelectric point (pI) of protein is less than 7, an anion exchange resin was used to separate on the basis of interaction of negatively charged amino acid residues. If the estimated pI of protein is high than 7, an cation exchange

resin was used separate on the basis of interaction of positively charged amino acid residues. Protein was initially loaded on to an anion exchange column DEAE sepharose-CL6B (Amersham Biosciences, Sweden) or CM sepharose fast flow cation exchange(Amersham Biosciences, Sweden) packed into column with a 40 ml bed volume and connected to AKTA prime plus(GE Healthcare, UK) Fast Protein Liquid Chromatography (FPLC) purification system. Column was packed according to the manufacturer's protocol. A steep salt gradient (0-500 mM NaCl in 100 ml of 50 mM Tris pH7.5) was used to elute specific protein. FPLC system collected 5 ml in each fraction, speeded at 2.0 ml/s. The fractions containing of interest were analyses by SDS-PAGE.

2.5.5 Protein concentration determination:

Bradford assay (Bradford, 1976) was used to measure protein concentration in each step, and was performed using Bio-Rad Protein Assay (Bio-Rad). The relative measurement of protein concentration was done according to protocols from the manufactures.

2.5.6 Desalting and buffer-exchanging of protein samples:

Pre-packed PD-10 Desalting column (GE Healthcare, UK) was used to prepare a small amount of protein in various salt and pH buffers in this project. The matrix of PD-10 column is sephadex G-25 with the exclusion limit Mr. 5000. The relative protein desalting and buffer exchanging procedures were done according to manufacturer's instruction.

2.6 Analytical techniques

2.6.1 SDS-PAGE

SDS-PAGE was used for analysis protein samples for analyzing the molecular weight, relative concentrations, and haem domain presenting and also the immunological response to antibodies.

Gels were prepared as the protocol described in Table 2.6. Protein samples were mixed with SDS loading buffer (3:1) and boiled at 90 °C for 5 minutes. All the protein samples and protein ladder (PageRuler™ Prestained Protein Ladder, Thermo Scientific) are carefully loaded in each well of the set gel. Gels were run at 200 V for 1 hour or 150V for 90 minutes (for better protein separation). To visualize the separated protein, the gel must be stained for proteins.

Component	Resolving Gel (15%)	Stacking Gel (5%)
Deionized water	2.54ml	5.49ml
Resolving Buffer 1.5M Tris pH8.8	2.50ml	-----
Stacking Buffer 0.5M Tris pH 6.8	-----	2.50ml
30% Acrylamide *	4.75ml	1.70ml
10% SDS	0.10ml	0.10ml

Mix well, then Add TEMED and APS before casting the gel

10% APS*	0.1	0.1
TEMED*	0.01ml	0.01ml
<p>Sample loading buffer:</p> <p>1M Tris/HCl pH 6.8 2.4ml</p> <p>20% SDS 3.0ml</p> <p>Glycerol 3.0ml</p> <p>Bromophenol blue 0.006 g</p> <p>deionized water 1.6 ml</p> <p>5 X SDS Running buffer:</p> <p>15g, Tris, 72g glycine, 5g SDS, made up to 1 liter deionized water.</p>		

Table 2. 6: Protocol for preparation of SDS-PAGE: * 30% Acrylamide (Protogel) gel stock contains 30% acrylamide, 0.8% bis-acrilamide; APS, ammonium persulfate; TEMED, N,N,N',N'-Tetramethylethylenediamine

2.6.2 Coomassie stain:

SDS-PAGE gel was stained for protein using Coomassie Brilliant Blue. Gels were stained in a solution of 0.2 % (w/v) Coomassie Brilliant Blue, 50% methanol, and 10% acetic acid and incubated with gentle shaking at room temperature for 1 hour. The gel was then rinsed with dsH₂O and then destained with a solution of 10% acetic acid, 10% methanol with gentle shaking at room temperature until protein bands could be visualized.

2.6.3 Western blot

Western blot was carried out, after protein samples were separated by 12.5% SDS-PAGE gels. The gel was placed in transfer buffer (25 mM Tris, 192 mM glycine, 20 % (v/v) methanol) in a few minutes and then sandwiched with a nitrocellulose membrane (GE, Amersham) in a pre-soaking blotting apparatus in transfer buffer at 100 volt for 90 minutes. To ensure transfer has occurred correctly, the transferred proteins need to be visualized, and stained with Ponceau S. The membrane was reversibly stained with 0.1% Ponceau S (w/v) in 5% acetic acid to check the protein transfer efficiency. It was then destained two or three washes with dsH₂O on the rocker for 2 minutes each time. The membrane was then washed with 20 ml of Tris buffered saline (TBS 50 mM Tris, 150 mM NaCl, pH 7.6) to remove the Ponceau stain further. Then it was replaced TBS with blocking solution (TBS plus 0.1 % (v/v) Tween 20 with 5 % (w/v) Marvel dried milk powder). Membrane was blocked on the rocker for 1 hour at room temperature. Then the membrane was transferred to with antibody solution containing primary antibody (10 ml of TBS+0.1 % (v/v) Tween20 + 1 % (w/v) Marvel + 0.005% primary antibody) and placed on a rocker overnight at 4°C. The following day, it was removed from antibody solution and washed 3 to 4

times with TTBS (TBS +0.1 % (v/v) Tween 20) 15 minutes once. The probe the primary antibody, membrane was transferred to TTBS with secondary antibody (10 ml of TTBS + 1 % Marvel + 0.01% anti-rabbit IgG peroxidase conjugate) and placed on a rocker at room temperature. Then it was washed 3 to 4 times with TTBS (TBS +0.1 % (v/v) Tween20) 15 minutes once. Chemiluminescence substrates 'SuperSignal West Dura Substrate' (Perbio Science, UK) were mixed, spread across the membrane, and allowed to develop for 5 minutes. Membrane was drained the reagents off the blot and sandwiched between acetate sheets in a bag. It was exposed to X-ray film (FUJI, Japan) for approximately 1-5 minutes to achieve an optimum luminescence signal.

2.6.4 Haem stain (Chemiluminescent method)

Gels were blotted onto nitrocellulose membranes following standard method. Ponceau S was used to check protein transferred efficiently, and nitrocellulose membrane was destained with distilled water. Chemiluminescent method (Vargas *et al.*, 1993) was used for haem staining to detect c-type haem containing cytochromes. 200µl of each reagent of ' SuperSignal West Dura Substrate' by Pierce (Perbio Science, UK) were mixed and spreaded across nitrocellulose membrane which was sandwiched between two acetate sheets for 5 minutes. The membrane was exposed to X-ray film (FUJI, Japan) for 1 - 5 minutes to achieve an optimum luminescence signal.

2.6.5 Spectra of protein samples:

UV-visible spectra were measured between 200-700 nm in a UV-1001 SHIMADZU spectrophotometer (Shimadzu, Baltimore, MD). 250 μ M sodium dithionite was used as a reduction agent, and 10%(w/v%) ammonia persulfate was used as an oxidizing agent.

2.6.6 Pyridine haemochrome

The pyridine haemochrome method (Berry and Terumpower 1987) was used to measure the c-type cytochrome concentration in each sample. 0.5ml of stock solution (200mM NaOH, 40%(w/v) pyridine and 3 μ l of 0.1 M $K_3Fe(CN)_6$) and 0.5 ml aliquot of sample were added in 1ml glass cuvette with thorough mixing, and the oxidized spectrum at 550 nm was recorded within 1 minute.

About 3 mg of sodium dithionite was added to the mixture. Spectra of the reduced pyridine haemochrome were recorded at 550 nm. Based on Beer-lambert law, the absorbance difference at 550 nm was divided by extinction coefficients of absorbance difference of c-type cytochrome at 550 nm ($\epsilon_{550(R-O)}$) to calculate the haem c content in the sample.

2.7 Stopped-flow kinetics experiment:

SX20 Stopped-Flow Spectrometer (Applied Photophysics, UK) was used to study the kinetics of fast biochemical reactions initiated by rapid mixing and stopping of the reactants. Stopped-flow kinetics of electron-transfer experiment from reduced form cytochrome proteins to nitrite reductase AniA was performed in 50 mM Tris buffer (pH 7.5) at room temperature, and monitored at a wavelength of 402 nm. To

keep the pseudo-first-order conditions, the concentration of AniA is always in large excess over cytochrome protein. The concentration of AniA was varied. The pseudo-first-order rate constants ($K_{\text{obs}}\text{s}^{-1}$) were calculated by fitting the experimental data with a 3 parameter single exponential function or a 5 parameter double exponential function (depending on electron transfer rate is contributed by one or two events) by SigmaPlot software. The second order electron-transfer rate constant ($\text{M}^{-1} \text{s}^{-1}$) was estimated from the slope of the plots of AniA concentration (μM) versus electron transfer rate $K_{\text{obs}}\text{s}^{-1}$.

2.8 *In vivo N. meningitidis* nitrite usage assay:

The nitrite concentration in the *N. meningitidis* liquid growing culture was measured by colorimetric assay (Nicholas and Nason 1957). Nitrite is converted to nitrous acid in the acidic medium and followed by diazotization of sulphanilic acid and the formation of diazonium salt. The diazonium salt is associated with N-naphthylethylenediamine to form a bright pink color, which can be detected by spectrophotometer at wavelength 540 nm. A standard curve of NaNO_2 was created between 0-12.5 μM , and mixed with 850 μl of sulphanilic in 1M HCl then 100 μl of 0.02% N-naphthylethylenediamine in HCl. After the pink color was fully developed, the absorbance at 540nm was read and standard graph then was generated (ABS_{540} vs. $[\text{NaNO}_2]\mu\text{M}$). From each of the sample culture, 50 μl of sample taken in triplicates and mixed with 850 μl of sulphanilic in 1M HCl then 100 μl of 0.02% N-naphthylethylenediamine in HCl. The mixture was measured at absorbance 540 nm and recorded and the average results were converted to nitrite concentration in μM using the linear equation from the standard graph. Each sample's result was average within triplicate.

Chapter 3

Localization of redox proteins in *Neisseria* species

3.1 Introduction:

Typically, redox proteins of respiratory chains in Gram negative bacteria, which function as electron donors or redox enzymes are localized in the cytoplasmic membrane or the periplasm to allow the generation of ion gradients to drive the synthesis of ATP. Many enzymes and electron donors of denitrification pathways are localized within the periplasm. However, in the *Neisseria* species, a number of redox proteins are predicted to be associated with the outer membrane.

AniA is the only nitrite reductase encoded in the *Neisseria* species. It was originally identified in *N. gonorrhoeae* and distinguished as being a outer membrane protein by the detergent solubilisation method (Clark 1987). *N. gonorrhoeae* colonies were lysed and selectively solubilised by sodium lauroyl sarcosinate (Clark 1987). The localization of AniA in other *Neisseria* species (*N. meningitidis* and other commensal *Neisseria* species, *N. lactamica*, *N. cinerea*, *N. subflava et. al.*) were predicted to be associated with the outer membrane by the same detergent solubilisation method (Hoehn and Clark 1990).

There are several c-type cytochromes that have been identified in the *Neisseria* species. The localization of each cytochrome was based on genetic prediction. Typical c-type cytochromes found in *Neisseria* species include cytochrome *cbb₃*, *bc₁*, *c_x*, *c₄*, *c₅*, *c'* and *CCP* (only in *N. gonorrhoeae*). Based on genetic analysis, cytochrome *c_x* and *c₄* were predicted to encode a periplasmic monohaem protein and

a periplasmic dihaem protein, respectively. Cytochrome c_5 was predicted to encode a membrane associated dihaem cytochrome and to attach to the membrane by a trans-membrane helix. There are two c-type cytochromes that are predicted, lipoproteins c' and CCP. In Gram- negative bacteria, lipoproteins (including AniA and Laz) can either be anchored to the inner or to the outer membrane facing towards periplasm. Due to the difficulties of separating gonococcus inner and outer membranes, the localization of lipoprotein cytochrome c' was shown to associate with the outer membrane, based on results obtained by heterologous expression of c' in *E. coli* (Turner et al. 2005).

As described before, based on a mutagenesis study, a c_5 mutant *N. meningitidis* MC58 strain could not reduce nitrite under microaerobic conditions (Deeudom et al. 2008). Cytochrome c_5 appears to be the major electron donor to nitrite reductase AniA in *N. meningitidis*. The width of Gram-negative bacteria periplasm is predicted approx. 170Å (1Å=0.1nm) (Matias et al. 2003; Tamura et al. 2005). The globular domain of AniA is able to span 45 Å, whereas dihaem cytochrome c_5 may access 60 Å, thus 105 Å in total across the periplasm (Figure 3.1). It presents a potential problem for electron transfer from the inner membrane respiratory complex to the outer membrane electron acceptors/respiratory electron acceptor reductase.

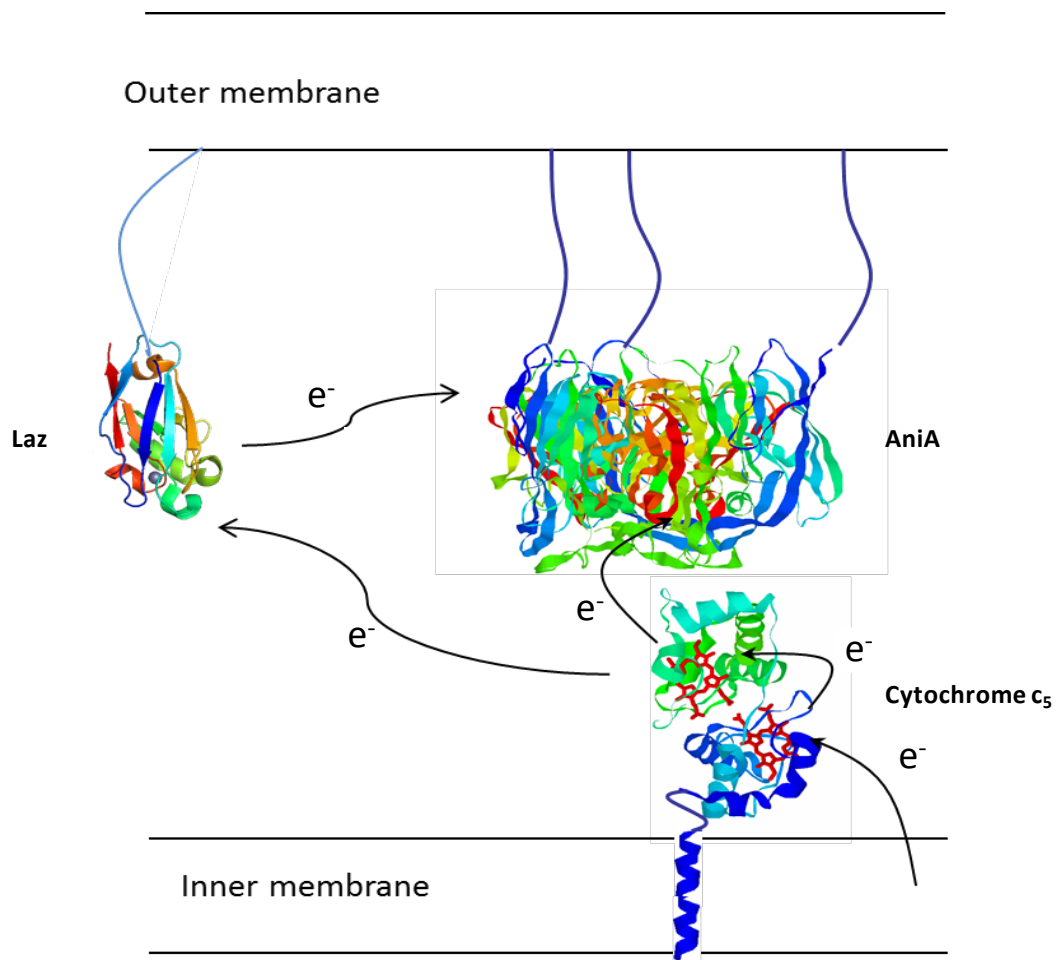


Figure 3.1: Electron flow from electron donors to nitrite reductase AniA in *N. meningitidis*. Both of cytochrome c_5 and Laz are predicted to be electron donors to AniA.

Pathogenic *N. meningitidis* and *N. gonorrhoeae* Laz is involved in defence against hydrogen peroxide and survival with in epithelial cells (Wu et al. 2005). Compared to the wild type strain, the survival of *N. gonorrhoeae* laz mutant strain is decreased in epithelial cells and highly sensitive to H_2O_2 (Wu et al. 2005). There is no obvious evidence suggesting Laz is essential for *Neisseria* growth under aerobic or anaerobic conditions. A c_5 mutant *N. meningitidis* failed to utilize nitrite during incubation under microaerobic conditions with nitrite present (Deeudom et al. 2008) . It

suggests that Laz could not receive electrons on its own from cytochrome *bc₁* and transfer to nitrite reductase AniA. If Laz is involved in nitrite reduction, a *laz* mutant strain will show the deficiency in nitrite utilization under denitrifying conditions. The other prediction is that Laz might receive electrons from cytochrome *c₅* and transfer to AniA as an electron mediator under certain conditions. In previous work, the *Neisseria* outer membrane and inner membrane were separated by introducing detergent Sarkosyl, and blotted by an anti-Laz specific antibody (Trees and Spinola 1989). The location of Laz was predicted to be localized in the outer membrane (Trees and Spinola 1989).

We are limited to small volume culture for the pathogenic *Neisseria*, and therefore we set out to investigate the localization of the redox proteins in the commensal *N. lactamica*, which can be cultured in a large volume. In this chapter, we are aiming to provide the evidence regarding location of redox proteins in *Neisseria* species.

3.2 Commensal *Neisseria lactamica* is closely related to *Neisseria meningitidis*:

In order to interpret the cellular location of redox proteins in *Neisseria* species, we choose the non-pathogenic strictly commensal *N. lactamica* ST640 (Genome sequence obtained from Wellcome Trust Sanger Institute) as the candidate. *N. lactamica* is similar to *N. meningitidis*, in many respects, but differs owing to its relative lack of virulence and ability to ferment lactose. All *N. meningitidis* MC58 genes associated with respiration are shown to have a homologous partner in *N. lactamica* ST640 (Table 3.1). In addition, the lipoprotein *N. meningitidis* AniA is highly identical to *N. lactamica* AniA including the N-terminal putative flexible linker regions (Figure 3.2). *N. meningitidis* Laz is also highly identical to *N. lactamica* Laz including the N-terminal putative flexible linker regions (Figure 3.3).

<i>N. meningitidis</i> MC58 gene	<i>N. lactamica</i> ST640 sequence homology identities	P-value
AniA(NMB1623)	626/657 (95%)	4.6e-131
Laz(NMB 1533)	162/193 (84%)	2e-98
C ₅ (NMB1677)	804/840(95%)	1.2e-170
C _x (NMB 0717)	305/379(80%)	1.8e-49
C ₄ (NMB 1805)	561/625(89%)	3.5e-110

Table 3.1: Results of NCBI Blast searches: *N. meningitidis* MC58 redox genes were searched against *N. lactamica* ST640 to find homologous sequences and identities.

```

N. lac AniA MKRQALAAMIASLFLAACCGGEPAAQAPAETPAASAEAASSAAQTAAETPSGELPVIDAV 60
N. men AniA MKRQALAAMIASLFLAACCGGEPAAQAPAETPAASAEAASSAAQTAAETPSGELPVIDAV 60
*****:*****

N. lac AniA TTHAPEVPPAIDRDYPKVRVKMETVEKTMKMDGVEYRYWTFDGDVPGRMIRVREGDTV 120
N. men AniA TTHAPEVPPAIDRDYPKVRVKMETVEKTMKMDGVEYRYWTFDGDVPGRMIRVREGDTV 120
*****.*****

N. lac AniA EVEFSNNPSSTVPHNVDFHAATGQGGGAAATFTAPGRTSTFSFKALQPGLYIYHCAVAVP 180
N. men AniA EVEFSNNPSSTVPHNVDFHAATGQGGGAAATFTAPGRTSTFSFKALQPGLYIYHCAVAVP 180
*****

N. lac AniA GMHIANGMYGLILVEPKVDEKDFYIVQGDFTYKGGKGAQGLQPFMDKAVAEQPEY 240
N. men AniA GMHIANGMYGLILVEPKVDEKDFYIVQGDFTYKGGKGAQGLQPFMDKAVAEQPEY 240
*****

N. lac AniA VVFNGHVGSIAGDNALKAKAGETVRMYVGNNGPNLVSSFHVICEIFDKVYVEGGKLINE 300
N. men AniA VVFNGHVGSIAGDNALKAKAGETVRMYVGNNGPNLVSSFHVICEIFDKVYVEGGKLINE 300
*****:*****

N. lac AniA VQSTIVPAGGSAIVEFKVDIPGSYTLVDHSIFRAFNKGALGQLKVEGAENPEIMTQKLS 360
N. men AniA VQSTIVPAGGSAIVEFKVDIPGSYTLVDHSIFRAFNKGALGQLKVEGAENPEIMTQKLS 360
*****

N. lac AniA TAYAGNGAASAASAPAASAPAASASEKSVY 390
N. men AniA TAYAGNGAASAASAPAASAPAASASEKSVY 390
*****.*****

```

Figure 3.2: Primary structure comparison of AniA in *N. meningitidis* MC58 (N. men) and *N. lactamica* ST640 (N. lac). The primary protein sequences show both of the proteins are identical. Putative flexible linker regions from *N. lactamica* and *N. meningitidis* AniA are highlighted in yellow colour. The regions shown begin after the predicted type II signal peptidase cleavage sites (LAAC, red in color), and leaves cysteine residue at the N-terminus, and end at the beginning of predicted globular domain of AniA in *N. meningitidis*. Amino acids alanine (A), glutamate (E), proline (P), serine (S) and threonine (T) are in bold and are predicted to be involved in forming the linker region.

```

N.lac Laz      MKAYLALISA AVIGLAACSQEPAAPAAEATSASEAPAEAETASAPEAPAAEAPAAEAAAGD 60
N.men Laz      MKAYLALISA AVIGLAACSQEPAAPAAEATPAAEAP-----ASEAPAAEAAPDAAE-- 52
*****:*****:*****:*****:*****:*****:*****:*****:*****:*****:*****

N.lac Laz      AAAPAAGNCAATTVEANDAMQFNTKEIQVSKACKEFTITLKHTGTQPKTSMGHNIVIGKAE 120
N.men Laz      --APAAAGNCAATVESNDNMQFNTKDIQVSKACKEFTITLKHTGTQPKASMGHNLVIAKAE 110
*****:*****:*****:*****:*****:*****:*****:*****:*****:*****:*****

N.lac Laz      DMDGIFKDG VGAADTDYVKPDDARVVAHTKLIGGEEASLTLDPAKLAGGEYKFACTFPG 180
N.men Laz      DMDGVFKDG VGAADTDYVKPDDARVVAHTKLIGGEEASLTLDPAKLADGEYKFACTFPG 170
*****:*****:*****:*****:*****:*****:*****:*****:*****:*****:*****

N.lac Laz      HGALMNGKVTLVD 193
N.men Laz      HGALMNGKVTLVD 183
*****:*****:*****:*****:*****:*****:*****:*****:*****:*****:*****

```

Figure 3.3: Primary structure comparison of Laz of *N. meningitidis* MC58 (*N. men*) and *N. lactamica* ST640 (*N. lac*). The primary protein sequences show Laz in both of *Neisseria* species are highly identical. Putative flexible linker regions from *N. lactamia* and *N. meningitidis* Laz are highlighted in yellow colour. The regions shown begin after the predicted type II signal peptidase cleavage sites (LAAC, red in colour), and leaves cysteine residue at the N-terminus, and end at the beginning of predicted globular domain of Laz in *N. meningitidis*. Amino acids (AAs) alanine, glutamate, proline, serine and threonine are shown in bold to emphasize that most of the AAs from the linker region to these types.

3.3 Subcellular localization of c-type cytochrome proteins:

The purpose was to identify and characterize the subcellular localization of c-type cytochrome proteins in *Neisseria* species. The *N. lactamica* ST640 strain was cultured under aerobic conditions and fractionated into periplasm, cytoplasm, and solubilized membrane (prepared by 1% dodecyl maltoside (DDM)). Soluble fractions of periplasmic, cytoplasmic fraction and solubilized membrane were separated by SDS-PAGE and stained for haem-dependent peroxidase activity. As described before, the majority of c-type cytochromes are predicted to be localized either in periplasm or associated with membrane (including two lipoprotein CCP and c').

There are 5 c-type cytochromes detected by haem staining. One has molecular weight 40kDa and is predicted to be CcoP which is a subunit of *cbb₃* oxidase. One has molecular weight 25kDa and is predicted to be cytochrome *c₅*. One has molecular weight 20kDa and is predicted to be cytochrome *c₄* or CcoO. One has molecular weight 15 kDa and is predicted to be cytochrome *c'*.

Haem-dependent peroxidase activity of c-type cytochromes could only be found in the membrane fraction, but not in periplasm or cytoplasm (Figure 3.4). This result does not agree with previous predictions that cytochrome *c₄* is a periplasmic protein. In order to determine localization of c-type cytochrome further, bacterial membrane needs to be further separated into inner membrane and outer membrane.

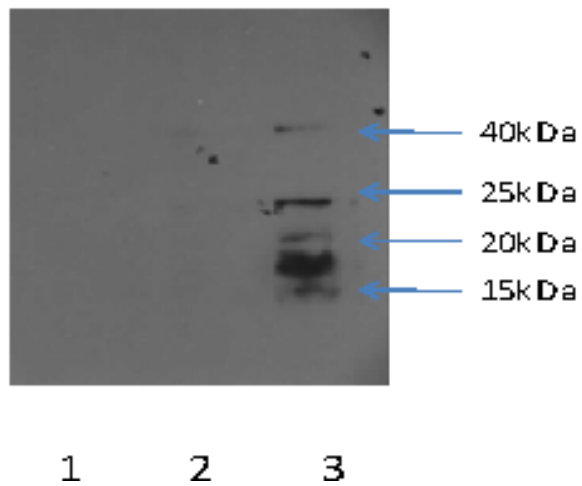


Figure 3.4: *N. lactamica* cells were fractionated into periplasm, cytoplasm and membrane. Localization of haem containing cytochrome proteins into periplasm, cytoplasm and membrane are shown in panels 1-3. 1. Haem staining of periplasmic fraction; 2. Haem staining of cytoplasmic fraction; 3. Haem staining of solubilized membrane. The majority of c-type cytochrome proteins could only be found in the membrane fraction, but not in periplasm or cytoplasm.

3.4 Membrane localization of redox proteins:

Attempts to separate *Neisseria* membranes by sucrose gradient centrifugation were successful in our study. *N. lactamica* ST640 were incubated and fractionated into periplasm, cytoplasm, membrane by lysozyme treatment and osmotic shock without adding any detergent. *Neisseria* membrane fractions containing redox proteins were prepared in 50mM Tris pH 8.0 buffer, mixed with the same volume of 50% (w/v) sucrose, loaded on to a sucrose step gradient (30%-55%) and separated by ultracentrifugation. Samples presumed to be inner membrane and outer membrane were extracted from the top and bottom of gradient and protein content of both fractions were analysed by SDS-PAGE, which was stained by Coomassie Blue (Figure 3.5). The major band from Coomassie blue stained gel is a porin protein (PorA) (approximately 35 kDa), a major outer membrane protein in *N. meningitidis* with a molecular weight of 40 kDa (Figure 3.5 A) (Tauseef et al. 2013). No porin protein was detected in inner membrane fractions, which indicates that the separation of inner membrane and outer membrane proteins has been achieved. Haem dependent peroxidase activity, due to all c-type cytochromes, was only detected in the inner membrane fraction (Figure 3.5 D). The expression of AniA was detected by using western blotting using a primary antibody against AniA. AniA with a molecular weight of about 55kDa is mainly associated with the outer membrane (Figure 3.5 B). The expression of Laz was detected by using western blotting using a primary antibody against Laz. Laz with a molecular weight of about 23 kDa is also mainly associated with the outer membrane (Figure 3.5 C).

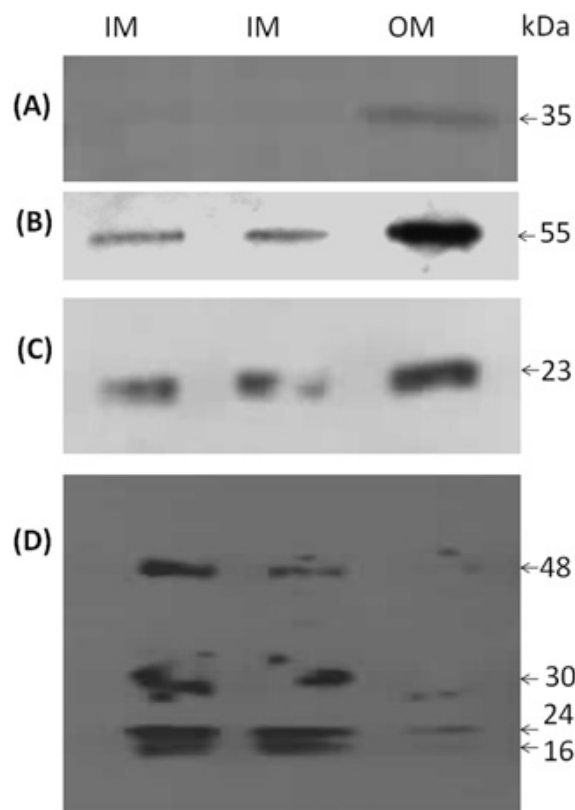


Figure 3.5: *N. lactamica* cells were fractionated into periplasm, cytoplasm and membrane using lysozyme treatment and osmotic shock. Localization of proteins into the inner membrane (IM) or outer membrane (OM) fractions are shown in panels (A-D). (A) The major band from a Coomassie Blue-stained gel is a porin, only seen in outer membranes. (B) Western blot with anti-AniA antibodies shows that AniA is mainly associated with outer membrane. (C) Western blot with anti-Laz antibodies shows that Laz is mainly associated with outer membrane. (D) Haem staining shows that c-type cytochromes are mainly associated with the inner membrane (48 kDa, CcoP; 30 kDa, cytochrome c_5 /PetC; 24kDa, CcoO/cytochrome c_4 ; 16 kDa, cytochrome c').

3.5 Discussion:

Like other Gram negative bacteria, the *Neisseria* species own a classical two-membrane cell envelope. In this work, we have demonstrated an approach to separate commensal *N. lactamica* inner and outer membrane by sucrose density-gradient centrifugation without introducing any detergent. It was found that nearly all major redox proteins are highly conserved between two related *Neisseria* species.

Western blotting and haem peroxidase staining were utilized to determine the subcellular localization of redox proteins in *N. lactamica*. The localization of the majority of c-type cytochromes was determined to be associated with membrane, but not in cytoplasm or periplasm. Further experiment confirmed that all c-type cytochromes are associated with the inner membrane.

Cytochrome c_4 was determined to be associated with inner membrane, although it was previously predicted as a periplasmic protein. Presumably c_4 is tightly associated with the other inner membrane associated proteins and not released in periplasm. Cytochrome c_5 was originally determined as a membrane associated protein and determined to associate with the inner membrane.

Haem staining relies on the peroxidase activity of c-type cytochromes and is affected by the maturation state of the protein folding around haem group (Diederix et al. 2002). Cytochrome c_x cannot be detected in either *N. gonorrhoeae* or *N. meningitidis* cell extracts, so presumably the peroxidase activity of cytochrome c_x is very low (Deeudom et al. 2008 ; Turner et al. 2005). The expression of cytochrome c_x is confirmed in *N. gonorrhoeae* strain F62 by western analysis (Hopper et al. 2013). The primary antibody used to detect 3 ×FLAG-tagged version of cytochrome c_x in

the bacteria was anti-FLAG monoclonal antibody (Hopper et al. 2013). The localization of cytochrome c_x in *Neisseria* species could be analysed by Western analysis in the future.

In addition, the localization of *N. gonorrhoeae* cytochrome c' was originally determined as being associated with the outer membrane, based on its heterologous expression in *E. coli* (Turner et al. 2005). In our work, cytochrome c' with molecular weight 16 kDa was determined as being associated with the inner membrane in *Neisseria* species.

The subcellular localization of nitrite reductase AniA and lipid-modified azurin (laz) in *Neisseria* species was originally predicted to be associated with the outer membrane by the detergent solubilisation method. Western blot with anti-laz and anti-AniA antibody suggests that *N. lactamica* Laz and AniA are mainly associated with the outer membrane. AniA was detected with a molecular weight of 55 kDa. Laz was determined with a molecular weight of 23 kDa. Both of *N. meningitidis* AniA and Laz share a high degree of similarity with *N. lactamica* AniA and Laz, including the N-terminal part consisting of the predicted type II signal sequences, followed by the extended low complexity region (LCR). It is reasonable to presume that AniA and Laz are also outer membrane associated proteins in *N. meningitidis*.

In conclusion, our data provides a useful confirmation that AniA and Laz are only found in the outer membrane, whereas all c-type cytochromes are associated with membranes, indeed the inner membrane. AniA and cytochrome c_5 are localized in different membranes. Electron donor c_5 is the sole electron donor to nitrite reductase AniA in *N. meningitidis*. It suggests there is a novel mechanism of electron transfer in *Neisseria* species.

AniA and Laz have a similar N-terminus which consists of predicted signal sequences, followed by the extended low complexity region (LCR), which seems to be a *Neisseria* specific addition to NirK, and rich in alanine, proline, glutamate. The translational distance between amino acids along the peptide chain will be between 1.5Å (in α -helix) and 3Å (in collagen). Given that the LCR has 30 amino acids, we estimate the globular domain of AniA is able to span about 45Å to 90Å from the surface of the inner leaflet of outer membrane (Figure 3.6). LCR may form an unstructural elongated linker region that would allow the globular domain of Laz or AniA to get access to electrons from the c-type cytochrome (c_5) associated with the inner membrane. If tethers are able to span up to 60Å, the outer membrane associated protein AniA should be allowed to extend sufficiently from the inner leaflet of the outer membrane to form a complex with the inner membrane associated dihaem cytochrome c_5 .

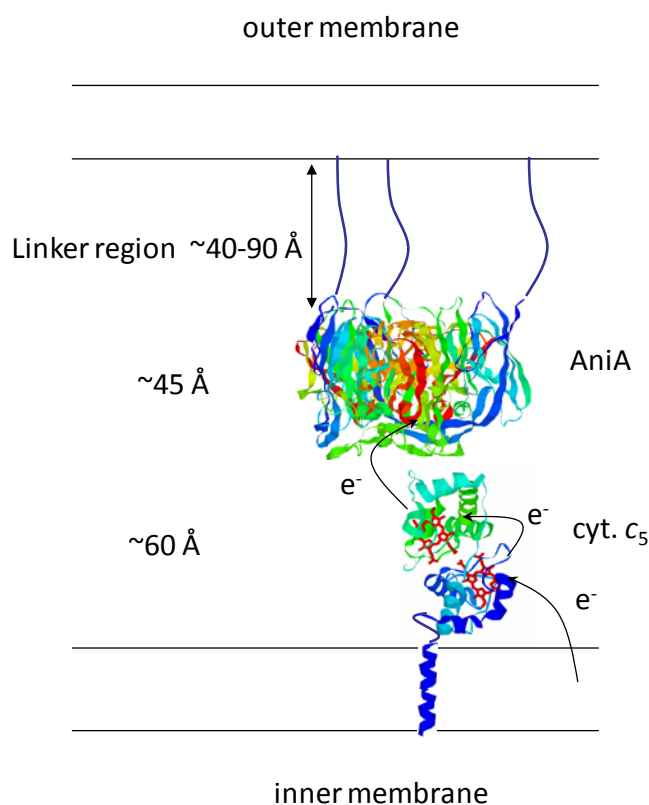


Figure 3.6: Predicted model of electron flow between membranes in *N. meningitidis*. Each LCR is expected to span about 40-90 Å to allow AniA to get access electrons from cytochrome c_5 .

In *N. meningitidis*, AniA is a trimer and tethered to outer membrane by three distinct peptides. In a system where AniA is free to move and rotate in periplasm, the diffusion rate should be much higher than AniA which is tethered to outer membrane, and the enzyme active site is facing to inner membrane. In addition, each tether (about 30 amino acids) is not long enough to wrap around the enzyme, three tethering peptides thus also prevent the core enzyme to rotate freely in the periplasm. These tethers are also attached to the core enzyme in such a way as to ensure redox-accepting sites are facing to cytoplasmic membrane. The mobility of tethered AniA may also be further reduced by peptidoglycan with in the periplasm. The sole electron donor cytochrome c_5 is associated with cytoplasmic membrane with a predicted membrane span α -helix. The second haem domain of cytochrome c_5 is predicted to be the direct donor to AniA.

Compared to free tumbling electron partners, c_5 and AniA interaction has a significantly decreased degree of freedom. It should be able to translate this into a kinetic advantage of an increasing rate of appropriate collision between the two electron partners during the denitrification process. This conformation of tethered enzymes is unusual in nature. The limited dynamic movement of AniA may be able to increase the opportunity for interaction with electron donor cytochrome c_5 , but there is also decreased flexibility to form interactions with other potential electron carriers in a multi-branch respiratory chain.

These unusual tethers of Laz might also be involved in host immune response against *Neisseria*. The LCR of the Laz protein is similar to a repeat sequence motif known as H-8 antigen. H-8 epitope with the lipobox presented at the N-terminus is able to allow Laz protein surface to be exposed in the *Neisseria* species (Hong et al. 2006). It has been demonstrated that antibodies specific to H-8 antigen of Laz or Lip are able to block the serum-dependent killing of meningococcal cells (Ray et al. 2011). *Neisseria* Laz is the defence enzyme at the outer membrane involved in protection against external hydrogen peroxides and copper toxicity, and survival in cervical Epithelial cells (Wu et al. 2005). It was also found the azurin from *Pseudomonas aeruginosa* is important in protection from oxidative stress, but not involved in nitrite reduction (Vijgenboom et al. 1997).

In conclusion, unlike other gram negative bacteria redox cofactor - containing respiratory proteins located within periplasm, it is determined that *Neisseria* employ tethering of redox proteins to the outer membrane and c-type cytochromes to inner membrane in two membrane Gram negative cell envelopes. Tethering redox protein AniA to outer membrane could reduce the movement and orientation of the core enzyme and benefit the formation of electron transfer couples in the *Neisseria* species. The attachment of redox proteins (AniA and Laz) may also affect the exposure of the host to redox proteins in the host microbe interaction, resulting in affecting the host response to *Neisseria* infection.

Chapter 4

Biochemical basis of inter-protein electron transfer for nitrite reduction in denitrification in *N. meningitidis*:

4.1 Introduction:

N. meningitidis encodes a partial denitrification pathway under microaerobic conditions; nitrite is converted to nitrous oxide via nitric oxide by two important enzymes, nitrite reductase AniA and nitric reductase NorB. AniA is responsible for converting nitrite to nitric oxide in the system. The denitrification pathway is crucial for *N. meningitidis* to gain a growth advantage under microaerobic conditions and also enables the protection against exogenous nitric oxide in the environment (Rock et al. 2005).

The nitrite reductase protein in the meningococcus is predicted to be expressed by only one gene, the *aniA* gene (NMB1623). The resultant AniA protein is a di-copper containing nitrite reductase. Localization of AniA in the *Neisseria* species was determined to associate with outer membrane in our work (refers to Chapter 3) (Li et al. 2012).

There are three electron carrying low spin c-type cytochromes predicted to function as electron transfer proteins that carry electrons in the periplasm from the *bc₁* complex to the terminal reductase in the *Neisseria* species. These include monohaem periplasmic *c_x*, dihaem periplasmic *c₄* and inner membrane associated dihaem *c₅* (Deeudom et al.

2008). It is possible that some of these c-type cytochromes could have similar roles or overlapping functions in *N. meningitidis* respiratory chain. The differences in their biophysical and biochemical properties may give them advantages to function most effectively under different conditions or with particular redox partners.

Cytochrome c_5 is predicted to encode a membrane associated di-haem cytochrome with molecular mass of 28,755 Da. It is highly conserved among the *Neisseria* species. This protein has an N-terminal membrane span, and followed by two soluble domains each containing a covalently bound haem c. The two haem containing domains of cytochrome c_5 show high degree of similarity (more than 50% sequence identity at protein level) of sequence to each other. The localization of cytochrome c_5 was also determined as an inner membrane associated protein in chapter 3.

Cytochrome c_5 and nitrite reductase AniA are localized in different membranes. Under microaerobic condition, the c_5 deleted mutant of *N. meningitidis* strain failed to reduce nitrite (Deeudom et al. 2008), suggesting that c_5 is the important electron donor to AniA in *N. meningitidis*. It also indicates there is a novel mechanism of inter-membrane electron transfer in *N. meningitidis*. The width of the gram negative periplasm is about 170 Å based on electron microscopy measurements and on structural information of a homologous monohaem cytochrome c_5 from *Shewanella putrefaciens*. It is predicted that two globular haem domains of cytochrome c_5 may access 60 Å across the periplasm (Deeudom et al. 2008). The globular domain of nitrite reductase AniA is able to span approx. 45 Å. Based on the predicted width of cytochrome c_5 and AniA is 105 Å, it presents a potential problem for inter-protein

electron transfer for nitrite reduction in *Neisseria* species. The aim of this chapter was to investigate whether cytochrome c_5 donates electrons to AniA directly *in vitro*.

4.2 Purification and characterization of cytochrome c_5

4.2.1 Construction and purification of cytochrome c_5

The purpose was to produce a large amount of stable soluble cytochrome c_5 to allow kinetics of electron transfer to be studied. In order to get soluble cytochrome c_5 protein, the gene was cloned into a pET vector and over-expression of cytochrome c_5 achieved in *E. coli*

Recombinant expression of cytochrome c_5 was performed in *E. coli* expression strain BL21 λ DE3 transformed with the pST2 plasmid to allow for the cytochrome to be expressed correctly. *E. coli* was routinely cultured in AI medium or on LB plates, supplemented with desired antibiotics. Broth culture were harvested and sonicated. Total extract needs to be filtered before applying to the column. The soluble fraction was applied to a nickel affinity column, which was used to isolate the target protein with His tag. The desired protein was confirmed by SDS-PAGE analysis (Figure 4.1). However, purity index soluble cytochrome c_5 is low and in a combination with other unspecific proteins following Ni affinity chromatography. As pI of cytochrome c_5 is 5.88, cytochrome c_5 was further purified by anion exchange chromatography. The desired outcome of anion exchange chromatography contains two major proteins of 27 kDa and 30 kDa. (Figure 4.1) The purified cytochrome c_5 always showed this feature.

Electrospray mass spectrometry revealed that the majority of the soluble cytochrome c_5 has molecular mass of 24801.5996 in 50mM Tris pH7.5 (Figure 4.2). If the cleavage of mature protein is between Proline (P) and Valine (V), predicted molecular mass of soluble cytochrome c_5 is about 24802Da (23570Da + two haems 1223Da). This corresponded correctly to the molecular mass of cytochrome c_5 protein with His tag and two covalently attached haems (24801.5996Da). If the cleavage of mature protein is between Methionine (M) and Glycine (G), predicted molecular mass of soluble cytochrome is about 24163Da (22940.47Da + two haems 1223Da). This is close to the molecular mass of a minor part of the cytochrome c_5 protein observed in mass spectrometry, in which the protein with His tag and two covalently attached haems yields a theoretical mass of 24181.5996Da. Other predictions for proteolytic cleavage compared to molecular mass measured by mass spectrometry are summarized in Figure 4.2 a.

It is presumed that random proteolytic cleavage of the soluble cytochrome c_5 occurs, and these water-soluble cleavage products are purified chromatographically. In addition, there is still some holo-cytochrome c_5 remaining in insoluble fractions following overexpression. However, in order to work with the insoluble cytochrome c_5 , detergent needed to be introduced into purification steps. We decided to purify the fortuitously soluble protein fraction, as it is easier to work with.

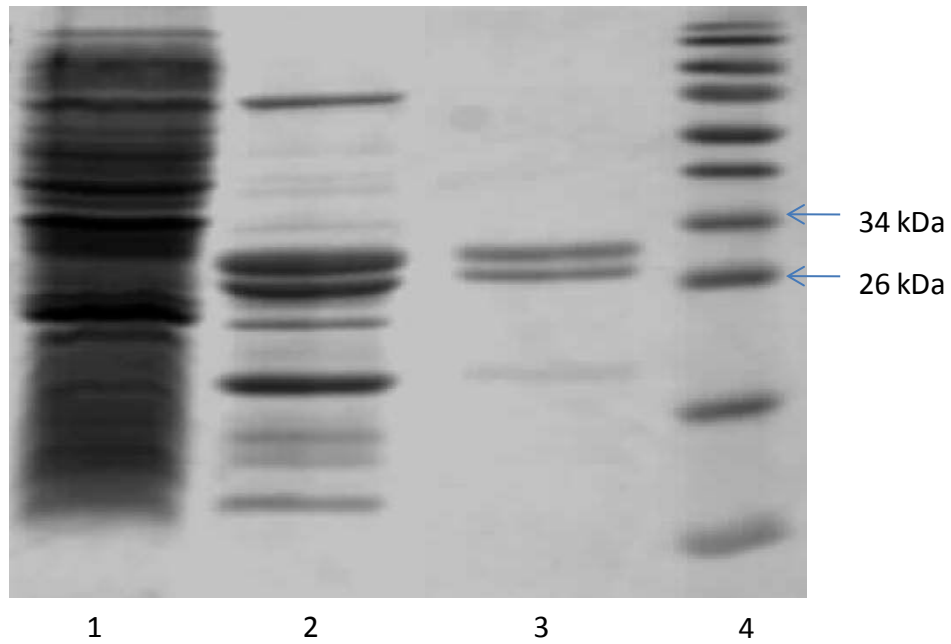


Figure 4.1 SDS-PAGE analysis of cytochrome c_5 from each step of purification process. Molecular weight of c_5 is about 27-30 kDa. 1: *E. coli* crude extract; 2: c_5 purified by Ni-His column; 3: c_5 purified by anion exchange column; 4: Protein ladder.

a.

MKQLRDNKAQGSALFTLVSGIVIVIAVLYFLIKLAGSGSFGDVDATTEAATQTRIQ↓P↓VGQ↓L
TM↓GDGIPVGERQGEQIFGKICIQCHAADSNVPNAPKLEHNGDWAPRIAQGFDTLQHALN
GFNAMPAKGGAADLTDQELKRAITYMANKSGGSFPNPDEAAPADNAASGTASAPADSAAPAE
AKAEDKGAAAPAVGVDGKKVFEATCQVCHGGSSIPGIPGIGKKDDWAPRIKKGKETLHKHALEG
FNAMPAKGGNAGLSDDEVKAAVDYMANQSGAKFHHHHHH

b.

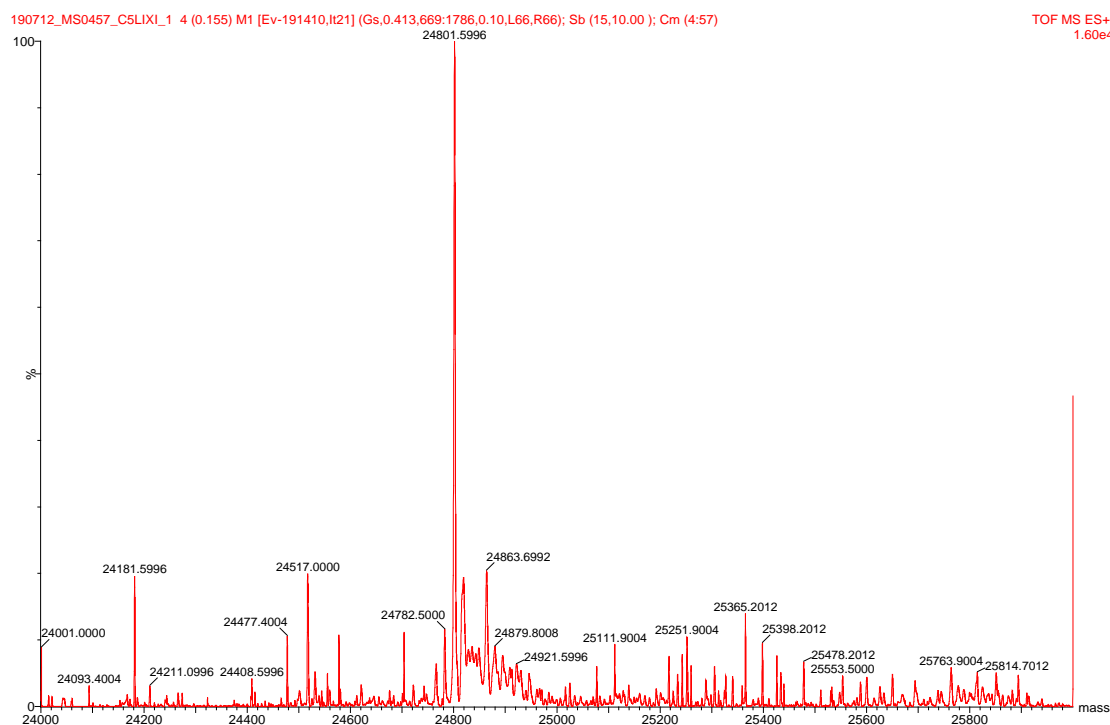


Figure 4.2 Molecular mass of soluble c_5 detected by electrospray mass spectrometry. a. Primary structure of expressed soluble cytochrome c_5 is highlighted in yellow color. Haem domains with haem-binding sites are underlined. Red and blue arrows are potential cleavage sites. b. Molecular mass of cytochrome c_5 detected by electrospray mass spectrometry. The major fraction of the soluble cytochrome c_5 has a molecular mass of 24801.5996Da.

4.2.2. Characterization of cytochrome c_5

4.2.2.1 Spectra properties of reduced and oxidized cytochrome c_5

Purified cytochrome c_5 was found to be in the reduced form as cytochrome c_5 shows the Soret band at 417nm and β and α bands at 523nm and 554nm respectively. When an oxidant was added, the Soret band moves to 406nm, and α and β band become one broad feature, as is typical for low spin c-type cytochromes. (Figure 4.3)

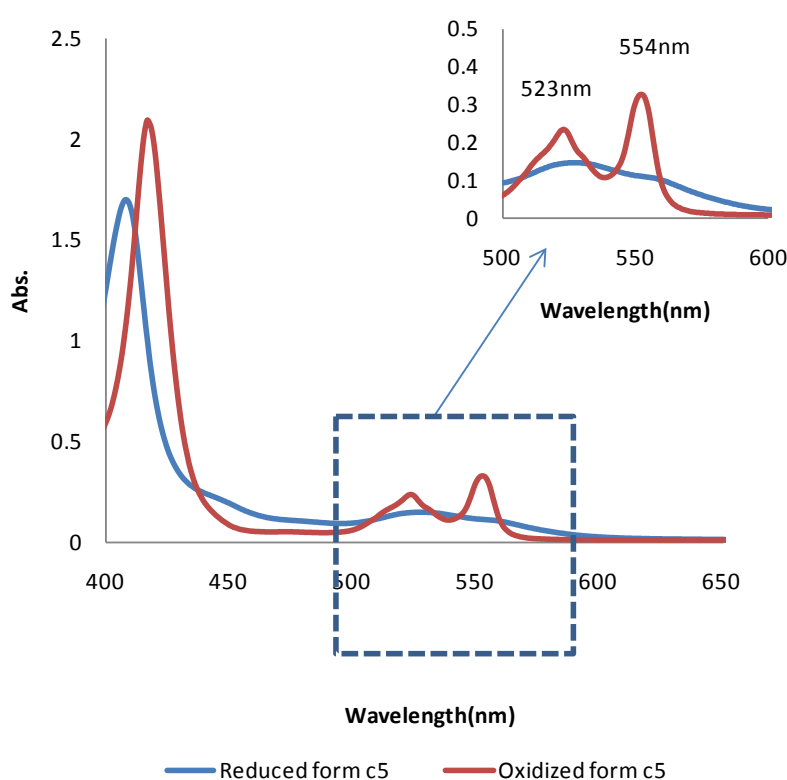


Figure 4.3: Absorption spectra of purified cytochrome c_5 : spectra were recorded at room temperature in 50mM Tris buffer (pH7.5). The oxidized (blue line) and reduced (red line) state shown absorbance peak at 406nm in oxidized form, and at 417nm, 523nm, 554 nm in the reduced form. The insert figure shows a zoom in on the α and β bands of the spectrum. The concentration of cytochrome c_5 is 2.24×10^{-3} mM.

4.2.2.2 Pyridine haemochrome to measure the concentration of cytochrome c_5

In order to determine the haem concentration in a cytochrome c_5 prep, the difference in absorbance at 550nm was measured under reduced versus oxidized conditions and compared to the known extinction coefficient of pyridine haemochrome.

For the particular preparation described below, the individual cytochrome c_5 concentration was 2.24×10^{-3} mM.

Reduced form cytochrome c_5 absorbance at 550 nm following pyridine haemochrome	0.055
Oxidized form cytochrome c_5 absorbance at 550 nm following pyridine haemochrome	0.006
$\Delta A = 0.055 - 0.006 = 0.049$ $\epsilon_{550} = 21.84(\text{R-O})$ $A = \epsilon cl \quad [c] = A / \epsilon l = 0.049 / 21.84 = 2.24 \times 10^{-3} \text{ mM}$ $[c]$ is the concentration of haem. The cytochrome protein was diluted 2-fold, and cytochrome c_5 is a dihaem protein. So the concentration of c_5 is 2.24×10^{-3} mM	

Calculation of extinction coefficient of reduced c_5 at 554nm (ϵ_{554R}) and extinction coefficient of reduced minus oxidised c_5 at 554nm ($\epsilon_{554(R-O)}$)

Reduced form cytochrome c_5 absorbance at 554 nm by dithionite	0.090
Oxidized form cytochrome c_5 absorbance at 554 nm by APS	0.055
$A_{(R-O)} = 0.090 - 0.055 = 0.035$ Extinction coefficients of reduced minus oxidized c_5 at 555nm $\epsilon_{554(R-O)} = \Delta A_{554} / cl = 0.035 / 2.24 \times 10^{-3} \text{ mM} \times 1 \text{ cm} = 15.6 \text{ mM}^{-1} \text{ cm}^{-1}$	
$A_R = 0.09$ Extinction coefficient of reduced c_5 at 554nm $\epsilon_{554R} = A_R / cl = 0.09 / 2.24 \times 10^{-3} \text{ mM} \times 1 \text{ cm} = 40.2 \text{ mM}^{-1} \text{ cm}^{-1}$	

These values were subsequently used to measure cytochrome c_5 concentration in other protein preparations.

4.3 Purification and characterization of nitrite reductase AniA

N. meningitidis AniA was expressed as a soluble protein by subcloning only the region following the signal peptidase site, downstream of a periplasmic leader sequence in the pET22b+ expression vector resulting in a stable genetic construct (designed by Dr. Melanie Thomson). The pET22b+ vector which has *peIB* leader sequence allows desired protein targeting to the periplasm of the BL21 (λ)DE3 expression strain. Soluble AniA was extracted from *E. coli* strain BL21 (λ)DE3 by the periplasm extraction method (described in Material and Method section). The AniA periplasmic extract was further purified by anion exchange column chromatography, as the predicted pI of truncated AniA is predicted to be 5.17. AniA protein eluted at approximately 250 mM NaCl when chromatography was conducted over a gradient of 0-500mM NaCl in 50mM Tris pH 7.5.

The molecular weight of soluble AniA protein on 15% SDS-PAGE gel is approximately 50 kDa (Figure 4.4). The predicted molecular weight of the truncated AniA is 26,981 Da. The anomalous running of AniA copper type nitrite reductase has been previously observed (Dr. Melanie Thomson, PhD thesis, unpublished data) and always shown higher molecular weight in SDS-PAGE than predicted. The visible spectrum of AniA as prepared is the oxidised form and characterized by absorbance maxima of 460 and 598 nm consistent with the blue color of sAniA in 50mM Tris buffer. In reduced form, AniA exhibits very low absorption and is colorless (Figure 4.5).

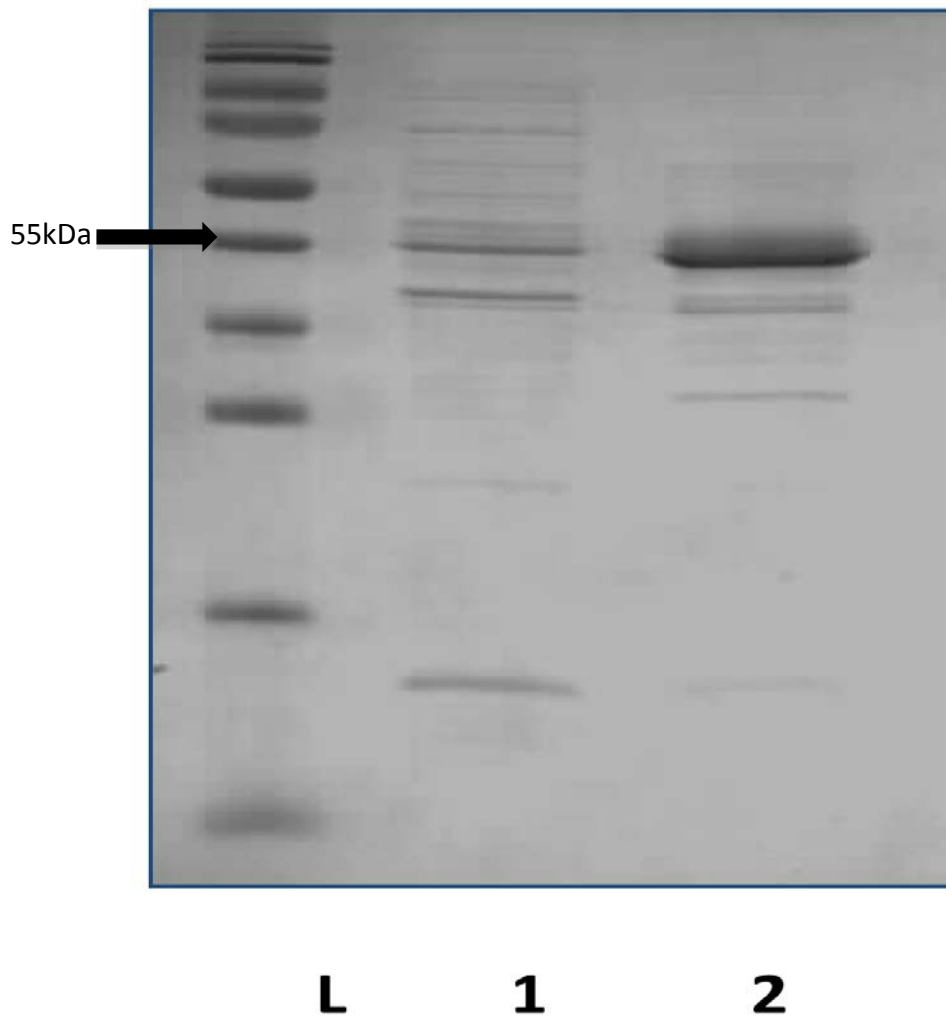


Figure 4.4: SDS-PAGE analysis of Anion exchange chromatography fractions of crude periplasmic extract and purified AniA. AniA has predicted MW approx. 55 kDa. Lane 1 is *E. coli* periplasmic crude extraction, lane 2 is purified AniA.

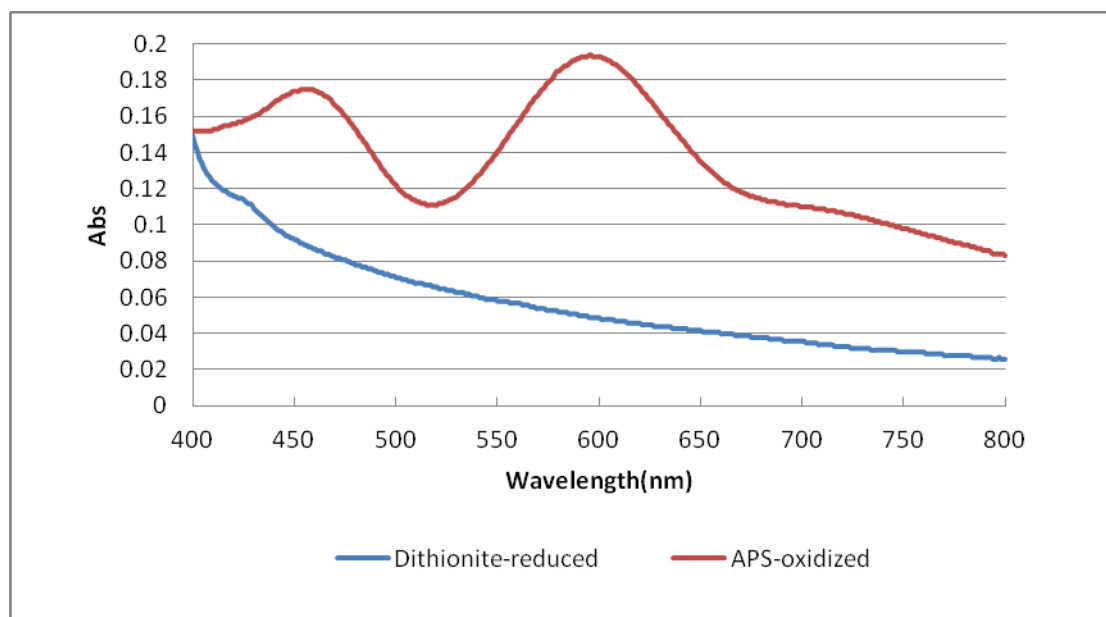


Figure 4.5: Spectral features of reduced and oxidized AniA by UV-VIS spectroscopy. Blue copper proteins absorb visible light around 600 nm. Oxidized AniA exhibits broad absorption with maximum absorption at 598 nm and 460 nm (red line). Reduced AniA exhibits very low absorption (blue line). The concentration of AniA is 516.8 μ M.

4.4 Steady state cytochrome c_5 nitrite reductase AniA interaction:

The purpose was to identify any role of cytochrome c_5 as an electron donor to AniA nitrite reductase. Cytochrome c_5 and nitrite reductase AniA were expressed and purified separately. Cytochrome c_5 as prepared is in the reduced form, AniA is kept in the oxidized form. The oxidation of cytochrome c_5 by AniA nitrite reductase was observed in this work.

Spectral analysis of reduced c_5 and oxidized AniA interaction was measured between 350 nm-650nm by spectrophotometer. Blue line (Control) is the reduced c_5 with water. Red line (Test) is the reduced cytochrome c_5 mixed with AniA. Green line is the absorbance difference between cytochrome c_5 with and without AniA. Upon adding AniA nitrite reductase, the absorbance difference shows an increase at 402nm, there was a relative decreased absorbance at 520nm and 555nm (Figure 4.6).

The observed absorbance differences are due to the oxidation of cytochrome c_5 and the concomitant reduction of AniA is not seen, presumably due to the broad nature and relatively low absorbance of AniA spectra compared to cytochrome c_5 . The absorbance difference changes the most at 402nm. It indicates that reduced cytochrome c_5 has been oxidized by AniA.

The result supports the idea that reduced cytochrome c_5 can be oxidized by nitrite reductase AniA directly. To test the kinetic competence of this interaction in supporting electron flow to nitrite reduction, the interaction between the two redox proteins was further examined by stopped flow kinetics.

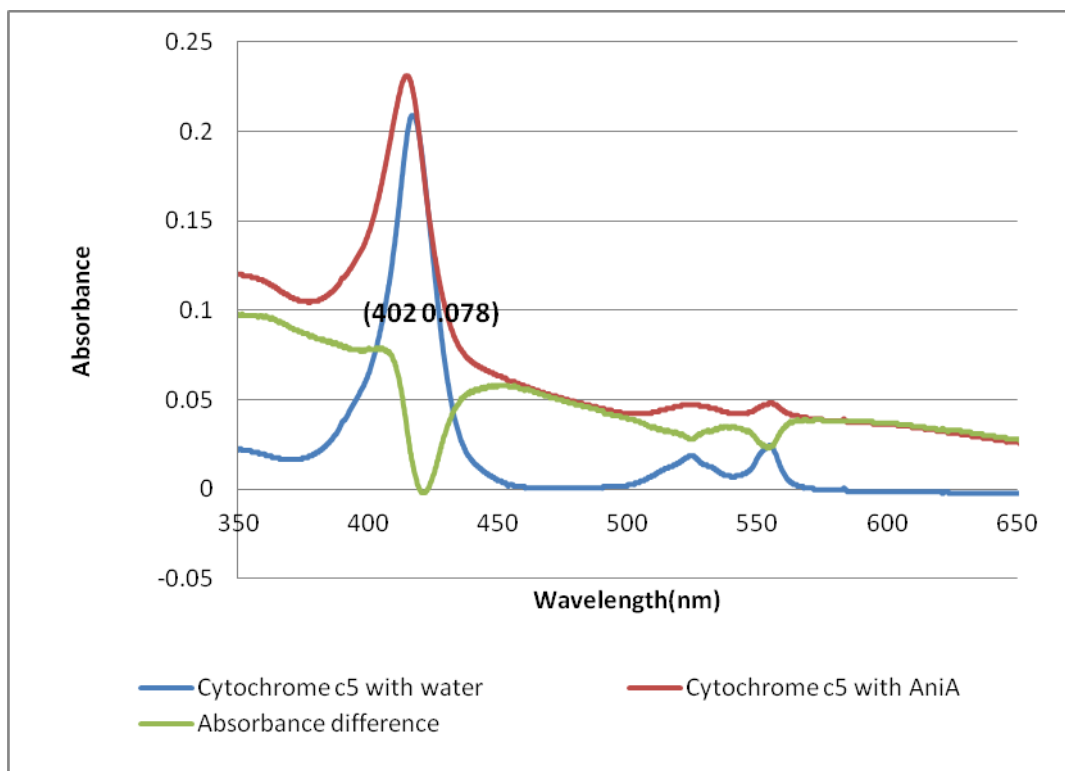


Figure 4.6: Spectral analysis of reduced c_5 and oxidized AniA interaction is measured between 350nm-650nm. The spectra of 500 μ l of 6.2 μ M reduced c_5 mixed with 500 μ l of 34 μ M oxidized AniA (red line); Control the spectra of 500 μ l of 6.2 μ M reduced c_5 with 500 μ l of water. Green line is the absorbance difference. The absorbance change shown an increase at 402nm.

4.5 Stopped flow kinetics of cytochrome c_5 and nitrite reductase AniA interaction:

4.5.1 The second order electron transfer rate constant between cytochrome c_5 and nitrite reductase AniA

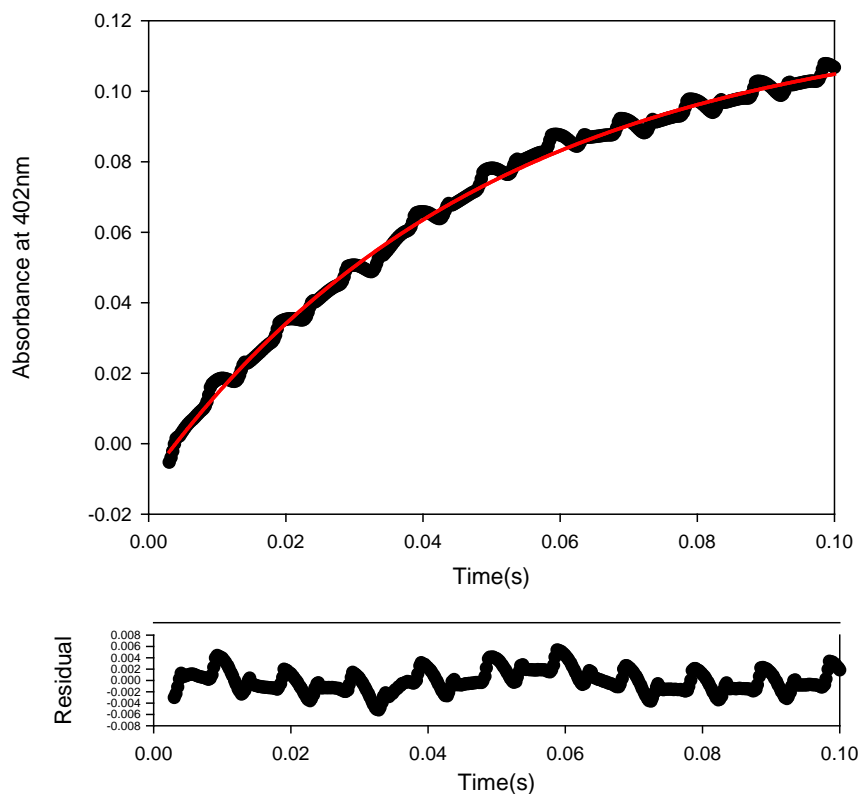
To investigate the kinetic relationship between nitrite reductase AniA and cytochrome c_5 , the formation of a functional electron transfer complex between these two proteins was analyzed by stopped-flow kinetics.

The kinetics of electron transfer from the reduced cytochrome c_5 to oxidized AniA was monitored at a wavelength of 402nm which had been previously determined by steady state experiments. To keep the pseudo first order, the concentration of AniA (from 33 μM to 132 μM) is always in large excess over the concentration of c_5 (7.5 μM). 1000 data points were collected for 1s in each stopped-flow experiment. By using the data over a short time period (6ms-100ms) we can measure a single rate constant using a 3 parameter single exponential rise to maximum function ($f=y_0+a*(1-\exp(-b*x))$) by Sigmaplot (Figure 4.7a). The second order electron transfer rate constant between the two proteins was estimated from the slope of the plots of AniA concentration versus $K_{\text{obs}}(\text{s}^{-1})$ (Figure 4.7b). The rapid increase of the absorbance is due to the oxidation of cytochrome c_5 and concomitant reduction of AniA.

The second order electron transfer rate constant between the two proteins is $(1.535 \pm 0.0114) \times 10^5 \text{M}^{-1} \text{s}^{-1}$, strongly supporting the idea that inner membrane

cytochrome c_5 interacts functionally with outer membrane associated nitrite reductase AniA as an electron donor.

a.



b.

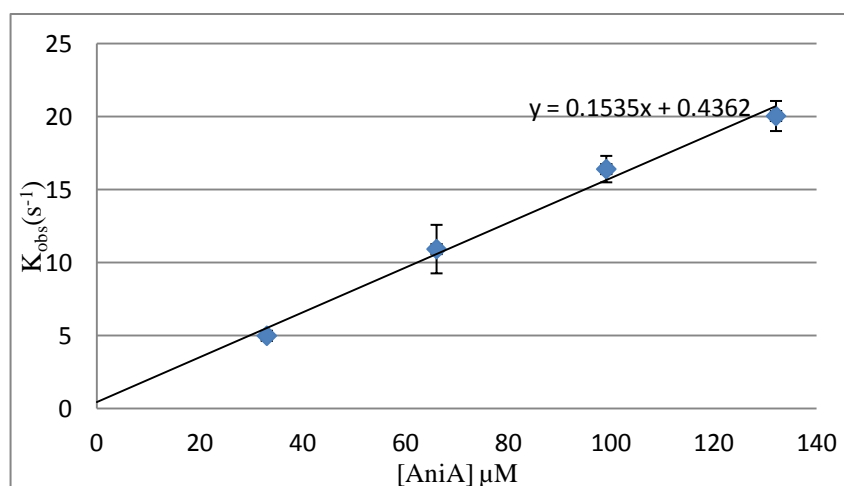


Figure 4.7: The electron-transfer between AniA and cytochrome c_5 was performed in 50mM Tris(pH 7.5). a. Stopped-flow kinetics of inter-protein electron-transfer reaction from reduced cytochrome c_5 to AniA. The black line

represents the observed data; red line is a fitting curve.

b. Plots of $K_{\text{obs}}s^{-1}$ vs. AniA concentrations (μM). The 2nd order electron transfer rate constant between the two proteins is $(1.535 \pm 0.0114) \times 10^5 \text{M}^{-1} \text{s}^{-1}$. The concentration of AniA (from 33 μM to 132 μM) is always in large excess over the concentration of c_5 (7.5 μM). Error bars denote standard deviation.

4.5.2 Salt dependence of cytochrome c_5 and AniA interaction:

The physiologically relevant salt concentration of human blood serum and saliva are approximately 140mM NaCl and 40mM NaCl, respectively (White et al. 1955). If electron transportation between the two partners persists under high salt conditions, this would support the notion that cytochrome c_5 is the direct electron donor to AniA under physiologically relevant conditions.

Stopped flow experiments were carried out as before, except with the following adaptation both of cytochrome c_5 (7.5 μM) and AniA (192 μM) were buffer-exchanged into different salt concentration buffers (0mM NaCl 50mM Tris pH7.5; 62.5mM NaCl 50mM Tris pH7.5; 125mM NaCl 50mM Tris pH7.5; 250mM NaCl 50mM Tris pH7.5; 500mM NaCl 50mM Tris pH 7.5). The protein concentrations of cytochrome c_5 and nitrite reductase AniA in different buffers were kept the same.

It was found that there is a limited effect on interaction between two partners (Figure 4.8). Electron transfer rate ($K_{\text{obs}} s^{-1}$) between cytochrome c_5 and AniA with no salt

present (35 s^{-1}) was only 30% higher than experiments performed in same buffer with salt present (from 62.5 mM-500mM NaCl). Electron transfer between these two partners can occur at a range of different salt concentrations.

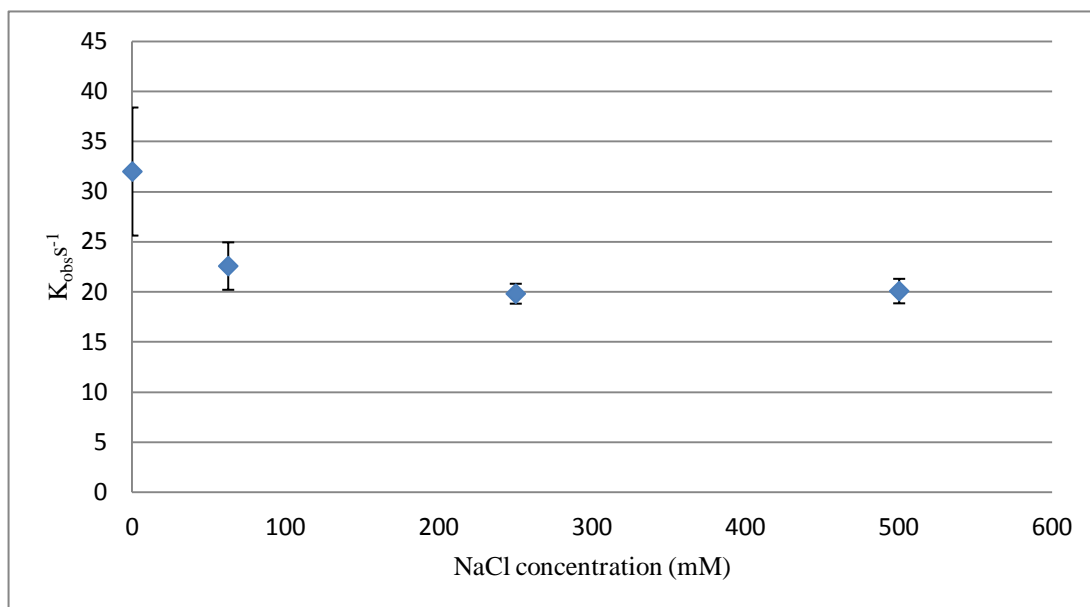


Figure 4.8: The salt dependence of cytochrome c_5 and AniA interaction was performed in 50mM Tris(pH 7.5)with salt present(0mM-500mM) : Plots of $K_{\text{obs}} \text{ s}^{-1}$ at different salt concentrations(mM). Stopped-flow kinetics of inter-protein electron-transfer reaction from reduced cytochrome c_5 to AniA was performed at different salt concentrations. The concentration of cytochrome c_5 ($7.5 \mu\text{M}$) and AniA ($192 \mu\text{M}$) were always kept the same at different buffer conditions. Error bars denote standard deviation.

4.5.3 pH dependence of cytochrome *c*₅ and AniA interaction:

It has been shown that the binding of NO₂⁻ to isolated nitrite reductase is pH dependent, the binding constant becoming 10-fold tighter as the pH is lowered from 7.5 to 5.2. In addition, the pH-dependence of copper type nitrite reductase activity is biphasic with an optimum at 5.2 and a plateau between 6.1 and 5.8, indicating the involvement of at least two protonation events (Stefanelli et al. 2008). The aim of this work is to check the pH dependence of electron transfer under different conditions.

Stopped flow experiments were carried out as before, except with the following adaptation: cytochrome *c*₅ (7.5 μM) and AniA (40 μM) were buffer-exchanged into different pH buffers (50mM HEPES pH5.5; 50mM HEPES pH6.5; 50mM Tris pH7.5; 50mM Tris pH 8.5). The protein concentrations of cytochrome *c*₅ and nitrite reductase AniA in different buffers were kept the same.

It is found that pH has a limited effect on interaction between two partners (Figure 4.9). Electron transfer rate ($K_{\text{obs}} \text{ s}^{-1}$) between cytochrome *c*₅ and AniA with pH 7.5 was not different than experiments performed in same buffer with different pH assays (from pH 5.5-8.5). Electron transfer between these two partners can occur at a range of different pH conditions.

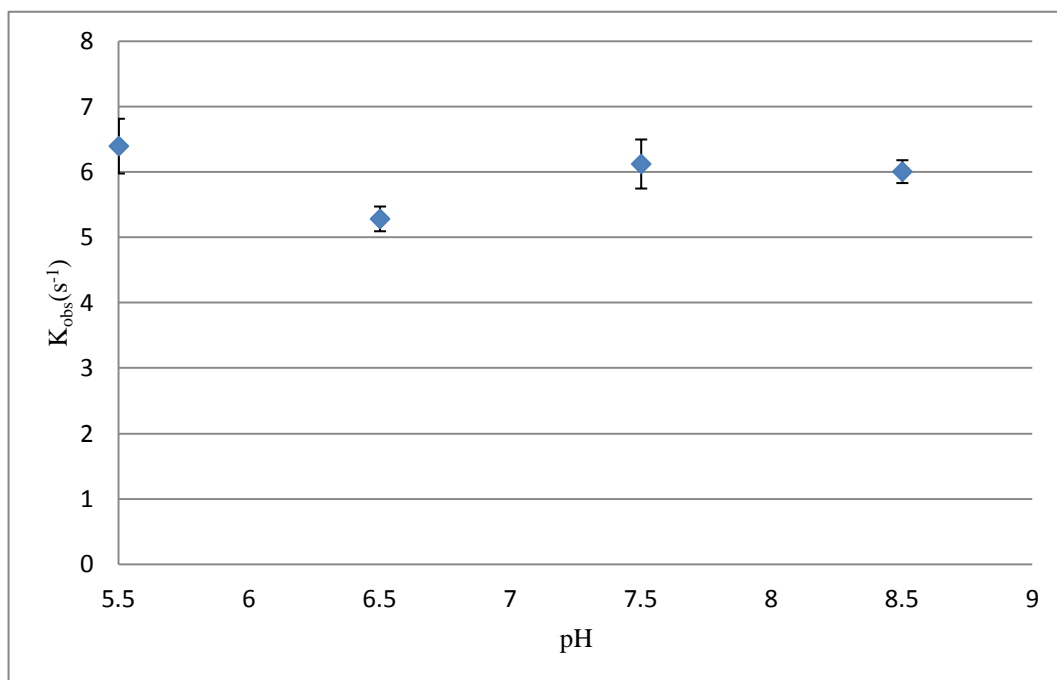


Figure 4.9: pH-dependence of AniA and cytochrome c_5 interaction was performed in 50 mM Tris with vary pH conditions (5.5-8.5): Plots of $K_{\text{obs}}(\text{s}^{-1})$ at different pH conditions. Stopped-flow kinetics of inter-protein electron-transfer reaction from reduced cytochrome c_5 to AniA at pH conditions. The concentration of cytochrome c_5 (7.5 μM) and AniA (40 μM) were always kept the same at different buffer conditions. Error bars denote standard deviation.

4.6: Over-expression of monohaem domains of cytochrome c_5 :

The purpose was to produce a large amount of soluble first haem domain and second haem domain of cytochrome c_5 for further kinetics studies.

As previously described, cytochrome c_5 contains a cytoplasmic domain, a membrane spanning domain, and two globular haem periplasmic domains. The amino acid residue 1-32 are predicted to be either exposed in cytoplasm or located in cytoplasmic membrane. The first haem binding domain was highlighted in grey color; the second haem binding domain was highlighted in blue color. 1st haem domain of c_5 is encoded by 134 amino acids, 2nd haem domain of c_5 encoded by 100 amino acids (Table 4.1). In order to produce soluble first haem domain of cytochrome c_5 (1st Hc₅) and second haem domain of cytochrome c_5 (2nd Hc₅) protein, cloning of 1st Hc₅ and 2nd Hc₅ gene and over expression of 1st Hc₅ and 2nd Hc₅ protein in *E. coli* have been done in this work (Figure 4.10).

Two haem domains of cytochrome c_5 were expressed in periplasm separately. First haem domain gene encoding 134 amino acids and second haem domain gene encoding 100 amino acids were cloned and expressed in *E. coli*. The cytochrome c_5 gene from genomic DNA of *N. meningitidis* MC58 amplified by PCR using GoTaq polymerase. Restriction enzyme sites were included towards the ends of primers in order to facilitate insertion to pET22b(+) vector.

pET22b(+) vectors were digested with MscI and XhoI to generate a sticky end and a blunt end for insertion. PCR products were purified and digested with PvuII and XhoI

to generate a sticky end and a blunt end with desired gene (Figure 4.10 and 4.12). The digested PCR products were then ligated into pET22b(+) vectors.

This results in a stable genetic construct where the monohaem domain is fused to a periplasmic leader sequence. The ligated plasmid were transformed to *E. coli* strain DH5 α . The monohaem domains have been successfully inserted into pET22b+ vector as confirmed by colony PCR (Figure 4.11 and 4.13) and DNA sequencing.

Recombinant expression of monohaem of cytochrome c_5 was performed in *E. coli* expression strain BL21 λ DE3 (pST2) cells. The expression procedure is the same as the expression of dihaem cytochrome c_5 protein.

N. meningitidis $1^{\text{st}}\text{H } c_5$ and $2^{\text{nd}}\text{H } c_5$ were highly expressed in *E. coli* and purified in a soluble form and yielded a large amount of soluble pure protein under aerobic conditions. Soluble $2^{\text{nd}}\text{H}c_5$ occurred in a single isoform as judged by SDS-PAGE (Figure 4.14 b). However, soluble $1^{\text{st}}\text{H } c_5$ occurred in two isoforms as also judged by SDS-PAGE (Figure 4.14 a). Despite appearing as two bands on the gel, there is only one peak of 14973.8994 Da detectable by MS, compared with a predicted mass of 14972.5 Da (Figure 4.15).

```

MKQLRDNKAQGSALFTLVSGIVIVIAVLYFLIKLAGSGSFGDV DATTEAATQTRIQPVGQLTMG
DGIPVGERQGEQIFGKICIQCHAADSNVNPAPKLEHNGDWAPRIAQGFDTL FQHALNGFNA
MPAKGGAADLTDQELKRAITYMANKSGGSFPNPDEAAPADNAASGTASAPADSAAPAEAKA
EDKGAAAPAVGVDGKKVFEATCQVCHGGSSIPGIPGIGKKDDWAPRIKKGKETLHKHALEGFN
AMPAKGGNAGLSDDDEVKAAVDYMANQSGAKF

```

Table 4.1: Primary sequences of first haem domain and second haem domain of cytochrome c_5 from *N. meningitidis* MC58. 134 amino acid highlighted in gray first haem domain of cytochrome c_5 ; 100 amino acid highlighted in blue second haem domain of cytochrome c_5 . Two haem binding sites are underlined.

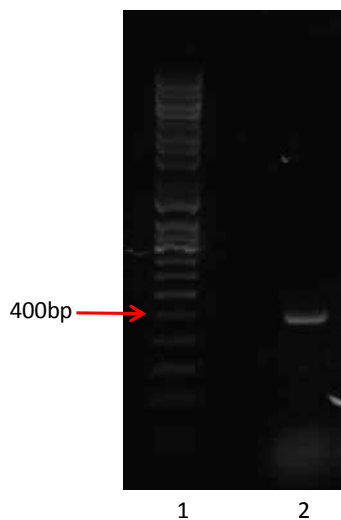


Figure 4.10: PCR product of first haem domain of cytochrome c_5 with flanking regions. The first haem domain of cytochrome c_5 exhibits size of 402 bp. Lane 1 is Q-step 4 DNA ladder; lane 2 is 1st haem of cytochrome c_5 .

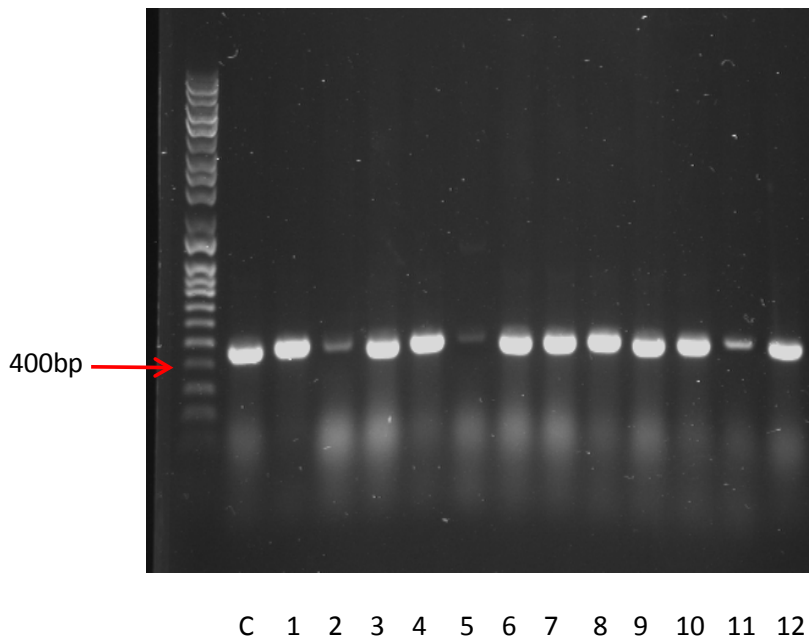


Figure 4.11: Colony PCR screens of *E. coli* DH5 α transformants for pET22b+ plasmid with insertion of first haem domain of cytochrome c_5 gene. C is control, *N. meningitidis* MC58 used as template in PCR cycle; 1-12 are the colony number 1-12.

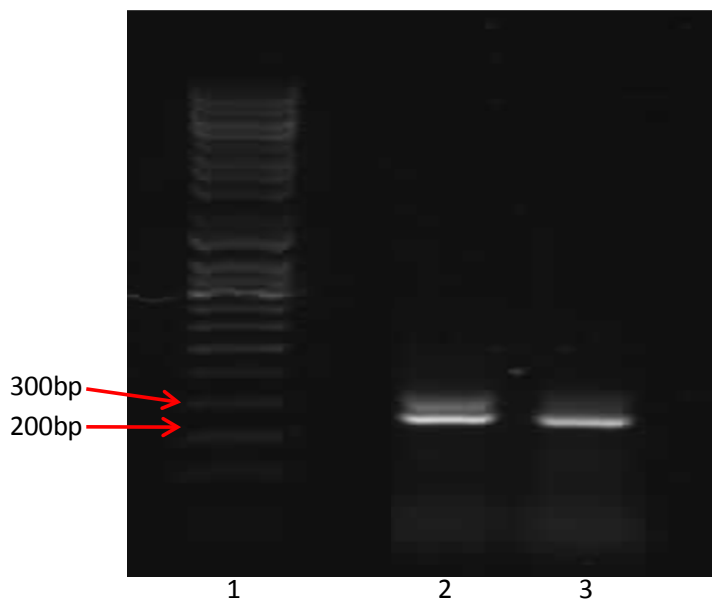


Figure 4.12: PCR product of the second haem domain of cytochrome c_5 with flanking regions. The second haem domain of cytochrome c_5 shows size of 264 bp. Lane 1 is Q-step 4 DNA ladder; lane 2&3 is the 2nd haem of cytochrome c_5 .

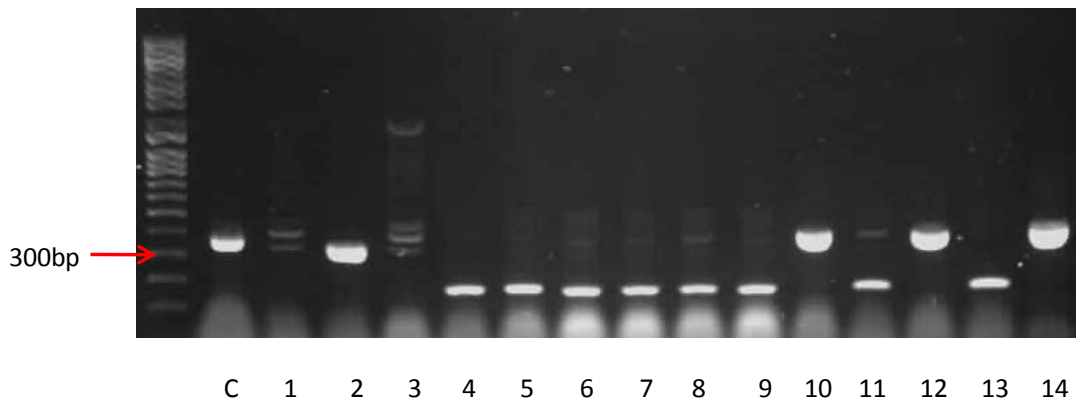


Figure 4.13: Colony PCR screen of *E. coli* DH5 α transformants for pET22b⁺ plasmid with insertion of second haem domain of cytochrome *c*₅ gene. C is control, *N. meningitidis* MC 58 used as template in PCR cycle; 1-14 are the colony number 1-14.

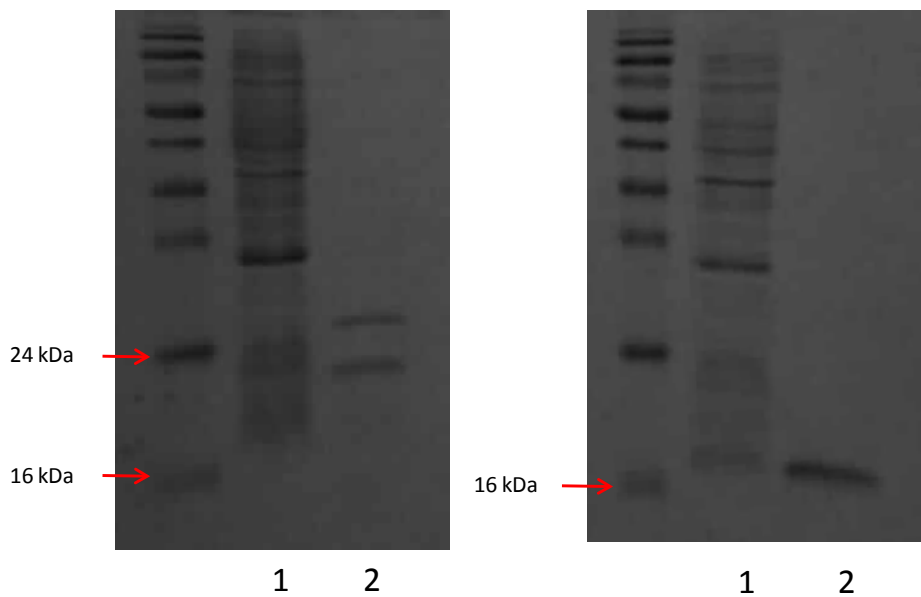
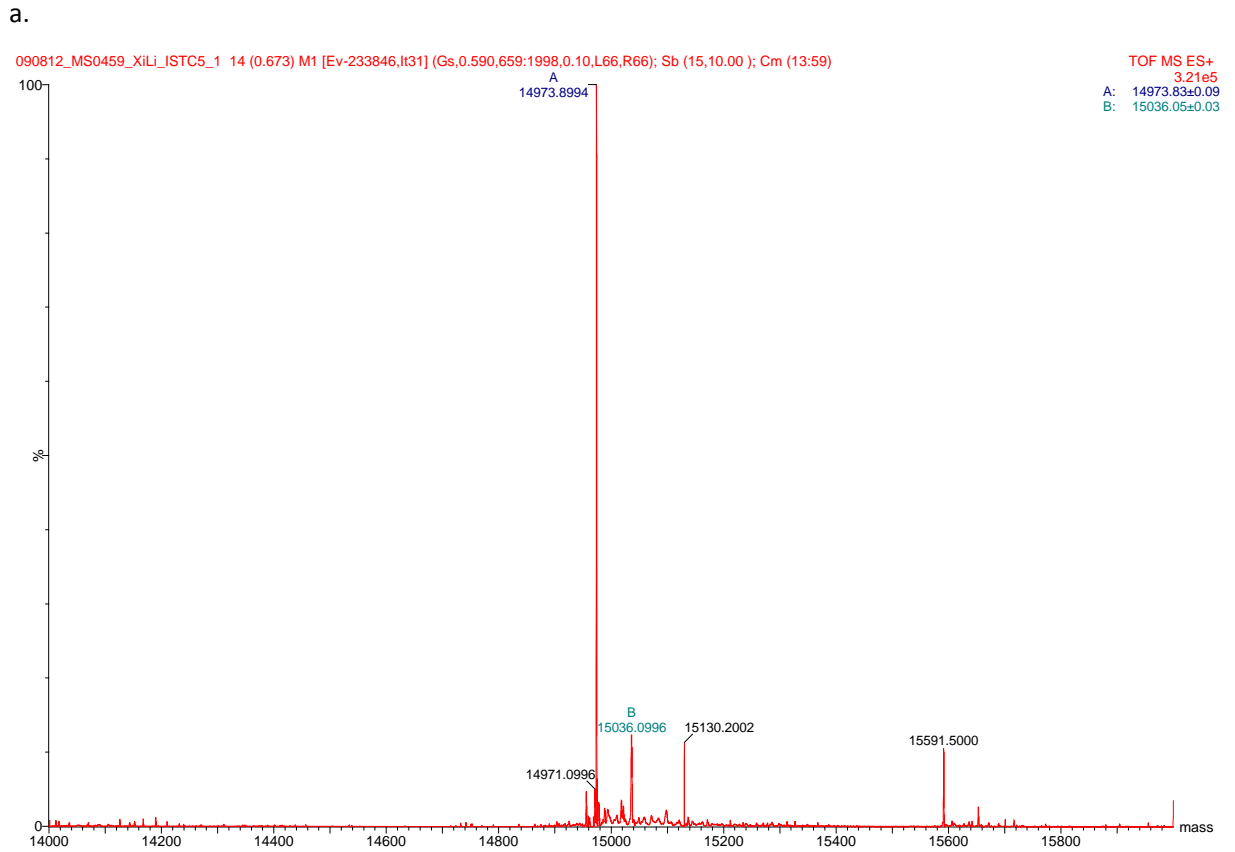


Figure 4.14: Expression of the 1st haem domain and the 2nd haem domain of cytochrome *c*₅ protein in *E. coli*. (a). Purified the 1st haem domain of *c*₅ from nickel affinity chromatography: 1 soluble crude extract 2. Purified the first haem domain of *c*₅; (b) purified the 2nd haem domain of *c*₅ from nickel affinity chromatography: 1 soluble crude extract 2. Purified the 2nd haem domain of *c*₅;



b.

HHHHHHAGSG SFGDVDATE AATQTRIQPV GQLTMGDGIP VGERQGEQIF GKICIQCHAA
 DSNVPNAPKL EHNGDWAPRI AQGFDTLFFQH ALNGFNAMPA KGGAADLTDQ ELKRAITYMA
 NKSGGSFPNP DEAAPA

Figure 4.15: Molecular mass of the first haem domain of cytochrome c_5 detected by electrospray mass spectroscopy. a. 1st haem domain of cytochrome c_5 has a molecular mass of 14973.8994 Da in 10 mM Tris buffer (pH7.5). b. Primary structure of first haem domain of cytochrome c_5 with N-terminal His tag (predicted molecular mass is 14972.5Da).

4.7: Stopped-flow kinetics of inter-protein electron transfer reaction from the reduced first haem domain and second haem domain of cytochrome c_5 to nitrite reductase AniA.

The aim is to investigate which haem-containing domain of cytochrome c_5 is the direct donor to nitrite reductase AniA in *N. meningitidis*. The formation of a functional electron transfer complex between these candidates (the first and the second haem domain of c_5) and AniA was analysed by stopped-flow kinetics.

4.7.1: Stopped-flow kinetics of the first haem domain of cytochrome c_5 and AniA interaction

If the first haem domain of cytochrome c_5 is the direct donor to nitrite reductase AniA, electron transportation between two partners should be able to persist under high salt conditions.

Stopped-flow kinetics were carried out as before, except with the following adaptation 1^{st}Hc_5 and AniA were buffer-exchanged into different salt concentration buffers (0mM NaCl 50mM Tris pH7.5; 62.5mM NaCl 50mM Tris pH7.5; 125mM NaCl 50mM Tris pH7.5; 250mM NaCl 50mM Tris pH7.5; 500mM NaCl 50mM Tris pH 7.5). The protein concentrations of reduced form 1^{st}Hc_5 (7.5 μM) and oxidized form AniA (35 μM) were always kept the same in vary buffers. It was found that there is no inter-protein electron transfer between 1^{st}Hc_5 and AniA with no salt present (A_{402} change less than 0.004) (Figure 4.16). With increasing salt concentration, there is still

no effect on the inter-protein electron transformation between 1stHc₅ and AniA.

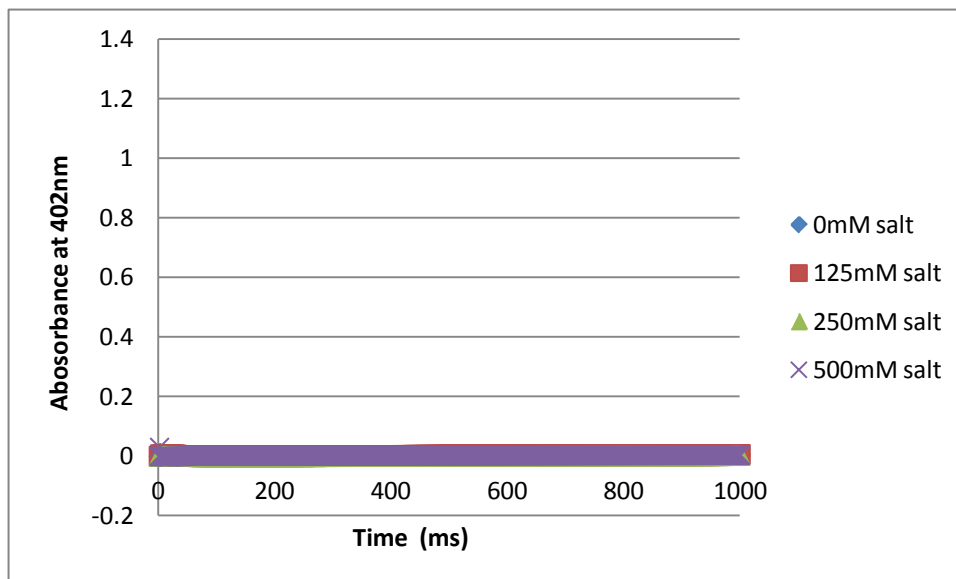


Figure 4.16: The salt dependence of first haem domain of cytochrome *c*₅ and AniA interaction was performed in 50mM Tris (pH 7.5) with salt present (0mM-500mM): Stopped-flow kinetics of inter-protein electron-transfer reaction from reduced first haem domain of cytochrome *c*₅ to AniA was performed at different salt concentrations. The protein concentrations of reduced form 1stHc₅ (7.5 μ M) and oxidized form AniA (35 μ M) were always kept the same at different salt conditions.

4.7.2 Stopped flow kinetics of second haem domain of cytochrome c_5 with AniA:

Second haem domain of cytochrome c_5 was predicted to donate electrons to AniA directly. To elucidate whether the second haem of cytochrome c_5 is the direct donor to AniA, the formation of a functional electron transfer complex between these two proteins was analysed in a stopped-flow experiment. The kinetics of electron transfer from the reduced 2^{nd}Hc_5 to oxidized AniA was monitored at a wavelength of 402nm, the same as c_5 and AniA stopped-flow kinetics. The concentration of 2^{nd}Hc_5 ($7.5 \mu\text{M}$) was kept the same as full length cytochrome c_5 . The concentration of AniA is from $8.5 \mu\text{M}$ to $35 \mu\text{M}$. The rapid increase of the absorbance is due to the oxidation of 2^{nd}Hc_5 and reduction of AniA (Figure 4.17). Second order rate constant was $2.8 \times 10^5 \text{ M}^{-1}\text{s}^{-1}$ is *approx.* 2 times faster than second order rate constant of inter-protein electron transfer between holo- c_5 and AniA. If the second haem domain of cytochrome c_5 is the direct donor to nitrite reductase AniA, electron transportation between two partners should persist under high salt conditions.

Stopped flow was carried out as before, except with the following adaptation second haem domain of cytochrome c_5 ($7.5 \mu\text{M}$) and AniA($30 \mu\text{M}$) were buffer-exchanged into different salt concentration buffers (0mM NaCl 50mM Tris pH7.5; 62.5mM NaCl 50mM Tris pH7.5; 125mM NaCl 50mM Tris pH7.5; 250mM NaCl 50mM Tris pH7.5; 500mM NaCl 50mM Tris pH 7.5). The protein concentrations of second haem domain

of cytochrome c_5 and nitrite reductase AniA in different buffers were always kept the same. It was found that with increasing salt concentration, there is limited effect on the inter-protein electron transfer between second haem domain of c_5 and AniA (Figure 4.18). Cytochrome c_5 is a membrane associated di-haem low spin c type cytochrome. The second order rate of electron transfer rate constant between $2^{\text{nd}}\text{H}c_5$ and AniA is $2.8 \times 10^5 \text{M}^{-1} \text{s}^{-1}$, strongly supporting the idea that second haem domain interacts functionally with nitrite reductase AniA as the electron donor.

First haem domain of cytochrome c_5 could not donate electrons to AniA directly. It suggests that first haem domain might be the electron donor to second haem domain.

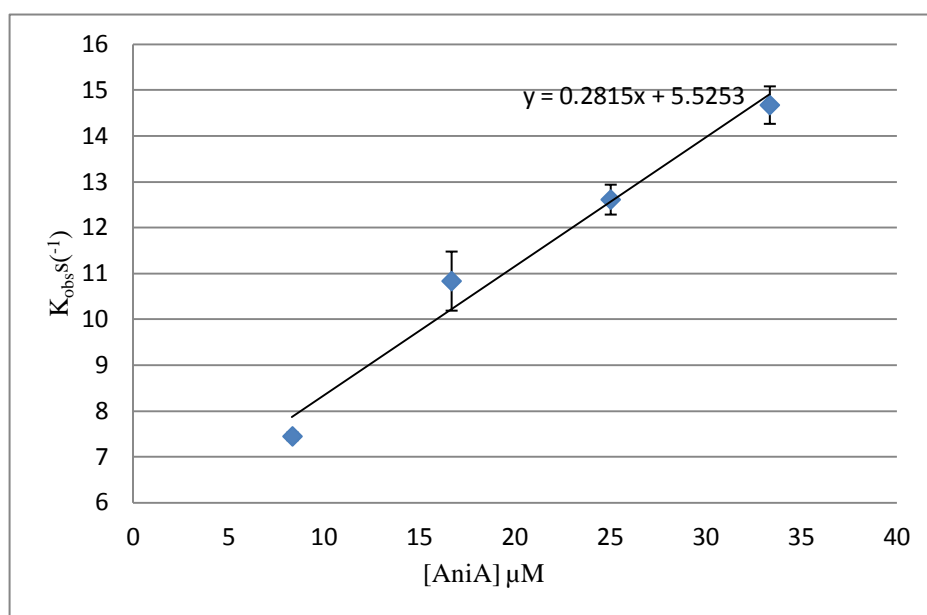


Figure 4.17: The electron-transfer between AniA and second haem domain of cytochrome c_5 was performed in 50mM Tris(PH7.5). Plots of K_{obs} (s^{-1}) vs. AniA concentration (μM). The 2^{nd} order electron transfer rate constant between the two proteins is $(2.8 \pm 0.0298) \times 10^6 \text{M}^{-1} \text{s}^{-1}$. The concentration of $2^{\text{nd}}\text{H}c_5$ ($7.5 \mu\text{M}$) is always kept the same as the full length cytochrome c_5 . The concentration of AniA is from $8.5 \mu\text{M}$ to

35 μM . Error bar denote standard deviation.

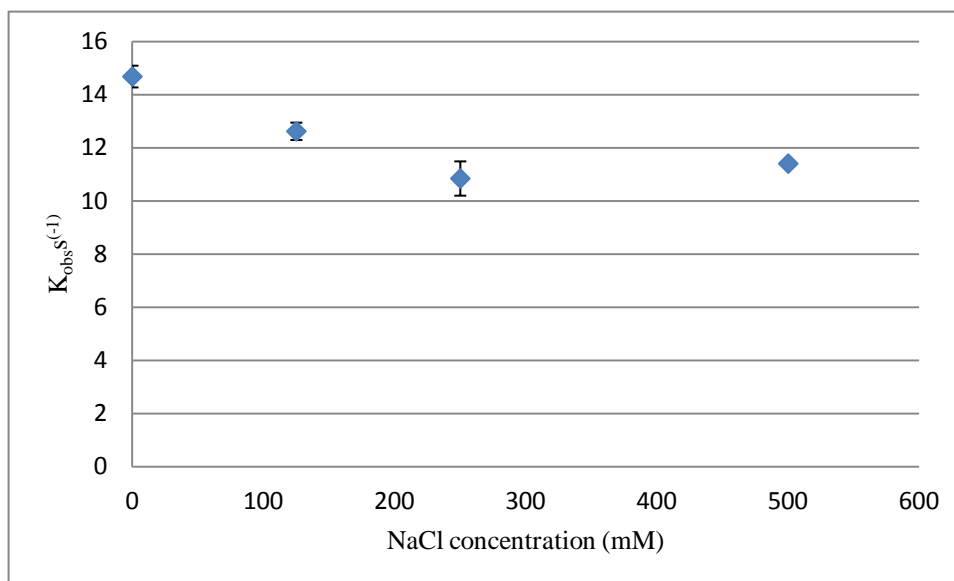


Figure 4.18: The salt dependence of the second haem domain of cytochrome c_5 and AniA interaction was performed in 50mM Tris(pH 7.5) with salt present (0mM-500mM): Plots of $K_{\text{obs}}(\text{s}^{-1})$ vs. salt concentration. Stopped-flow kinetics of inter-protein electron-transfer reaction from reduced second haem domain of cytochrome c_5 to AniA was performed at different salt concentrations. The concentration of second haem domain of cytochrome c_5 (7.5 μM) and AniA (30 μM) were always kept the same into different salt concentration buffers. Error bars denote standard deviation.

4.8: Over-expression of Cytochrome c_x and c_4 :

As the control experiment of c_5 and AniA nitrite reduction, c-type cytochrome c_x and c_4 were used to confirm the theory that specificity of c_5 and AniA redox partner interaction in nitrite reduction in *N. meningitidis*. Based on mutagenesis study, c_x and c_4 mutant strains could reduce nitrite at the similar rate as the wild type strain under denitrifying conditions (Deeudom et al. 2008). It suggests c_x and c_4 are not functioning as electron donor to nitrite reductase AniA in *N. meningitidis*. *N. meningitidis* c_x mutant and c_4 mutant strains have the significant deficiency in oxygen reduction, indicating both of cytochrome c_x and c_4 are important electron donors to terminal cytochrome oxidase cbb_3 complex. The purpose was to produce a large amount of stable soluble cytochrome c_x and c_4 for kinetics studies. If c_x or c_4 could not donate electrons to AniA or donate electrons to AniA at relatively low electron transfer rate, it indicates they are not involved in nitrite reduction in *N. meningitidis*.

In order to produce soluble cytochrome c_x protein, subcloning and over-expression of cytochrome c_x in *E. coli* have been done. The cytochrome c_x gene was originally cloned into the pETYSBLIC3C expression plasmid, which contains a His tag at its N-terminus. However, like cytochrome c_5 , soluble preparations of c_x appeared to lack an N-terminal His tag, presumably due to a cleavage of the mature protein in the expression process. Another His tag was introduced to the C-terminus of the cytochrome c_x gene. In a round of PCR cycles these primers anneal to *N. meningitidis* MC58 cytochrome c_x gene cloned in pETYSBLIC3C plasmid, replicating the plasmid DNA with a C-terminal His-tag insertion (Figure 4.19). Purification of cytochrome c_x

is visualized by SDS-PAGE and further confirmed by MS. The size of cytochrome c_x protein on 15% SDS-PAGE gel is approximately 13 kDa (Figure 4.20a). The predicted molecular weight of the processed c_x is 13.4 kDa. There is only one major peak of 13474.00 Da was detectable by MS (Figure 4.20b).

Cytochrome c_4 was ligated into pETYSBLIC3C expression plasmid. The successfully construct c_4 - pETYSBLIC3C was kindly donated by Dr. James Edwards. Soluble cytochrome c_4 was extracted from *E. coli* strain BL21 (λ)DE3(pST2) by periplasm extraction method. The c_4 periplasmic extract was further purified by cation exchange column chromatography, as the predicted pI of cytochrome c_4 is 9.25. Soluble c_4 protein was eluted at approximately 250 mM NaCl, when chromatography was conducted over a gradient of 0-500mM NaCl in 50mM Tris pH 7.5. Desired protein was confirmed by SDS-PAGE analysis (Figure 4.21). The size of cytochrome c_4 protein on 15% SDS-PAGE gel is approximately 20 kDa. The predicted molecular weight of the processed c_4 is 21989 Da. However, the purity of cytochrome c_4 needs to be improved in the future work.

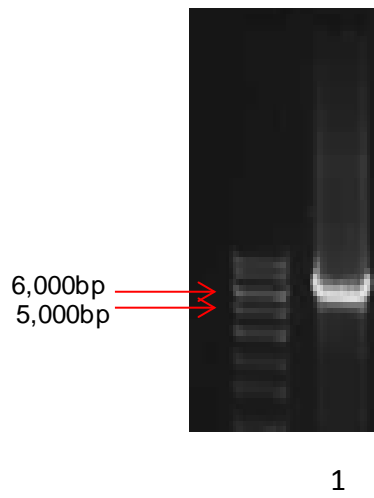
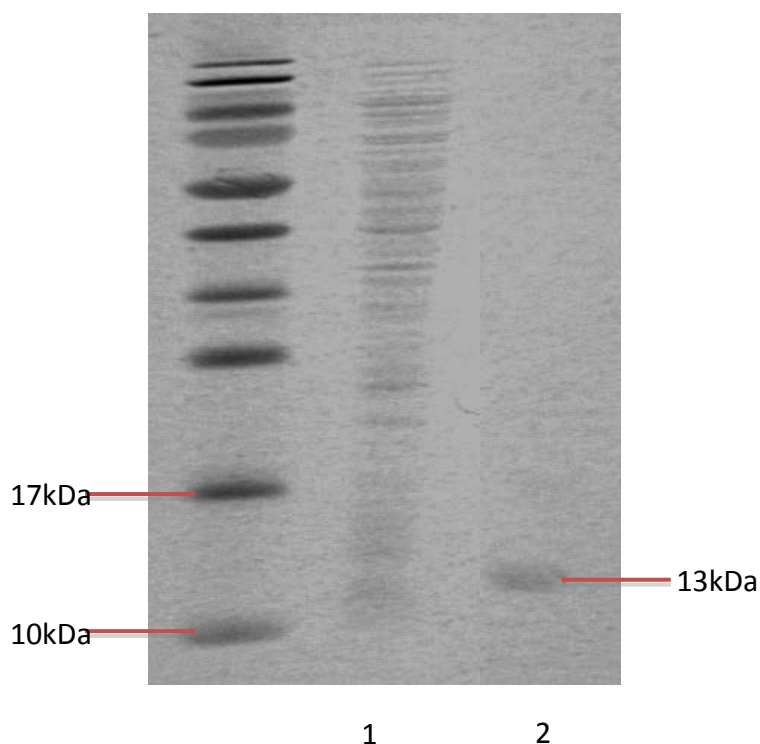


Figure 4.19: PCR product of plasmid c_x -pETYSBL3C. pETYSBL3C exhibits size of 6000bp. c_x gene exhibits size of 417bp. Lane 1 is the c_x -pETYSBL3C plasmid

a.



b.

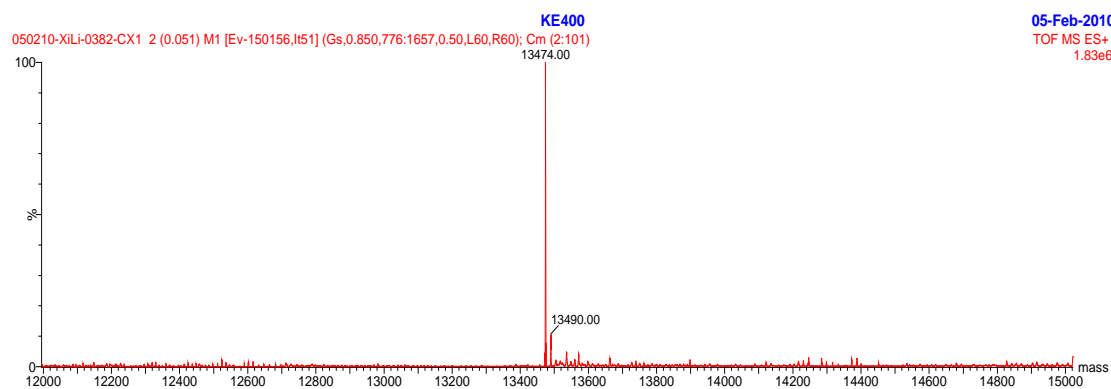


Figure 4.20: Purified soluble cytochrome c_x from nickel affinity chromatography: (a). Purified c_x from nickel affinity chromatography analyzed by SDS-PAGE: cytochrome c_x has a molecular mass of *approx.* 13 Da in 50 mM Tris buffer (pH7.5). 1: soluble crude extract; 2: purified cytochrome c_x (b). Molecular mass of cytochrome c_x detected by electrospray mass spectroscopy. Cytochrome c_x has a molecular weight of 13474.00Da (predicted molecular mass is 13.4kDa)

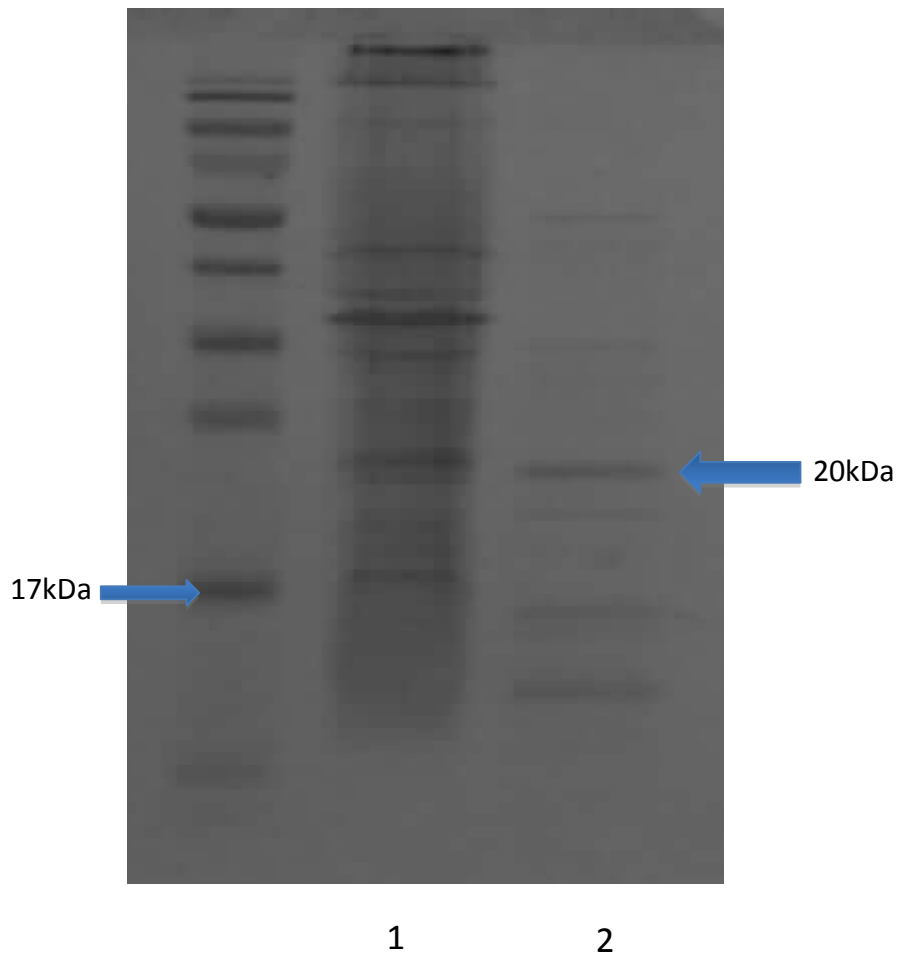


Figure 4.21: Purification of cytochrome c_4 protein in from ion exchange chromatography analyzed by SDS-PAGE: 1. Soluble cell crude extract; 2. Purified soluble cytochrome c_4 with molecular weight of approximately 20kDa.

4.9: Stopped-flow kinetics of inter-protein electron transfer reaction from reduced cytochrome c_x to nitrite reductase AniA.

If inter-protein electron transportation between the two partners persists under high salt conditions, this would support the notion that cytochrome c_x is the direct electron donor under physiologically relevant conditions.

Stopped-flow experiments were carried out as before, except with the following adaptation: cytochrome c_x and AniA were buffer-exchanged into different salt concentration buffers (0mM NaCl 50mM Tris pH7.5; 62.5mM NaCl 50mM Tris pH7.5; 125mM NaCl 50mM Tris pH7.5; 250mM NaCl 50mM Tris pH7.5; 500mM NaCl 50mM Tris pH 7.5). The protein concentrations of cytochrome c_x (7.5 μ M) and nitrite reductase AniA (85 μ M) in different buffers were kept the same.

It was found that salt could completely shut down interaction between two redox partners. Electron transfer rate ($K_{\text{obs}} \text{ s}^{-1}$) between cytochrome c_x and AniA with no salt present is *approx.* 3.4 s^{-1} (analyzed by 3 parameter single exponential rise to maximum function ($f=y_0+a*(1-\exp(-b*x))$), by Sigmaplot), which is lower than $k_{\text{obs}} \text{ s}^{-1}$ between cytochrome c_5 and AniA interaction (13.48 s^{-1}) at the same AniA concentration. In addition, it is also significantly higher than experiments performed in the same buffer with salt presented (from 125mM-500mM NaCl). Electron transfer between these two redox partners cannot occur at a range of different salt concentration. It suggests cytochrome c_x is not the electron donor to nitrite reductase AniA in *N. meningitidis*.

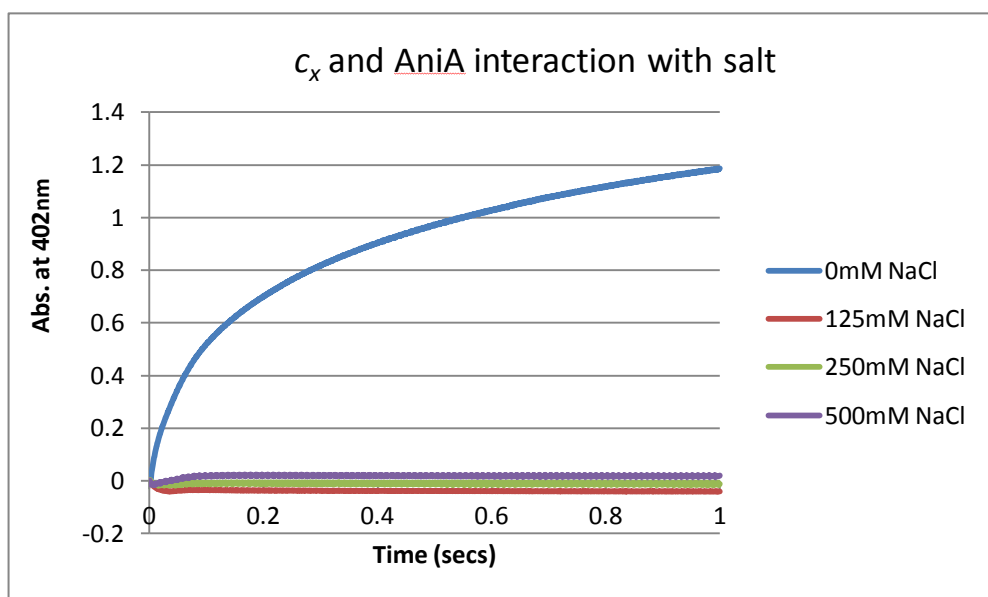


Figure 4.22: Salt dependence of cytochrome c_x and AniA interaction by stopped-flow kinetics: Stopped-flow kinetics of inter-protein electron-transfer reaction from reduced cytochrome c_x to AniA was performed in 50 mM Tris buffer (pH 7.5) with salt present (from 0mM-500mM NaCl). The protein concentrations of cytochrome c_x ($7.5 \mu\text{M}$) and nitrite reductase AniA ($85 \mu\text{M}$) were kept the same in different buffers.

To investigate the kinetic relationship between nitrite reductase AniA and cytochrome c_4 , the formation of a functional electron transfer complex between these two proteins was analyzed by stopped-flow kinetics. The kinetics of electron transfer from the reduced cytochrome c_4 to oxidized AniA was monitored at a wavelength of 402 nm. To keep the pseudo first order, the concentration of AniA is always in large excess

over the concentration of cytochrome c_4 (7.5 μ M). The second order electron transfer rate constant between the two proteins was estimated from the slope of the plots of AniA concentration versus $K_{\text{obs}}(\text{s}^{-1})$. The increase of the absorbance is due to the oxidation of cytochrome c_4 and concomitant reduction of AniA. The second order electron transfer rate constant between the two proteins is $0.147 \times 10^5 \text{ M}^{-1}\text{s}^{-1}$. It is *approx.* 10 times slower than that of cytochrome c_5 and AniA interaction. It supports the notion that cytochrome c_4 cannot interact functionally with outer membrane associated nitrite reductase AniA as an electron donor.

If electron transportation between the two partners persists under high salt conditions, this would support the notion that cytochrome c_4 is the direct electron donor under physiologically relevant conditions.

Stopped flow experiments were carried out as before, except with the following adaptation cytochrome c_4 and AniA were buffer-exchanged into different salt concentration buffers (0mM NaCl 50mM Tris pH7.5; 62.5mM NaCl 50mM Tris pH7.5; 125mM NaCl 50mM Tris pH7.5; 250mM NaCl 50mM Tris pH7.5; 500mM NaCl 50mM Tris pH 7.5). The protein concentrations of cytochrome c_4 (7.5 μ M) and nitrite reductase AniA (85 μ M) in different buffers were kept the same.

Although salt could not completely shut down interaction between two partners, electron transfer rate ($K_{\text{obs}} \text{ s}^{-1}$) between cytochrome c_4 and AniA is very low. It suggests, cytochrome c_4 is not the electron donor to nitrite reductase AniA.

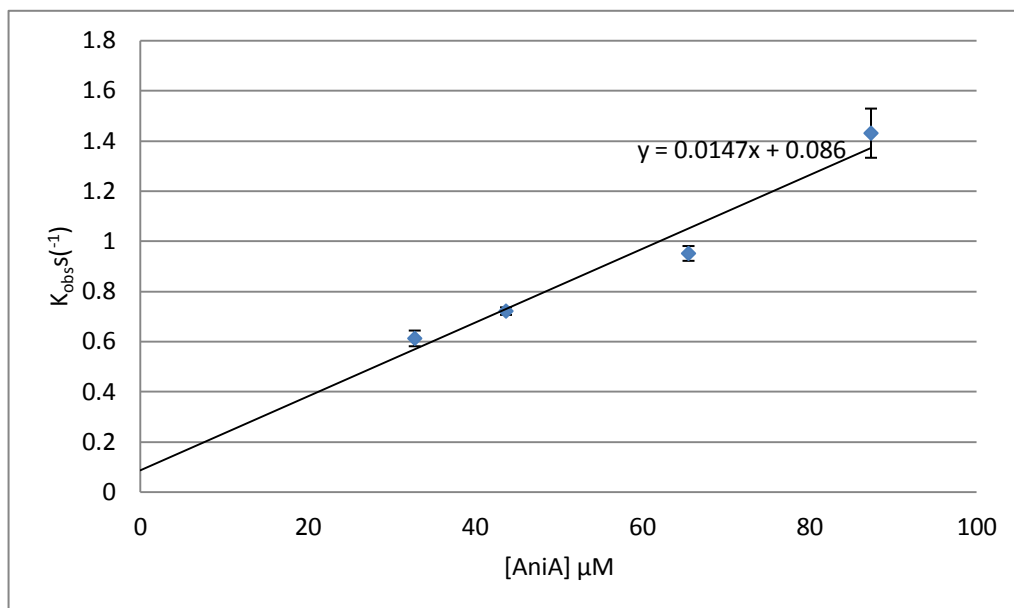


Figure 4.23: The electron-transfer between AnIA and cytochrome c_4 . Stopped-flow kinetics of inter-protein electron-transfer reaction from reduced cytochrome c_4 to AnIA performed in 50 mM Tris (pH7.5). Plots of $K_{\text{obs}}\text{s}^{-1}$ vs. AnIA concentrations (μM). The 2nd order electron transfer rate constant between the two proteins is $(0.147) \times 10^5 \text{M}^{-1}\text{s}^{-1}$. The concentration of AnIA is always in large excess (32.7–87.3 μM) over the concentration of c_4 (7.5 μM). Error bar denote standard deviation.

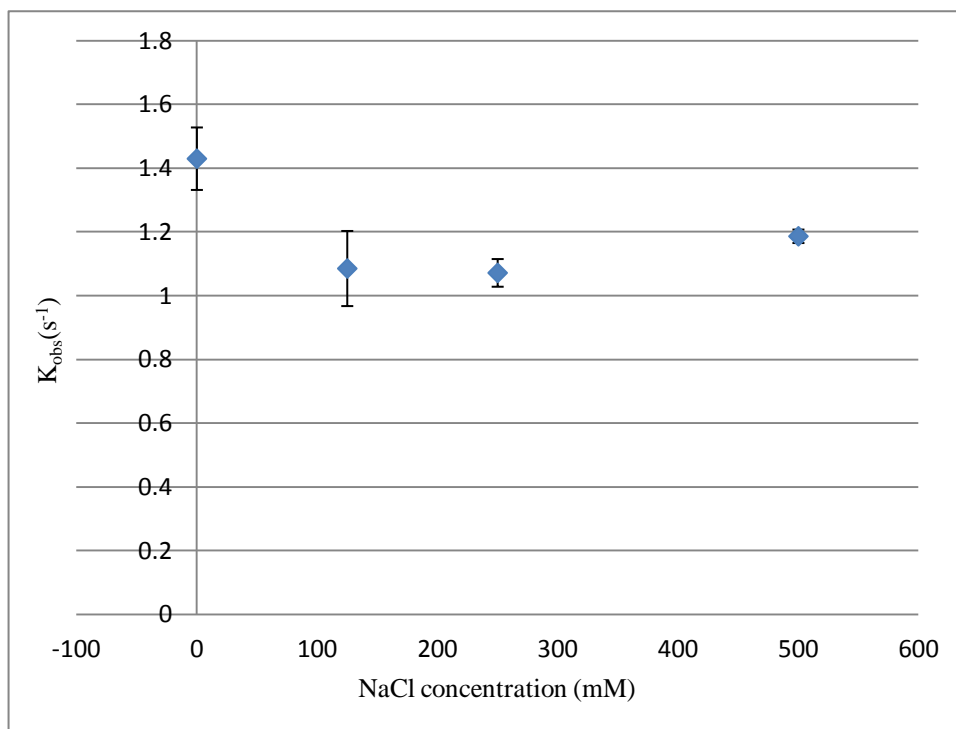
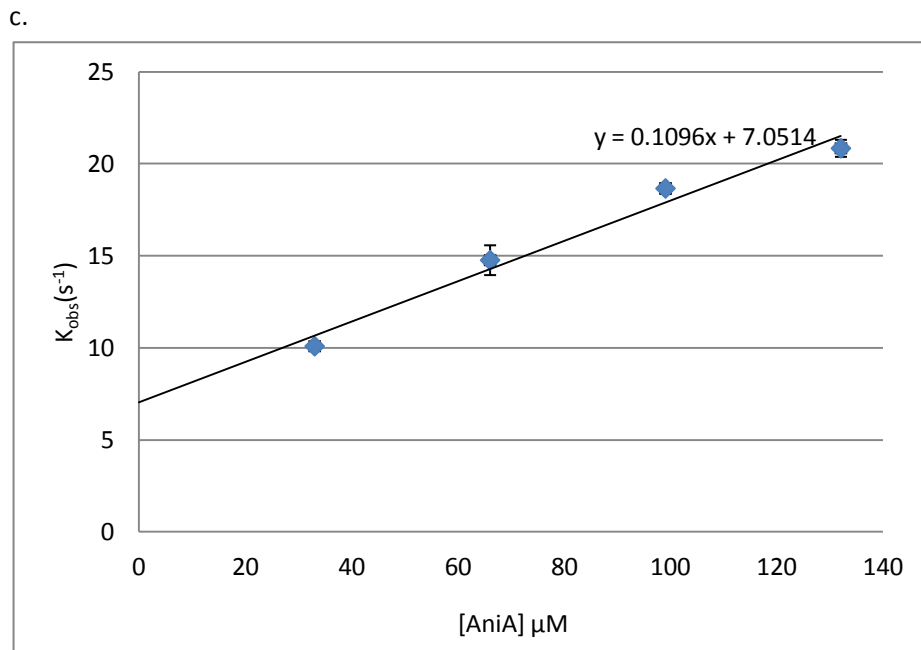
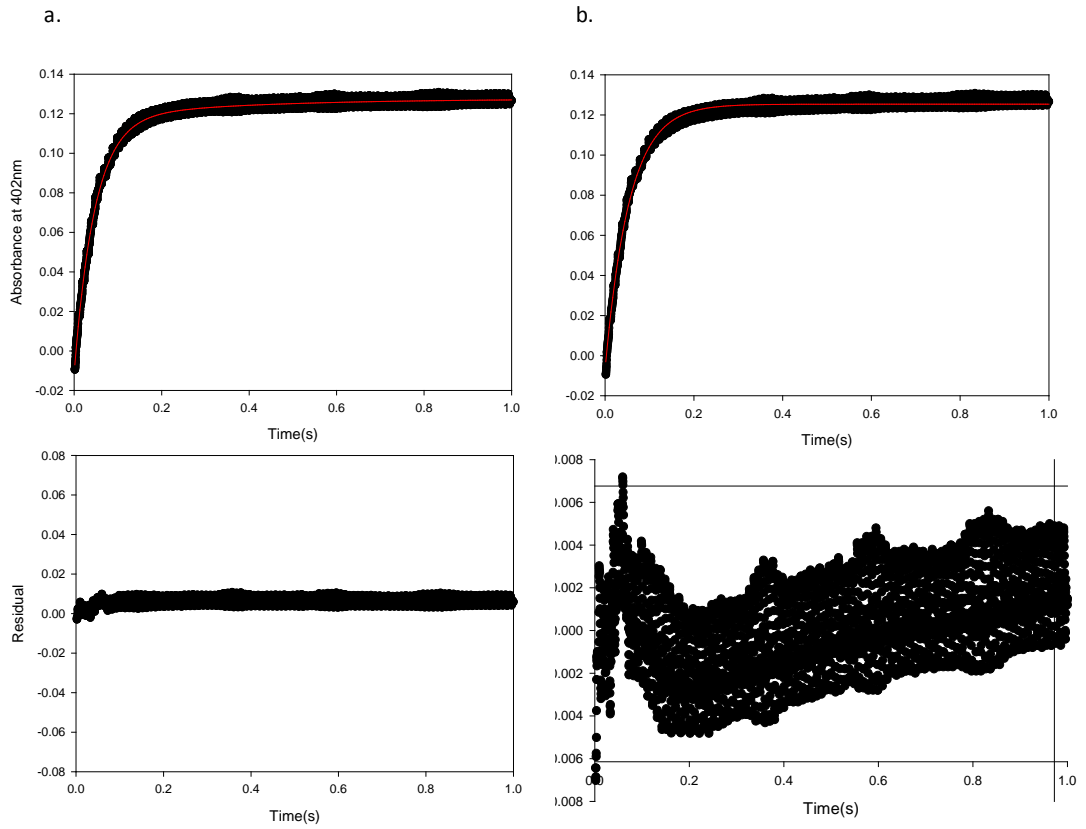


Figure 4.24: The salt dependence of cytochrome c_4 and AniA interaction by stopped flow kinetics: Plots of K_{obs} (s^{-1}) vs. salt concentrations. Stopped-flow kinetics of inter-protein electron-transfer reaction from reduced cytochrome c_4 to AniA was performed in 50mM Tris buffer(pH7.5) with salt presented (from 0mM-500mM NaCl). The protein concentrations of cytochrome c_4 ($7.5 \mu M$) and nitrite reductase AniA ($85 \mu M$) in different buffers were kept the same. Error bars denote standard deviation.

4.10: Intra-protein electron transfer between two haem containing domains of c_5 during nitrite reduction:

As mentioned above (refers to section 4.4.1), stopped-flow kinetics were initially analyzed over the first 100ms, a period over which data could be fitted to a single exponential equation assumed to be due to inter-protein electron transfer between c_5 and AniA. In order to understand the intra-protein electron transfer between two haem containing domains of c_5 , we used of the same set of data as before, but analysed absorbance change over 1 second at the same wavelength. The experimental data was fitted to a double exponential equation with 5 parameters ($f=y_0+a*(1-\exp(-b*x))+c*(1-\exp(-d*x))$) by Sigmaplot (Figure 4.25 a). This equation is able to separate the rate contributed to by two different events, (I) Inter-protein electron transfer between c_5 and AniA (fast rate, K_1); (II) intra-protein electron transfer between two haem containing domains of c_5 (slow rate, K_2). In addition, the experimental data was also fitted to a single exponential equation with 3 parameters (Figure 4.25 b). However, it produces the poor fitting and the large residuals, comparing with the double exponential fit. The second order electron transfer rate constant between the two proteins is $1.09 \times 10^5 \text{M}^{-1}\text{s}^{-1}$, compared to $(1.535) \times 10^5 \text{M}^{-1}\text{s}^{-1}$ calculated from the initial 100ms of the experiment (Figure 4.25 c.).



d.

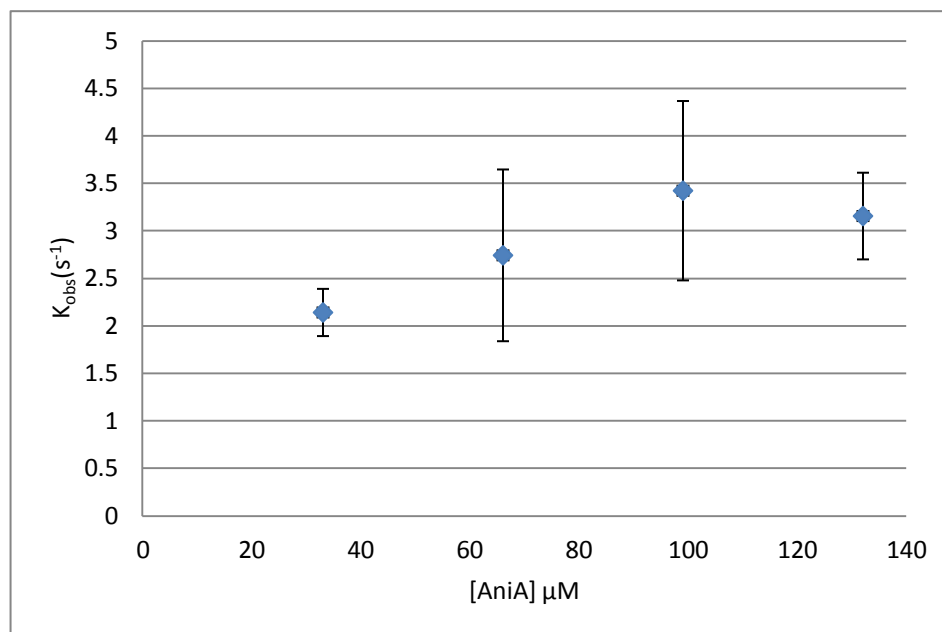


Figure 4.25: The electron-transfer between Ania and cytochrome c_5 analyzed by 5-parameter double exponential equation. a&b. Stopped-flow kinetics of inter-protein electron-transfer reaction from reduced cytochrome c_5 to Ania over 1 second fitted by single exponential function(a) and double exponential function(b). The black line represents the observed data; red line is a fitting curve. c. Plots of fast rate $K_{\text{obs}} (\text{s}^{-1})$ at different Ania concentrations(μM). The 2nd order electron transfer rate constant between the two proteins is $1.096 \times 10^5 \text{M}^{-1} \text{s}^{-1}$ d. Plots of slow rate $K_{\text{obs}} (\text{s}^{-1})$ at different Ania concentration(μM). The concentration of Ania (from 33 μM to 132 μM) is always in large excess over the concentration of c_5 (7.5 μM). The experiment is performed in 50 mM Tris(pH7.5). Error bars denote standard deviation.

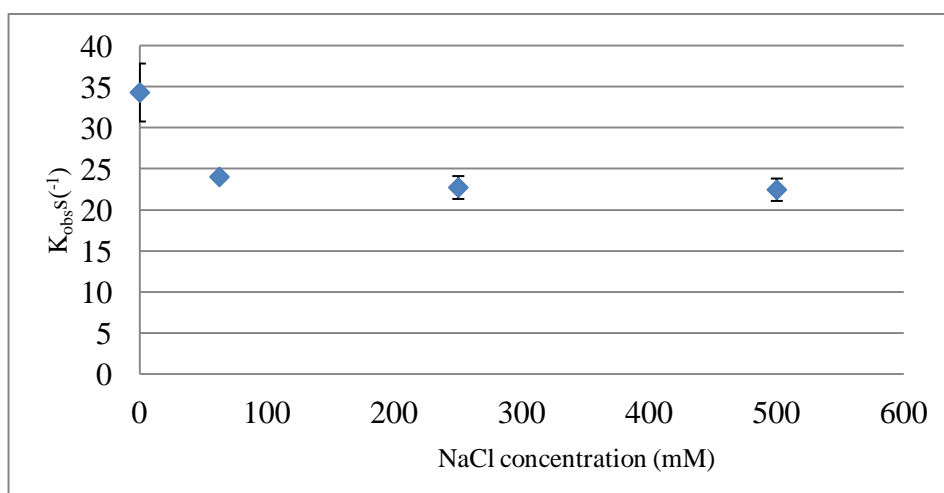
The one-way ANOVA on intra-protein electron transport rate revealed no significant difference between rate at different AniA concentrations, $F(3,11)=1.957$, $p > 0.05$ (Figure 4.25 d). In conclusion, the slow rate (K_2) showed no significant difference between AniA concentrations indicating that this is due to electron transfer between the two haem containing domains within cytochrome c_5 . The rate of electron transfer between the 2nd haem domain of c_5 and AniA is faster than the intra-protein electron transfer between two haem containing domains of c_5 .

4.11: Salt and pH dependence of intra-protein electron between two haem containing domains of c_5 :

In order to understand salt and pH dependence of the intra-protein electron transfer between two haem containing domains of c_5 , we used the same set of data before (Section 4.5.2 and 4.5.3), but analysed absorbance change over 1 second at the same wavelength. The experimental data was fitted to a double exponential with 5 parameters ($f=y_0+a*(1-\exp(-b*x))+c*(1-\exp(-d*x))$) by Sigmaplot.

Compared with section 4.5.2, fast rate K_1 agreed with inter-protein electron transfer obtained from initial 100ms of stopped flow experiment (Figure 4.26. a). The one-way ANOVA on intra-protein electron transport rates revealed no significant difference between salt concentrations, $F(3,11)= 0.589$, $p>.05$. This indicates that salt has no effect on intra-protein electron transfer between haem containing domains of cytochrome c_5 .

a.



b.

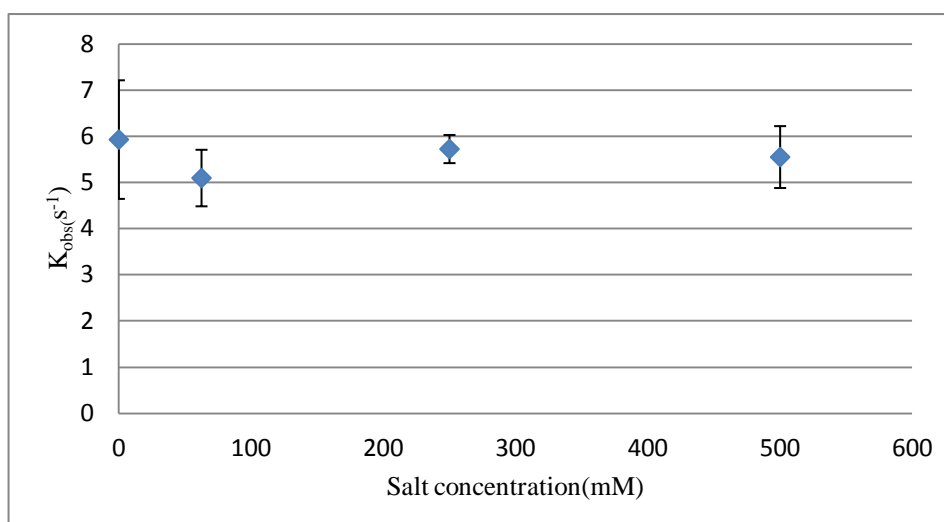
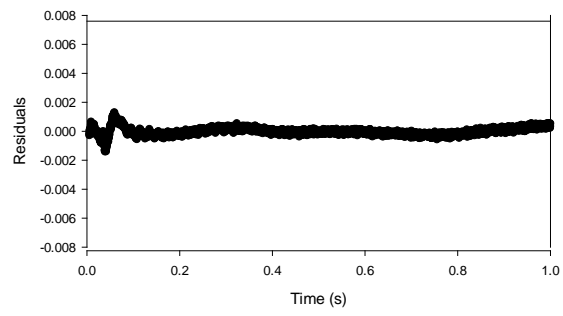
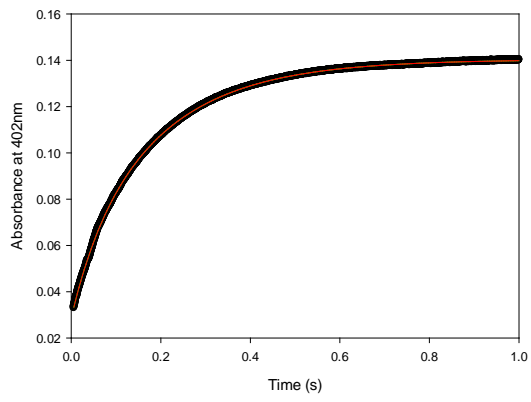
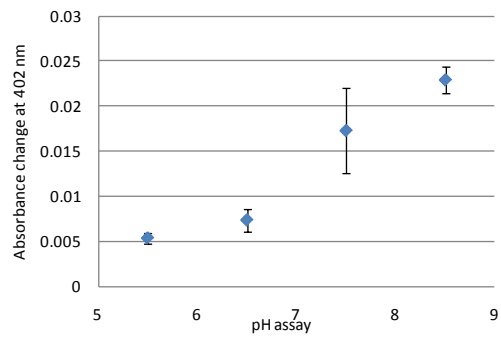


Figure 4.26 Salt dependence of intra-protein electron transfer between two haem containing domains of cytochrome c_5 was performed in 50mM Tris(pH7.5) with salt present(0mM-500mM). a. Plots of fast rate $K_{obs}(s^{-1})$ at different salt concentration (mM) b. Plots of slow rate $K_{obs}(s^{-1})$ at different salt concentration (mM). The concentration of cytochrome c_5 (7.5 μ M) and AniA (192 μ M) were always kept the same at different buffer conditions. Error bars denote standard deviation.

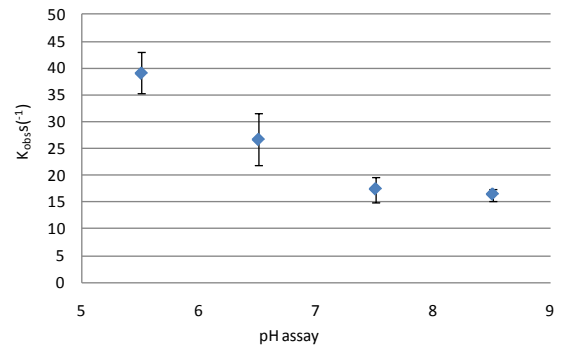
a.



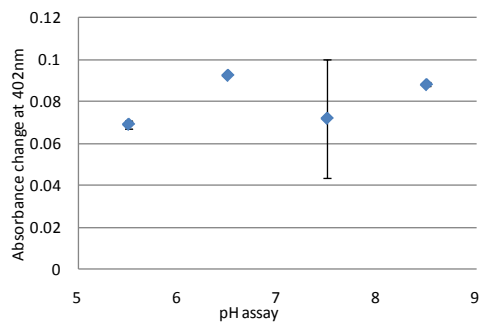
b.



c.



d.



e.

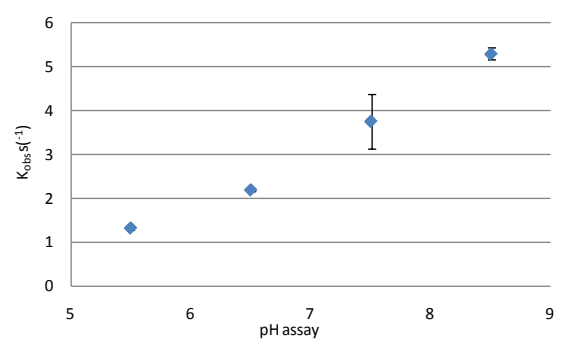


Figure 4.27: pH dependence of intra-protein electron transfer between two haem containing domains of cytochrome c_5 was performed in 50 mM Tris with vary pH (5.5–8.5). a. Stopped-flow kinetics of electron-transfer reaction from reduced cytochrome c_5 to AniA. The red line represents the observed data; black line is a fitting curve. b. the absorbance change of inter-protein electron transfer between the second haem domain of cytochrome c_5 and AniA at different pH assays; c. the inter-protein electron transfer between the second haem domain of cytochrome c_5 and AniA at different pH assays. d. The absorbance change of intra-protein electron transfer between two haem containing domains of cytochrome c_5 at different pH assays. e. The intra-protein electron transfer between two haem containing domains of cytochrome c_5 at different pH assays. The concentration of cytochrome c_5 (7.5 μM) and AniA (40 μM) were always kept the same at different buffer conditions. Error bars denote standard deviation.

As mentioned before, the experimental data was fitted by double exponential 5 parameter equation, which is able to separate two events contributed by inter-protein electron transfer rate and also intra-protein electron transfer rate (Figure 4.27). The difference between observed data and fitting curve are significantly small (Figure 4.27.a). The fast rates (inter-protein electron transfer rates) are significantly higher than that obtained from initial 100ms (Figure 4.27.b). In addition, the absorbance changes at 402 nm are decreased with the increasing pH assay (Figure 4.27.c). The

slow rates (intra-protein electron transfer rates) increased with pH (Figure 4.27.d), and the absorbance changes at 402 nm are staying constant (Figure 4.27.e). It is possible to calculate that pH affects the intra-protein electron transfer between two haem containing domains of cytochrome *c*₅.

4.12: Discussion

Soluble cytochrome c_5 and nitrite reductase AniA were expressed and purified separately. Cytochrome c_5 as prepared is in the reduced form, whereas truncated AniA is in the oxidized form. Coomassie blue staining of cytochrome c_5 showed that the majority of expressed soluble cytochrome c_5 exhibits molecular mass of 27 kDa and 30 kDa, as analyzed by SDS-PAGE. Two isoforms of cytochrome c_5 might be due to proteolytic cleavage of mature protein. However, molecular mass of cytochrome c_5 detected by mass spectrometry indicates only a single species is present. *N. meningitidis* AniA was also expressed as a soluble protein. Purification of the protein was confirmed by SDS-PAGE analysis.

Steady state experiments confirmed that reduced cytochrome c_5 is able to be oxidized by nitrite reductase AniA. To elucidate the kinetic competence of electron transfer between nitrite reductase AniA and cytochrome c_5 , the formation of a functional electron transfer complex between these two proteins was analyzed by stopped-flow kinetics. As cytochrome c_5 is a dihaem protein, only first 100ms was analyzed to assumed to be due to inter-protein electron protein between cytochrome c_5 and AniA. The second order electron transfer rate constant between the two proteins is $(1.535 \pm 0.0243) \times 10^5 \text{ M}^{-1} \text{ s}^{-1} (K_1)$, which strongly supports the idea that inner membrane cytochrome c_5 interacts functionally with outer membrane associated nitrite reductase AniA as an electron donor. The second order electron transfer rate constant between *Achromobacter xylosoxidans* Cyt c_{551} and blue copper CuNIR (A_{xg}NIR) is $(4.8 \pm 0.02) \times 10^6 \text{ M}^{-1} \text{ s}^{-1}$ (Nojiri et al. 2009). Inter-molecular electron transfer from

pseudoazurin to copper containing nitrite reductase is $7.3 \times 10^5 \text{ M}^{-1}\text{s}^{-1}$ in *A. xylosoxidans* (Kataoka et al. 2004). It indicates that the stability of redox partner and nitrite reductase form a functional electron transfer couple is in the range of 10^5 - $10^7\text{M}^{-1}\text{s}^{-1}$.

As previously described (Chapter 3), the core enzyme AniA is tethered to outer membrane by three putative flexible linker regions. In addition, the active sites of AniA core enzyme facing to electron donor cytochrome *c*₅ have a significantly decreased number of degrees of freedom compared with freely tumbling NirK in the periplasm (Li et al. 2012). Thus in theory, the second order rate constant between cytochrome *c*₅ and AniA should be much higher *in vivo* than the measurement *in vitro*.

As described before, the enzyme activity of AniA is pH-dependent, and reaches its optimum activity at around pH 5.5 (Abraham et al. 1997; Stefanelli et al. 2008). This pH dependency of AniA might relate to the physiology of *N. meningitidis*. During invasion, maintaining the optimum activity of nitrite reductase to support meningococcal growth in neutral-acidic CSF as increasing circulating of lactate is important for *N. meningitidis* spreading at last phases of infective process (Stefanelli et al. 2008). In *A. xylosoxidans*, NirK was also shown pH-dependency of the enzyme catalysis, but not the affinity of the enzyme for nitrite (Abraham et al. 1997). The physiologically relevant salt concentration of human blood serum and saliva are approximately 140mM NaCl and 40mM NaCl, respectively (White et al. 1955). It is important that inter-protein electron transfer of nitrite reduction in denitrification is

independent from varied physiological stresses from the external environment. In this work, inter-protein electron transfer between AniA and cytochrome c_5 is confirmed to have a high tolerance to salt concentration and pH.

Both of cytochrome c_x and c_4 were previously determined as important electron donors to cbb_3 terminal reductase in *N. meningitidis* (Deeudom et al. 2008). Under denitrifying conditions, mutants strains deficient in c_x and c_4 have no effect on NirK-dependent nitrite reduction. It indicated both of cytochrome c_x and c_4 are not the redox partner of AniA in *Neisseria*. The 2nd order rate inter-protein electron transfer constant between c_4 and AniA interaction is *approx.* 10 times smaller than that of c_5 and AniA interaction. Although salt has limited affect on electron transportation, the absorbance change is still too small to be accounted. Cytochrome c_x is able to donate electrons to AniA at considerably low rate without any salt present. However, inter-protein electron transportation between c_x and AniA is completely shut down by external physiological stress (salt). It indicates unlike cytochrome c_5 , dihaem cytochrome c_4 and monohaem cytochrome c_x are not the direct donor to AniA or involved in NirK dependent denitrification pathway in *N. meningitidis*. This also confirmed the specificity of c_5 and AniA redox partners interaction in nitrite reduction.

Which haem containing domains of c_5 makes the direct contact with AniA? As cytochrome c_5 is a dihaem protein, there is no information on which haem containing domain is the direct donor to AniA. However, based on analysis of the width of Gram negative periplasm, inner membrane associated first haem domain of cytochrome c_5 is unlikely to get access to the outer membrane associated redox protein AniA, and form a functional electron transfer couple in *Neisseria*.

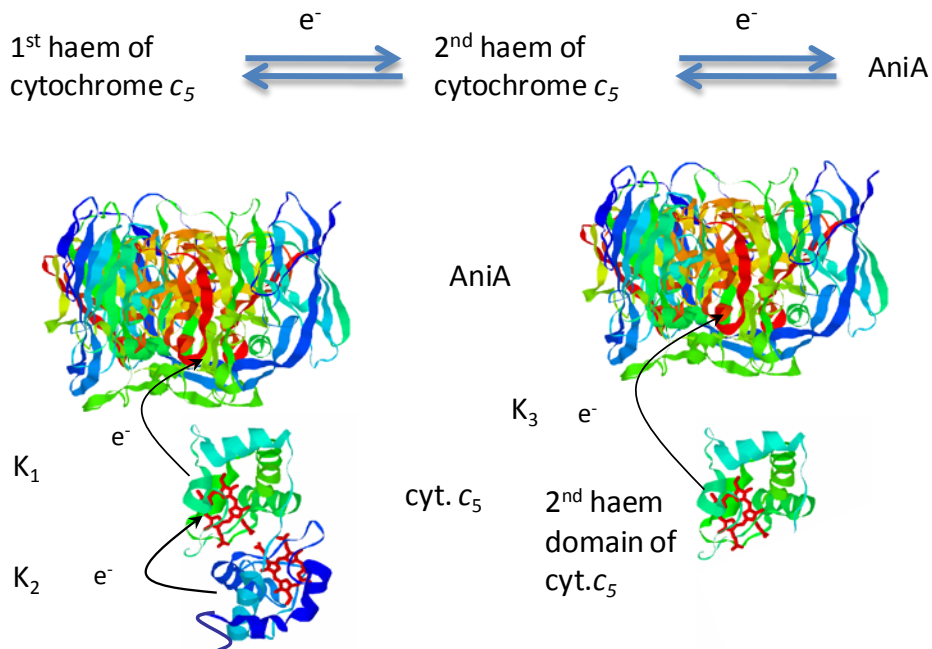
In order to determine any roles of two haem containing domains in nitrite reduction in *N. meningitidis*, two mono-haem domains of cytochrome c_5 were expressed heterologously and purified separately. Both of two monohaem domains of cytochrome c_5 as prepared were in the reduced form. 1st Hc₅ was highly expressed in *E. coli* and purified in a soluble form under aerobic conditions, but exhibited in two isoforms as judged by SDS-PAGE. Despite appearing as two bands on the gels, a single peak was detected by MS. The probable explanation is the protein at two different redox forms run at different positions. 2nd Hc₅ was highly expressed and purified in a soluble form under aerobic condition as judged by SDS-PAGE.

The second order electron transfer rate constant between second haem domain of cytochrome c_5 and AniA is $2.8 \times 10^6 \text{ M}^{-1} \text{ s}^{-1}$ (K_3), which is 2 times higher than that of c_5 and AniA interaction. In addition, first haem domain of cytochrome c_5 is unable to donate electrons to AniA directly. The two covalently bound haem c in cytochrome c_5 are connected by AlaSerPro-rich LCR. First haem c is predicted to be the electron entry site of cytochrome c_5 , and second haem c constitutes the center from where the electron is transferred to terminal reductase AniA.

As experiment followed pseudo-first order, it is assumed that all electron transport is towards AniA at the beginning of the reaction. However, K_3 (2nd haem domain of c_5 and AniA) has been calculated is $2.8 \times 10^6 \text{ M}^{-1}\text{s}^{-1}$, K_1 (holo- c_5 and AniA) is $1.4 \times 10^6 \text{ M}^{-1}\text{s}^{-1}$ under the same experimental conditions. It indicates intra-protein interaction between two haem containing domains may affect the inter-protein electron transport between c_5 and AniA.

Dihaem cytochrome c_5 and AniA interaction is predicted to have a two-step reaction *in vitro* (Figure 4.28). Both of haem c containing domains of c_5 were kept in a stable reduced form. The second haem domain of c_5 was initially oxidized by AniA. Subsequently, electrons started to flow from the first haem domain to the second haem domain of c_5 . The first haem domain was then oxidized by the second haem domain of c_5 , and till reached their equilibrium. We also found the intra-protein electron transfer between two mono-haem domains of cytochrome c_5 are statistically no difference between AniA concentrations. It indicates that intra-protein electron transfer between two haem domains of c_5 is constant and independent on AniA concentration. K_3 is 2 times higher than K_1 . One possible explanation is the first haem binding domain of c_5 might structurally prevent electron flow from the second haem binding domain of c_5 to AniA (Figure 4.28.b).

a.



b.

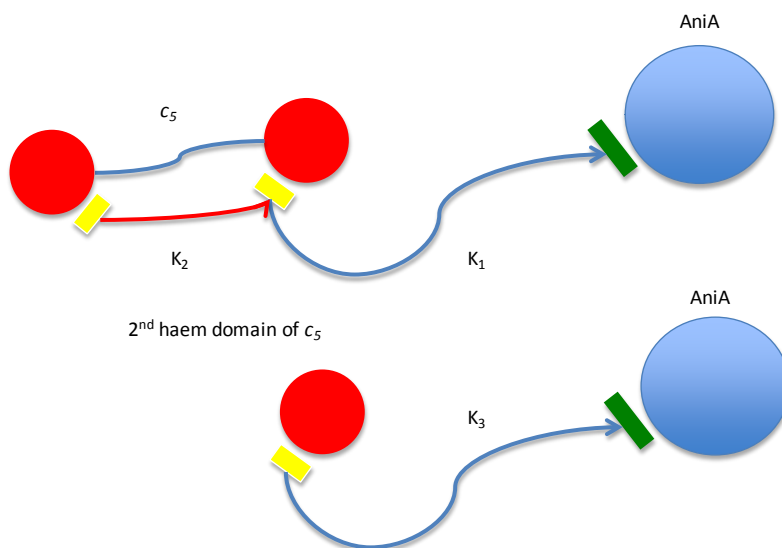


Figure 4. 28: Proposed model of soluble c_5 and AniA interaction *in vitro*: **a.** free tumbling soluble c_5 and AniA in 50 mM Tris buffer (pH7.5) K₁ is the electron transfer rate constant from dihaem cytochrome c_5 to AniA; K₂ is the electron transfer from second haem domain of c_5 to first haem domain

of c_5 ; K_3 is the electron transfer rate constant from second haem domain of c_5 to AniA. **b.** The cartoon model of comparison of electron transfer from c_5 to AniA and electron transfer from the 2nd haem domain of c_5 and AniA. The yellow square is predicted as the cytochrome c_5 electron donating/accepting sites. The green square is predicted as the AniA electron accepting sites.

It was also shown pH affects the intra-protein electron transfer between two monohaem domains of cytochrome c_5 , but not salt. As described in literature, there are three major types of inter-molecular interactions between c-type cytochrome protein and its electron donor, including oppositely charged interaction, van der Waals interaction, and also inter-protein hydrogen bonding (Nojiri et al. 2009; Axelrod et al. 2002). As electrostatic surface of copper I binding site of *N. gonorrhoeae* soluble AniA has negative potentials (Boulanger and Murphy 2002) (Figure 4.29). It is reasonable to predict that the electrostatic surface of electron donating surface of the haem containing domains of cytochrome c_5 have positive potentials.

Based on data observed in this study, different pH assays affect the intra-protein electron transfer between two monohaem containing domains of c_5 *in vitro*. Under basic conditions, there are fewer protons in the environment, which increases the intra-protein electron transfer between two monohaem domains of cytochrome c_5 (Figure 4.29). Under acidic conditions, there are more protons in the assay, which results in two haem domains of cytochrome c_5 repelling each other as they became increasing positively charged and the second haem domain favours a functional

electron transfer couple with AniA (Figure 4.29). As the AlaSerPro-rich LCR separates the two haem domains within dihaem cytochrome c_5 , the association of haem containing domains of cytochrome c_5 is not tethered together as a solid complex. The LCR might be able to form unstructured elongated linker to allow the active second haem domain of c_5 to donate electrons to AniA.

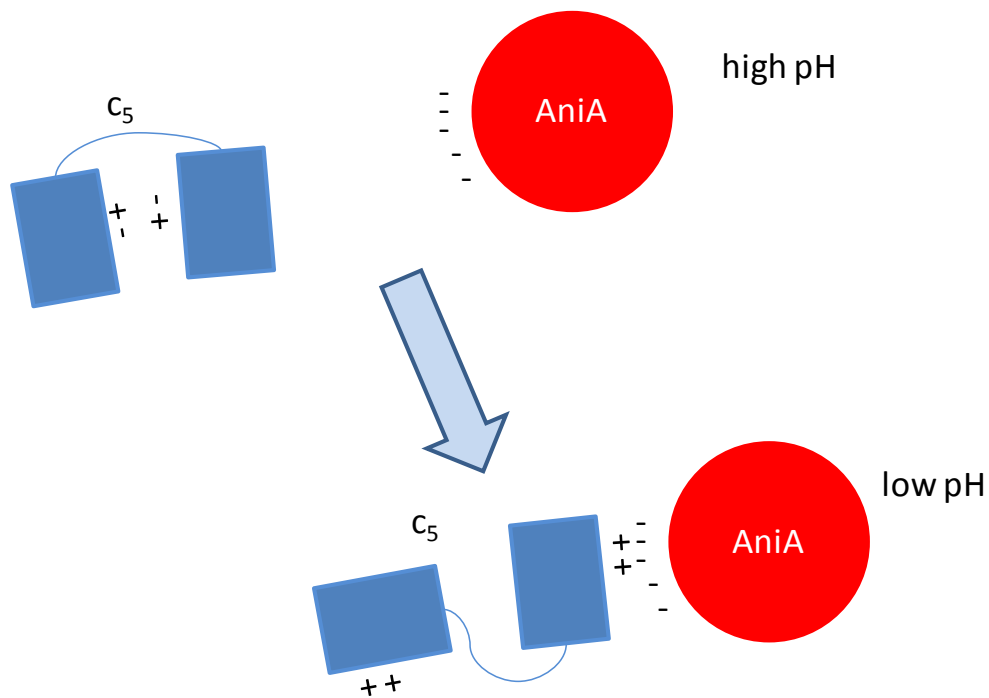


Figure 4.29: pH dependence of intra-protein electron transfer between two monohaem domains of cytochrome c_5 . Intra-protein electron transfer between two haem domain is predicted to be enhanced by increasing pH in the assay (less protons).

From combined data of inter-protein electron transport between c_5 and AniA, second order rate constant, pH and salt independency, there is a good evidence that cytochrome c_5 is the direct and efficient electron donor to AniA nitrite reductase in *N. meningitidis*. Based on electron transfer between second haem domain of cytochrome c_5 and AniA, second order rate constant, pH and salt independency, it also provides a good evidence that second haem domain of c_5 is the direct donor to AniA. Cytochrome c_x and c_4 also confirmed the specificity of c_5 and its redox partner AniA.

As both of redox partners are located in different membrane, understanding the mechanism of the movement of AniA and c_5 is important. There are two predictions. (I) As described before, N-terminal linker LCR of AniA tethering to outer membrane might form a unstructured elongated linker region will allow the globular active domain move from the surface of the inner leaflet of the outer membrane to get access electrons from c_5 (Li et al. 2012). (II) AlaSerPro-rich LCR that encompassed the attachment sites of its glycan between two haem containing domains of cytochrome c_5 might allow the active site of second domain of c_5 to make the direct contact with AniA and form a functional electron transfer couple. Both of these predictions need to be investigated in the future.

Chapter 5

Inter-protein electron transfer for nitrite reduction in denitrification in other *Neisseria* species:

5.1 Introduction:

Like *N. meningitidis*, the gonococcus could also use nitrite and nitric oxide as alternative electron acceptors during oxygen limiting conditions (Hopper et al. 2009; Rock et al. 2005). It also employs this partial denitrification to reduce nitrite to nitrous oxide via nitrite oxide. There is only one nitrite reductase (AniA) encoded in meningococcal and gonococcal chromosome, which is a membrane of the NirK (copper containing) family of nitrite reductase and also an outer membrane associated membrane lipoprotein (refer to Chapter 3). Comparing with other bacteria, electrons are predicted to be transferred from cytochrome *bc₁* complex in the cytoplasmic membrane to nitrite reductase AniA by either c-type cytochromes or azurin (Hopper et al. 2009). Laz is the only azurin homologue in *N. gonorrhoeae* and also mainly associated with outer membrane. However, there is little evidence suggesting Laz is a physiologically important electron donor to nitrite reductase AniA in *N. meningitidis*. *N. meningitidis* *c₅* mutant strains could not reduce nitrite at all, suggesting cytochrome *c₅* is the only electron donor to AniA in *N. meningitidis* (Deeudom et al. 2008). However, *N. gonorrhoeae* *c₅* mutant strains could still reduce nitrite to support oxygen-limited growth and convey a selective advantage for survival in their host

(Amanda Hopper 2009). It suggests there are other alternative routes for nitrite reduction in NirK-dependent nitrite reduction in *N. gonorrhoeae*.

As mentioned in the introduction, cytochrome oxidase *cbb₃* complex is the only terminal oxidase in *Neisseria*, and has high affinity for oxygen. It has four subunits, CcoO, CcoN, CcoQ, and CcoP. The core enzyme CcoO-CcoN is catalytically active in oxygen reduction without the presence of CcoP subunit. *N. meningitidis* and *N. gonorrhoeae* share a high level of sequence similarity ($\geq 98\%$ in house keeping genes). *CcoP* subunit of cytochrome *cbb₃* of *N. meningitidis* is a dihaem protein; however, *CcoP* subunit of cytochrome *cbb₃* of *N. gonorrhoeae* is a trihaem protein (Figure 5.1). The second haem domain of cytochrome *c₅* has high identity ($> 70\%$) with 3rd haem domain of trihaem *CcoP* of the cytochrome *cbb₃* oxidase of *N. gonorrhoeae* (Figure 5.2). Our hypothesis is the 3rd haem domain of CcoP is able to donate electrons to AniA in *N. gonorrhoeae* directly.

There is another cytochrome *c₅* homologue found in *Neisseria elongata* subsp. *glycolytica* ATCC 29315. It has more than 70% sequence similarity with the second haem domain of cytochrome *c₅* (Figure 5.3). In this non-pathogenic *Neisseria* species, it is possible this *c₅* homologue could provide another electron donating pathway to nitrite reductase AniA. We hypothesize *N. elongata* cytochrome *c* is also able to donate electrons to AniA directly.

The aim of this chapter is to identify the roles of the 3rd haem domain of CcoP and *N.*

elongata cytochrome *c* in the AniA-dependent denitrification in *Neisseria* species.

This approach will involve heterologous expression of 3rd haem domain of CcoP and *N. elongata* cytochrome protein *c* and identification of their function biochemically.

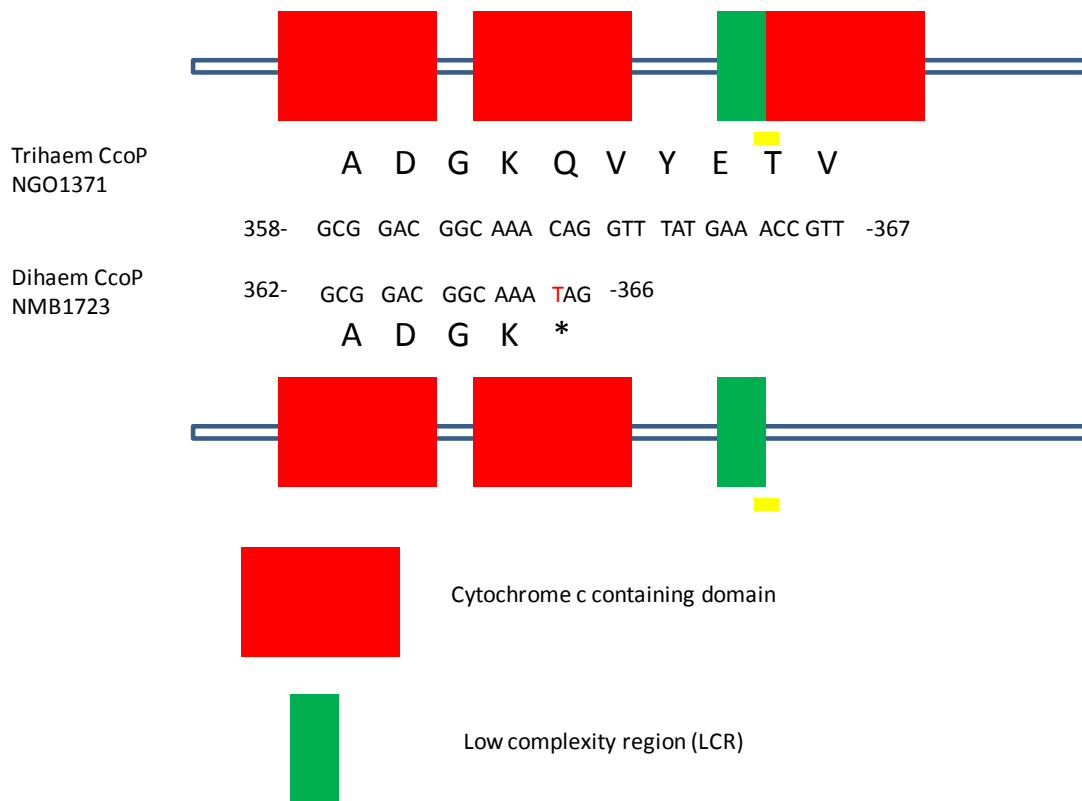


Figure 5.1: Domain architectures of neisserial CcoP subunit of *cbb*₃ oxidase: Modular structures of *N. gonorrhoeae* trihaem CcoP and *N. meningitidis* dihaem CcoP. The region encompassing the premature stop codon resulting in CcoP truncation and the corresponding region in tri-haem CcoP are indicated by yellow rectangles and the specific residues and the corresponding codons are numbered according to those of intact polypeptides The single base changed (C to T) creates

a premature stop codon at the end of *N. meningitidis* CcoP (highlighted in red; stop codon labeled with *). A SNP leads to the truncation of the CcoP subunit of *cbb*₃ oxidase associated with *N. meningitidis*. In *N. gonorrhoeae*, the AlaSerPro-rich low complexity region (LCR) separates the 2nd and 3rd haem binding domains of trihaem CcoP and also encompasses the glycan attachment site (Vik et al. 2009).

```

NGO1371      300  VWGLSNKDGKAPVKKAEPAPAAEPAPSAPAEAAQAASEAKPAAAEPKAEKKAAPAAKADG 360
NMB1677      144  TY-MANKSGGSFNPDEAAPADN---AASGTASAPADSAAPAEKAEDKGAAAPAVGVGDG 200
      .: ::*:* : : *.*** : : *.. *: .*..* ** *:.: : ****. **
NGO1371      KQVYETVCAACHGNAIPGIPHVGTKADWADRIKKGKDTLHKHAIEGFNTMPAKGGRGDLS 420
NMB1677      KKVFPEATCQVCHGGSIPGIPGIGKDDWAPRIKKGKETLHKHAIEGFNAMPAKGGNAGLS 260
      *:*:*. * .**.:***** :*. * ** *****:*****:*****:*****...**

NGO1371      DDEVKAAVDYMVNQSGGKF 439
NMB1677      DDEVKAAVDYMANQSGAKF 279
      *****.***.*

```

Figure 5.2: Primary protein sequence comparison of *N. gonorrhoeae* CcoP (NGO 1371) and *N. meningitidis* c_5 (NMB 1677). *N. gonorrhoeae* CcoP contains three haem binding sites. The 3rd haem binding domain of *N. gonorrhoeae* CcoP has high sequence similarity with second haem domain of cytochrome c_5 . The haem binding domains of the 3rd haem domain of trihaem CcoP and 2nd haem domain of cytochrome c_5 are highlighted in red. Both of haems are predicted to have hexacoordinate with Met as the sixth ligand (highlighted in yellow)

```

NEIELOOT00905      -----AAPAAKVDGKAVYEATCKACHSGTIPGTPGVGKKDEWEPRIKQGQETLH 49
NMB1677            180 PAEAKAEDKGAAAPAVGVDGKKVFEATCQVCHGGSSIPGIPGIGKKDDWAPRIKKGKETLH 240
                   ****. **** *:****:.*.*:*** **:****:* ****:****
NEIELOOT00905      KHAIEGFKGMPAKGGNEG----- 67
NMB1677            KHAIEGFNAMPAKGGNAGLSDEVKAAVDYMANQSGAKF 279
                   ***:***:.****** *

```

Figure 5.3: Primary protein sequence comparison of *N. elongata* cytochrome c (NEIELOOT_00905) and cytochrome *c*₅ (NMB 1677). NEIELOOT_00905 has high sequence similarity with second haem domain of *c*₅. The haem binding domains of *N. elongata* cytochrome c and 2nd haem domain of cytochrome *c*₅ are highlighted in red. Both of haems are predicted to have hexacoordinate with Met as the sixth ligand (highlighted in yellow)

5.2 Over-expression and characterization of the third haem domain of CcoP of cytochrome *cbb*₃ complex from *N. gonorrhoeae*.

The initial purpose was to produce a large amount of the 3rd haem domain of CcoP protein for further kinetics experiments. In order to produce soluble 3rd haem domain of CcoP, the subcloning and expression of 3rd haem domain of *N. gonorrhoeae ccoP* procedure is the same as that used for construction of the monohaem domains of cytochrome *c*₅ (Figure 5.4). The restriction sites (PvuII and XhoI) were included in sequence in order to insert the 3rd haem domain of *ccoP* product compatible for cloning into pET22b+ vector directly. The constructed 3rd haem *ccoP*-pET22b⁺ plasmid (3CcoPpET22b) was verified by colony PCR screen (Figure 5.5) and DNA sequencing.

Recombinant expression of 3rd haem domain of CcoP was performed in pET22b(+) vectors in *E. coli* cells BL21 λDE3(pST2). It was purified aerobically and yielded large amounts of pure soluble protein. The desired protein was confirmed by SDS-PAGE analysis. Predicted molecular mass of soluble 3rd haem of CcoP with the N-terminal His-tag and one covalently attached haem domain is 10406 Da (9789.95 Da + one haem domain 616 Da). The desired outcome of Ni affinity chromatography contains one major protein of *approx.* 10 kDa, as analyzed by SDS-PAGE (Figure 5.6). Purified 3rd haem domain of cytochrome CcoP as prepared was in the reduced form. The spectrum of CcoP shows typical low spin c-type cytochrome features: the Soret band at 419nm, and β and α bands at 523nm and 553nm, respectively. In the oxidized

form, the Soret band moves to 406nm, and α and β band become one broad feature (Figure 5.7).

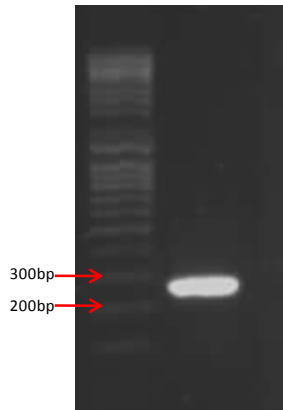


Figure 5.4: PCR product of 3rd haem domain of *ccoP*. The 3rd haem domain of *ccoP* exhibits size of 258 bp. Lane 1 is 3rd haem domain of *ccoP* gene.

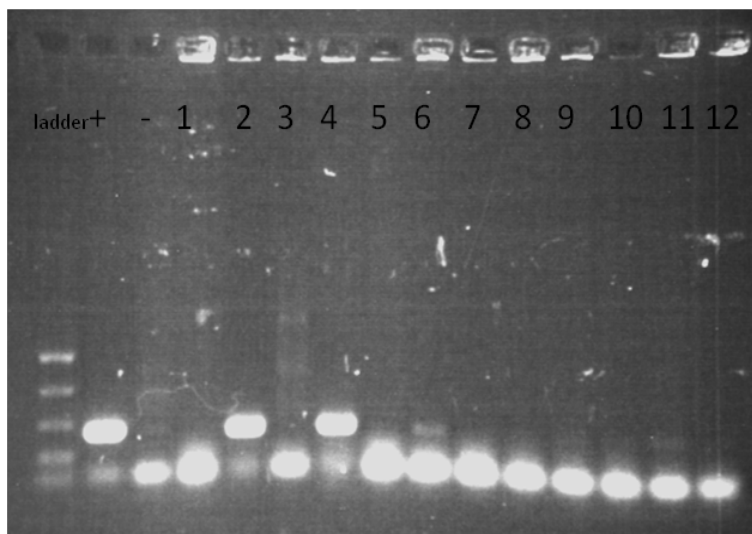


Figure 5.5: Colony PCR screen of 3rd haem domain of *ccoP* of *N. gonorrhoeae*. +. Positive control, boiled *N. gonorrhoeae* colony as template; -. Negative control, undigested empty pET22b(+) as template; 1-12, colony candidates No. 1- No.12.

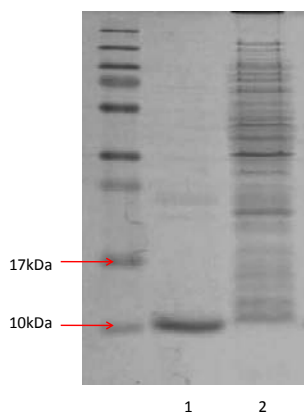


Figure 5.6: SDS-PAGE analysis of Ni affinity chromatography fractions of crude periplasmic extract and purified 3rd haem domain of *N. gonorrhoeae* CcoP. 3rd haem domain of *N. gonorrhoeae* CcoP has predicted MW. approximately 10 kDa. Lane 1: purified 3rd haem domain of *N. gonorrhoeae* CcoP protein. Lane 2: periplasmic fraction.

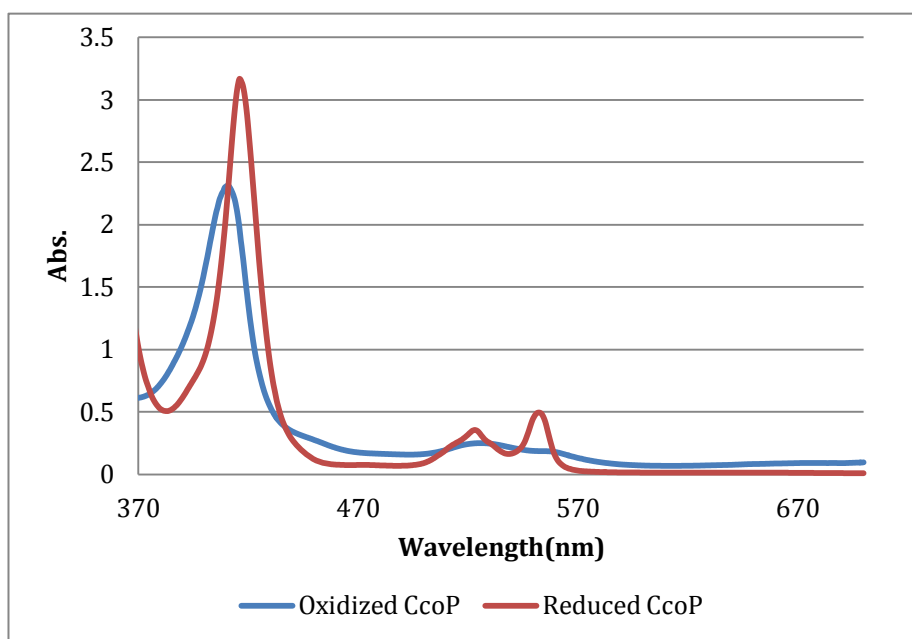


Figure 5.7: Absorption spectra of purified cytochrome CcoP: spectra were recorded at room temperature in 50mM Tris buffer (pH7.5). The oxidized (blue line) and reduced (red line) state shown absorbance peak at 406nm in oxidized form, and at 419nm, 523nm 553 nm in the reduced form. The concentration of cytochrome CcoP is 1.23×10^{-2} mM.

5.3 Stopped-flow kinetics of inter-protein electron transfer reaction from reduced third haem domain of CcoP of *cbb*₃ to nitrite reductase AniA.

5.3.1 The second order electron transfer rate constant between 3rd haem domain of *N. gonorrhoeae* CcoP and nitrite reductase AniA

To elucidate the physiological relationship between nitrite reductase AniA and the 3rd haem domain of CcoP of *cbb*₃ oxidase of *N. gonorrhoeae*, the formation of a functional electron transfer complex between these redox partners was analyzed by stopped-flow kinetics. The kinetics of electron transfer from the reduced 3rd haem domain of CcoP to oxidized AniA was monitored at a wavelength of 402nm. In order to keep pseudo first order, the concentration of the 3rd haem domain of CcoP was 7.5μM, substantially lower than AniA concentration (from 150μM to 40μM). The rapid increase of the absorbance is due to the oxidation of the 3rd haem domain of CcoP and concomitant reduction of AniA (Figure 5.8 a.). The 2nd order electron transfer rate constant between the two proteins, $(3.378 \pm 0.0167) \times 10^5 \text{ M}^{-1} \text{ s}^{-1}$ (Figure 5.8 b), strongly supports the idea that 3rd haem domain of *N. gonorrhoeae* CcoP interacts functionally with outer membrane associated nitrite reductase AniA as an electron donor.

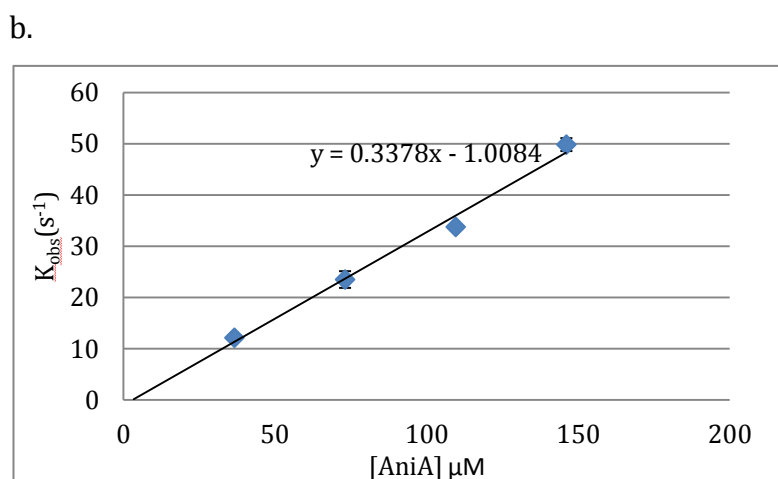
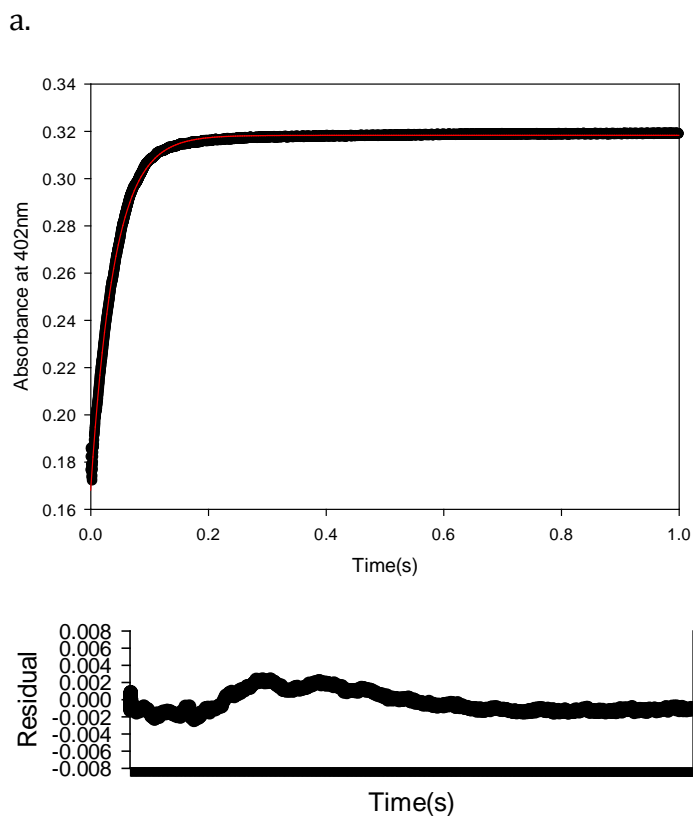


Figure 5.8: Stopped-flow kinetics of inter-protein electron-transfer reaction from reduced cytochrome CcoP to AniA was performed in 50mM Tris (pH7.5). a. The black line represents the observed data; red line is a fitting curve. b. Plots of K_{obs} (s^{-1}) vs. AniA concentrations. Error bar denote standard deviation. The concentration of the 3rd haem domain of CcoP was 7.5 μ M, substantially lower than AniA

concentration (from 150 μ M to 40 μ M). Error bars denote standard deviation.

5.3.2 Salt dependence of the 3rd haem domain of *N. gonorrhoeae* CcoP and nitrite reductase AniA interaction

We investigated whether 3rd haem domain of CcoP could donate electrons at similar rate with salt present, which would support this cytochrome protein being a physiologically relevant electron donor to nitrite reductase AniA.

Stopped flow experiments were carried out as before, except with the following adaptation 3rd haem domain of *N. gonorrhoeae* CcoP and AniA were buffer-exchanged into different salt concentration buffers (0mM NaCl 50mM Tris pH7.5; 62.5mM NaCl 50mM Tris pH7.5; 125mM NaCl 50mM Tris pH7.5; 250mM NaCl 50mM Tris pH7.5; 500mM NaCl 50mM Tris pH 7.5). The concentration of the 3rd haem domain of CcoP was 7.5 μ M lower than constant AniA concentration (96 μ M). The protein concentrations of 3rd haem domain of *N. gonorrhoeae* CcoP and nitrite reductase AniA in different buffers were kept the same.

It was found that there is a limited effect on interaction between two redox partners (Figure 5.6). Electron transfer rate K_{obs} (s^{-1}) between 3rd haem domain of *N. gonorrhoeae* CcoP and AniA with no salt present was only 30% higher than experiments performed in same buffer with salt present (from 100mM-500mM NaCl) (Figure 5.9). Electron transfer between these two partners can occur at a range of salt concentrations.

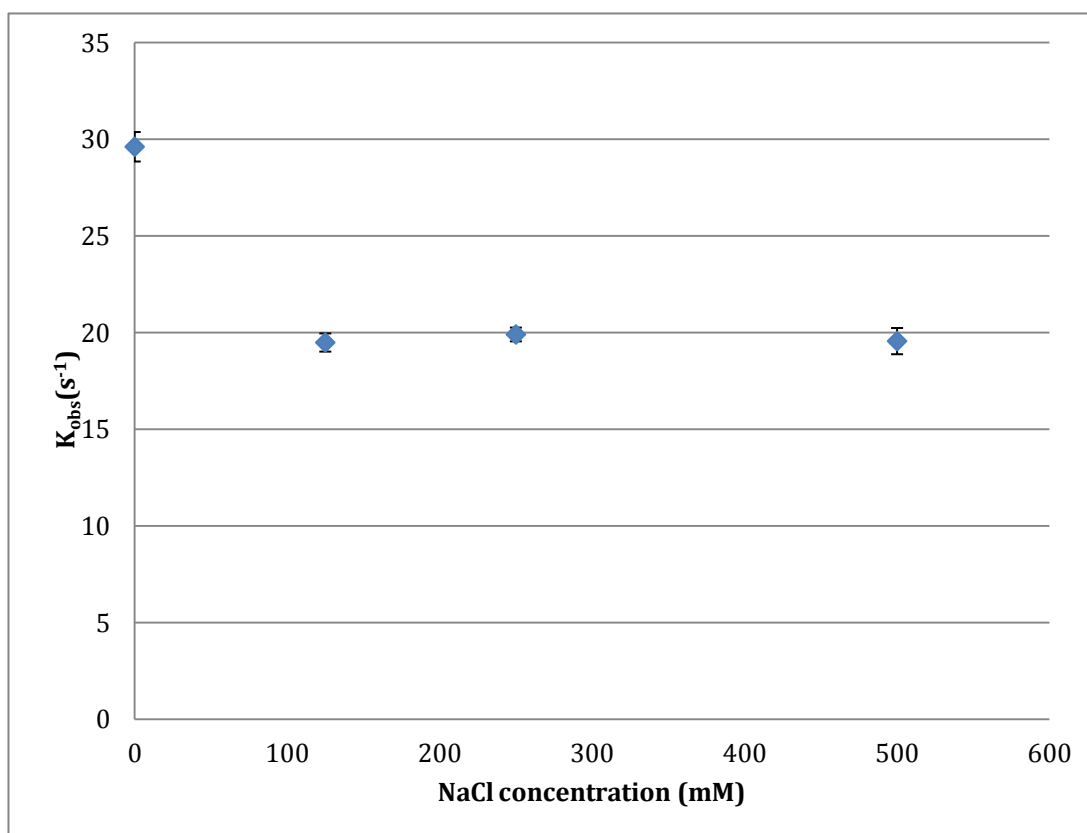


Figure 5.9 The salt dependence of reduced 3rd haem domain cytochrome CcoP and AniA was performed in 50 mM Tris(pH7.5 with salt present (0-500mM): Plots of $K_{obs} s^{-1}$ vs. salt concentration. Stopped-flow kinetics of inter-protein electron-transfer reaction from reduced 3rd haem domain cytochrome CcoP to AniA was performed at different salt concentrations. The concentration of the 3rd haem domain of CcoP was 7.5 μ M lower than constant AniA concentration (96 μ M). Error bars denote standard deviation.

5.3.3 pH dependence of 3rd haem domain of *N. gonorrhoeae* CcoP nitrite reductase AniA interaction.

The pH dependence of electron transfer between two partners is also addressed in this work. If the 3rd haem domain of CcoP could donate electrons at similar rates in varied pH assays, it would suggest this cytochrome protein is an effective electron donor to nitrite reductase AniA in *N. gonorrhoeae*. A stopped-flow experiment was performed as before, except the following adaptation: the 3rd haem domain of *N. gonorrhoeae* CcoP and AniA were buffer-exchanged into different pH assays (50mM HEPES pH5.5; 50mM HEPES pH6.5; 50mM Tris pH7.5; 50mM Tris pH 8.5). The concentration of 3rd haem domain of CcoP was 7.5 μ M lower than constant AniA concentration (30 μ M). Protein concentrations of the 3rd haem domain of CcoP and AniA in different buffers were always kept the same.

It is found that pH has a limited effect on interaction between two partners. Electron transfer rate $K_{\text{obs}}(\text{s}^{-1})$ between 3rd haem domain of CcoP and AniA with pH 7.5 was not different than experiments performed in same buffer with different pH assays (from pH 5.5-7.5) (Figure 5.10) . However, $K_{\text{obs}}(\text{s}^{-1})$ between 3rd haem domain of CcoP and AniA was decreased at higher pH (pH8.5). Electron transfer between these two partners can occur at a range of pH conditions.

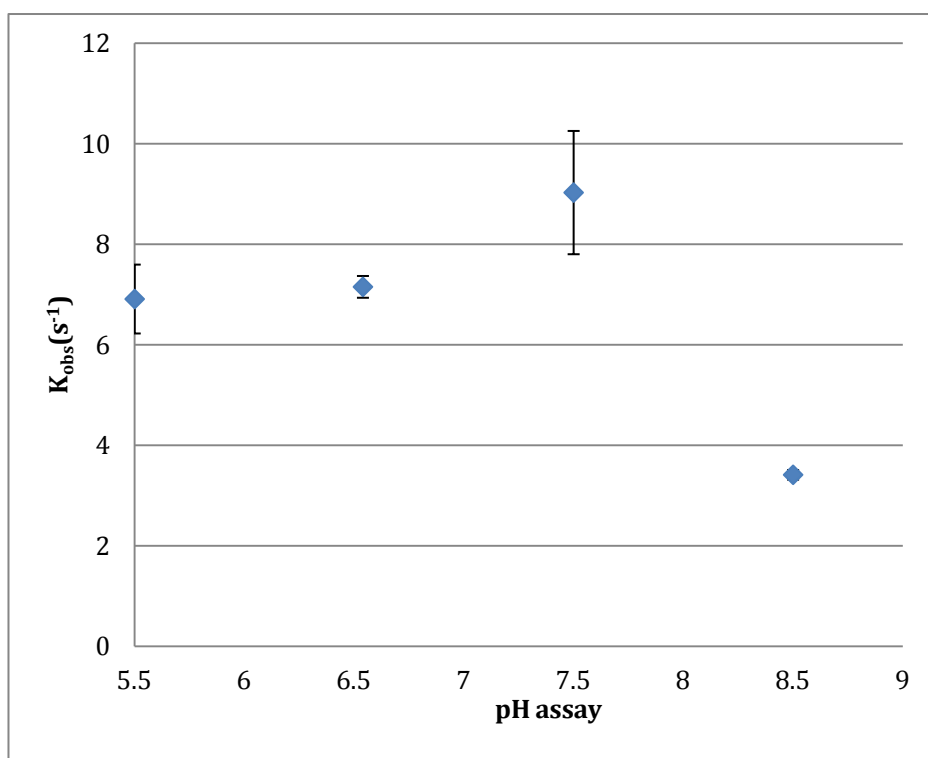


Figure 5.10: pH-dependence of AnIA and reduced cytochrome CcoP interaction was performed in 50mM Tris with vary pH conditions(5.5-8.5): Plots of $K_{obs}(s^{-1})$ vs. pH conditions. Stopped-flow kinetics of inter-protein electron-transfer reaction from reduced cytochrome CcoP to AnIA at pH conditions. The concentration of 3rd haem domain of CcoP was 7.5 μ M lower than constant AnIA concentration (30 μ M). Error bar denote standard deviation.

5.4 Over-expression and characterization of cytochrome *c* family protein from *N. elongata*

As mentioned in the introduction, *N. elongata* cytochrome (NEIELOOT_00905) shares more than 70% sequence similarity with second domain of cytochrome *c*₅. Our prediction is that the *c*₅ homologue in *N. elongata* has a role in denitrification process in *Neisseria* species. In order to produce soluble *N. elongata* cytochrome *c*, the cloning and expression of cytochrome *c* family protein from *N. elongata* in *E. coli* have been done (Figure 5.10). This gene contains nucleotide sequences of 201bp encoding for a sequence of 67 amino acids. PCR product was double digested and ligated into linearized pET22b⁺ vector directly. Successfully constructed NEIELOOT00905-pET22b⁺ plasmids were verified by colony PCR and DNA sequencing (Figure 5.12). This results in an expression construct where cytochrome domain is fused to a periplasmic leader sequence. *N. elongata* cytochrome *c* was purified aerobically and yielded large amounts of pure soluble protein. Predicted molecular weight of soluble *N. elongata* cytochrome *c* with His tag and one covalently attached haem domain is 8381.71 Da (Figure 5.13). Compared to other *c*-type cytochrome expressed in this work, *N. elongata* cytochrome *c* as prepared was in the oxidized form. It shows the typical low spin *c*-type cytochrome features. In the reduced state, cytochrome shows Soret band at 418nm, and α and β bands at 530nm and 555nm. In the oxidized state, Soret band moves to 406nm and α and β bands become on broad feature. However, *N. elongata* cytochrome *c* shows a band at 655nm

in both reduced and oxidized spectra (Figure 5.14) .

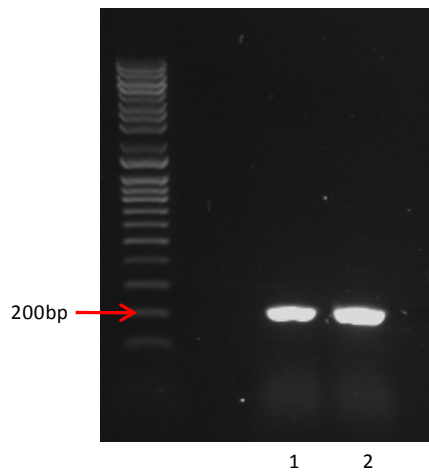


Figure 5.11: PCR product of cytochrome c family protein from *N. elongata*. The *N. elongata* cytochrome exhibits size of 201 bp. Lane 1 is *N. elongata* cytochrome gene with *N. elongata* subsp. *Glycolytica* 1043-haem (kindly donated by Dr. Mike Koomey) as template. Lane 2 is *N. elongata* cytochrome gene with *N. elongata* subsp. *Glycolytica* 6171 chromosomal DNA kindly donated by Dr. Mike Koomey) as template.

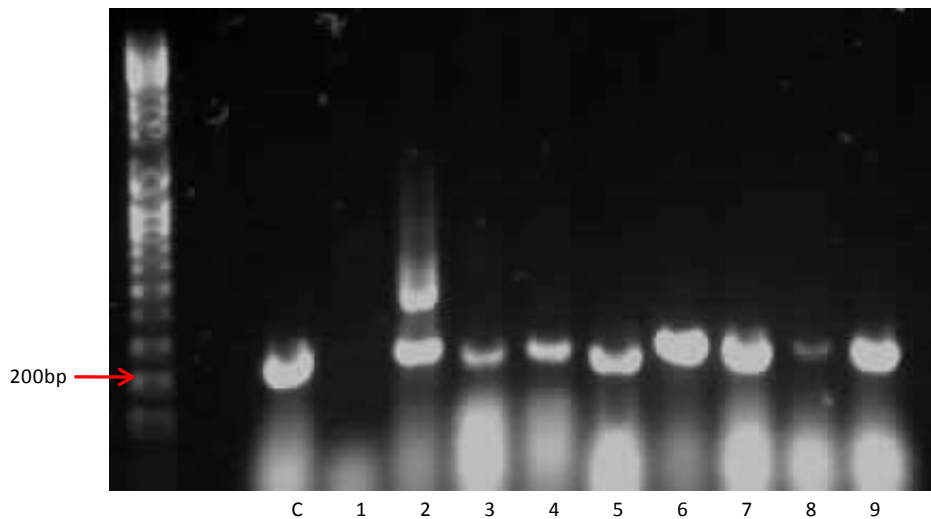


Figure 5.12: Colony PCR screen of cytochrome c family protein from *N. elongata* gene ligated into pET22b+ vector inserted in *E. coli* DH5 α transformants. c. control, *N. elongata* subsp. *Glycolytica* 6171 chromosomal DNA as template; 1-9, colony candidates No. 1- No.9.

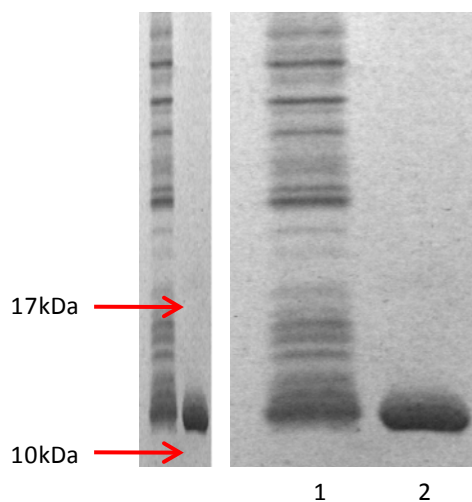


Figure 5.13: SDS-PAGE analysis of Ni affinity chromatography fractions of crude periplasmic extract and purified cytochrome c family protein from *N. elongata*. 3rd haem domain of *N. elongata* cytochrome has predicted MW. Approximately 10 kDa. Lane 1 periplasmic fraction. Lane 2: purified *N. elongata* cytochrome c.

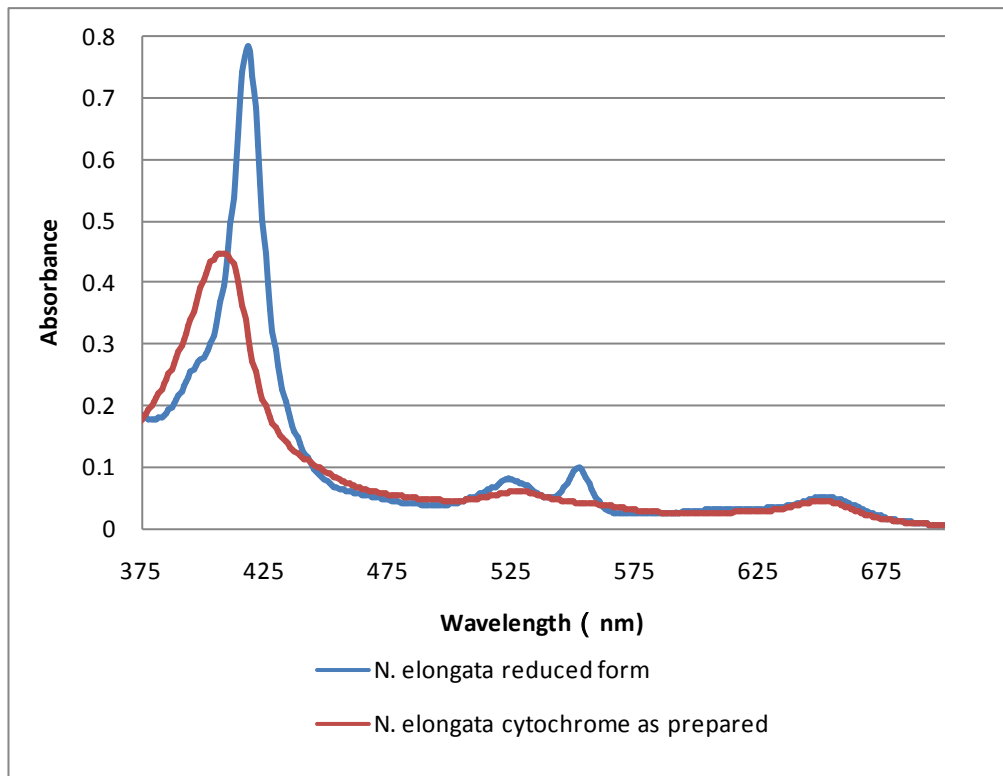


Figure 5.14: Absorbance spectra of purified *N. elongata* cytochrome *c*: Spectra were recorded at room temperature in 50mM Tris buffer (pH7.5). The oxidized state and reduced state show absorbance peaks at 406nm in oxidized form, and at 418nm, 530 and 555nm in the reduced form. Both of reduced and oxidized form *N. elongata* cytochrome *c* shown peak at the same wavelength 650nm. The concentration of *N. elongata* cytochrome *c* is 0.56×10^{-3} mM.

5.5 Steady state *N. elongata* cytochrome c and nitrite reductase AniA interaction:

The purpose was to identify any role of *N. elongata* cytochrome as an electron donor to AniA nitrite reductase. *N. elongata* cytochrome and nitrite reductase AniA were expressed and purified separately. *N. elongata* cytochrome is kept in reduced form under anaerobic conditions, and AniA is in oxidized form. The oxidation of *N. elongata* cytochrome by AniA nitrite reductase was observed. Spectral analysis of reduced *N. elongata* cytochrome and oxidized AniA interaction was measured between 350 nm-700nm by spectrophotometer under anaerobic conditions. Blue line (Control) is the spectra of 500 μ l of 12 μ M *N. elongata* cytochrome with water. Red line (Test) is the spectra of 500 μ l of 12 μ M reduced *N. elongata* cytochrome mixed with 500 μ l of 30.5 μ M AniA. Green line is the absorbance difference between *N. elongata* cytochrome with and without same amount of AniA. Upon adding AniA nitrite reductase, the absorbance difference (Green line) shows a major decrease at 425nm, there are also decreased absorbance at 525nm and 555nm. (Figure 5.15)

These observed absorbance differences are due to the oxidation of *N. elongata* cytochrome, the concomitant reduction of AniA is not seen, presumably due to the broad nature and relatively low absorbance of AniA spectra compared to *N. elongata* cytochrome. The absorbance difference changes the most at 425nm.

The result supports the idea that reduced *N. elongata* cytochrome can be oxidized by nitrite reductase AniA directly. To test the kinetic competence of this interaction in supporting electron flow to nitrite reduction, the interaction between the two redox

proteins was further examined by stopped flow kinetics.

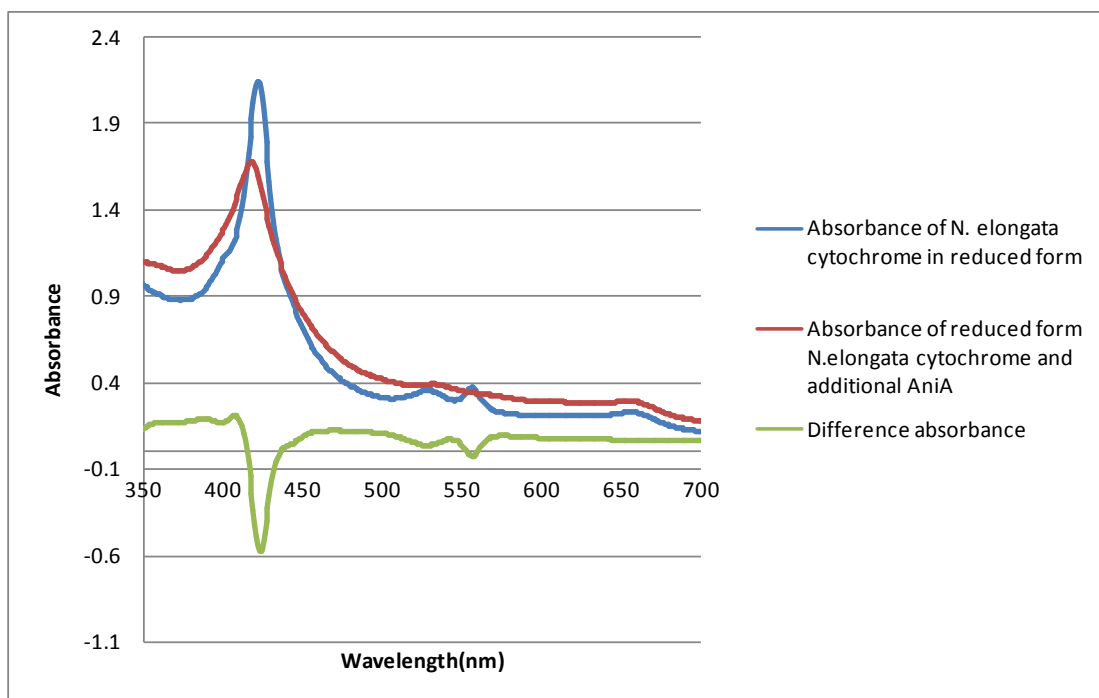


Figure 5.15: Spectral analysis of *N. elongata* cytochrome and oxidized AniA interaction is measured between 350nm to 700nm. The spectra of 500 μ l of 12 μ M reduced *N. elongate* cytochrome c mixed with same amount of 30.5 μ M oxidized AniA; control the spectra of 500 μ l of 12 μ M reduced *N. elongata* cytochrome with 500 μ l water. Green line is the absorbance difference.

5.6 Stopped-flow kinetics of inter-protein electron transfer reaction from reduced *N. elongata* cytochrome c to nitrite reductase AniA.

To investigate the kinetic relationship between nitrite reductase AniA and *N. elongata* cytochrome the formation of a functional electron transfer complex between these two proteins was analyzed by stopped-flow kinetics.

The kinetics of electron transfer from the reduced *N. elongata* cytochrome c to oxidized AniA was monitored at a wavelength of 425 nm, which had been previously determined by steady state experiments. To keep the pseudo first order, the concentration of AniA is always in large excess over the concentration of *N. elongata* cytochrome. As *N. elongata* cytochrome is easily oxidized in lab conditions, to keep *N. elongata* cytochrome in the reduced form, all the protein samples were prepared in an anaerobic chamber.

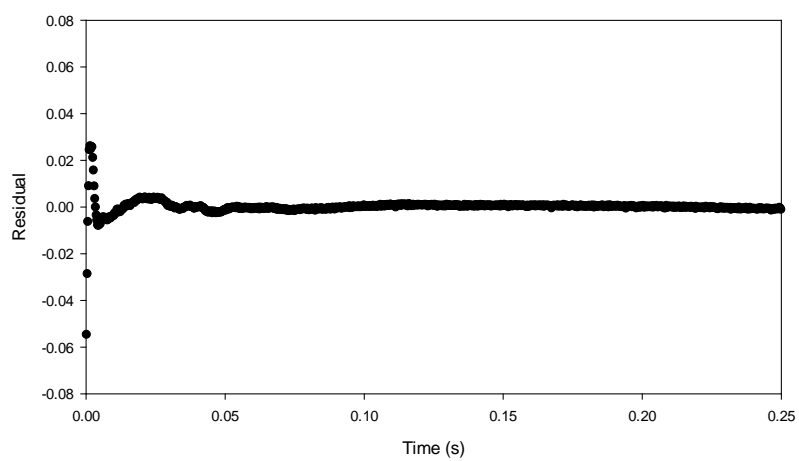
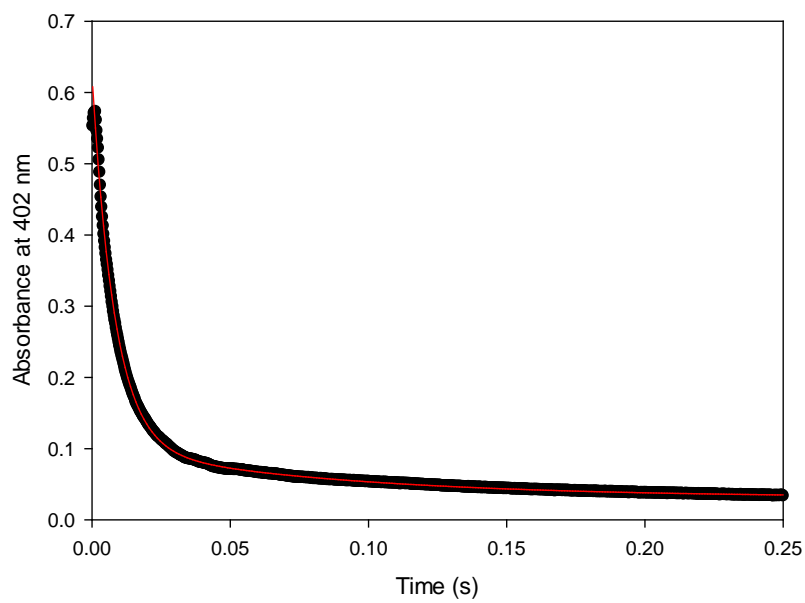
1000 data points were collected for 0.25s in each stopped-flow experiment. By using the data over a short time period (0ms-250ms) we can measure two rate constant using a 5 parameter double exponential rise to maximum function by Sigmaplot (Figure 5.16 a). There are two individual events happening at the same time. As reduced *N. elongata* cytochrome is not stable in the stopped flow equipment, the auto-oxidation of reduced *N. elongata* cytochrome is happening all the time. The other event is the reduced *N. elongata* cytochrome is oxidized by nitrite reductase AniA.

The second order electron transfer rate constant between the two proteins was estimated from the slope of the plots of AniA concentration versus $K_{obs}(s^{-1})$ (Figure 5.16 b).The rapid decrease of the absorbance is due to the oxidation of *N. elongata*

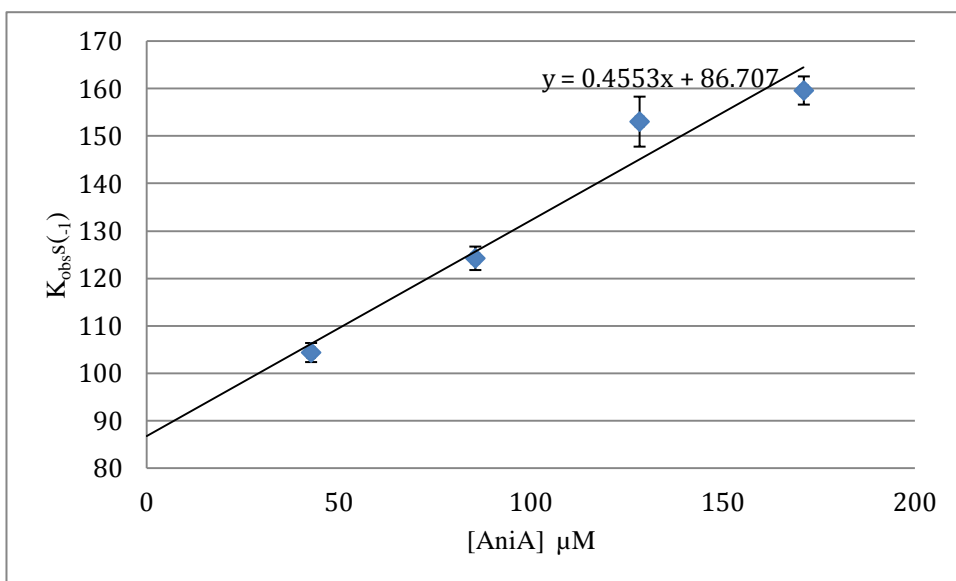
cytochrome and concomitant reduction of AniA. The slow rate is the *N. elongata* cytochrome auto-oxidation rate, which is about $20(\text{s}^{-1})$ (Figure 5.16 c). It is independent from AniA concentration.

The second order electron transfer rate constant between the two proteins is $4.5 \times 10^5 \text{M}^{-1} \text{s}^{-1}$, strongly supporting the idea that *N. elongata* cytochrome interacts functionally with outer membrane associated nitrite reductase AniA as an electron donor.

a.



b.



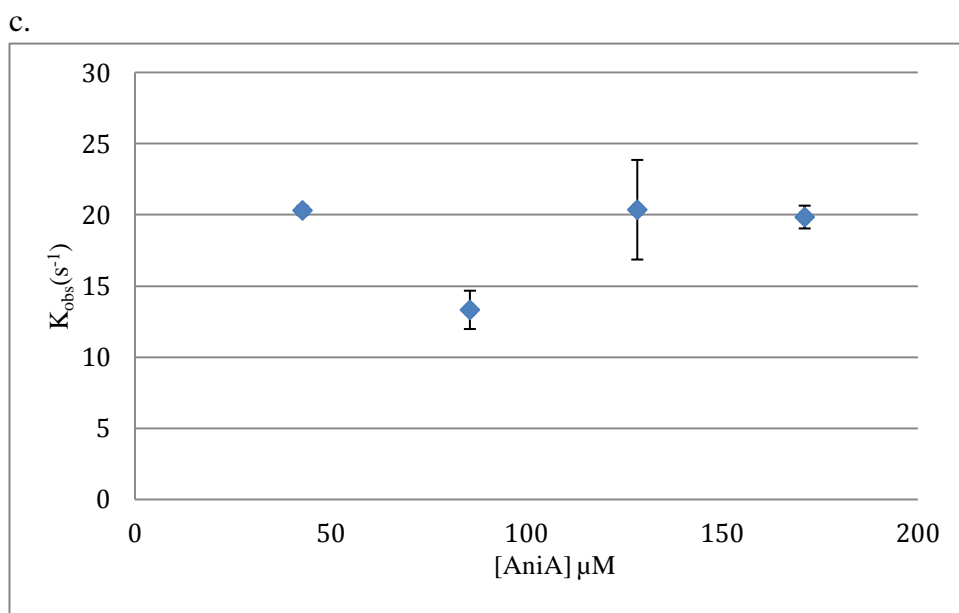


Figure 5.16: The electron transfer between Ania and *N. elongata* cytochrome c was performed in 50mM Tris (pH7.5). a. stopped-flow kinetics of inter-protein electron transfer reaction between reduced *N. elongata* cytochrome to Ania. The black line represents the observed data; red line is fitting curve. b. Plots of $K_{obs}(s^{-1})$ (fast rate) vs. Ania concentrations. Error bar denote standard deviation. The second order rate is $4.5 \times 10^5 M^{-1}s^{-1}$. c. plots of $K_{obs}(s^{-1})$ (auto-oxidation rate) vs. Ania concentration. The concentration of *N. elongata* cytochrome c was $7.5\mu M$, substantially lower than Ania concentration (from $171\mu M$ to $42.75 \mu M$). Error bar denotes standard deviation.

5.7 Discussion:

3rd haem domain of *cbb₃* oxidase of *N. gonorrhoeae* has been successfully cloned and heterologously expressed in *E. coli*. The 3rd haem domain of CcoP was expressed with C-terminal His tag, and exhibits molecular mass of *approx.* 10 kDa analyzed by SDS-PAGE. The predicted molecular mass is 10401Da. Reduced CcoP spectra shows typical c type cytochrome features :the Soret band at 419 nm, and α and β bands at 523 nm and 553 nm respectively. In the oxidized form, the soret band moves to 406 nm, and α and β bands become one broad feature.

The role of the 3rd haem domain of CcoP in electron transportation has been addressed in this work. To elucidate the physiological relationship between nitrite reductase AniA and the 3rd haem domain of CcoP, the formation of a functional electron transfer complex between these two proteins was analyzed by stopped-flow experiment. The second order rate of electron transfer from the reduced form 3rd haem domain of *CcoP* to oxidized form AniA is $3.3 \times 10^5 \text{M}^{-1} \text{s}^{-1}$, which strongly supports the idea that the 3rd haem domain of *N. gonorrhoeae* CcoP interacts functionally with outer membrane protein AniA. The second order rate constant of CcoP and AniA interaction is higher than cytochrome *c₅* and AniA interaction.

The change in salt or pH stress could not significantly affect the inter-protein electron transfer between two redox partners. As *N. gonorrhoeae* is an obligate human pathogen colonized in genitourinary tract with varying pH and salt concentrations, the pH and salt independence of inter-protein electron transfer between AniA and 3rd haem domain of CcoP would dramatically benefit nitrite reduction in *N. gonorrhoeae*.

In vitro, reduced the 3rd haem domain of *N. gonorrhoeae* CcoP is oxidized by AniA at a physiological relevant rate, indicating 3rd haem domain of CcoP transfer electrons directly to outer membrane AniA in *N. gonorrhoeae*. A *N. gonorrhoeae* double mutant (*c*₅ and the 3rd haem of CcoP) strain could not reduce nitrite at all under denitrifying conditions (Aspholm et al. 2010). It suggests that cytochrome *c*₅ and trihaem CcoP are the only direct donors to AniA in *N. gonorrhoeae*. Here we have provided a biochemical confirmation that a component of cytochrome terminal oxidase *cbb*₃ complex is involved in nitrite reduction.

N. elongata subsp. *Glycolytica* ATCC 29315 cytochrome c family protein has been successfully cloned and heterologously expressed in *E. coli* BL21 λDE3(pST2). Different from the other expressed c-type cytochromes, *N. elongata* cytochrome as prepared was in an oxidized form and dark brown color. The predicted molecular mass of *N. elongata* cytochrome c with N-terminal His tag and one covalently attached haem domain is 8377.21 Da. It exhibits molecular mass of *approx.* 10 kDa, as analyzed by SDS-PAGE. Reduced form *N. elongata* cytochrome was prepared by dithionite, and desalted in an anaerobic chamber. The reduced form *N. elongata* cytochrome spectra show the Soret band at 417nm, and α and β bands at 525 nm and 552 nm respectively. In the oxidized form, the soret band moves to 410nm, and α and β bands become one broad feature. However unlike other low spin cytochrome c, both of reduced and oxidized *N. elongate* cytochrome c spectra show a band at 655nm.

The formation of a functional electron transfer complex between these two proteins was also analyzed by stopped-flow experiment. Although all the protein samples are prepared and desalted carefully in the anaerobic chamber, reduced form *N. elongata* cytochrome can be oxidized by oxygen in the stopped-flow equipment, which is kept under aerobic conditions at room temperature. The auto-oxidation of reduced *N. elongata* cytochrome is happening all the time at a constant rate ($k_{\text{obs}} (\text{s}^{-1}) = \text{approx. } 20 (\text{s}^{-1})$) and also confirmed independent from AniA concentration. The other event is the reduced *N. elongata* cytochrome is oxidized by nitrite reductase AniA. The second order rate constant of electron transfer from the reduced *N. elongata* cytochrome *c* to oxidized AniA is $4.5 \times 10^5 \text{ M}^{-1} \text{ s}^{-1}$. Comparing with cytochrome *c*₅ and AniA interaction, the second order rate of *N. elongata* cytochrome and AniA is about 2 times higher than that of *c*₅ and AniA interaction.

Reduced *N. elongata* cytochrome can be oxidized by nitrite reductase AniA directly at a physiological relevant rate. We also demonstrate the auto-oxidation rate of *N. elongata* cytochrome *c* is independent from AniA concentration at room temperature. In conclusion, *N. elongata* cytochrome *c* is a direct and efficient electron donor to nitrite reductase AniA in this non-pathogenic species.

As a subunit of *cbb*₃ complex, the function of CcoP is to support terminal oxidase activity. *N. meningitidis* could be more adapted under more aerobic conditions and low nitrite concentration. Nitrite reduction comes with significant metabolic cost as NO is toxic and growth inhibitory (Overton et al. 2006). Although *N. meningitidis* expressed nitric oxide reductase NorB which converting nitric oxide to nitrous oxide, the expression of norB is activated by NO by acting on NsrR (NO-sensing transcription factor) (Overton et al. 2006). Toxic NO accumulates so quickly that growth inhibition occurs before sufficient NorB expressed in the system. Two different studies have shown *aniA* gene was found to contain mutations in 32% or 34% of sequenced *N. meningitidis* strains, resulting in either premature termination of translation or deletion of entire gene (Barth et al. 2009; Ku et al. 2009). In addition, a conserved and functional AniA is not essential for *N. meningitidis* survival (Stefanelli et al. 2008). However, all *N. gonorrhoeae* strains are predicted to express AniA implying the crucial role for AniA in gonococcus (Ku et al. 2009). Nitrite reduction is more important in *N. gonorrhoeae* than *N. meningitidis*. It suggests that tri haem CcoP evolved to enable *N. gonorrhoeae* to utilize AniA denitrification more effectively under microaerobic condition.

N. meningitidis and *N. gonorrhoeae* share more than 98% sequence similarity in house-keeping genes and normally should be included in the single species. The important fact dividing them into different species is the diseases they cause.

Primary habitat of all human hosted *Neisseria* species is colonized in the nasopharynx, except *N. gonorrhoeae* which colonize urogenital mucosal sites. The extreme

uniformity of *N. gonorrhoeae* housekeeping gene suggests that it may have arisen as a clone of *N. meningitidis* colonizing the genital tract (Vazquez et al. 1993). The evolutionary origin of trihaem *ccoP* may have been a unique gene duplication gene fusion event between cytochrome *c₅* and primordial dihaem CcoP. This hypothesis is supported by high sequence similarity between C-terminal CcoP and *c₅*, and also length of AlaSerPro stretches and overall alanine richness between the two candidates. A cytochrome *c₅* and CcoP hybrid *N. gonorrhoeae* strain (a translational fusion consisting of the amino-terminus of *c₅* and the 3rd haem domain of *N. gonorrhoeae* CcoP was constructed) in a cytochrome *c₅* deficient strain and expression of dihaem CcoP background is still able to support nitrite reduction and nitrite dependent microaerobic growth (Aspholm et al. 2012). It demonstrated the identical function of the terminal haem domain of *c₅* and trihaem CcoP, when displayed in the context of otherwise structurally identical polypeptides. Taking all these together, *N. gonorrhoeae* CcoP could provide strong evidence for molecular based evolution in *Neisseria* species (Aspholm et al. 2012).

In conclusion, the ability of the 3rd haem domain of CcoP to act as an electron carrier in nitrite reduction that can transfer electrons to nitrite reductase AniA reshape the organization of respiration, and provides boarder connectivity to electron transport from cytochrome *bc₁* complex to AniA through electron carriers cytochrome *c₅*, *c₃*, and *c₄* (Figure 5.17). It is also the first example of a terminal reductase involved in nitrite reduction. Both of 3rd haem domain of CcoP and *N. elongata* cytochrome share high degree similarity with the direct donor 2nd haem domain of cytochrome *c₅*, and

also show the ability of donating electrons to AniA at a physiological relevant rate. Based on biochemical interactions established in this work between CcoP and *N. elongata* cytochrome, we favor a model both of the corresponding gene *c5* product donating electrons to AniA. In addition, in this model electron donors (CcoP or *N. elongata* cytochrome) have to be capable of close contact with AniA.

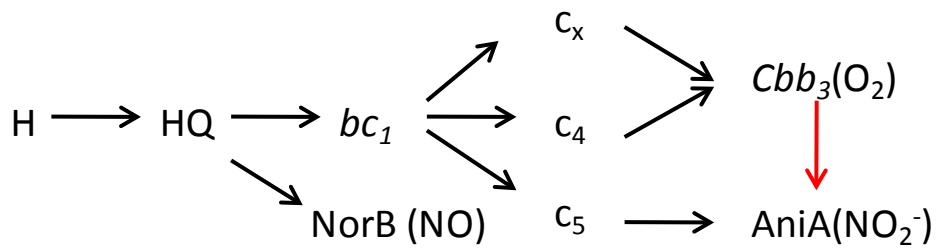


Figure 5.17: Proposed pathways for electron transfer from NADH dehydrogenase(H) to terminal reductase (cbb_3 , AniA and NorB) in *N. meningitidis* and *N. gonorrhoeae*. The model is based on data obtained from this work and also from(Hopper et al. 2009; Aspholm et al. 2010; Deudom et al. 2008)

Chapter 6

Characterization of lipid-modified Azurin (Laz)

6.1 Introduction:

The *laz* gene (NMB 1533) of *N. meningitidis* strain MC58 is predicted to encode lipid modified azurin (Laz). Laz is predicted to have three domains, including the lipoprotein signal peptide, the flexible linker peptide, and the globular azurin domain. In addition, it is determined to be associated with the outer membrane (Chapter 3). Mature Laz consists of 182 amino acids including the C-terminal globular azurin domains (residue 63-182) with the flexible linker peptide (residue 18-62) and the N-terminal lipoprotein signal peptide (residue 1-17) (Figure 6.1.a). It can be cleaved by signal peptidase II between Ala 17 and Cys 18. The predicted pI of Laz protein is 4.6. The globular domain of Laz is very similar to a conventional periplasmic azurin, which is a copper-containing protein in the cupredoxin superfamily. Cupredoxins are normally described as important electron carriers in electron transport and energy metabolism. Pseudoazurins, rusticyanin, plastocyanin, amicyanin are other members of the cupredoxin superfamily. Cupredoxins absorb visible light at around 600nm (due to S to Cu charge transfer). Cupredoxins exhibit a strong blue colour at oxidized state, which can be detected by using visible spectrophotometry. The copper binding site consists of two histidines, one cysteine and one methioine, and is conserved among cupredoxins and is within eight-stranded Greek key β -barrel structure (Figure 6.1. b).

a.



b.

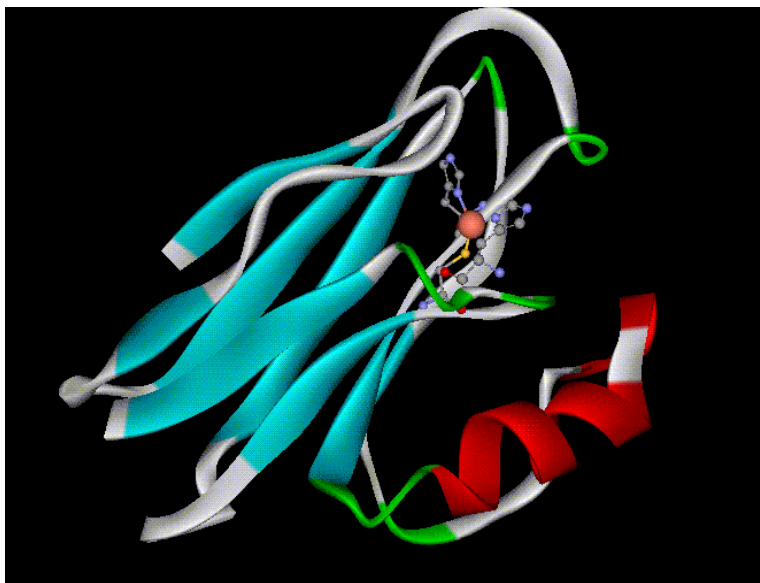


Figure 6.1: Predicted *Neisseria* Laz structure: a. Predicted *Neisseria* Laz domain structure. Mature Laz consists of three domains including N-terminal lipoprotein, flexible linker, and C-terminal globular azurin. b. Predicted tertiary structure of globular azurin domain of Laz with the copper site. The azurin domain of Laz contains the copper site at His102, Cys166, His171 and Met175. Copper is red sphere. The predicted copper binding site is within eight-stranded Greek key β -barrel structure.

Laz is highly conserved in meningococcus and gonococcus. The N-terminal domain (39 amino acids) of mature Laz contains 5 repeats of highly conserved sequence

alanine-alanine-glutamate-alanine-proline (AAEAP) motif which are quite similar to the sequence in the paralogs of linker regions of Lip protein and AniA protein in *N. meningitidis*, and also includes an epitope recognized by the H. 8 monoclonal antibody (MAb) (Cannon 1989; Trees and Spinola 1989; Woods et al. 1989). MAb binds to all pathogenic *Neisseria* species including gonococci and meningococci, but not to other commensal *Neisseria* strains (Trees and Spinola 1989).

Pathogenic bacterium *Pseudomonas aeruginosa* azurin (Paz) is found as an inducer of apoptosis and has a regression effect on human melanoma and breast cancer (Punj et al. 2004). Laz H. 8 moiety is capable of disrupting the entry barrier in glioblastoma cells and attacking brain tumours (Hong et al. 2006). *Neisseria* uses the lipobox upstream of the H.8 moiety to bring the azurin to the surface, but it is the H. 8 moiety, lipidated or not, that is critical for entry in glioblastoma cells, presumably through disruption of any tight junction between the endothelial cells.

Neisseria Laz, Paz and H.8 fused in Paz could bind to merozoite surface protein of the malarial parasite *Plasmodium falciparum* to reduce parasitemia, and also bind to HIV-1 gp120, intercellular adhesion molecule ICAM-3 and the CD4 receptors of T cells to suppress HIV-1 growth in blood mononuclear cells at an early stage in the infection (Chaudhari et al. 2006). Laz could be a potential therapeutic target in the treatment of cancer, malaria and HIV-1 infection. *Neisseria* Laz is also involved in defence against oxidative stress and copper toxicity and survival within cervical epithelial cells (Wu et al. 2005).

The globular azurin domain (127 amino acids) has a high degree of similarity to the sequence of azurin from other bacteria *Pseudomonas*, *Alcaligenes*, and *Bordetella*. It suggests that there is a potential function of Laz involved in electron transportation

during respiration. It was found that azurin is an efficient electron donor to copper type nitrite reductase under denitrifying conditions in bacteria *Pseudomonas*, *Alcaligenes*, and *Bordetella* (Brittain et al. 1992; Murphy et al. 2002; Pearson et al. 2003). However, the azurin functioning as efficient electron carriers in respiration is not lipoprotein and does not have H. 8 MAb binding sites, which are present in *N. meningitidis* Laz. Furthermore, a *c₅* mutant *N. meningitidis* failed to utilize nitrite during incubation under microaerobic conditions with nitrite present (Deeudom et al. 2008) . It suggests that Laz could not receive electrons on its own from cytochrome *bc₁* and transfer to nitrite reductase AniA. If Laz is involved in nitrite reduction, a *laz* mutant strain will show the deficiency in nitrite utilization under denitrifying conditions. The other prediction is that Laz might receive electrons from cytochrome *c₅* and transfer to AniA as an electron mediator under certain conditions. The aim of this chapter is to investigate whether *Neisseria* Laz is involved in the respiratory mechanism in *Neisseria* species.

6.2 Over-expression and characterization of Laz:

The purpose was to produce soluble Laz protein for further kinetics study. Primers were designed to amplify truncated *laz* and to be inserted into the pET 22b⁽⁺⁾ vector which allows IPTG-inducible expression of the desired protein to be directed to the periplasm of the *E. coli* expression strain BL21 (λ)DE3 with *pelB* leader sequence. The *laz* primers were designed with NcoI site at 3' end and Eco RI site at 5' end. The *laz* gene with the size of 516 bp was amplified by PCR (Figure 6.2). There are two extra amino acids (Met, Ala) included at the N-terminus of protein to keep the reading in framed resulting in soluble Laz with 167 amino acids in total. The cloning of the truncated *laz* gene from the PCR product was digested by restriction enzymes and ligated with linearized pET22b⁽⁺⁾ vector directly.

The successfully constructed plasmid was transformed to *E. coli* DH5 α for checking the plasmid stability and expression strain *E. coli* BL21 (λ)DE3. A colony PCR screen was used to check the successful ligated plasmid with *laz* forward primer and T7 reverse primer (Figure 6.3). The ligated pET-22b⁽⁺⁾-*laz* plasmid was also confirmed by DNA sequencing and then ready for protein expression.

The expression of soluble Laz protein was achieved by incubating BL21 (λ)DE3 pET 22b⁺-Laz in LB broth with 1mM CuCl₂ at 30°C and induced with 1mM IPTG to achieve a high yield of soluble protein expression. The Laz periplasmic extraction was further purified by anion exchange column chromatography, as the predicted pI of Laz is 4.6. The predicted molecular mass of soluble Laz is 16985Da (without copper ion) analysed by mass spectroscopy (Dr. Manu Deedom, PhD thesis, unpublished data) The expressed protein was found to have a high molecular mass of

20 kDa or 27 kDa. This might be due to different redox states coexisting during SDS-PAGE (Figure 6.4).

The visible spectrum of Laz as prepared is characterized by an absorbance maximum of 626 nm consistent with the blue colour expected of Laz in 50mM Tris buffer (pH7.5). In reduced form, Laz exhibits very low absorption (Figure 6.5).



Figure 6.2: PCR product of *laz* gene with EcoRI and NcoI restriction digested sites exhibit a size of 516bp.

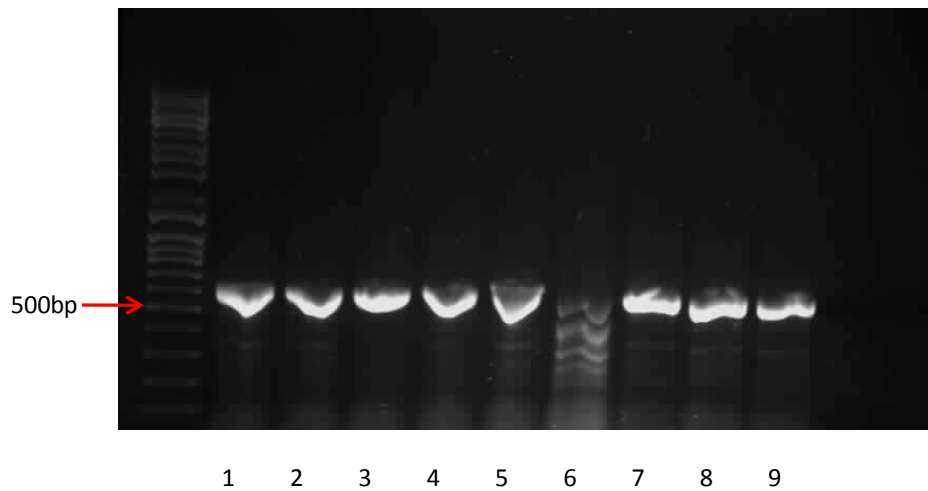


Figure 6.3: Colony PCR screen for *laz* inserted in pET 22b(+) plasmid. NO. 1-9 are the colony candidate numbers 1 to 9.

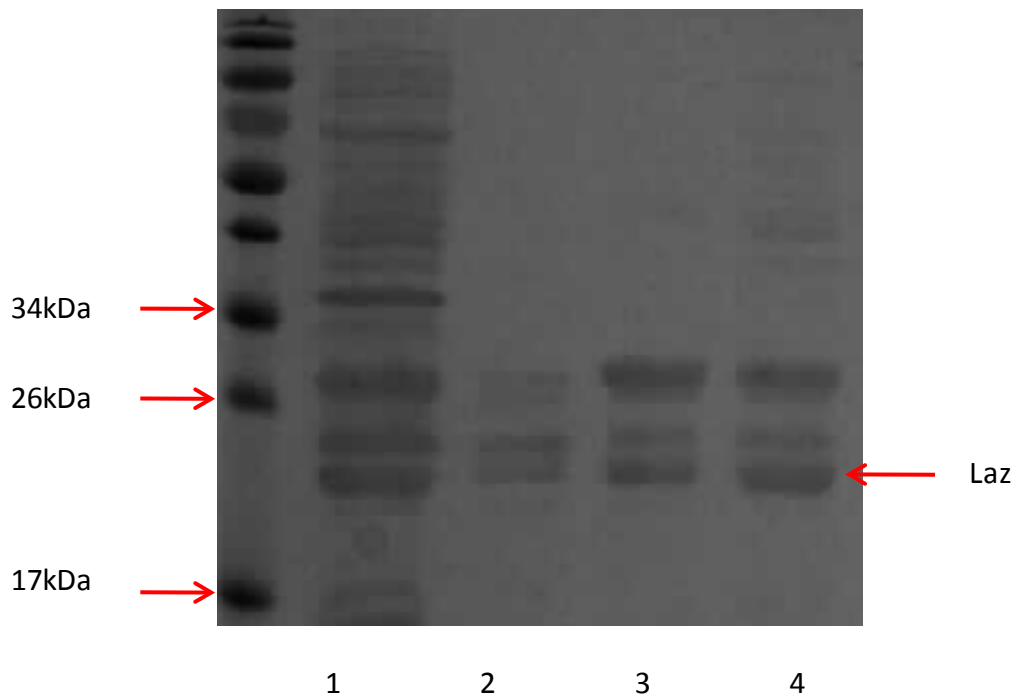


Figure 6.4: Expression of meningococcal sLaz protein in *E. coli*. SDS-PAGE analysis of soluble Laz(sLaz) from DEAE-sepharose anion exchange chromatography: Lane 1 is *E. coli* Periplasmic fraction containing sLaz protein. Lane 2, 3 and 4 are protein fractions containing purified sLaz from anion exchange chromatography.

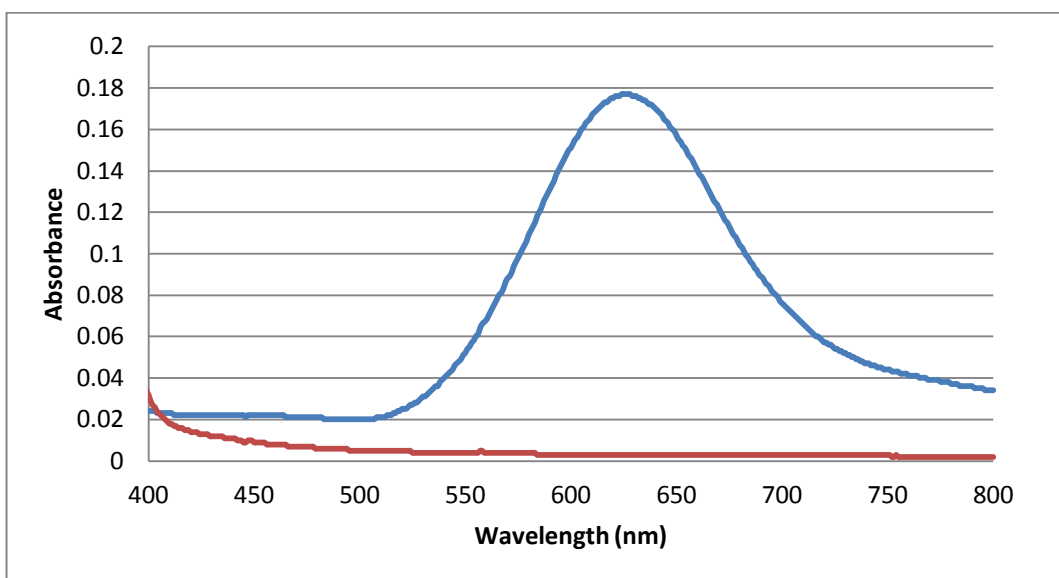


Figure 6.5: UV-visible spectrum of reduced and oxidized soluble Laz (19 μM) buffered in 50 mM Tris (pH7.5). Blue copper proteins absorb visible light around 600 nm. Oxidized Laz exhibits broad absorption with maximum absorption at 626 nm (blue line). Reduced Laz exhibits very low absorption (red line).

6.3 Steady state kinetics of inter-protein electron transfer reaction from Laz to nitrite reductase AniA, and cytochrome c_5 to Laz.

The purpose was to identify any role of Laz as an electron mediator between AniA nitrite reductase and cytochrome c_5 . Laz, cytochrome c_5 and nitrite reductase AniA were expressed and purified, separately. Cytochrome c_5 as prepared is in reduced form, Laz is in oxidized form. Spectral analysis of reduced c_5 and oxidized Laz interaction was measured between 400 nm-700nm by spectrophotometer. Blue line (Control) represents the spectra of 800 μ l 7 μ M reduced c_5 and 200 μ l water. The red line (Test) represents the spectra of 800 μ l 7 μ M reduced cytochrome c_5 mixed with 200 μ l 76 μ M Laz. The green line is the absorbance difference between cytochrome c_5 with and without Laz. Upon adding Laz, the absorbance difference has shown a decrease at 420nm, and also a decreased absorbance at 520nm and 555nm (Figure 6.6). These observed absorbance differences are due to the oxidation of cytochrome c_5 , the concomitant reduction of Laz is not seen, presumably due to the broad nature and relatively low absorbance of the spectra of Laz compared to that of cytochrome c_5 . The absorbance difference changes the most at 420nm. It indicates that reduced cytochrome c_5 has been oxidised by AniA.

The steady state interaction between Laz and AniA was performed in the same as the interaction between cytochrome c_5 and Laz, except for the following adaptation: Soluble Laz was prepared in the reduced form, whereas AniA was prepared in the oxidized form. Spectral analysis of reduced Laz and oxidized AniA interaction was measured between 400 nm-800nm by spectrophotometer. The blue line (Control) represents the spectra of 500 μ l 76 μ M reduced Laz with 500 μ l water. The red line (Test) represents the spectra of 500 μ l 76 μ M reduced Laz mixed with 500 μ l 68 μ M

oxidized AniA. The green line is the absorbance difference of Laz with and without AniA. Upon adding AniA nitrite reductase, the absorbance difference shows the bands at 605 nm, which differ from the spectra of oxidized AniA (600nm and 455 nm) (Figure 6.7). This might suggest that some of oxidized AniA is reduced by Laz. The interaction of electron transfer between Laz and AniA needs to be further confirmed by stopped-flow kinetics at different wavelengths.

The result supports the idea that reduced cytochrome c_5 can be oxidized by Laz directly. To test the kinetic competence of this interaction in supporting electron flow to nitrite reduction, the interaction between the two-redox proteins was further examined by stopped-flow kinetics. However, this experiment is unable to provide the evidence that Laz is the direct electron donor to AniA in *Neisseria* species.

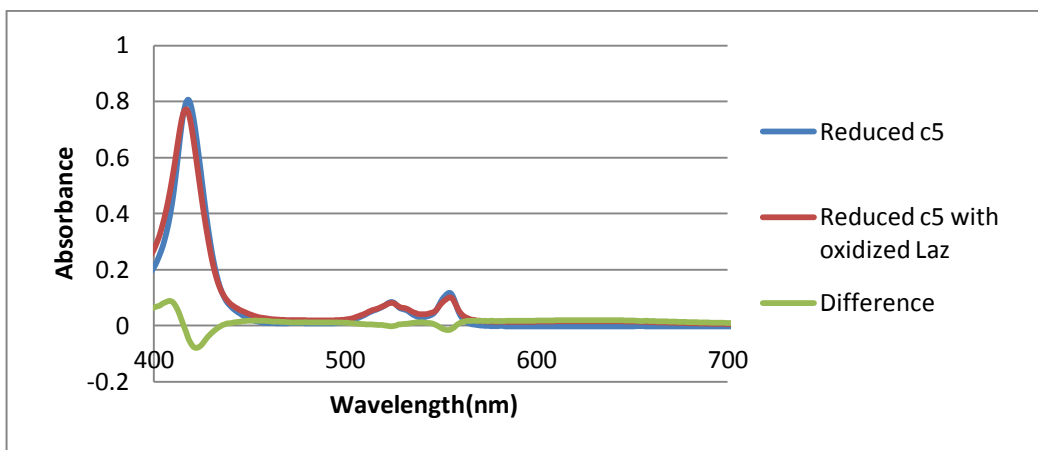


Figure 6.6: Spectral analysis of reduced c_5 and oxidized Laz interaction is measured between 400nm-700nm. The spectra of 800 μ l of 7 μ M reduced c_5 mixed with 200 μ l of oxidized 76 μ M Laz (red line); Control (blue line) the spectra of 800 μ l of 7 μ M reduced c_5 with 200 μ l of water. Green line is the absorbance difference

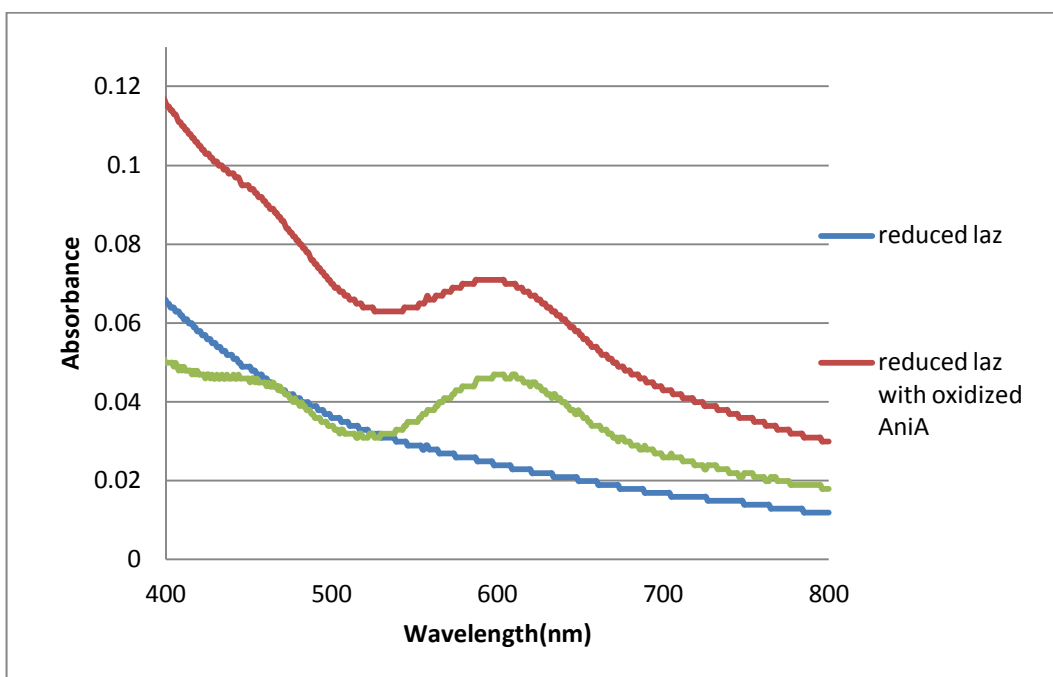


Figure 6.7: Spectral analysis of reduced Laz and oxidized AniA interaction is measured between 400nm-800nm. The spectra of 500 μ l of 76 μ M reduced Laz mixed with 500 μ l of 68 μ M oxidized AniA (red line); Control (blue line) the spectra of 500 μ l of 76 μ M reduced Laz with 500 μ l of water. Green line is the absorbance difference.

6. 4 Stopped flow kinetics of inter-protein electron transfer reaction from cytochrome c_5 to Laz, and from Laz to AniA

To investigate the kinetic relationship between Laz and cytochrome c_5 , the formation of a functional electron transfer complex between these two proteins was analysed by stopped-flow kinetics.

The kinetics of electron transfer from the reduced cytochrome c_5 to oxidized Laz was monitored at a wavelength of 402nm. To keep the pseudo first order, the concentration of Laz is always in large excess over the concentration of c_5 . Observed data was fitted by a single rate constant using a 3 parameter single exponential rise to maximum function by Sigmaplot. The rapid increase of the absorbance is due to the oxidation of cytochrome c_5 and concomitant reduction of Laz. The second order electron transfer rate constant between the two proteins was estimated from the slope of the plots of Laz concentration versus $K_{\text{obs}}(\text{s}^{-1})$ (Figure 6.8).

The second order electron transfer rate constant between the two proteins is *approx.* $(1.946) \times 10^5 \text{ M}^{-1}\text{s}^{-1}$, similar to the second order rate constant of cytochrome c_5 and AniA interaction. It strongly supports the idea that the inner membrane cytochrome c_5 interacts functionally with Laz as an electron donor.

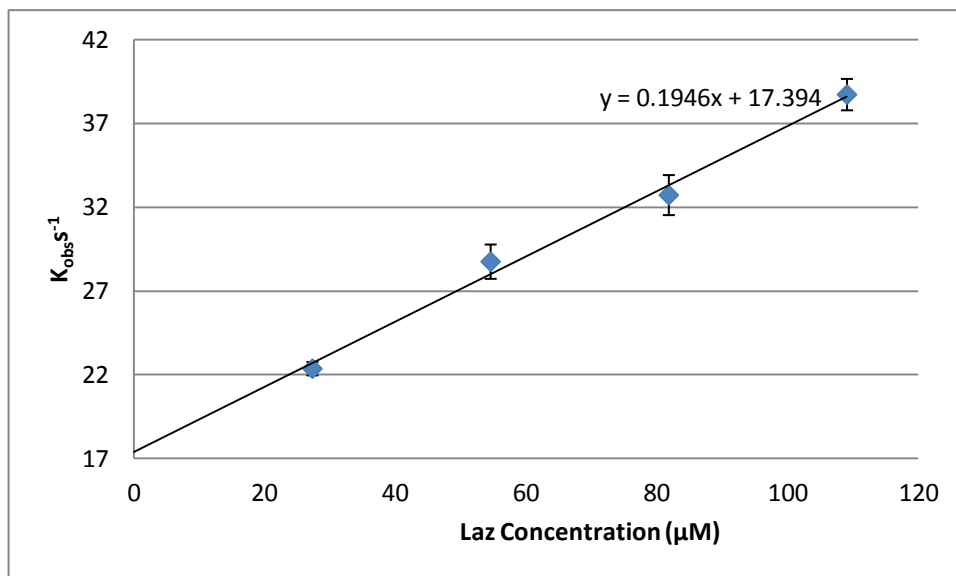


Figure 6.8: The 2nd order rate constant for cytochrome c_5 and Laz interaction. Plots of $K_{obs} s^{-1}$ vs. Laz concentration. Error bar denote standard deviation. The 2nd order electron transfer rate constant between the two proteins is $1.946 \times 10^5 M^{-1} s^{-1}$. The concentration of AniA (from 22.37 μM to 38.72 μM) is always in large excess over the concentration of Laz (7.5 μM). The experiment is performed in 50mM Tris(pH7.5). Error bars denote standard deviation.

To investigate the kinetic relationship between Laz and AniA, the formation of a functional electron transfer complex between these two proteins was analysed by stopped-flow kinetics. The kinetics of electron transfer from the reduced Laz to the oxidized AniA was monitored at the wavelength of 455nm, 600nm and 626nm (Figure 6.9). To keep the pseudo first order, the concentration of AniA (35 μM) is always in large excess over the concentration of Laz (7.5 μM). It was found that there is no inter-protein electron transfer between Laz and AniA at these wavelengths.

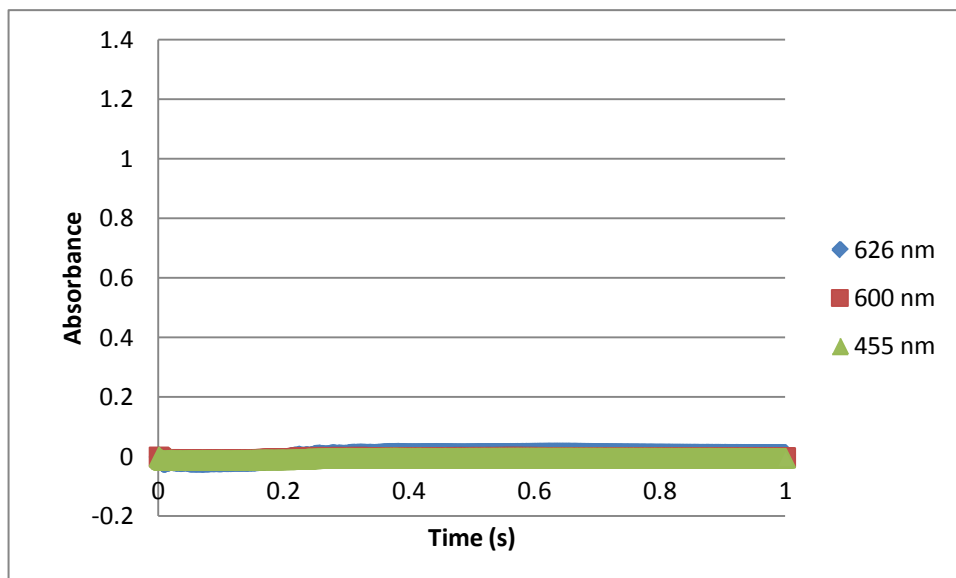


Figure 6.9: Stopped-flow kinetics of inter-protein electron-transfer reaction from reduced laz to AniA was performed at wavelength (455nm, 600nm, 626nm). The protein concentrations of reduced form Laz (7.5 μM) and oxidized form AniA (35 μM) were always kept the same in vary wavelengths. The experiment was performed in 50mM Tris(pH7.5).

6.5 Growth of *laz* mutant strain under microaerobic conditions

The purpose was to investigate the role of Laz in the *N. meningitidis* respiration chain and also to determine the ability of *laz* mutant strains to utilize nitrite as alternative electron terminal acceptors with a low oxygen supplement. The disrupted *laz* gene (constructed plasmid obtained from Dr. Manu Deedom) was transformed into *N. meningitidis* MC58, and the correct insertion was confirmed by colony PCR screen (Figure 6.10). To achieve growth under the denitrifying conditions, both of the wild type and mutant *N. meningitidis* strains were cultured in 20ml MHB in 25ml McCartney bottle with 10mM NaHCO₃ and 5mM nitrite supplement at 90 rpm.

Supplementing Laz and WT cultures with nitrite increased the growth optical density, which is consistent with a change from oxygen limitation to unrestricted growth (Figure. 6.11 a). Both of WT and *laz* mutant grew better with nitrite supplement than without nitrite supplement under microaerobic conditions (Figure. 6.11 a). The *laz* mutant strain is able to utilize nitrite as a respiratory substrate to support growth under oxygen limited conditions. The growth of *laz* mutant strains under the denitrifying conditions was still slightly poorer than WT strains. The *laz* mutant strain entered log phase 1 hour more slowly than that of the WT strain. However, both of strains reached the maximum optical density at the same time (after 9 hours incubation).

An increase in growth rate with the presence of nitrite was consistent with the expression of AniA and the disappearance of nitrite (Figure 6.11 b). Levels of nitrite were measured by nitrite assay after every hour of growth. The WT strains start to utilize nitrite at hour 4. And nitrite had disappeared at hour 8 in the WT strain. It was found that the *laz* mutant strain starts to utilize nitrite at the same time as the WT

strain. The level of nitrite in the *laz* mutant had disappeared at hour 9. Our study has shown the *laz* mutants reduce nitrite later than WT during growth under microaerobic conditions. In addition, the *laz* mutant strain is able to use nitrite as a respiratory substance under microaerobic conditions. It indicates that Laz is not crucial in the *N. meningitidis* nitrite reduction process.

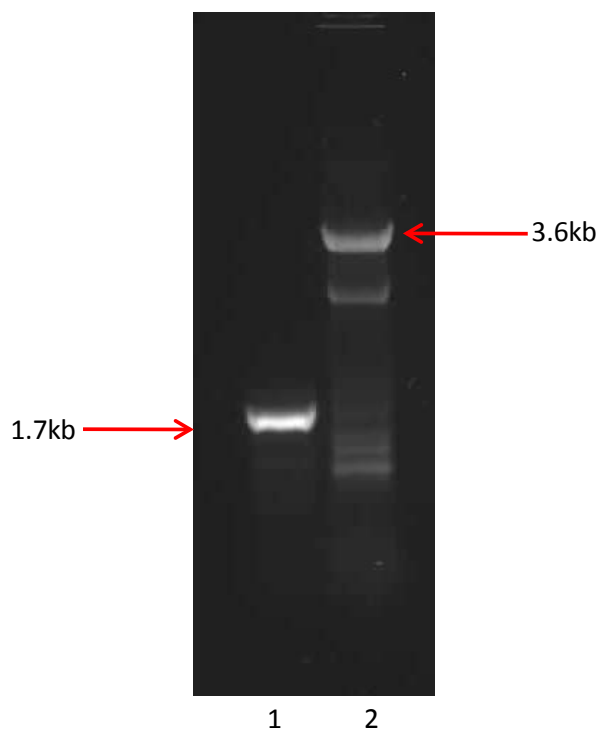
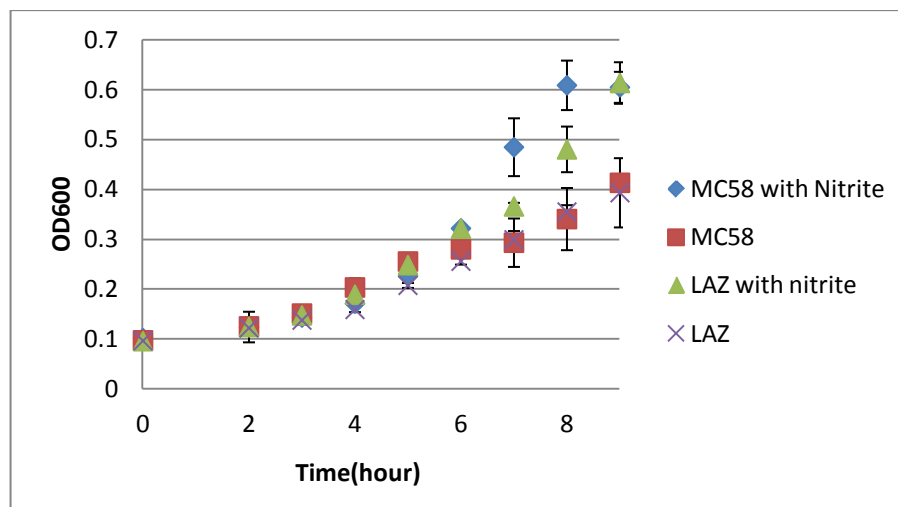


Figure 6.10: Colony PCR screen of *laz* with disrupted gene in *N. meningitidis* MC58. *laz* fragment (1.7 kb) without insert was found in lane 1; The *laz* + chl^r fragments (3.6 kb) were found in lane 2.

a.



b.

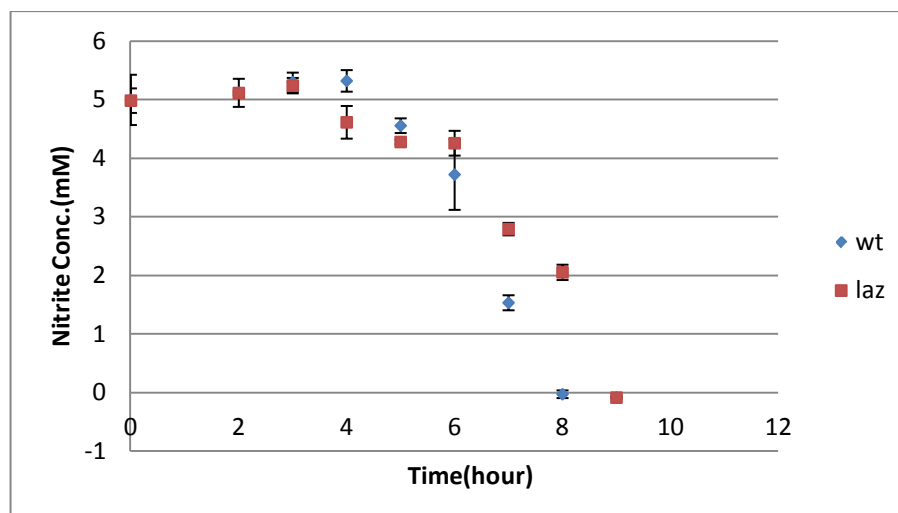


Figure 6.11: Growth of *N. meningitidis* under oxygen limited conditions. (a) The effect of nitrite on the growth of WT and *N. meningitidis laz* mutant. Growth curve is plotted as OD₆₀₀ versus time (hour). (b) Comparing nitrite reduction of wild type and *laz* mutant under denitrifying conditions. *Laz* showed ability to reduce nitrite to support growth under microaerobic condition. Error bar denote the standard deviation.

6.6 Discussion:

Our work described the establishment of an *E. coli* heterologous over expression system for Laz production that produced soluble Laz which was identified by UV-vis absorbance and SDS-PAGE methods. The *laz* gene has been successfully cloned and heterologously expressed in the *E. coli* cell. In order to produce the soluble Laz protein with copper ion, LB medium must be supplemented with 1mM CuCl₂. As the predicted pI of Laz is 4.6, anion exchange chromatography was used to purify soluble Laz. Laz protein was partially purified as visualised by SDS-PAGE. The visible spectrum of Laz as prepared is characterized by the maximum absorbance of 626 nm, and was consistent with the blue colour of azurins. In reduced form, sLaz exhibits very low absorption.

The function of Laz involved in the denitrification pathway has also been determined by kinetic studies. In a steady state experiment, reduced form cytochrome *c*₅ can be oxidized by sLaz. However, reduced form Laz cannot be oxidized by AniA. It suggests that Laz is able to receive electrons from cytochrome *c*₅ but cannot deliver electrons to nitrite reductase AniA *in vitro* in *Neisseria* species (Figure 6.12).

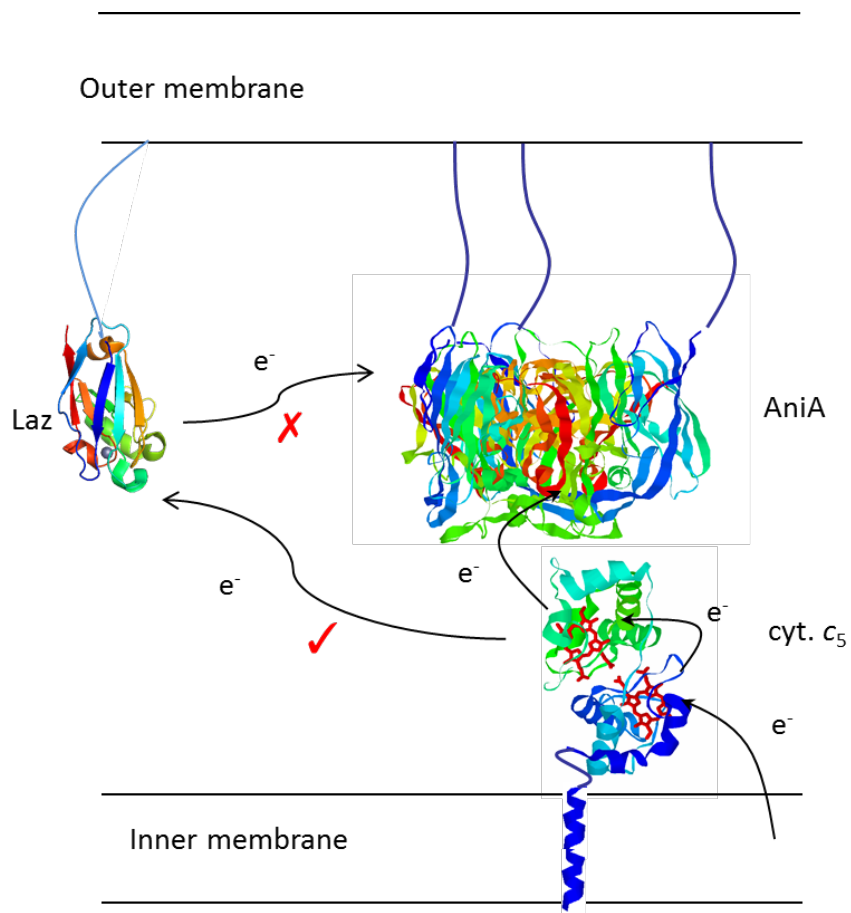


Figure 6.12: The predicted function of Laz in *N. meningitidis*. Laz was predicted as electron mediator between c_5 and AniA under certain conditions. In our study, *in vitro*, Laz is able to receive electrons from cytochrome c_5 , but cannot donate to AniA.

To elucidate the kinetic competence of electron transfer between Laz and cytochrome c_5 , the formation of a functional electron transfer complex between these two proteins was analysed by stopped-flow kinetics. The second order electron transfer rate constant between the two proteins is $1.94 \times 10^5 \text{ M}^{-1} \text{ s}^{-1}$, a similar rate to that of the c_5 and AniA inter-protein electron transfer, which strongly supports the idea that the inner membrane associated cytochrome c_5 interacts functionally with the outer membrane associated Laz as an electron donor.

Under denitrifying conditions, nitrite is not being utilized to support growth until oxygen becomes limited. If the *laz* gene is involved in nitrite reduction in *N. meningitidis*, the *laz* mutant strain will show a clear deficiency in growth and nitrite utilization under oxygen limiting conditions. The ability of *N. meningitidis laz* mutant strains reducing nitrite as alternative electron acceptor is similar to that of the wild type strain. It is directly linked to nitrite being used to support growth when oxygen becomes limited. However, the *laz* mutant strains do have a delay (about one hour) on starting to utilize nitrite. In addition, the *laz* mutant strains do not have a decreased ability to reduce nitrite and generate nitric oxide. The interruption of *laz* gene might have polar effect on the other gene(s) nearby, such as NMB1532 which is predicted to encode for hemerythrin. The function of this di-iron protein is unknown in this organism but in *Ralstonia eutropa* two hemerythrins domains are found in NorA protein which can bind nitric oxide and possibly act as a regulator of response to nitric oxide (Büsch *et al*, 2005 and Strube *et al*, 2007). Complementation of *laz* gene or deletion of hemerythrin should be undertaken to provide more understanding. In *laz* mutant, the response to nitric oxide might be disrupted and result in the decrease in removal of nitric oxide. However, in some occasions, *laz* mutant possibly overcome nitric oxide toxicity and strive to grow.

Laz has been determined to be mainly associated with the outer membrane. Inter-protein electron transport between Laz and cytochrome c_5 suggests that Laz is able to receive electrons from the electron carrier cytochrome c_5 at a physiologically relevant rate. However, Laz is unable to donate electrons to terminal reductase AniA. Typically, small soluble cytochrome c receives electrons from cytochrome bc_1 complex and transfers to terminal reductase. It is confirmed that c_5 is able to receive electrons from cytochrome bc_1 complex and transfer to Laz in *Neisseria*. However, this electron pathway is not clearly involved in the *Neisseria* respiration chains.

In conclusion, our study suggests that Laz is capable of interacting with cytochrome c_5 *in vitro*, but the *in vivo* data suggests that this interaction is not of importance under denitrifying conditions. Based on the characterization of the *laz* mutant strain in our work, it appears that the function of Laz is not involved in respiration and growth of the *N. meningitidis*.

Chapter 7:

Are cytochrome c_x and c_4 still electron donors to cbb_3 oxidase, when *N. meningitidis* is carrying an ectopic copy of *N. gonorrhoeae ccoP*?

7.1 Introduction:

Cytochrome cbb_3 type oxidases are usually expressed in response to microaerobic conditions to allow the colonization of anoxic tissues and may be an important determinant of pathogenicity (Pitcher and Watmough 2004). Cytochrome cbb_3 oxidase has high affinity for oxygen reduction. Both of cytochrome c_x and c_4 were previously determined to be electron donors to the only terminal oxidase cbb_3 in *N. meningitidis*. Based on a mutagenesis study, c_x and c_4 deficient strains have an impaired aerobic growth due to the inability to metabolize oxygen (83% \pm 5% and 59% \pm 5% rate of oxygen uptake compared to the wild type, respectively) (Deeudom et al. 2008). It indicated that *N. meningitidis* cytochrome c_x and c_4 are required for efficient oxygen respiration as electron acceptors (Deeudom et al. 2008). However, in *N. gonorrhoeae*, electron transfer to oxygen relies on cytochrome c_4 and c_5 involvement, not cytochrome c_x , providing electron transfer pathways from cytochrome bc_1 to cbb_3 oxidase (Ying Li 2010). In addition, the gonococcal and meningococcal c_5 deficient strains have a decreased in nitrite reduction, indicating that c_5 is the important electron

donor involved in nitrite reduction in *Neisseria* species (Aspholm 2010; Deudom et al. 2008).

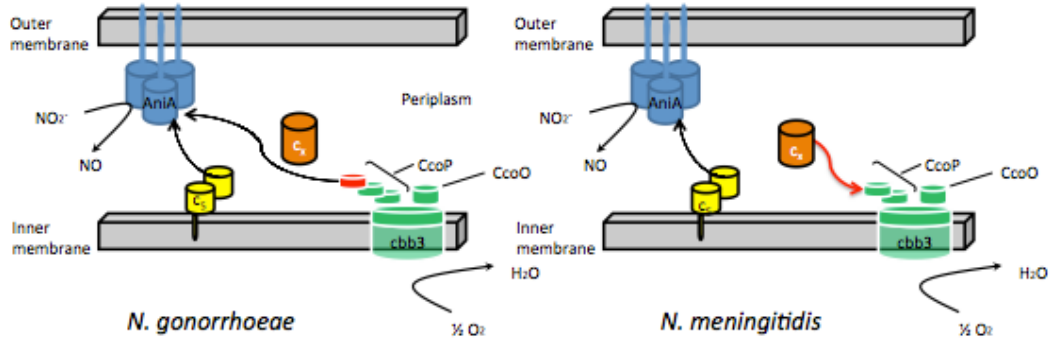
N. gonorrhoeae and *N. meningitidis* are highly conserved in terms of gene content and sequence similarity. Protein sequences of *N. meningitidis* c_x (NMB0717) and *N. gonorrhoeae* c_x (NGO0292) are highly conserved except N, C-terminal regions (Figure 7.1). The close similarity of the two proteins suggests the same function in two closely related organisms.

As mentioned before, cytochrome cbb_3 terminal oxidase is encoded by the *ccoNOQP* operon, and has four subunits, CcoO, CcoN, CcoQ and CcoP in *Neisseria* species. In addition, CcoP_{mme} (NMB1723) is a dihaem protein, whereas CcoP_{ngo} (NGO 0292) is a trihaem protein. The single base change (CAG to TAG; Q to stop) creates a stop codon in *N. meningitidis* CcoP.

The 3rd haem domain of CcoP is an effective electron donor to AniA in *N. gonorrhoeae*. Our prediction is that the 3rd haem domain of *ccoP*_{ngo} also blocks the electron-accepting site of cytochrome c_x on cbb_3 oxidase in *N. gonorrhoeae*, which would explain the apparent difference in role of c_x in oxygen reduction between the two closely related species. *N. meningitidis* MF64 (from Dr. Mike Koomey, Oslo) is *N. meningitidis* MC58 strain carrying an ectopic copy of *N. gonorrhoeae* *ccoP*. If our prediction is true, *N. meningitidis* MF64 strain, MF64 c_x deficient strain and MC58 c_x deficient strain should show growth at similar rates to one another but slower than that of the wild type strain MC58.

The aim of this chapter is to confirm that an ectopic copy of *N. gonorrhoeae ccoP* blocks the electron accepting site on *cbb₃* oxidase in *N. gonorrhoeae*. In addition, the involvement of *c_x* and *c₄* in oxygen reduction in *N. meningitidis* MF64 and MC58 is also characterized.

a.



b.

NGO0292	----MNTTRLPTAFILCCLCAAASAADNSIMTKGQKVYESN CIACHG KKGEGRGTAFFP 55
NMB0717	MKETPMNTRLPTALVLGCFCAAASAADNSIMTKGQKVYESN CVACHG KKGEGRGTMFFP 60
	*****:* *:*****:*****:***** **
NGO0292	LFRSDYIMNKPVLLHSMVKGINGTIKVNKTYNGF M PATAISDADIAAVATYIMNAFDN 115
NMB0717	LYRSDYIMNKPVLLHSMVKGINGTIKVNKTYNGF M PATAISDADIAAVATYIMNAFDN 120
	*:***:*:*:*****:*****:*****:*****:*****:*****
NGO0292	GGGSVTEKDVKQAKGKNQTDKMPSETGNPASDGIQIKPF 155
NMB0717	GGGSVTEKDVKQAKSKN----- 138
	*****:***

Figure 7.1: Comparison of cytochrome c_x difference in *N. meningitidis* (NMB0717) and *N. gonorrhoeae* (NGO0292). a. Comparison of c_x involvement in oxygen reduction in *N. meningitidis* MC58 and *N. gonorrhoeae* FC16 (Ying Li et al. 2010 ; Deudom et al. 2008). b. Multiple alignments of cytochrome c_x homologs in *N. meningitidis* MC58 and *N. gonorrhoeae* FC16. NGO 0292 and NMB 0717 are highly conserved. Cytochrome c_x homologs haem binding sites (green highlighted) are hexacoordinate with methionine (yellow highlighted) residue as the sixth ligand are conserved.

7.2 Visualization of cytochrome profiles in *N. meningitidis* MC58 and MF64 by haem staining:

The purpose was to identify the cytochrome profiles in *N. meningitidis* MC58 and MF64. MC58 and MF 64 cell extracts were separated by SDS-PAGE, blotted and visualized. There are 4 c-type cytochromes detected by haem dependent peroxidase activity (Figure 7.2). MC58 CcoP exhibiting a molecular weight of 43 kDa as predicted for NMB 1723, a cytochrome subunit CcoP domain of *cbb₃* terminal oxidase in *N. meningitidis* MC58. MF64 CcoP exhibiting a molecular weight of 55 kDa is predicted for NGO1371, a cytochrome subunit CcoP domain of *cbb₃* terminal oxidase in *N. gonorrhoeae* F62. The rest of the c-type cytochromes visualized were identical between these two strains, and molecular mass prediction is based on homologues in *N. gonorrhoeae* F62 (Hopper et al. 2009). The protein with approximately 22kDa is predicted to be cytochrome *c₄* with strong peroxidase activity. Two bands with molecular weight of 28kDa and 35kDa are predicted to be cytochrome *c₅* and PetC, respectively. Haem staining relies on the peroxidase activity of c-type cytochrome and is affected by the naturation state of the protein folding around the haem group (Diederix et al. 2002) . Cytochrome *c_x* cannot be detected in either *N. gonorrhoeae* or *N. meningitidis* cell extract, so presumably the peroxidase activity of cytochrome *c_x* is very low.

Mutant strains deficient in *c_x* and *c₄* were generated following the transformation of mutant constructs into *N. meningitidis* MC58 and MF64. *c_x* gene disrupted by the spectinomycin resistance gene and *c₄* gene disrupted by erythromycin resistance gene

were extracted from *N. meningitidis* c_x and c_4 mutant strains from Dr. Manu Deedom. Plasmids were transformed in *N. meningitidis* MF64 by the TSB method and selected by antibiotic selective plates. The replacement of the wild type copy of the gene with the copy containing an antibiotic resistance cassette was confirmed by the colony PCR screen (Figure 7.3). Cytochrome c_x DNA fragment with size 3.3 kb corresponds to c_x with the spectinomycin cassette. The cytochrome c_4 DNA fragment with sized 2.6 kb corresponds to c_4 with the erythromycin cassette.

In order to confirm the mutant strain, lysed cell extract of each strain was separated by SDS-PAGE, blotted and visualized by haem staining (Figure 7.4). The lane containing cytochrome c_4 mutants lacked an intense band with a molecular mass of 22 kDa, consistent with the absence of cytochrome c_4 (predicted molecular mass 21.5 kDa). As mentioned before, cytochrome c_x could not be detected by haem staining (Deedom et al. 2008). *N. meningitidis* MC58, MC58: c_x^- , MF64, MF64: c_x^- cell extracts show no difference in c-type cytochrome profile of each lane.

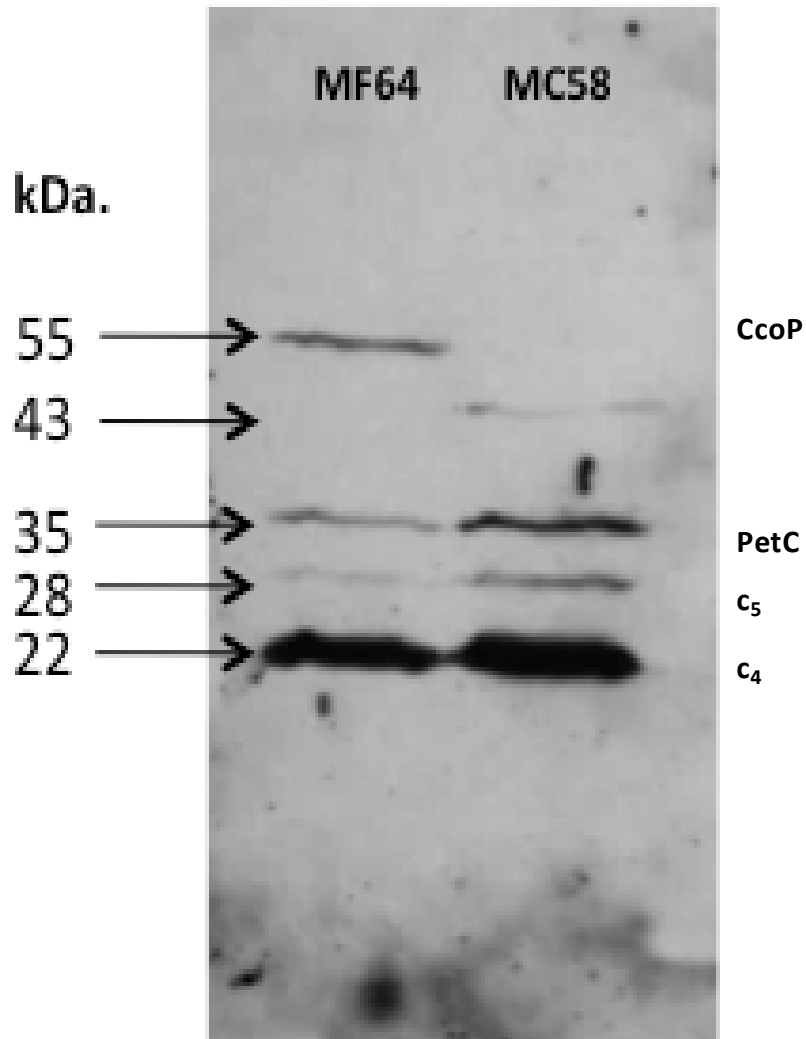


Figure 7.2: Cytochrome profiles of *N. meningitidis* MC58 and MF64. MC58 CcoP exhibiting a molecular weight of 43 kDa is predicted to be NMB 1723, MF64 CcoP exhibiting a molecular weight of 55 kDa is predicted to be NG01371.

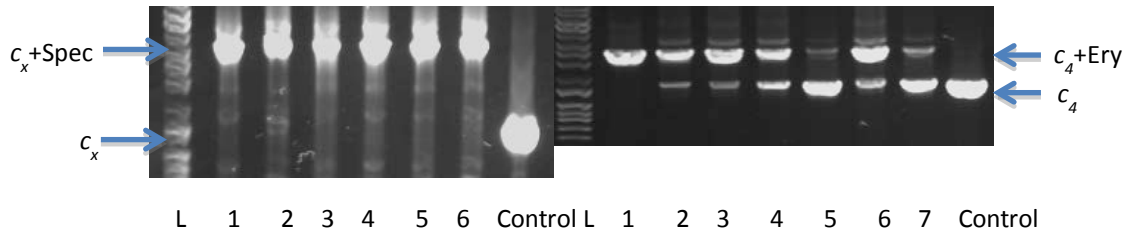


Figure 7.3: Colony PCR Colony PCR screen for c_x gene with erythromycin resistance gene cassette (ery^r) and c_4 gene with spectinomycin resistance gene cassette (spc^r) insert in *N. meningitidis* MF64 transformants. c_x (1.3 kb) with spc^r cassette 3.3kb; c_4 (1.4 kb) with ery^r cassette 2.6kb. L: protein ladder; No. 1-6: candidates 1-6.

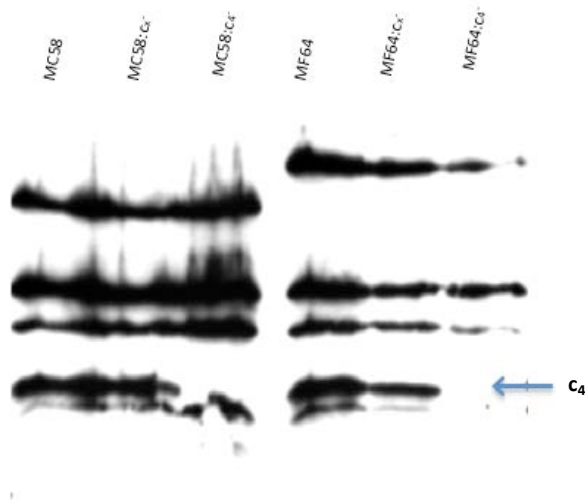


Figure 7.4: Cytochrome profiles of respiratory cytochrome c_x , c_4 mutant extracts show altered expression of cytochrome in *N. meningitidis* MC58 and MF64. Cytochrome c_4 has a predicted molecular mass of 21407.8Da; cytochrome c_x has a predicted molecular mass of 12651.2Da; MC58 CcoP has a predicted molecular mass of 40039.39Da; MF64 CcoP has a molecular mass of 47946.36Da. Haem staining of c_4 mutants in both MC58 and MF64 background show the missing c_4 cytochrome. Cytochrome c_x cannot be visualized by haem staining.

7.3: Growth properties of cytochrome deficient mutants of *N. meningitidis*

MC58 and MF64:

In order to test whether the 3rd haem domain of CcoP blocks the c_x electron-accepting site of *cbb₃* oxidase in *N. gonorrhoeae*, the growth of *N. meningitidis* MF64 and MC58 strains with a single mutation in c_x and c_4 under aerobic conditions were analysed. *N. meningitidis* c_x mutant strain is containing disrupted chromosomal copy of cytochrome c_x gene. Disruption of the cytochrome c_x gene was undertaken using a spectinomycin resistance gene cassette insertion. *N. meningitidis* c_4 mutant strain is containing disrupted chromosomal copy of cytochrome c_4 gene. Disruption of the cytochrome c_4 gene was undertaken using a erythromycin resistance gene cassette insertion. The aerobic cultures were sampled and measured at 600nm for optical density measurements.

It was found that *N. meningitidis* MC 58 and MF64 have no difference in growth of meningococcus under aerobic conditions (Figure 7.5). The ability of MF64 to utilize oxygen is the same as that of the wild type strain. It suggests that the ectopic copy of *N. gonorrhoeae* CcoP has no effect on cytochrome c_x dependent electron transportation.

MC58, MF64, MC58: c_x^- , and MC58: c_x^- grew at similar rates to one another under the same aerobic conditions (Figure 7.5). It is also notable that *N. meningitidis* MC58: c_x^- , MF64, and MF64: c_x^- grew to the same cell density as did in *N. meningitidis* MC58. All the strains entered exponential growth after 2 hours incubation and reached OD₆₀₀ of 2.0 at 8 hours.

Cytochrome c_4 mutant strains are highly sensitive to oxygen and failed to grow during aerobic incubation (Figure 7.6). All the c_4 deficient strains quickly entered the death phase. The inability of *N. meningitidis* MC58 and MF64 c_4 deficient strains to reduce oxygen indicates cytochrome c_4 is a major electron carrier (or even the only one) in *N. meningitidis*.

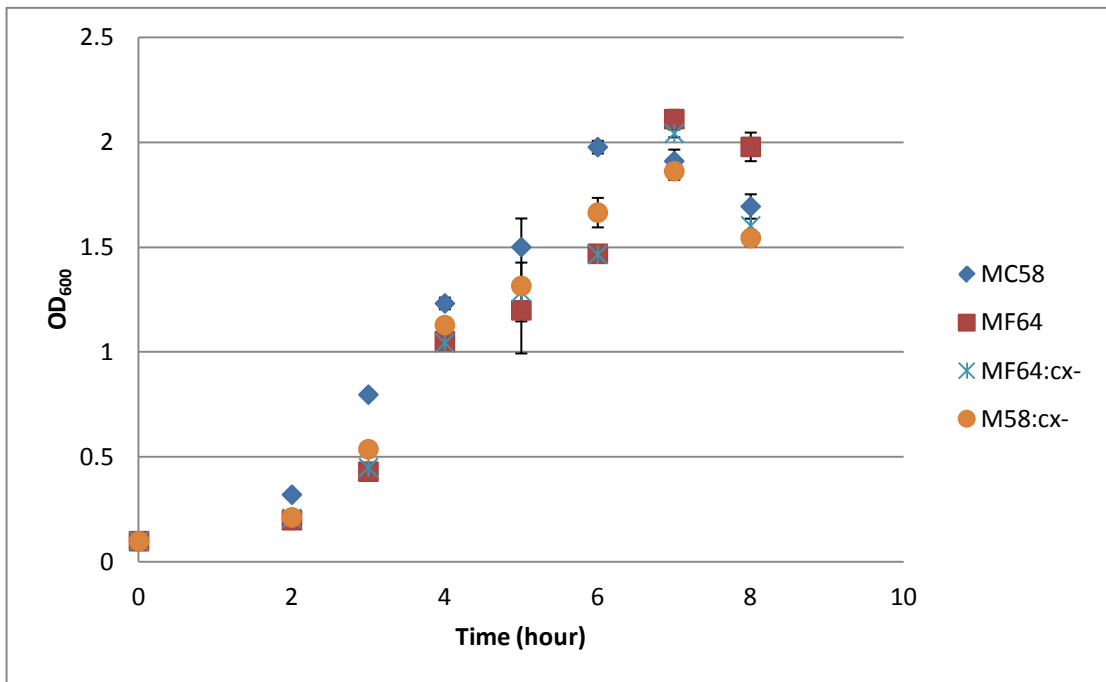


Figure 7.5: Growth of *N. meningitidis* cytochrome c_x mutants under aerobic conditions. All strains have the similar patterns. The *N. meningitidis* cytochrome c_x mutant in both MC58 and MF64 backgrounds showed no difference in growth patterns.

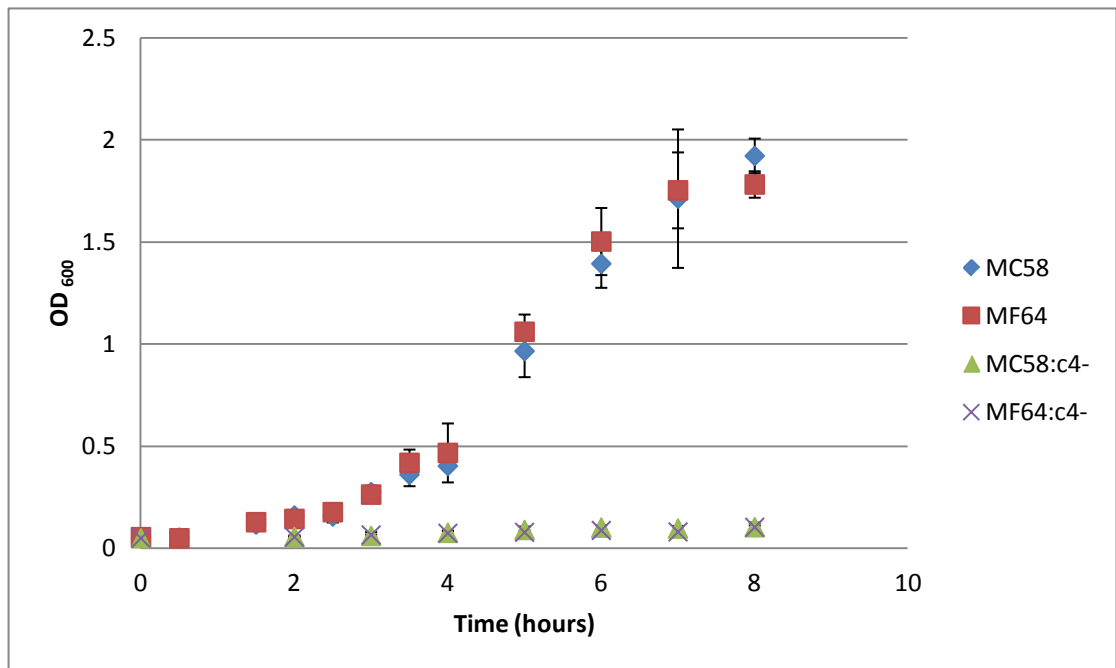


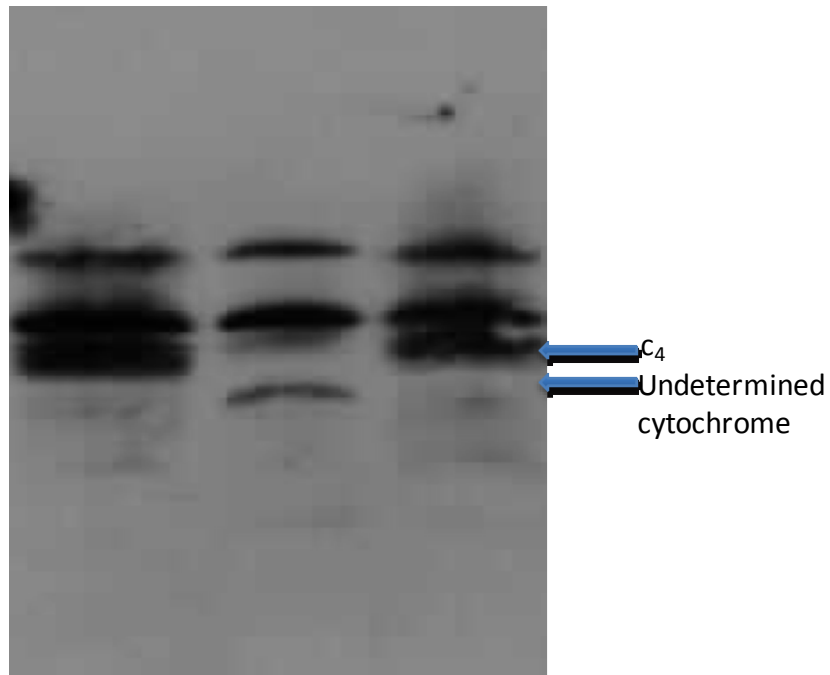
Figure 7.6: Growth of *N. meningitidis* cytochrome c_4 mutants under aerobic conditions. *N. meningitidis* cytochrome c_4 mutant in both MC58 and MF64 backgrounds have shown no difference in growth patterns. Cytochrome c_4 mutant strains are highly sensitive to oxygen.

7.4 Comparing *N. meningitidis* c_x mutants in published construct and new construct:

Based on Dr. Manu Deedom's paper, both cytochrome c_x and c_4 are electron donors to cbb_3 oxidase (Deedom et al. 2008). Double mutant cytochrome c_x and c_4 MC58 strain still had residual oxidase activity. It indicates that there are alternative pathways to cbb_3 oxidase in *N. meningitidis*.

As described in the method and material section, pCR-Blunt II TOPO- $c_x::\text{Sp}c^R$ plasmid was extracted from derivative of *N. meningitidis* MC58 with insertion in NMB 0717($\text{Sp}c^R$) (MDMC58 c_x^-) and transformed to *N. meningitidis* MC58(MC58 c_x^-) and *N. meningitidis* MF64(MF64 c_x^-). The performance of MDMC58 c_x^- and MC58 c_x^- under aerobic conditions is supposed to be the same. However, cytochrome c_4 appears to be the only electron donor to terminal oxidase cbb_3 complex in our experiment. Cytochrome c_x does not have a role in aerobic growth. Due to low peroxidase activity of cytochrome c_x , the expression of cytochrome c_x could not be detected by haem staining. The expression of cytochrome c_x is confirmed by comparing the spectral difference between *N. meningitidis* c_x mutant strain and wild type absorption (Dr. Manu Deedom, PhD thesis, unpublished data). The lost absorption in mutant strain represents the actual absorption by that c-type cytochrome. Cytochrome c_x mutant lost absorption peak at 554-555 nm in α band, suggesting that cytochrome c_x has α peak at 554-555 nm. Cytochrome c_x mutant lost absorption peak at 435 nm in Soret band, suggesting that cytochrome c_x has Soret peak at 435 nm.

Cytochrome c_x colony PCR screen confirmed that cytochrome c_x gene was disrupted by spectinomycin resistance cassette in both of the constructs (MDMC58 c_x^- and MC58 c_x^-). In order to compare these two constructs the cells were lysed, and visualized by haem staining. As cytochrome c_x can not be detected by haem staining due to low peroxidase activity, the rest of the components of cytochrome profiles of c_x mutant strains (either MDMC58 c_x^- or MC58 c_x^-) and wild type MC58 should be the same. However, MDMC58 c_x^- has one major cytochrome protein missing, which is predicted to be the sole electron carrier cytochrome c_4 to cytochrome cbb_3 oxidase. In addition, there is one cytochrome protein that is highly over-expressed compared to the wild type, but it is hard to determine why this cytochrome is highly expressed.



1 2 3

Figure 7.7 Cytochrome profiles of c_x mutant and wild type strains under the same growth conditions. Whole cell extracts were separated by SDS-PAGE, blotted and stained for haem peroxidase activity. 1: MC58 c_x^- ; 2: MDMC58 c_x^- ; 3: wild type MC58. Lane 2, cytochrome c_4 is missing. MDMC58 c_x^- strain appears to express a cytochrome protein with approximately 17 kDa.

7.5 Discussion:

This chapter focused on *N. meningitidis* carrying an ectopic copy of *N. gonorrhoeae* CcoP with the aim of determining whether this has any effect on cytochrome c_x and c_4 dependent electron transportation under aerobic conditions. Mutant strains deficient in c_x and c_4 were generated following the transformation of the constructs into *N. meningitidis* MC58 and MF64. Cytochrome profiles suggest that the *N. meningitidis* MF64 strain is carrying an ectopic copy of *N. gonorrhoeae* CcoP.

The ECL haem staining comparison of *N. meningitidis* MC58 and MF64 showed CcoP_{ngo} (Predicted mw. of 40039.39Da) and CcoP_{nm} (Predicted mw. of 47946.36Da) exhibits molecular weight of 40 kDa and 45 kDa, respectively on SDS-PAGE.

Constructed c_4 and c_x mutant plasmids were transformed into MC58 and MF64, respectively, and confirmed by colony PCR screen and haem staining. Cytochrome c_4 has strong peroxidase activity and exhibits a molecular mass of 22kDa, consistent with the absence of cytochrome c_4 (predicted molecular mass 21.5kDa) for these strains. However, cytochrome c_x could not be detected by haem staining (Deeudom et al. 2008).

It was hypothesized that the 3rd haem domain of CcoP_{ngo} may block the c_x electron transportation pathway in *N. gonorrhoeae*. However, it was found that cytochrome c_x is not a major electron donor in oxygen respiration under the conditions tested. *N. meningitidis* MF64 with an ectopic copy of CcoP may result in the same growth rate as a MC58 c_x mutant strain and MF64 c_x mutant strain. As c_4 was determined as an important electron donor in *N. meningitidis* and *N. gonorrhoeae*, cytochrome c_4

mutant strains in two different backgrounds MC58 and MF 64 were used as the control experiment (Deeudom et al. 2008; Li et al. 2010).

If both of cytochrome c_x and c_4 are the electron donors to the terminal reductase cbb_3 oxidase, either c_x or c_4 deficient in *N. meningitidis* MC58 and MF64 would show the deficiency in oxygen reduction. Compared with wild type *N. meningitidis* MC58, the additional third haem domain of CcoP does not have an effect on MF64 growth. It does not agree with the hypothesis that the MF64 third haem domain CcoP subunit blocks the c_x electron accepting site of cbb_3 oxidase. It indicates that CcoP_{ngo} does not block the c_x electron transportation to cbb_3 oxidase in *N. gonorrhoeae*. It is also agreed with the previously published result for *N. gonorrhoeae* that there is not a significant role of cytochrome c_x in electron transfer to cbb_3 oxidase (Li et al. 2010).

All c_4 -deficient strains were severely deficient in accepting electrons from bc_1 complex and donating to cbb_3 oxidase. It is possible cytochrome c_4 deficiency results in decreasing oxidation of cytochrome bc_1 complex and increasing the opportunity of interaction between O_2 and cytochrome bc_1 complex producing more superoxide radical. It indicates that cytochrome c_4 is the significant and crucial electron donor to terminal oxidase cbb_3 complex.

The role of dihaem cytochrome c_4 as an electron donor to cbb_3 oxygen reductase has been widely described, including in *V. cholera*, *P. stutzeri*. Bacteria within β and α -proteobacterial clades that contain a cbb_3 oxidase are likely also to contain a dihaem

cytochrome c_4 (Chang et al. 2010). It is reasonable to assume, cytochrome c_4 is the natural electron donor to cbb_3 oxidase.

A small soluble cytochrome is normally involved in electron transfer between bc_1 complex and cbb_3 oxidase in bacteria. It is possible c_x is fulfilling this role in the *Neisseria* species. Cytochrome c_x is the efficient electron donor to cbb_3 cytochrome oxidase during the respiratory growth of *Rhodobacter sphaeoides* (Daldal et al. 2001). Heterologously expressed soluble cytochrome c_{552} (homologous to c_x) acts as an electron donor to cytochrome c oxidase in *Paracoccus denitrificans* (Reincke et al. 1999). It indicates that it is possible to assume that c_x might have an overlapping function with c_4 as an electron donor to cbb_3 oxidase. However mutant deficient in cytochrome c_x in both MC58 and MF64 backgrounds showed similar growth patterns as in the wild type MC58 and MF64. It suggests cytochrome c_x does not have a role in donating electrons from cytochrome bc_1 complex to cbb_3 oxidase. It has been observed that the data does agree with the *N. gonorrhoeae* c_x mutant study. There are roles for cytochrome c_4 and c_5 but not cytochrome c_x in oxygen reduction in *N. gonorrhoeae* (Li et al. 2010). So cytochrome c_x lacks a significant role in electron transfer to cytochrome oxidase in the *Neisseria* species, under the condition tested.

Comparing the published data of the cytochrome profile of a c_x mutant *N. meningitidis* MC58 strain with that of c_x mutant strain in the same *N. meningitidis* MC58 background, there is a major respiratory cytochrome c_4 missing in the published construct, although cytochrome c_4 was shown to be prevent the c_x mutant strain in that

work (Deeudom et al. 2008). The reason for this inconsistency is unclear and will be the subject of future work.

In conclusion, cytochrome c_x does not have a role in oxygen reduction under aerobic conditions in *Neisseria* species. Cytochrome c_4 is the significant electron donor to cytochrome oxidase cbb_3 complex. When *N. meningitidis* is carrying an ectopic copy of *N. gonorrhoeae* CcoP, cytochrome c_4 is able to receive electrons from cytochrome bc_1 and to donate to cbb_3 oxidase.

It suggests that the 3rd haem domain of CcoP does not block c_x -accepting sites on the cbb_3 oxidase in *N. gonorrhoeae*. It also supports the idea that the *N. meningitidis* cytochrome c_4 is the chief electron carrier under aerobic conditions. In addition, *N. gonorrhoeae* 3rd haem domain of CcoP does not have a negative effect on oxygen reduction. High affinity oxygen respiration is solely dependent on electron carrier cytochrome c_4 . Cytochrome c_4 could be a potential therapeutic target for Meningococcal therapy and diagnosis in the future.

In addition, unlike previous predictions, *N. meningitidis* does not have a multiple-branched respiratory chains (Figure 7.8). It might potentially benefit from the high affinity of each cytochrome to terminal reductase, but also limit the survival *N. meningitidis* to survive in diverse environments.

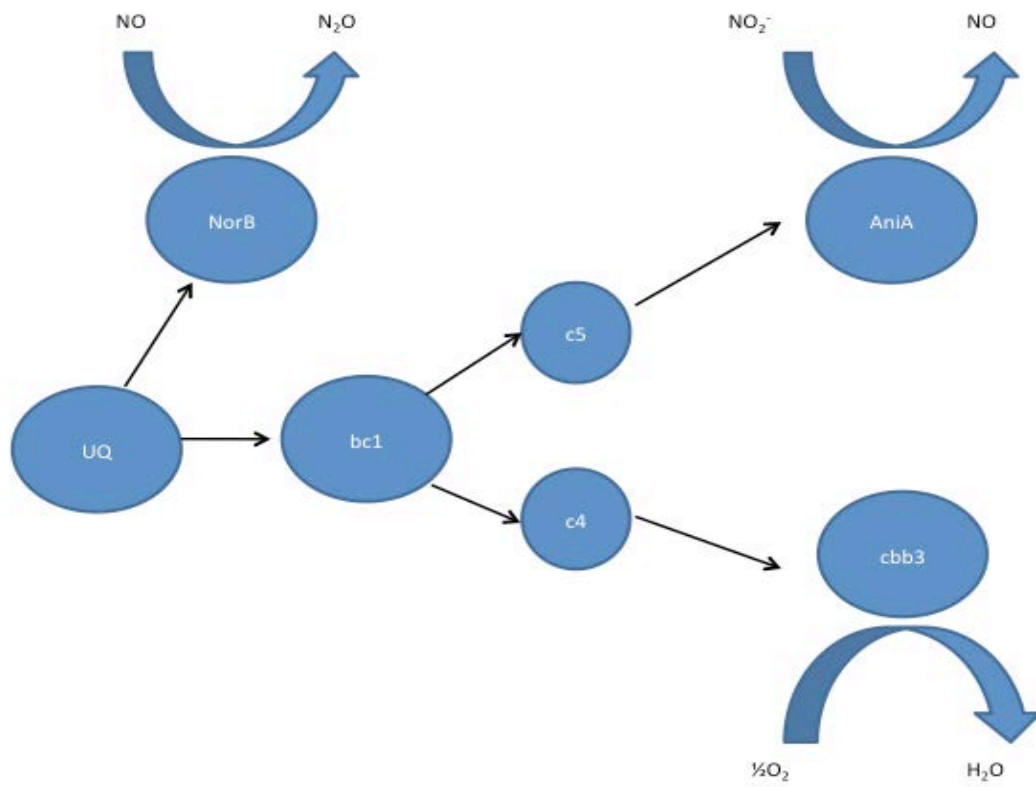


Figure 7.8 Proposed electron transport chains in *N. meningitidis* MC58.

Chapter 8

General discussion and conclusion:

N. meningitidis is hypothesized to have evolved to live in microaerophilic human nasopharynx. It is able to utilize oxygen, nitrite and nitric oxide as terminal electron acceptors and catalyse oxygen reduction and truncated denitrification. From data generated in this work, it is proposed that cytochrome *c₄* is the sole electron donor to cytochrome *cbb₃* oxidase, and cytochrome *c₅* is the sole electron donor to AniA nitrite reductase. In addition, cytochrome *c₅* and its redox partner AniA interaction was confirmed to tolerate variable pH, and salt conditions. It is important for *N. meningitidis* to survive in the wide range of physical and physiological conditions. Cytochrome *c_x* is not involved in oxygen reduction or nitrite reduction according to our data. Laz is an electron acceptor of cytochrome *c₅*, but cannot donate electrons to AniA *in vitro*. This also indicates that Laz might not be involved in aerobic or microaerobic respiration in the *Neisseria* species. Due to the limited number of respiratory components, and terminal reductases, the data generated from this work, also implies that *N. meningitidis* is a simple one-to-one model (one electron donor to one terminal reductase) of the respiratory chain and that there are limited options for electron flow to nitrite reductase and oxygen reductase. Despite the lack of metabolic versatility of *N. meningitidis*, it is reasonable to conclude that *N. meningitidis* has a less-branched respiratory chain, compared to other proteobacteria.

Comparative analysis of respiratory components of *N. meningitidis* and *N. gonorrhoeae* reveals that all components are highly conserved, except a key

difference that CcoP of *cbb*₃ oxidase of *N. gonorrhoeae* has an extra haem domain than that of *N. meningitidis*, and this has a high similarity with 2nd haem domain of *c*₅. The 3rd haem domain of CcoP of *cbb*₃ oxidase of *N. gonorrhoeae* is also confirmed as an effective electron donor to AniA in *N. gonorrhoeae*, compared with the efficiency of cytochrome *c*₅ donating electrons to AniA. It is interesting that one subunit of terminal oxidase is acting as an electron portal to a different electron acceptor in *Neisseria* species. This unexpected function of the terminal reductase dramatically reshapes the respiratory chain in *N. gonorrhoeae*. It provides *N. gonorrhoeae* flexible routes to AniA in nitrite reduction. Conservation of gene content and high sequence identity between *N. meningitidis* and *N. gonorrhoeae* is no guarantee of the same function. Due to the different environment they inhabit and diseases they cause, the two pathogenic species have to make (divergent) adaptations to their respiratory networks with respect to denitrification. The new proposed electron transport chains were shown in Figure 8.1.

In addition, in commensal *N. elongata*, cytochrome *c* (NEIELOOT 00905) has a high sequence similarity with 2nd haem domain of cytochrome *c*₅, and it is also confirmed as an efficient electron donor to AniA, compared with CcoP and *c*₅ as electron donors. *N. elongata* utilizes three electron transportation routes of nitrite reduction, which probably agrees with the physiological growth conditions of low oxygen and a nitrite rich environment. However, there is limited information about why *N. elongata* recruits multiple electron pathways to the sole nitrite reductase AniA (Figure 8.1).

In conclusion, the second order rate constants between predicted potential electron donors and AniA interaction in *Neisseria* species are summarized in Table 8.1. In

addition, it is reasonable to assume that any *Neisseria* cytochrome, which shares a high degree of similarity with the 2nd haem domain of *c*₅ is likely to be a potential electron donor to AniA.

Potential electron donors of AniA in <i>Neisseria</i> species	Rate constant (M ⁻¹ s ⁻¹) between the potential electron donor and AniA interaction
Cytochrome <i>c</i> ₅	1.535× 10 ⁵
Second haem domain of cytochrome <i>c</i> ₅	2.815× 10 ⁵
First haem domain of cytochrome <i>c</i> ₅	0
Cytochrome <i>c</i> ₄	0.147× 10 ⁵
Cytochrome <i>c</i> _x	0
The third haem domain of <i>N. gonorrhoeae</i> CcoP	3.378× 10 ⁵
<i>N. elongata</i> cytochrome <i>c</i>	4.553× 10 ⁵
Laz	0

Table 8.1: Summary of the rate constants for potential electron donors and AniA interaction in this work.

Nitrite reduction comes with a significant metabolic cost as NO is toxic and also inhibits growth (Overton et al. 2006). Two different studies have shown the *aniA* gene was found to have frameshift mutations in 32% or 34% of sequenced *N. meningitidis* strains, resulting in either premature termination of translation, and sometimes there is deletion of entire gene (Barth et al. 2009; Ku et al. 2009), i.e. a conserved and functional AniA is not essential for *N. meningitidis* survival (Stefanelli et al. 2008). However, all *N. gonorrhoeae* strains are predicted to express

AniA, implying the crucial role for AniA in gonococcus (Ku et al. 2009). Nitrite reduction is more important in *N. gonorrhoeae* than in *N. meningitidis*. It suggests that the trihaem CcoP, which evolved in the *Neisseria* species, is able to effectively control denitrification under microaerobic conditions. The loss of the third haem domain of CcoP is also shown as an adaptation at the species level.

The organization of redox proteins in the *Neisseria* species seems unusual. Laz and AniA are mainly associated with the outer membrane, whereas c-type cytochromes are associated with the inner membrane, as analysed in the closely related non-pathogenic *Neisseria* species, *N. lactamica*. As cytochrome c_5 is confirmed as the major electron carrier to AniA in *N. meningitidis*, it creates a potential problem of electron transfer from the inner membrane associated cytochrome c_5 to the outer membrane protein AniA. There are two predictions of the model of inter-protein electron transfer between cytochrome c_5 and AniA. One is the N-terminal linker LCR of AniA tethered to outer membrane might form an unstructured elongated linker region to get access to electrons from the 2nd haem domain of cytochrome c_5 (Figure 8.2). The other prediction is that the LCR that is between the two haem containing domains of cytochrome c_5 might allow the active site of the second domain of c_5 to make the direct contact with AniA and form a functional electron transfer couple (Figure 8.2). It was also confirmed that the second haem domain of cytochrome c_5 is the direct donor to AniA in vivo. As described before, AniA is a trimer, the N-terminal tethers of each monomer tethered the globular active AniA to the outer membrane to ensure the core enzyme active sites are facing towards the inner membrane. Each tether is not long enough to allow the globular domain of AniA to rotate around. This decreased dynamics of redox partners may be beneficial for AniA, allowing it to take advantage of the low cost of forming a functional

electron transfer couple with cytochrome *c*₅, but it would also decrease the opportunity of AniA functionally interacting with other potential electron donors in the periplasm. It might be another explanation of why *N. meningitidis* does not have a multiply branched respiratory chain.

Alternative to the biochemical arguments of redox proteins tethered to the outer membranes, other reasons related to the lifestyle of *Neisseria* species might explain the tethering of redox proteins. As mentioned before, *N. meningitidis* Laz is shown to be competent at entering glioblastoma cells and causing high levels of cytotoxicity (Hong et al. 2006). The ability of Laz entering mammalian cells is related to lipid attachment and exposure to the surface of the cell (Hong et al. 2006). It is also shown, apart from being involved in nitrite reduction, that the expression of AniA of *N. gonorrhoeae* has been shown to provide protection against killing by human sera (Cardinale and Clark 2000).

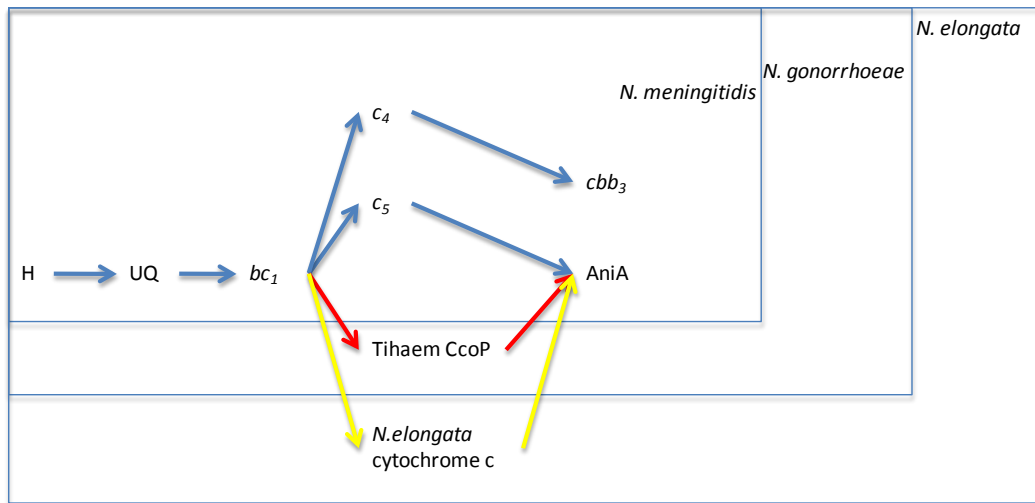


Figure 8.1: Proposed electron transport chains from NADH to nitric oxide, oxygen and nitrite in *N. meningitidis*, *N. gonorrhoeae* and *N. elongata*. Electron flow from cytoplasmic reductase to terminal reductase is shown by arrows. The unique pathway from trihaem CcoP to AniA is designated by red arrow in *N. gonorrhoeae*. The unique pathway from *N. elongata* cytochrome c to AniA is designated by yellow arrow in *N. elongata*.

outer membrane

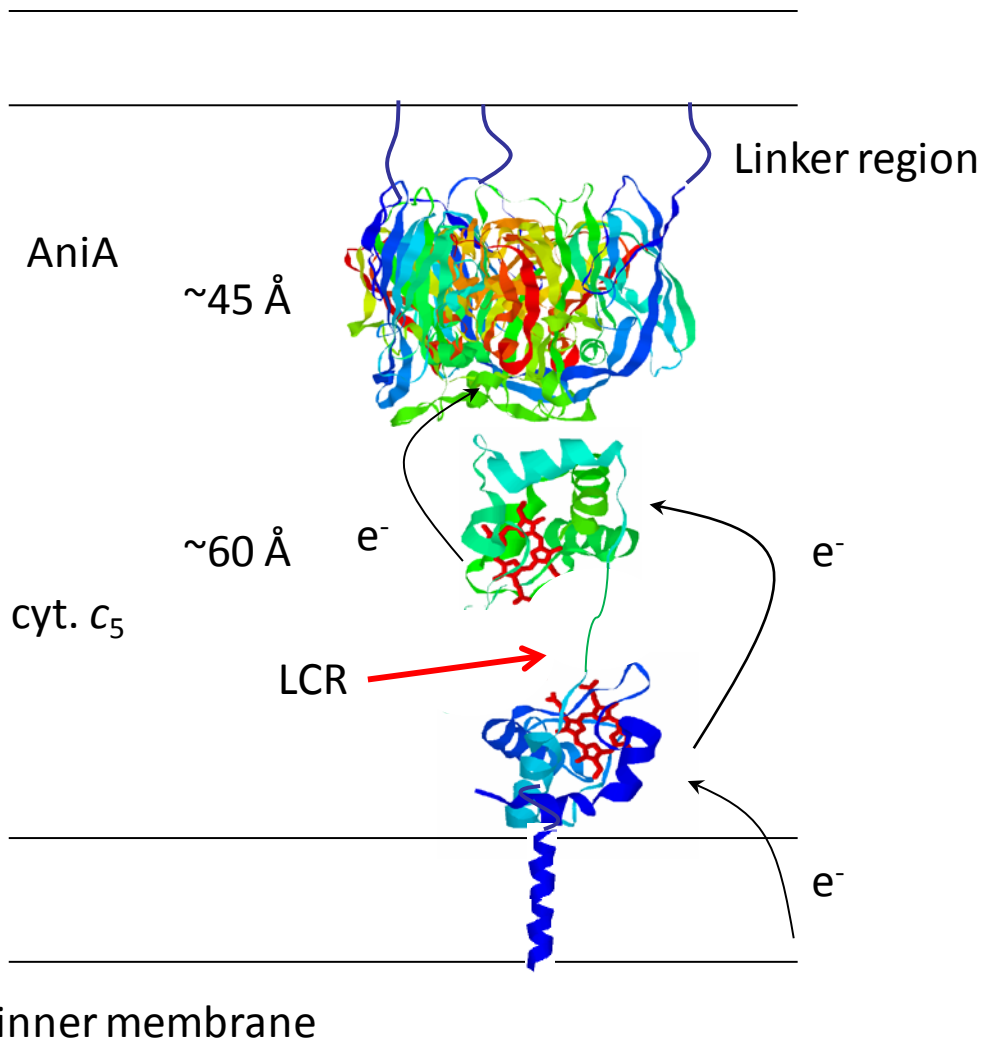


Figure 8.2: The predicted model of electron transfer between c_5 and AnIA in *Neisseria* species. AlaSerPro-rich LCR between two haem containing domains of cytochrome c_5 might allow c_5 to donate electrons directly to the active site of AnIA.

References

Abraham, Z. H. L., B. E. Smith, B. D. Howes, D. J. Lowe and R. R. Eady (1997). "pH-dependence for binding a single nitrite ion to each type-2 copper centre in the copper-containing nitrite reductase of *Alcaligenes xylosoxidans*." *Biochem. J.* 324: 511-516.

Anjum, M. F., T. M. Stevanin, R. C. Read and J. W. B. Moir (2002). "Nitric Oxide Metabolism in *Neisseria meningitidis*." *Journal of Bacteriology* 184(11): 2987-2993.

Ambler R.P.(1991) "Sequence variability in bacterial cytochromes c" *Biochimica et Biophysica Acta (BBA)* 1058(1): 42-47

Aspholm, M., Koomey, M et al. (2010). "Structural Alterations in a Component of Cytochrome c Oxidase and Molecular Evolution of Pathogenic *Neisseria* in Humans." *PLOS pathogens* 6(8).

Axelrod HL, Abresch EC, Okamura MY, Yeh AP, Rees DC, Feher G.(2002) "X-ray structure determination of the cytochrome c₂: reaction center electron transfer complex from *Rhodobacter sphaeroides*." *J Mol Biol.*319(2):501-15.

Barth, K. R., V. M. Isabella and V. L. Clark (2009). "Biochemical and genomic analysis of the denitrification pathway within the genus *Neisseria*." *Microbiology* 155(12):

4093-4103.

Bennett JS, Bentley SD, Vernikos GS, Quail MA, Cherevach I, White B, Parkhill J and Maiden MC(2010) "Independent evolution of the core and accessory gene sets in the genus *Neisseria*: insights gained from the genome of *Neisseria lactamica* isolate 020-06." *BMC genomics*;11;652

Bell LC, Richardson DJ, Ferguson SJ (1990) "Periplasmic and membrane-bound respiratory nitrate reductases in *Thiosphaera pantotropha*. The periplasmic enzyme catalyzes the first step in aerobic denitrification." *FEBS Lett.* 265(1-2):85-7.

Berry, E. and Trumpower B. (1987). "Simultaneous determination of hemes a, b, and c from pyridine hemochrome spectra." *Anal Biochem.*(161): 1.

Bogdan, J., Minetti C. and Blake M. (2006). "A one step method for genetic transformation of non-piliated *Neisseria meningitidis*." *Journal of Microbiological Methods* 49: 97-101.

Bok, J. and N. Keller (2012). "Fast and easy method for construction of plasmid vectors using modified quick-change mutagenesis." *Methods Mol Biol.* 944: 163-174.

Boulanger, J. M. and E. P. M. Murphy (2002). "Crystal Structure of the Soluble Domain of the Major Anaerobically Induced Outer Membrane Protein (AniA) from Pathogenic *Neisseria*: A New Class of Copper containing Nitrite Reductases." *J. Mol. Biol.* 315:

1111-1127.

Bradford, M. (1976). "A rapid and sensitive method for quantitation of microgram quantities of protein utilizing the principle of protein-dye-binding." *Analytical Biochemistry* 72: 248-254.

Brittain, T., Blackmore R., Greenwood C. and Thomson A. (1992). "Bacterial nitrite-reducing enzymes." *European Journal of Biochemistry* 209: 793-802.

Büsch, A., K. Strube, B. Friedrich and R. Cramm (2005). "Transcriptional regulation of nitric oxide reduction in *Ralstonia eutropha* H16." *Biochemical Society Transactions* 33: 193-194.

Cannon, J. G. (1989). "Conserved lipoproteins of pathogenic *Neisseria* Species Bearing the H.8 Epitope: Lipid-modified Azurin and H.8 Outer Membrane Protein. " *Clinical Microbiology Reviews* 2: S1-S4.

Cardinale, J. A. and V. L. Clark (2000). "Expression of AniA, the Major Anaerobically Induced Outer Membrane Protein of *Neisseria gonorrhoeae*, Provides Protection against Killing by Normal Human Sera." *INFECTION AND IMMUNITY* 68(7): 4368-4369.

Chang, H. Y., Y. Ahn, L. A. Pace, M. T. Lin, Y. H. Lin and R. B. Gennis (2010). "The diheme cytochrome c(4) from *Vibrio cholerae* is a natural electron donor to the respiratory cbb(3) oxygen reductase." *Biochemistry* 49(35): 7494-7503.

Chaudhari, A., A. M. Fialho, D. Ratner, P. Gupta, C. S. Hong, S. Kahali, Tohru Yamada, Kasturi Haldar, Wonhwa Cho, Virander S. Chauhan, T. K. D. Gupta and A. M. Chakrabarty "Azurin, *Plasmodium falciparum* Malaria and HIV/AIDS: Inhibition of Parasitic and Viral Growth by Azurin." *Cell Cycle* 5(15): 1642-1648.

Clark, V. L., Campbell, L.A., Palermo, D.A., Evans, T.M. and Klimpel, K.W. (1987). "Induction and repression of outer membrane proteins by anaerobic growth of *Neisseria gonorrhoeae*." *Infect. Immun.* 55: 1359-1364.

Daldal, F., S. Mandaci, C. Winterstein, H. Myllykallio, K. Duyck and D. Zannoni (2001). "Mobile Cytochrome c2 and Membrane-Anchored Cytochrome cy Are Both Efficient Electron Donors to the cbb3- and aa3-Type Cytochrome c Oxidases during Respiratory Growth of *Rhodobacter sphaeroides*." *Journal of Bacteriology* 183(6): 2013-2024.

De la Cerda, B., A. Diaz-Quintana, J. A. Navarro, M. Hervas and M. d. l. Rosa. (2002). "Site-directed mutagenesis of cytochrome c6 from *Synechocystis* sp PCC6803: the heme protein possesses a negatively charged area that may be isofunctional with the

acidic patch of plastocyanin." *J. Biol. Chem.* 274: 13292-13297.

Deeudom M, Rock J, Moir J.(2006) "Organization of the respiratory chain of *Neisseria meningitidis*." *Biochem. Soc. Trans.* 34:139-42.

Deeudom, M., M. Koomey and J. W. B. Moir (2008). "Roles of c-type cytochromes in respiration in *Neisseria meningitidis*." *Microbiology* 154(9): 2857-2864.

Diederix, R. E. M., M. Ubbink and G. Canters (2002). "Peroxidase Activity as a Tool for Studying the Folding of c-Type Cytochromes." *Biochemistry* 41: 13067-13077.

Edwards, J., D. Quinn, K. A. Rowbottom, Jean L. Whittingham, Melanie J. Thomson and James W. B. Moir (2012). "*Neisseria meningitidis* and *Neisseria gonorrhoeae* are differently adapted in the regulation of denitrification: single nucleotide polymorphisms that enable species-specific tuning of the aerobic-anaerobic switch." *Biochemical Journal* 445(1): 69-79.

Frasch, C. and A. Pollard (2001). "Development of natural immunity to *Neisseria meningitidis*." *Vaccine* 19: 1327-1346.

Fraser, A., A. Gafter-Gvili, M. Paul and L. Leibovici (2006). "Antibiotics for preventing meningococcal infections." *Cochrane Database Syst Rev.* 4.

Gotschlich EC, Goldschneider I, Artenstein MS. (1959) "Human immunity to the meningococcus. IV. Immunogenicity of group A and group C meningococcal polysaccharides in human volunteers. V. The effect of immunization with meningococcal group C polysaccharide on the carrier state." *J Exp Med.* 1969 Jun 1;129(6):1349-84.

Gupta, R., Z. He and S. Luan. (2002). "Functional relationship of cytochrome c6 and plastocyanin in Arabidopsis." *Nature* 417: 567-571.

Hanahan, D. (1983). "Studies on transformation of *Escherichia coli* with plasmids." *J Mol Biol.* 166(4): 557-580.

Haddow LJ, Mulgrew C, Ansari A, Miell J, Jackson G, Malnick H, Rao GG.(2003) "Neisseria elongata endocarditis: case report and literature review." *Clin Microbiol Infect.* 9(5):426-30.

Hart. CA and Thomson. AP (2006). "Meningococcal disease and its management in children." *Brit. Med. J.* 333: 685-690.

Hoehn, G. T. and Clark V. L. (1990). "Distribution of a protein antigenically related to the major anaerobically induced gonococcal outer membrane protein among other

Neisseria species." Infect. Immun. 58: 3929-3933.

Hong, C. S., T. Yamada, W. Hashimoto, A. M. Fialho, T. K. Das Gupta and A. M. Chakrabarty (2006). "Disrupting the entry barrier and attacking brain tumors: the role of the Neisseria H.8 epitope and the Laz protein." Cell Cycle 5: 1633-1641.

Hopper, A., Tovell N. and Cole J. (2009). "A physiologically significant role in nitrite reduction of the CcoP subunit of the cytochrome oxidase cbb3 from *Neisseria gonorrhoeae*." FEMS Microbiology Letters 301(2): 232-240.

Hopper A., Li Y., Cole J. (2013) "A Critical Role for the cccA Gene Product, Cytochrome c2, in Diverting Electrons from Aerobic Respiration to Denitrification in *Neisseria gonorrhoeae*." J. Bacteriol. 2013;195(11):2518-29.

Hsiao JF, Lee MH, Chia JH, Ho WJ, Chu JJ, Chu PH.(2008). "Neisseria elongata endocarditis complicated by brain embolism and abscess." J. Med. Microbiol. 57(3):376-81

Janzon, J., B. Ludwig and F. Malatesta (2007). "Electron transfer kinetics of soluble fragments indicate a direct interaction between complex III and the caa3 oxidase in *Thermus thermophilus*." IUBMB Life 59: 563-569.

Jones C. W. and Poole R. K.(1985). "The Analysis of Cytochromes" Methods in

Microbiology 18: 285–328

Kataoka, K., K. Yamaguchi, M. Kobayashi, T. Mori, N. Bokui and S. Suzuki (2004). "Structure-based engineering of *Alcaligenes xylosoxidans* copper-containing nitrite reductase enhances intermolecular electron transfer reaction with pseudoazurin." *J Biol Chem* 279(51): 53374-53378.

Kawai M, Nakao K, Uchiyama I, Kobayashi I. (2006). "How genomes rearrange: genome comparison within bacteria *Neisseria* suggests roles for mobile elements in formation of complex genome polymorphisms." *Gene* 383:52-63.

Ku, S. C., Schulz B. L., Power P. M. and Jennings M. P. (2009). "The pilin O-glycosylation pathway of pathogenic *Neisseria* is a general system that glycosylates AniA, an outer membrane nitrite reductase." *Biochem Biophys Res Commun* 378(1): 84-89.

Kukimoto M, Nishiyama M, Murphy ME, Turley S, Adman ET, Horinouchi S, Beppu T (1994). "X-ray structure and site-directed mutagenesis of a nitrite reductase from *Alcaligenes faecalis* S-6: roles of two copper atoms in nitrite reduction." *Biochemistry* 33:5246-5252.

Li, X., Parker S., Deedom M. and Moir J. W. (2012). "Tied down: tethering redox

proteins to the outer membrane in *Neisseria* and other genera." *Biochemical Society transactions* 39(6): 1895-1899.

Li, Y., Hopper A., Overton T., Squire D. J. P., Cole J. and Tovell N. (2010). "Organization of the Electron Transfer Chain to Oxygen in the Obligate Human Pathogen *Neisseria gonorrhoeae*: Roles for Cytochromes c4 and c5, but Not Cytochrome c2, in Oxygen Reduction." *Journal of Bacteriology* 192(9): 2395-2406.

Lipowski, G., U. Liebl, B. Guigliarelli, W. Nitschke and B. Schoepp-Cothenet (2006). "Conformation of the c552:aa3 electron transfer complex in *Paracoccus denitrificans* studied by EPR on oriented samples." *FEBS Lett* 580(25): 5988-5992.

Matias, V. R., Al-Amoudi, A. J. Dubochet and T. J. Beveridge (2003). "Cryo-transmission electron microscopy of frozen-hydrated sections of *Escherichia coli* and *Pseudomonas aeruginosa*." *J. Bacteriol.* 185: 6112-6118.

McGuinness, B., I. Clarke, P. Lambden, A. Barlow, J. Poolman, D. Jones and J. Heckels (1991). "Point mutation in meningococcal *porA* gene associated with increased endemic disease." *Lancet* 337: 514-517.

Morleya, S. L. and J. A. Pollardb (2001). "Vaccine prevention of meningococcal disease, coming soon?" *Vaccine* 20(5-6): 666-687.

Murphy LM, Dodd FE, Yousafzai FK, Eady RR, Hasnain SS. (2002). "Electron Donation Between Copper Containing Nitrite Reductases and Cupredoxins: the Nature of Proteinprotein Interaction in Complex Formation." *Journal of Molecular Biology* 315: 859-871.

Nicholas, D. and Nelson A. (1957). *Methods in Enzymology* 3: 981.

Nojiri, M., Koteishi H., Nakagami T., Kobayashi K., Inoue T., Yamaguchi K. and Suzuki S. (2009). "Structural basis of inter-protein electron transfer for nitrite reduction in denitrification." *Nature* 462(7269): 117-120.

Overton, T. W., R. Whitehead, Y. Li, L. A. S. Snyder, N. J. Saunders, H. Smith and J. A. Cole (2006). "Coordinated Regulation of the *Neisseria gonorrhoeae*-truncated Denitrification Pathway by the Nitric Oxide-sensitive Repressor, NsrR, and Nitrite-insensitive NarQ-NarP." *Journal of Biological Chemistry* 281(44): 33115-33126.

Otten MF, van der Oost J, Reijnders WN, Westerhoff HV, Ludwig B, Van Spanning RJ.(2001). "Cytochromes c(550), c(552), and c(1) in the electron transport network of *Paracoccus denitrificans*: redundant or subtly different in function?" *J. Bacteriol.* 183(24):7017-26.

Pearson, I. V., Page M. D., Van Spanning R. J. M. and Ferguson S. J. (2003). "A Mutant of *Paracoccus denitrificans* with Disrupted Genes Coding for Cytochrome c550 and Pseudoazurin Establishes These Two Proteins as the In Vivo Electron Donors to Cytochrome cd1 Nitrite Reductase." *Journal of Bacteriology* 185(21): 6308-6315.

Pitcher, R. S. and N. J. Watmough (2004). "The bacterial cytochrome cbb3 oxidases." *Biochimica et Biophysica Acta (BBA) - Bioenergetics* 1655: 388-399.

Punj, V., S. Bhattacharyya, D. Saint-Dic, C. Vasu, E. A. Cunningham, J. Graves, T. Yamada, A. I. Constantinou, K. Christov, B. White, G. Li, D. Majumdar, A. M. Chakrabarty and T. K. Das Gupta (2004). "Bacterial cupredoxin azurin as an inducer of apoptosis and regression in human breast cancer." *Oncogene* 23(13): 2367-2378.

Ray, T. D., L. A. Lewis, S. Gulati, P. A. Rice and S. Ram (2011). "Novel blocking human IgG directed against the pentapeptide repeat motifs of *Neisseria meningitidis* Lip/H.8 and Laz lipoproteins." *J Immunol* 186(8): 4881-4894.

Reincke, B., Thony-Meyer L., Dannehl C., Odenwald A., Aidim M., Witt H., Ruterjans H. and Ludwig B. (1999). "Heterologous expression of soluble fragments of cytochrome c552 acting as electron donor to the *Paracoccus denitrificans* cytochrome c oxidase." *Biochimica et Biophysica Acta* 1411: 114-120.

Rock, J. D., M. R. Mahnane, M. F. Anjum, J. G. Shaw, R. C. Read and J. W. Moir (2005). "The pathogen *Neisseria meningitidis* requires oxygen, but supplements growth by denitrification. Nitrite, nitric oxide and oxygen control respiratory flux at genetic and metabolic levels." *Mol. Microbiol.* 58(3): 800-809.

Stefanelli, P., G. Colotti, A. Neri, M. L. Salucci, R. Miccoli, L. Di Leandro and R. Ippoliti (2008). "Molecular characterization of nitrite reductase gene (*aniA*) and gene product in *Neisseria meningitidis* isolates: is *aniA* essential for meningococcal survival?" *IUBMB Life* 60(9): 629-636.

Stevanin, T. M., Moir J. W. and Read R. C. (2005). "Nitric oxide detoxification systems enhance survival of *Neisseria meningitidis* in human macrophages and in nasopharyngeal mucosa." *Infect. Immun.* 73(6): 3322-3329.

Strube, K., S. de Vries and R. Cramm (2007). "Formation of a dinitrosyl iron complex by NorA, a nitric oxide-binding di-iron protein from *Ralstonia eutropha* H16." *Journal of Biological Chemistry* 282: 20292-20300.

Tamura, N., Murakami S., Oyama Y., Ishiguro M. Yamaguchi and A. (2005). "Direct interaction of multidrug efflux transporter AcrB and outer membrane channel TolC detected via site-directed disulfide cross-linking." *Biochemistry* 44: 11115-11121.

Tauseef I. , Ali YM., Bayliss CD. (2013) "Phase variation of PorA, a major outer

membrane protein, mediates escape of bactericidal antibodies by *Neisseria meningitidis*." *Infect Immun.* 2013;81(4):1374-80.

Tetelin, H., N. Saunders, J. Heidelberg, A. Jeffries, K. Nelson, J. Eisen and H. D. Ketchum KA, Peden JF, Dodson RJ, Nelson WC, Gwinn ML, DeBoy R, Peterson JD, Hickey EK, Haft DH, Salzberg SL, White O, Fleischmann RD, Dougherty BA, Mason T, Ciecko A, Parksey D, Blair E, Cittone H, Clark EB, Cotton MD, Utterback TR, Khouri H, Qin H, Vamathevan J, Gill J, Scarlato, Massignani D, Pizza M, Grandi G, Sun Li, Smith HO, Fraser CM, Moxon ER, Rappuoli R, and Venter JC (2000). "Complete genome sequence of *Neisseria meningitidis* serogroup B strain MC58." *Science* 287: 1809-1815.

Trees, D. L. and S. M. Spinola (1989). "Localization of and Immune Response to the Lipid-Modified Azurin of the Pathogenic *Neisseria*." *J Infect Dis.* 161(2): 336-339.

Turner, S. M., J. W. B. Moir, L. Griffiths, T. W. Overton, H. Smith and J. A. Cole (2005). "Mutational and biochemical analysis of cytochrome c, a nitric oxide-binding lipoprotein important for adaptation of *Neisseria gonorrhoeae* to oxygen-limited growth." *Biochem. J.* 388: 545-553.

van Deuren, M., P. Brandtzaeg and J. van der Meer (2000). "Update on Meningococcal Disease with Emphasis on Pathogenesis and Clinical Management." *Clin Microbiol*

Rev. 13(1): 144-166.

Van Driessche, G., Hu G. v. d. W. W., Selvaraj F., McManus J. D., Blankenship R. E and Beeumen J. J. v. (1999). "Auracyanin A from the thermophilic gliding bacterium *Chloroflexus aurantiacus* represents an unusual class of small blue copper proteins." *Protein Sci.* 8: 947-957.

Van Niel EW, Braber KJ, Robertson LA, Kuenen JG (1992). "Heterotrophic nitrification and aerobic denitrification in *Alcaligenes faecalis* strain TUD." *Antonie Van Leeuwenhoek.* 62(3):231-7.

Vargas, C., McEwan A. and Downie J. (1993). "Evidence for specific secretion rather than autolysis in the release of some *Helicobacter pylori* proteins." *Analytical Biochemistry* 209(2): 323-326.

Vazquez JA, Berron S, O'Rourke M, Smith NH, (1993). "Ecological separation and genetic isolation of *Neisseria gonorrhoeae* and *Neisseria meningitidis*." *Curr. Biol.* 3: 567-572.

Vik, A., F. Aas, J. Anonsen and e. al. (2009). "Broad spectrum O-linked protein glycosylation in the human pathogen *Neisseria gonorrhoeae*." *Proc Natl Acad Sci USA* 106: 4447-4452.

Vijgenboom, E., J. E. Busch and G. W. Canters. (1997). "In vivo studies disprove an obligatory role of azurin in denitrification in *Pseudomonas aeruginosa* and show that *azu* expression is under control of *rpoS* and ANR." *Microbiology* 143: 2853-2863.

White, A. G., P. Entmacher, G. Rubin and L. Leiter (1955). "Physiological and pharmacological regulation of human salivary electrolyte concentrations; with a discussion of electrolyte concentrations of some other exocrine-secretions." *J Clin Invest.* 34(2): 246-255.

Woods, J. P., J. F. Dempsey, T. H. Kawula, D. S. Barritt and J. G. Connon (1989). "Characterization of the neisserial lipid-modified azurin bearing the H.8 epitope. ." *Molecular Microbiology* 3(5): 583-591.

Wu, H. J., Seib K. L., Edwards J. L., Apicella M. A., McEwan A. G. and Jennings M. P. (2005). "Azurin of pathogenic *Neisseria* spp. is involved in defense against hydrogen peroxide and survival within cervical epithelial cells." *Infect Immun* 73(12): 8444-8448.

Yi, K., Rasmussen A. W., Gudlavalleti S. K., Stephens D. S. and Stojiljkovic I. (2004). "Biofilm formation by *Neisseria meningitidis*." *Infect Immun* 72(10): 6132-6138.

Zufferey, R., Preisig O., Hennecke H. and Thöny-Meyer R. L. (1996). "Assembly and function of the cytochrome cbb3 oxidase subunits in *Bradyrhizobium japonicum*." *J. Biol. Chem.* 271(15): 9114-9119.